



Production of silver-loaded zeolites and investigation of their antimicrobial activity

A thesis presented for the award of
Doctor of Philosophy

Bright Kwakye-Awuah

December

2008

Production of silver-loaded zeolites and investigation of their antimicrobial activity

Bright Kwakye-Awuah

B.Sc., M.Sc.

A thesis submitted in partial fulfilment of the requirements of the University of Wolverhampton for the degree of
Doctor of Philosophy

December 2008

This work or any part thereof has not previously been presented in any form to the University or to any other body whether for the purpose of assessment, publication or for any other purpose (unless otherwise stated). Save for any express acknowledgements, references and/or bibliographies cited in the work, I confirm that, the intellectual content of the work is the result of my own efforts and of no other person.

The right of Bright Kwakye-Awuah to be identified as the author of this work is asserted in accordance with ss. 77 and 78 of the Copyright, Designs and Patents Act 1988. At this date copyright is owned by the author.

Signature:

Date: 3 December 2008

Abstract

The production of silver-loaded zeolites either by ion exchange method or by isomorphous substitution of silver ions into zeolites frameworks and their antimicrobial activity is presented. Silver-loaded zeolites produced by ion-exchange in this work include silver-exchanged zeolite X, silver-exchanged zeolite A and silver-exchanged high-alumina Phillipsite. Silver-doped Analcime was produced by isomorphous substitution of silver ions into the Analcime framework. The silver-loaded zeolites were characterized by X-ray diffraction (XRD) analysis, scanning electron microscopy (SEM), energy dispersive X-ray (EDX) analysis, particle size analysis and Fourier transformed infrared (FTIR) spectroscopy.

Studies showed that the amount of silver ions loaded into the zeolites frameworks differed for each zeolite. XRD analysis showed little or no changes in the phase purity of all zeolites before and after ion exchange or before and after substitution of silver ions. SEM analysis and particle size analysis showed that the morphology of each zeolite particles was closely related before and after ion exchanged or before and after substitution of silver ions.

The antimicrobial activity of these silver-loaded zeolites was investigated by exposing *Escherichia coli* K12W-T, *Staphylococcus aureus* NCIMB6571 and *Pseudomonas aeruginosa* NCIMB8295 suspended in tryptone soya broth (TSB) to the silver-loaded zeolites. The first stage of the investigation involved the exposure of the strains to silver-loaded zeolites in TSB for a duration of 24 hours at different concentration of silver-loaded zeolites. The second stage involved the exposure of the strains to silver-loaded zeolites in TSB over a period of two hours. The persistency of antimicrobial activity of silver-loaded zeolites was investigated by retrieving

each silver-loaded zeolite from the first exposure cultures, washed copiously with de-ionised water and adding to fresh bacterial suspensions. To understand the mode of antimicrobial activity of the silver-loaded zeolites, the uptake of silver ions by the strains, composition of fatty acid, as well as the DNA content of *Escherichia coli* K12W-T was studied.

The results obtained showed silver ions appeared to elute from the zeolites frameworks into the TSB in anomalous trend. All three microorganisms were completely inhibited within one hour with the silver-loaded zeolites retaining their antimicrobial activity. The release of silver ions from the zeolites frameworks followed first-order kinetics with varying rate constants and half-lives. The fatty acid composition of all strains as well as the DNA content of *Escherichia coli* K12W-T were affected by the action of silver ions.

Acknowledgements

I am extremely grateful to my Lord, my God and my saviour Christ Jesus for his unceasing love, grace, peace, providence and protection for my life. I thank my director of studies, *Dr Iza Radecka*, my first and second supervisors; *Prof Craig D. Williams* and *Dr Ken Kenward* for their encouragements and constructive discussions throughout the research period.

My appreciation also goes to *Prof Trevor Hocking* Associate Dean and director of Research Centre in Applied Sciences (RCAS) for his patience and support. I am also grateful to *Dr James Vickers* for his assistance in the use of the Flow Cytometer. Special thanks go to the following technical support staff in the School of Applied Science, University of Wolverhampton: *Dianne Spencer, Barbara Hodson, Andrew Brook, Ann Dawson, Balbir Bains, Keith Jones* and *Dave Townrow*.

My next thanks goes to fellow researchers in Room MA 028 namely, *Rob Verlinden, Gopal Kedia, Carlos Rios, Abishek Gupta* and *Chris Rogers*.

Finally, my heartfelt gratitude go to my beloved wife *Lydia Kwakye-Awuah* and my daughter *Bridget A. B. Kwakye-Awuah* for their outstanding love, bravery, and encouragements throughout my studies.

Dedications

This work is dedicated to my Lord, God and Saviour *Christ Jesus*

to my wife,

Lydia Kwakye-Awuah

and my daughter

Bridget A. B. Kwakye-Awuah

List of Tables

Table 1: Mechanism of antimicrobial action of gluteraldehyde (Adapted from Russell, 2003)	5
Table 2: Description of silver	9
Table 3: Intrinsic resistance in bacteria to biocides (Adopted from McDonnell and Russell 1999)	18
Table 4: Mechanisms of plasmid-encoded resistance to biocides (Adapted from McDonnell and Russell, 1999)	19
Table 5: Various zeolites with their channel systems (Szostak, 1989)	26
Table 6: Sub-factors influencing zeolite crystallisation (Szostak, 1989)	36
Table 7: Summary of experimental procedure used in the antimicrobial testing of silver-loaded zeolite X	62
Table 8: Summary of experimental procedure used in the repeated retrieval and re-use of silver-loaded zeolite X	64
Table 9: Elemental composition of zeolite X before and after ion exchange	77
Table 10: General infrared assignments in zeolites	79
Table 11: Elemental composition of zeolite A before and after ion exchange	83
Table 12: EDX chemical composition analysis of high-alumina Phillipsite before and after ion exchange	87
Table 13: EDX microanalysis of the elemental composition with various loading of silver ions into the analcime framework ($N = 4$)	92
Table 14: Amount of Ag^+ detected in the supernatant (ICP-AES) for undoped analcime and for various loadings of Ag^+	95
Table 15: Results showing the antimicrobial activity of silver exchanged zeolite X against <i>E. coli</i> for a duration of 24 hours with different concentrations of silver-exchanged zeolite X	101
Table 16: Results showing the antimicrobial activity of silver exchanged zeolite A against <i>S. aureus</i> for duration of 24 hours with different concentrations of silver-exchanged zeolite A.	108

Table 17: Results showing the antimicrobial activity of silver exchanged high-alumina Phillipsite against <i>P. aeruginosa</i> for duration of 24 hours. Different concentrations of silver-exchanged high-alumina Phillipsite used are shown in the graph	114
Table 18: Results showing the antimicrobial activity of silver-doped analcime on <i>P. aeruginosa</i> for duration of 24 hours. Different concentrations of silver-exchanged zeolite X used are shown in the graph.	118
Table 19: Rate constants and half-lives of silver zeolite X in <i>E. coli</i> , <i>S. aureus</i> and <i>P. aeruginosa</i>	129
Table 20: Mean concentration of silver ions released from silver-exchanged zeolite X into TSB containing either <i>E. coli</i> , <i>S. aureus</i> or <i>P. aeruginosa</i> at time, $t = 0.5$ hours ($N = 4$; $P \leq 0.05$)	130
Table 21: Mean concentration of silver ions released from silver-exchanged zeolite X into TSB containing either <i>E. coli</i> , <i>S. aureus</i> or <i>P. aeruginosa</i> at time, $t = 1.5$ hours ($N = 4$; $P \leq 0.05$)	131
Table 22: Rate constants and half-lives of silver zeolite A in <i>E. coli</i> , <i>S. aureus</i> and <i>P. aeruginosa</i>	133
Table 23: Mean concentration of silver ions released from silver-exchanged zeolite A into TSB containing either <i>E. coli</i> , <i>S. aureus</i> or <i>P. aeruginosa</i> at time, $t = 0.5$ hours ($N = 4$; $P \leq 0.05$)	134
Table 24: Mean concentration of silver ions released from silver-exchanged zeolite A into TSB containing either <i>E. coli</i> , <i>S. aureus</i> N or <i>P. aeruginosa</i> at time, $t = 1.5$ hours ($N = 4$; $P \leq 0.05$)	135
Table 25: Rate constants and half-lives of AgHAP in <i>E. coli</i> , <i>S. aureus</i> and <i>P. aeruginosa</i>	137
Table 26: Summary of rate constants and silver-loading for zeolites X, A and high-alumina Phillipsite	138
Table 27: Mean concentration of silver ions released from silver-exchanged high-alumina into TSB containing either <i>E. coli</i> , <i>S. aureus</i> or <i>P. aeruginosa</i> at time, $t = 0.5$ hours ($N = 4$; $P \leq 0.05$)	140

Table 28: Mean concentration of silver ions released from silver-exchanged high-alumina into TSB containing either <i>E. coli</i> , <i>S. aureus</i> or <i>P. aeruginosa</i> at time, $t = 1.5$ hours ($N = 4$; $P \leq 0.05$)	140
Table 29: Profile of fatty acids obtained from <i>E. coli</i> grown in the presence of zeolite X and silver-exchanged zeolite X	145
Table 30: Profile of fatty acids obtained from <i>S. aureus</i> grown in the presence of zeolite X and silver exchanged zeolite X	146
Table 31: Profile of fatty acids obtained from <i>P. aeruginosa</i> grown in the presence of zeolite X and silver-exchanged zeolite X	147
Table 31: General band assignment of bacteria	150
Table 32: List of reagents, suppliers and abbreviations or chemical formula	163
Table 33: List of abbreviations for silver-loaded zeolites	164
Table 34: List of media/microorganisms, suppliers and their abbreviations	164
Table 35: List of instruments, their abbreviations and locations	165

Appendices

2.1 Descriptive statistics of silver loaded zeolite X on <i>E. coli</i> , <i>S. aureus</i> and <i>P. aeruginosa</i>	186
2.2 One-way ANOVA analysis	187
2.3: Statistical descriptives of viable cell counts obtained by one-way ANOVA analysis for the retrieval and reuse of silver-exchanged zeolite X on <i>S. aureus</i>	188
2.4 Statistical descriptives of viable cell counts obtained by one-way ANOVA analysis for the retrieval and reuse of silver-exchanged zeolite X on <i>P. aeruginosa</i> NCIM8295	189

3. Descriptive statistics of silver ions eluted from silver-exchanged zeolite X	190
3.1 Statistical descriptives of silver ions eluted from silver-exchanged zeolite X obtained by one-way ANOVA analysis during exposure of <i>E. coli</i>	190
3.2: Statistical descriptives of silver ions eluted from silver-exchanged zeolite X obtained by one-way ANOVA analysis during exposure of <i>S. aureus</i>	190
3.3: Statistical descriptives of silver ions eluted from silver-exchanged zeolite X obtained by one-way ANOVA analysis during exposure of <i>P. aeruginosa</i>	191
4. Descriptive statistics of antibacterial testing of silver-exchanged zeolite A	191
4.1: Statistical descriptives of silver ions eluted from silver-exchanged zeolite A obtained by 191 one-way ANOVA analysis during exposure of <i>E. coli</i>	191
4.2 Statistical descriptives of silver ions eluted from silver-exchanged zeolite A obtained by one-way ANOVA analysis during exposure of <i>S. aureus</i>	192
4.3 Statistical descriptives of silver ions eluted from silver-exchanged zeolite A obtained by one-way ANOVA analysis during exposure of <i>P. aeruginosa</i>	192
4.4 Viable cell counts obtained for <i>E. coli</i> K12W-T, <i>S. aureus</i> and <i>P. aeruginosa</i> NCIMB8295 for the retrieval and reuse of silver-exchanged zeolite A	193
4.5 Statistical descriptives of silver ions eluted from silver-exchanged zeolite A obtained by one-way ANOVA analysis during exposure of <i>E. coli</i>	194
4.6 Statistical descriptives of silver ions eluted from silver-exchanged zeolite A obtained by one-way ANOVA analysis during exposure of <i>S. aureus</i>	194
4.7 Statistical descriptives of silver ions eluted from silver-exchanged zeolite A obtained by one-way ANOVA analysis during exposure of <i>P. aeruginosa</i>	195
4.8 Statistical descriptives of silver ions eluted from silver-exchanged high-alumina Phillipsite obtained by one-way ANOVA analysis during exposure of <i>E. coli</i>	195

4.9 Statistical descriptives of silver ions eluted from silver-exchanged high-alumina Phillipsite obtained by one-way ANOVA analysis during exposure of <i>S. aureus</i>	196
4.10 Statistical descriptives of silver ions eluted from silver-exchanged high-alumina Phillipsite obtained by one-way ANOVA analysis during exposure of <i>P. aeruginosa</i>	196

List of Figures

Figure 1: General pattern of biocide entry into different types of microorganisms (Adapted from McDonnell and Russell, 1999)	3
Figure 2: (a) Diagram of a gram-negative cell wall: (b) Electron Micrograph of a Gram-Negative cell wall (http://student.ccbcmd.edu/bio141)	12
Figure 3: (a); Structure of a gram-positive bacterium and (b); Electron micrograph of a gram-positive cell wall (http://student.ccbcmd.edu/bio141)	15
Figure 4: Structure of mycobacterial cell wall. (http://student.ccbcmd.edu/bio141)	16
Figure 5: Hypothetical growth curve of bacteria (Madigan, 2000)	17
Figure 6: Tetrahedra framework structure of zeolites (http://www.bza.org/zeolites.html)	25
Figure 7: Secondary building units recognized in zeolite frameworks. Single 4, 5, 6, and 8 rings (S4R, S5R, S6R and 8SR), double rings (4DR, 6DR and 8DR) and complex rings (Adapted from Szostak, 1989)	27
Figure 8: Framework structure of zeolite X showing location of exchangeable sites (Yeom and Kim, 1997)	31
Figure 9: Framework structure of zeolite A (LTA) (http://izasc.ethz.ch/fmi/xsl/IZA-SC/ftc_fw.xsl?-db=Atlas_main&-lay=fw&-max=25&STC=LTA&-find)	32
Figure 10: Framework structure of Phillipsite (PHI) (http://izasc.ethz.ch/fmi/xsl/IZA-SC/ftc_fw.xsl?-db=Atlas_main&-lay=fw&-max=25&STC=LTA&-find)	33
Figure 11: Framework structure of Analcime (ANA)	33

(http://izasc.ethz.ch/fmi/xsl/IZA-SC/ftc_fw.xsl?-db=Atlas_main&-lay=fw&-max=25&STC=LTA&-find)

Figure 12: Schematics of zeolite synthesis	34
Figure 13: Schematics of the X-Ray diffraction spectrometer (British Museum, 2005)	52
Figure 14: Schematics of the FTIR spectrometer (British Museum, 2005)	57
Figure 15: Schematics of ICP (British Museum, 2005)	65
Figure 16: Schematics of the Flow Cytometer (www.ab-direct.com)	66
Figure 17: SEM micrographs of zeolite X with silver loadings (left) and without (right)	75
Figure 18: SEM micrographs of silver-exchanged zeolite X showing varying sizes	76
Figure 19: EDX spectra of zeolite X with (left) and without (right) silver loading	76
Figure 20: Particle size distribution of zeolite X with (blue bars) and without (brown bars) silver ions	78
Figure: 21 XRD pattern for zeolite silver-exchanged X along with the reference pattern 38 - 237	78
Figure 22: Results of the FTIR spectra of zeolite X with and without silver ions	80
Figure 23: SEM micrographs of zeolite A with silver loadings (left) and without silver loadings (right)	82
Figure 24: EDX spectra of zeolite A with silver loadings (left) and without (right) silver loading	82
Figure: 25: XRD pattern for zeolite A with silver loadings (red line) and without silver loadings (blue line) along with the reference pattern 39 - 222	83
Figure 26: Particle size distribution of zeolite A with (blue bars)	84

and without (brown bars) silver ions

Figure 27: FTIR spectrum of zeolite A with silver-loading (blue line) and without silver loading (red line) 85

Figure 28: SEM micrograph of high aluminium Phillipsite with silver loading (left) and without silver loading (right) 86

Figure 29: EDX spectra of high-alumina Phillipsite with silver loading (left) and without silver loading (right) 87

Figure 30: XRD spectra for high aluminium Phillipsite with silver loading (top) and without silver loading (bottom) 88

Figure 31: FTIR spectra of high aluminium Phillipsite with silver loading (blue line) and without silver loading (red line) 89

Figure 32: XRD spectra of silver-doped analcime with different loading of silver ions 90

Figure 33: SEM micrograph of silver-doped analcime obtained with (top left): no loading of silver ions, (top right): 5 % loading of silver ions, (bottom left): 10 % loading of silver and (bottom right): 20 % loading of silver ions 91

Figure 34: Energy dispersive X-ray spectra of (a): undoped analcime, (b): analcime doped with 5 % Ag^+ , (c): analcime doped with 10 % Ag^+ and (d) analcime doped with 20 % Ag^+ 92

Figure 35: Particle size distribution of analcime doped with 0, 5, 10 and 20 % doping of silver ions 93

Figure 36: Fourier transformed infrared spectroscopy spectra of (a): undoped analcime, (b): analcime doped with 5 % Ag^+ , (c): analcime doped with 10 % Ag^+ and (d) analcime doped with 20 % Ag^+ 94

Figure 37: Bacteriostatic activity of silver-loaded zeolite X at 37 °C. (a): *E. coli* (b): *S. aureus* and (c): *P. aeruginosa*. Cells were treated with zeolite X and with silver-loaded zeolite X at 0, 0.15, 0.25, 0.50 and 1.00 g l⁻¹ in TSB. The pH remained fairly constant within the range of 7.1 – 7.3. 102

Figure 38: Silver ions released from silver-exchanged zeolite X into TSB with or without (a): *E. coli* (b): *S. aureus* and (c): *P. aeruginosa* with time at concentration of 0.15 g l⁻¹ silver-exchanged zeolite X. 103

Figure 39: Silver ions released from silver-exchanged zeolite X into TSB with or without (a): <i>E. coli</i> (b): <i>S. aureus</i> and (c): <i>P. aeruginosa</i> with time at a concentration of 0.25 g l ⁻¹ silver-exchanged zeolite X.	104
Figure 40: Silver ions released from silver-exchanged zeolite X into TSB with or without (a): <i>E. coli</i> (b): <i>S. aureus</i> and (c): <i>P. aeruginosa</i> with time at concentration of 0.50 g l ⁻¹ silver-exchanged zeolite X.	105
Figure 41: Silver ions released from silver-exchanged zeolite X into TSB with or without (a): <i>E. coli</i> (b): <i>S. aureus</i> and (c): <i>P. aeruginosa</i> with time at concentration of 1.0 g l ⁻¹ silver-exchanged zeolite X.	106
Figure 42: Bacteriostatic activity of silver-loaded zeolite A at 37 °C for (a): <i>E. coli</i> (b): <i>S. aureus</i> and (c): <i>P. aeruginosa</i> cells were treated with zeolite A and with silver-loaded zeolite A at 0, 0.15, 0.25, 0.50 and 1.00 g l ⁻¹ in TSB. The pH remained fairly constant within the range of 7.1 – 7.3	109
Figure 43: Silver ions released from silver-exchanged zeolite A into TSB with or without (a): <i>E. coli</i> (b): <i>S. aureus</i> and (c): <i>P. aeruginosa</i> with time at concentration of 0.15 g l ⁻¹ silver-exchanged zeolite A.	110
Figure 44: Silver ions released from silver-exchanged zeolite A into TSB with or without (a): <i>E. coli</i> (b): <i>S. aureus</i> and (c): <i>P. aeruginosa</i> with time at concentration of 0.25 g l ⁻¹ silver-exchanged zeolite A	111
Figure 45: Silver ions released from silver-exchanged zeolite A into TSB with or without (a): <i>E. coli</i> (b): <i>S. aureus</i> and (c): <i>P. aeruginosa</i> with time at concentration of 0.50 g l ⁻¹ silver-exchanged zeolite A.	112
Figure 46: Silver ions released from silver-exchanged zeolite A into TSB with or without (a): <i>E. coli</i> (b): <i>S. aureus</i> and (c): <i>P. aeruginosa</i> with time at concentration of 1.0 g l ⁻¹ silver-exchanged zeolite A	113
Figure 47: Bacteriostatic activity of silver-exchanged high-alumina Phillipsite at 37 °C. (a): <i>E. coli</i> (b): <i>S. aureus</i> and (c): <i>P. aeruginosa</i> . Cells were treated with high-alumina Phillipsite and with silver-exchanged high-alumina Phillipsite at 0, 0.15, 0.25, 0.50 and 1.00 g l ⁻¹ in TSB. The pH remained fairly constant within the range of 7.1 – 7.3	115
Figure 48: Left: Silver ions released from silver-exchanged high-alumina Phillipsite into TSB with or without (a): <i>E. coli</i> (b): <i>S. aureus</i> and (c): <i>P. aeruginosa</i> with time	116

at concentration of 0.15 g l⁻¹ silver-exchanged high-alumina Phillipsite. Right: Silver ions released from silver-exchanged high-alumina Phillipsite into TSB with or without (a): *E. coli* (b): *S. aureus* and (c): *P. aeruginosa* with time at concentration of 0.25 g l⁻¹ silver-exchanged high-alumina Phillipsite

Figure 49: Left: Silver ions released from silver-exchanged high-alumina Phillipsite into TSB with or without (a): *E. coli* (b): *S. aureus* and (c): *P. aeruginosa* with time at concentration of 0.50 g l⁻¹ silver-exchanged high-alumina Phillipsite. Right: Silver ions released from silver-exchanged high-alumina Phillipsite into TSB with or without (a): *E. coli* (b): *S. aureus* and (c): *P. aeruginosa* with time at concentration of 1.0 g l⁻¹ silver-exchanged high-alumina Phillipsite 117

Figure 50: Bactericidal activity of silver-loaded high-doped analcime at 37 °C. (a): *E. coli* (b): *S. aureus* and (c): *P. aeruginosa* cells were treated with analcime (○) and with silver-doped analcime at 0 (×), 0.15 (△), 0.25 (□), 0.50 (◇) and 1.00 (▲) g l⁻¹ in TSB. 119

Figure 51: Results from the retrieval experiments for silver-loaded zeolite X at concentration of 1.5 g l⁻¹. 126

Figure 52: Concentrations of silver remaining in silver-zeolite X before and after each exposure to (a): *E. coli*, (b): *S. aureus* and (c) *P. aeruginosa* cultures. Each experiment lasted for 2 hours. 127

Figure 53: Concentration profile of silver ions eluted from zeolite X as a function of time for (a): first exposure, (b): first retrieval, (c): second retrieval and (c): third retrieval of silver-exchanged zeolite X. 129

Figure 54: Results from the retrieval experiments for silver-loaded zeolite A at concentration of 1.5 g l⁻¹ on (a): *E. coli*, (b): *S. aureus* and (c): *P. aeruginosa*. 131

Figure 55: Concentrations of silver remaining in silver-zeolite A before and after each exposure to (a): *E. coli*, (b): *S. aureus* and (c) *P. aeruginosa* cultures 132

Figure 56: Concentration profile of silver ions eluted from zeolite A into TSB containing *E. coli*, *S. aureus* and *P. aeruginosa* as a function of time for (a): first exposure, (b): first retrieval, (c): second retrieval and (c): third retrieval of silver-exchanged zeolite A 133

Figure 57: Results from the retrieval experiments for 136

silver-exchanged high-alumina Phillipsite at concentration of 1.5 g l^{-1} on (a): *E. coli*, (b): *S. aureus* and (c): *P. aeruginosa*.

Figure 58: Concentrations of silver remaining in silver-exchanged high-alumina Phillipsite before and after each exposure to (a): *E. coli*, (b): *S. aureus* and (c) *P. aeruginosa* cultures. 138

Figure 59: Concentration profile of silver ions eluted from high-alumina Phillipsite into TSB containing *E. coli*, *S. aureus* and *P. aeruginosa* as a function of time for (a): first exposure, (b): first retrieval, (c): second retrieval and (c): third retrieval of silver-exchanged high-alumina Phillipsite 139

Figure 60: Retrieval and re-use of silver-doped analcime against *E. coli* in TSB 141

Figure 61: Typical plots showing fluorescence for stained (black line) and PI-stained (other lines) cells of left: *E. coli* and right: *S. aureus* assessed by Flow Cytometry. 143

Figure 62: Above (a): Dot plot of cells of *E. coli* with silver-exchanged zeolite X (b): without silver-exchanged zeolite X. Below: Fluorescence of *E. coli* obtained with cells stained with (c): SYTOX 22 and (d): PI and SYTOX 22. 144

Figure 63: Above (a): Dot plot of cells of *S. aureus* with silver-exchanged zeolite X (b): without silver-exchanged zeolite X. Below: Fluorescence of *S. aureus* obtained with cells stained with (c): SYTOX 22 and (d): PI and SYTOX 22. 144

Figure 64: FTIR spectra of λ DNA, Ag/ λ DNA, isolated DNA of *E. coli* and isolated Ag/ λ DNA of *E. coli*. 149

Appendices

1.1: SEM micrographs of zeolite X with silver loading (left) and without silver loading (right) with different magnifications. 183

1.2: SEM micrographs of zeolite A with silver loading (left) and without silver loading (right) with different magnifications. 183

1.3C: SEM micrographs of zeolite X with silver loading (left) and without silver loading (right) with different magnifications. 184

1.4: SEM micrographs of Analcime with silver loading (left) and without silver loading (right) with same magnifications. 184

Contents	Page
Abstract	i
Acknowledgements	iii
Dedications	iv
List of Tables	v
List of Figures	ix
Chapter 1:	1
Introduction and literature review	
1.1 Antimicrobial agents	2
1.1.1 Introduction and literature review	2
1.1.2 Adsorption and uptake of different classes of antimicrobial agents	3
1.1.3 Action of individual classes of antimicrobial agents	4
1.1.3.1 Aldehydes	4
1.1.3.2 Alcohols	6
1.1.3.3 Phenols, bisphenols and halophenols	6
1.1.3.4 Cationic biocides	8
1.1.3.5 Halogen releasing compounds	8

1.2 Silver and silver compounds	8
1.2.1. Description and properties of silver	8
1.2.2 History of silver use	9
1.2.3 Silver and its application as antimicrobial agent	10
1.2.4 Mode of antimicrobial activity of silver	11
1.3 Bacteria	12
1.3.1 Gram-Negative cell	12
1.3.1.1 Surface structures	12
(a) Flagella motility	13
(b) Pili	13
(c) Capsules	14
(d) Lipoteichoic acid	14
(e) Lipopolysaccharides	14
1.3.1.2 Plasma membrane	14
1.3.2 Gram-positive cell	15
1.3.3 Mycobacterial cell	16
1.3.4 Bacterial growth	17
1.4 Microbial resistance	18
1.4.1 Microbial resistance to antimicrobial agents	18
1.4.2 Microbial resistance to silver	20

1.5 Zeolites	21
1.5.1 Historical background	21
1.5.2 Introduction to molecular sieves	22
1.5.3 Classification of zeolites	23
1.5.4 Nomenclature of zeolites	24
1.5.5 Structures of zeolites	24
1.5.5.1 Channels and pore openings	25
1.5.5.2 Secondary building units (SBUs)	26
1.5.6 Diffusion in zeolites	27
1.5.7 Zeolite chemistry	29
1.6 Structures studied in this work	30
1.6.1 Zeolite X	30
1.6.2 Zeolite A	31
1.6.3 High Aluminium Phillipsite	32
1.6.4 Analcime	33
1.7 Synthesis of zeolites	34
1.7.1 Introduction	34
1.7.2 Factors affecting zeolite formation during synthesis	35
1.7.2.1 Molar composition	36
1.7.2.2 Temperature	37
1.7.2.3 Time	37

1.7.2.4 History-dependent factors influencing zeolite formation	38
1.8 Properties of zeolites	39
1.9 Application of zeolites	39
1.9.1 Adsorption	39
1.9.2 Zeolite catalysis	40
1.9.3 Ion exchange	40
1.9.4 Aquaculture	41
1.9.5 Swimming pool filters	41
1.9.6 Removal of solid wastes	42
1.10 Silver-zeolite technology	42
1.11 Hypothesis	44
1.12 Aims and objectives	45

Chapter 2:	47
Methodology and experimental design	48
PART A:	49
Production and characterisation of silver zeolites	49
2.1 Synthesis of zeolites	49
2.1.1 Synthesis of zeolite X	49
2.1.2 Synthesis of zeolite A	50
2.1.3 Synthesis of High Aluminium Phillipsite	51
2.1.4 Synthesis of silver-doped analcime	52
2.2 Characterisation of zeolites	52
2.2.1 X-ray Diffraction (XRD)	53
(a) Introduction	53
(b) Principle of XRD	53
(c) Experimental method	54
2.2.2 Energy Dispersive X-ray analysis (EDX)	55
(a) Introduction	55
(b) Principle of EDX	55
2.2.3 Scanning Electron Microscopy (SEM)	55
(a) Introduction	55
(b) Principle of SEM	56

2.2.4 Particle size analysis	56
(a) Introduction	56
(b) Principle of Particle size X bed analyzer	56
(c) Experimental method	56
2.2.5 Fourier Transformed Infrared Spectroscopy	57
(a) Introduction	57
(b) Principle of FTIR	57
(c) Experimental method	58
2.3 Ion exchange of zeolites	59
2.3.1 Zeolite X	59
2.3.2 Zeolite A	59
2.3.3 High Aluminium Phillipsite	59
PART B:	60
Antimicrobial activity of silver-loaded zeolites	60
2.4 Media preparation	60
2.4.1 Preparation of tryptone Soya Agar (TSA)	60
2.4.2 Preparation of tryptone Soya Broth (TSB)	60
2.4.3 Preparation of Ringer's solution	60

2.5 Antimicrobial activity of silver-exchanged zeolite X	61
2.5.1 Introduction	61
2.5.2 Influence of concentration with time	61
2.5.3 Concentration dependence over shorter time	63
2.5.4 Repeated zeolite retrieval and re-use	63
2.6 EDX analysis of each retrieved zeolites	64
2.7 Analysis of silver released silver-loaded zeolites by ICP-AES spectroscopy	74
2.8 Analysis of silver released and its effect on bacteria	75
2.8.1 ICP-AES analysis	75
2.8.2 Flow Cytometry analysis of zeolite X on <i>E. coli</i>	76
2.8.2.1 Introduction	76
2.8.2.2 Principle of Flow Cytometry	76
2.8.2.3 Material and media preparation	77
2.8.2.4 Instrumental settings	78
2.8.2.5 Experimental procedure	78
2.9 Analysis of fatty acid composition by chromatography (GC)	78
2.9.1 Media preparation	78
2.9.2 Preparation of cell cultures	79

2.9.3 Fatty acid extraction	79
2.9.4 Determination of fatty acid composition	80
2.10 Analysis of DNA content of <i>E. coli</i> K12W-T by FTIR	81
2.10.1 DNA Extraction	81
2.10.2 FTIR analysis of extracted DNA	81
2.11 Statistical analysis	82
Chapter 3:	83
Results and discussion	83
Synthesis, ion exchange and characterization of silver-loaded zeolites	81
3.1 Synthesis, ion exchange and characterization of zeolite X	84
3.1.1 Synthesis	84
3.1.2 Ion exchange	84
3.1.3 Characterization	84
3.2 Synthesis, ion exchange and characterization of zeolite A	90
3.2.1 Synthesis	90
3.2.2 Ion exchange	90
3.2.3 Characterization	90

3.3 Synthesis, ion exchange and characterization of high-alumina Phillipsite (HAP)	94
3.3.1 Synthesis	94
3.3.2 Characterisation	95
3.3.3 Ion exchange	95
3.4 Synthesis and characterization of silver-doped Analcime	99
3.4.1 Synthesis	99
3.4.2 Characterisation	99
3.5 Discussion	105
Chapter 4:	109
Results and discussion	109
Antimicrobial activity of silver-loaded zeolites	109
4.1 Antimicrobial activity of silver-exchanged zeolite X (AgZ-X)	110
4.1.1 Influence of concentration of (AgZ-X) over longer period	110
4.1.2 Influence of concentration of (AgZ-X) over shorter period	111
4.1.3 ICP-AES analysis of silver ions eluted from (AgZ-X)	112
4.2 Antimicrobial activity of silver-exchanged zeolite A (AgZ-A)	116

4.2.1 Influence of concentration of (AgZ-A) over a 24-hour duration	116
4.2.2 Influence of concentration of (AgZ-A) over shorter period	117
4.2.3 ICP-AES analysis of silver ions eluted from (AgZ-A)	118
4.3 Antimicrobial activity of silver-exchanged high-alumina Phillipsite (AgHAP)	122
4.3.1 Influence of concentration of AgHAP over a 24-hour duration	122
4.3.2 Influence of concentration of AgHAP over shorter period	122
4.3.3 ICP-AES analysis of silver ions eluted from AgHAP	124
4.4 Antimicrobial activity of silver-doped Analcime	125
4.4.1 Influence of concentration of silver-doped Analcime over longer period	125
4.4.2 Influence of concentration of silver- doped Analcime over shorter period	126
4.5 Discussion	128
4.5.1 Discussion of antimicrobial activity of silver-loaded zeolites	128
4.5.2 Discussion of silver ions eluted from silver-loaded zeolites	130
Chapter 5:	133
Results and discussion	133
Persistency in antimicrobial activity of silver-loaded zeolites	133

5.1 Continuous retrieval and re-use of AgZ-X	134
5.1.1 Antimicrobial activity	134
5.1.2 EDX analysis of silver ions left in AgZ-X after each retrieval	135
5.1.3 ICP-AES analysis of silver ions eluted from AgZ-X	137
5.2 Continuous retrieval and re-use of AgZ-A	139
5.2.1 Antimicrobial activity	139
5.2.2 EDX analysis of silver ions left in AgZ-A after each retrieval	139
5.2.3 ICP-AES analysis of silver ions eluted from AgZ-A	141
5.3 Continuous retrieval and re-use of AgHAP	143
5.3.1 Antimicrobial activity	143
5.3.2 EDX analysis of silver ions left in AgHAP after each retrieval	144
5.3.3 ICP-AES analysis of silver ions eluted from AgHAP	145
5.4 Continuous retrieval and re-use of silver-doped Analcime	147

Chapter 6:	149
Results and discussion	149
Effect of silver ions on bacterial components	149
6.1 Flow Cytometry analysis	150
6.2 Analysis of fatty acid composition	152
6.3 Effect of silver-exchange zeolite X on DNA of <i>E. coli</i>	155
6.4 Discussion	158
Chapter 7:	161
Overall discussion and conclusion	161
7.1 Overall discussion	162
7.1.1 Silver release and uptake by microorganisms	162
7.1.2 Mode of action of antimicrobial activity of silver	165
7.1.3 Bacterial resistance to silver	167
7.2 Overall conclusion	168
7.3 Limitations of this study	169

7.4 Suggestions for further work	169
List of abbreviations	164
References	167
Appendices	184
1. Synthesis of silver-loaded zeolites	184
1.1 SEM micrographs of zeolite X with and without silver loading	184
1.2 SEM micrographs of zeolite A with and without silver loading	184
1.3 SEM micrographs of high-alumina Phillipsite with and without silver loading	185
1.4 SEM micrographs of zeolite-doped Analcime	185
2. Descriptive statistics of antibacterial testing of silver-exchanged zeolite X	185
2.1 Descriptive statistics of antimicrobial activity silver loaded zeolite X on <i>E. coli</i> K12W-T, <i>S. aureus</i> NCIMB6571 and <i>P. aeruginosa</i> NCIMB8295	186
5. List of publications, posters and conferences attended	197
6. Theoretical calculations of Ag in zeolites	198
6.1 Number of moles of Ag in zeolite X	198
6.2 Number of moles of Ag in zeolite A	198
6.3 Number of moles of Ag in high-alumina Phillipsite	198

6.4 Number of moles of Ag in analcime	199
7. Conferences attended during time of study	199

Chapter 1

Introduction and Literature review

This chapter reviews the various antimicrobial agents and their mode of antimicrobial action. Descriptions of gram-negative, gram-positive and bacterial cells are also presented. A review of literature on silver-zeolite technology and its antimicrobial activity is discussed in the latter part of this chapter. Finally, the hypothesis on which this work is based along with the aims and objectives are given.

1.1 Antimicrobial agents

1.1.1 Introduction

Antimicrobial agents are chemical compounds biosynthetically or synthetically produced which either destroy or usefully suppress the growth or metabolism of a variety of microscopic or submicroscopic forms of life (Blondelle and Houghten, 1996). Hence, antimicrobial agents are used as antiseptics, disinfectants or preservatives (Russell, 1990a, 1994, 1996; McDonnell and Russell, 1999). Due to the chemical nature of antimicrobial agents they are often referred to as biocides. Biocides differ in their antimicrobial activity (McDonnell and Russell, 1999). Hence terms such as ‘static’ is used to describe biocides that inhibit microbial growth (e.g. bacteriostatic, fungistatic, sporistatic) (McDonnell and Russell, 1999) and ‘cidal’ which refers to biocides that kill the target organism (e.g. bactericidal, sporicidal, virucidal) (Russell and Hugo, 1994; Russell, 1996; McDonnell and Russell, 1999; Niku-Paavola *et al.*, 1999).

Antimicrobial agents also include antibiotics, which are naturally occurring or synthetic substances which inhibit selective bacteria at relatively low concentrations. Other terms used to describe the nature of antimicrobial activity of biocides are sterilization; a physical or chemical process that completely destroys or removes all microbial life and preservation, defined as the prevention of multiplication of microorganisms (McDonnell and Russell, 1999).

1.1.2 Adsorption and uptake of different classes of antimicrobial agents

The general pattern of biocide entry into different types of microorganisms is shown in Figure 1.

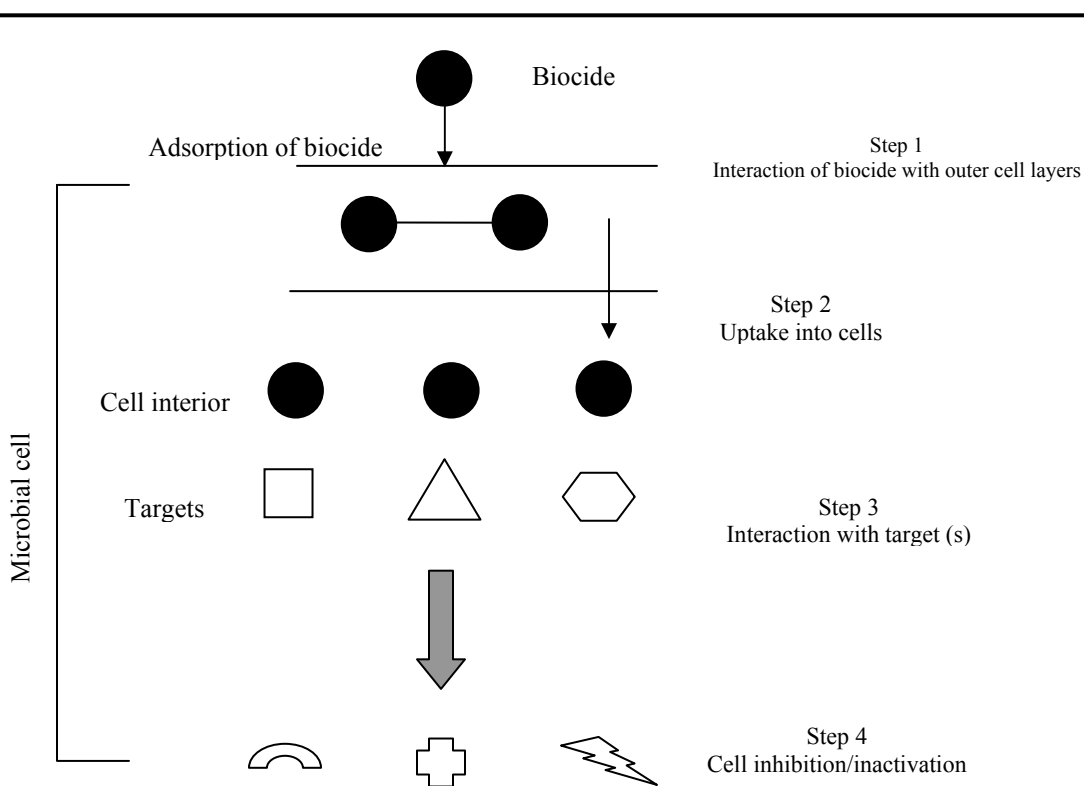


Figure 1: General pattern of biocide entry into different types of microorganisms (Adapted from McDonnell and Russell, 1999).

The entry begins with adsorption of biocides to the cell surface. There are five different classes of adsorption (Russell and Hugo, 1994). These are: (i) an S-shaped pattern, in which a biocide molecule in the form a solute is oriented vertically and meets strong competition from solvent molecules or by another adsorbed molecule; (ii) L-shaped pattern, where it becomes increasingly difficult for biocide molecule to fill target sites as it fills them; (iii) an H-shaped pattern, (which is the product formed) after the molecule is adsorbed; (iv) C-pattern, the product obtained when the solute penetrates more readily into the adsorbate than the solvent and (v) Z-pattern, in which

there is a sharp break in the pattern followed by an increase in uptake caused by a breakdown of the adsorption species and a formation of a new species (Hugo, 1991). Following interaction with the outer cell layers, the biocide traverse the outer cell layer(s) to reach their target sites, usually present within microbial cells (Figure 1). The mechanism of biocide uptake into the interior of microbial depends on the composition of the outer membrane and the chemical nature of the biocide (Russell *et al.*, 1991; Russell, 1996). After entry into the interior of the cell the biocide interact with their target. Target sites in the interior of the cell include cytoplasmic membrane cytoplasmic constituents (Maillard, 2002). Most biocides interact with more than one target (Russell, 1990a; Russell *et al.*, 1991; Maillard, 2002) resulting in the inhibition of the cell.

1.1.3 Action of individual classes of antimicrobial agents

A comprehensive list, description and uses of antimicrobial agents along with their chemical structures are given below.

1.1.3.1 Aldehydes

Aldehydes such as glutaraldehyde have broad spectrum of activity against bacteria and their spores, fungi and viruses and are used for disinfection, sterilization and preservation (Gorman *et al.*, 1980; Maillard, 2002). Due to its cross-linking effects on amino groups in bacterial proteins (El-Falaha *et al.*, 1985b) it has the ability to act on non-sporulating and sporulating bacteria by agglutinating their cells thereby increasing their settling rates (Mavarro and Monsan, 1976). Glutaraldehyde is also used as fixative in electron microscopy. The mode of the bactericidal (Russell, 1990b; Russell, *et al.*, 1991; McDonnell and Russell, 1999) and sporicidal (Power and Russell, 1990; McDonnell and Russell, 1999; Tennen *et al.*, 2000) activity of glutaraldehyde showed a strong interaction of glutaraldehyde with the outer layers of *E. coli* and *S. aureus*

(Hughes and Thurman, 1970; Gorman and Scott, 1977; Russell, 1994). A summary of some antimicrobial agent such as glutaraldehyde and its target site(s) of action is shown in Table 1: In addition, glutaraldehyde also inhibits transport in gram-negative bacteria (Gorman and Scott, 1977), inhibits dehydrogenase activity (Russell, 1990a) and of periplasmic enzymes (Gorman and Scott, 1977). In addition it prevents lysosthaphin-induced lyses in *Staphylococcus aureus* (Russell *et al.*, 1997) and of sodium lauryl sulphate-induced lyses in *Escherichia coli* (Russell, 1990b). Mycobactericidal activity of glutaraldehyde has been documented although no critical review has been undertaken (Russell, 1994, 1996).

Table 1: Mechanism of antimicrobial action of glutaraldehyde (Adapted from Russell, 2003)

Target microorganism	Glutaraldehyde action
Bacterial spores	Low concentrations inhibit germination; high concentrations are sporicidal, probably as a consequence of strong interaction with outer cell layers
Mycobacteria	Action unknown, but probably involves mycobacterial cell wall
Other non-sporulating bacteria	Strong association with outer layers of gram-positive and gram-negative bacteria; cross-linking of amino groups in protein; inhibition of transport processes into cell
Fungi	Fungal cell wall appears to be a primary target site, with postulated interaction with chitin
Viruses	Actual mechanisms unknown, but involve protein- DNA cross-links and capsid changes
Protozoa	Mechanism of action not known

The mode of fungicidal activity of glutaraldehyde has been studied (Navarro Monsan, 1976) with the major target site being the fungal cell wall. The potency of the antifungal activity of glutaraldehyde was against hepatitis B surface antigen ([HBcAg] in hepatitis B virus [HBV]) and against lysine residues on the surface of the hepatitis A virus [HAV] (Passagot, 1987; Chambon *et al.*, 1992).

Formaldehyde has been known to be extremely reactive compound (Russell, 1994; Power, 1995; Russell *et al.*, 1991) that reacts with protein DNA and RNA (McDonnell and Russell, 1999). It is

sporicidal and inhibits DNA synthesis of bacteria (McDonnell and Russell, 1999). *Ortho*-phthalaldehyde (OPA) is an aromatic dialdehyde whose antimicrobial action has been undertaken against gram-positive staphylococci, mycobacteria and spores and gram-negative *E. coli* and *Pseudomonas aeruginosa* (Walsh *et al.*, 1999; 2001; Fraud *et al.*, 2001). Although the mechanism of antimicrobial action of *ortho*-phthalaldehyde is not known, preliminary studies showed that the mechanism of action is similar to that of gluteraldehyde (Walsh *et al.*, 1999).

1.1.3.2 Alcohols

Several alcohols are known to exhibit antimicrobial activity (McDonnell and Russell, 1999). Ethanol and isopropanol act as membrane disrupters of most bacteria resulting in the inhibition of enzymes involved in glycolysis, fatty acids and phospholipids synthesis (Russell and Chopra, 1996). They inhibit DNA, RNA and peptidoglycan of *E. coli*. In addition ethanol was found to induce intracellular material from *Saccharomyces cerevisiae* (Russell, 1996). Other alcohols such as phenyl alcohol (PEA) and phenoxyethanol (POE) have been found to produce membrane disruption at low concentrations (McDonnell and Russell, 1999). POE is used as uncoupling agent to induce translocation in *E. coli* whilst PEA was found to inhibit the growth of several gram-negative bacteria (Gilbert *et al.*, 1990).

1.1.3.3 Phenols, bis-phenols and halophenols

Phenols are known to induce progressive loss of intracellular constituents from treated bacteria producing an overall membrane damage as a result of intracellular coagulations at higher concentrations (Hugo, 1991). At lower concentrations phenols lyse growing cells of *E. coli*, staphylococci and streptococci (McDonnell and Russell, 1999). Fenticlor, a chlorinated bis-phenol was found to affect the metabolic activities of *E. coli* and *S. aureus* (Hugo and

Bloomfield, 1974). As a result the selective permeability of the membrane to protons was increased with a consequent dissipation of protomotive force (PMF) and an uncoupling of oxidative phosphorylation (Bloomfield, 1974). The antifungal properties of phenols involve damage to the plasma membrane resulting in the leakage of intracellular constituents (Russell, 1996; McDonnell and Russell, 1999).

Bis-phenols are hydroxyl-halogenated derivatives of phenolic groups connected by bridges (Russell *et al.*, 1991; Russell and Day 1993; Russell *et al.*, 1997). Triclosan (5-chloro-2-(2,4-dichlorophenoxyphenol) and hexachlorophene (2,2'-methylenebis(3,4,6-trichlorophenol)) are two bis-phenol compounds with broad-spectrum antimicrobial activity (Joswick *et al.*, 1971; Russell *et al.*, 1991; Schweizer, 2001). Triclosan is a membrane-active agent (Phan and Marquis, 2006) although other studies have shown that it inhibits the growth of *E. coli*, *S. aureus* and other bacterial strains (McMurry *et al.*, 1998). Hexachlorophene on the other hand is reported to inhibit the membrane-bound parts of the electron transport chain (Silvernale *et al.*, 1971; Joswick *et al.*, 1971).

Chloroxylenol (4-chloro-3,5-dimethylpheno:*p*-chloro-*m*-xylenol) is a halophenol used in disinfectants and antiseptic formulations although little is known about its mechanism of antimicrobial action. It is bactericidal except to *P. aeruginosa* and moulds (Russell, 1990a; Bruch, 1996).

1.1.3.4 Cationic biocides

Quaternary ammonium compounds (QACs) and Chlorohexidine (CHX) salts are used as surfactants, antiseptics and disinfectants (El-Falaha *et al.*, 1985a; Russell and Day; 1993; 1996). They cause significant membrane damage to gram-negative, gram-positive bacteria (Hugo, 1991; Denyer, 1995; Russell, 1996) and yeasts (Hiom *et al.*, 1996). The target site is predominantly the

cytoplasmic membrane in mycobacteria (Russell, 1996) or the plasma membrane in yeasts (Fraud *et al.*, 2001). Low concentrations were reported to be mycobacteriostatic. QACs have been found to induce remarkable changes in the fatty acid composition of *P. aeruginosa* (McDonnell and Russell, 1999).

1.1.3.5 Halogen releasing compounds

Chlorine releasing compounds such as hypochlorites are powerful oxidizing agents with bactericidal, fungicidal and sporicidal activity (McDonnell and Russell, 1999). Their primary effects are either or all the progressive oxidation of thiol groups to disulphides, sulphoxides and disulphoxides (Hugo, 1991; Denyer *et al.*, 1993; Russell, 1996). Chlorine also has detrimental effects on DNA synthesis as a result of the formation of chlorinated derivatives of nucleotide bases (Russell and Hugo, 1994; McDonnell and Russell, 1999).

Iodine, in the form of aqueous potassium iodide or alcoholic solution exhibit effective microbicidal activity against bacteria and their spores, yeasts, moulds and viruses (Gottardi, 1985; McDonnell and Russell, 1999). Iodine interacts with thiol groups in enzymes and proteins (Hugo, 1991; Denyer, 1995; Russell, 1996) making it bactericidal, fungicidal and sporicidal (McDonnell and Russell, 1999).

1.2 Silver

1.2.1 Description and properties of silver

Pure silver (Ag) has a brilliant white metallic lustre (Silver, 2003). It occurs in ores including Argentite (Ag₂S) and Horn Silvers (AgCl). Pure silver has the highest electrical and thermal conductivity of all metals. Silver possesses the lowest contact resistance of all metals. There are different forms of silver. Typical nanocrystalline silver contains 90 % of ionic silver whilst the

remaining 10 % of the silver content is in the form of silver particles. It is stable in clean air and water, although it tarnishes upon exposure to ozone, hydrogen sulphide, or air containing sulphur (Silver, 2003). Silver exists in solution as ions (Ag^+), also called ionic silver.

Table 2 shows a summary of the properties of silver:

Table 2: Description of silver (Adapted from Silver, 2003)

Characteristic	Description/ value
Melting point	961.3 °C
Boiling point	2212 °C
Density at 20 °C	10.5 g cm ⁻³
Atomic number	47
Atomic weight	107.868 gmol ⁻¹
Electronic configuration	[Kr] 4d ¹⁰ 5s ¹
Covalent radius	1.34 Å
Valency	+1 or +2

1.2.2 History of silver use

The use of silver and silver compounds as antimicrobial agents has been known since ancient times and is well documented (Russell and Hugo, 1994; Russell *et al.*, 1997; Dunn and Edward-Jones., 2004). As cited by Silver (2003), Carl Crede in 1844 pioneered the installation of dilute silver nitrate in the eye of neonates to prevent ocular infections. As cited in Silver (2003), Von Behring then followed in 1887 and showed that 0.25 % and 0.01 % of silver nitrate solutions were effective against typhoid and anthrax. Halstead (1900) treated non-healing wounds with hammered foils and colloidal silver. By the late 1920s, colloidal silver was accepted by the Food

and Drug Agency in the United States for wound treatment (Silver, 2003). However, the development of antibiotics led to a decline in the research into silver and silver compounds until mid 1960s when Moyer and Monafó started using 0.5 % silver nitrates solutions on burn wounds. Then came 1968, when Fox introduced 1 % silver sulfadiazine cream which became one of the leading topical agents used in burn wounds (Yin *et al.*, 1999).

1.2.3 Silver and its application as antimicrobial agent

Several products have incorporated silver for use as topical antimicrobial agent (Grier, 2000; Atiyeh *et al.*, 2007). These products include silver nitrate (AgNO_3), silver sulfadiazine (SSD), silver sulfadiazine/chlorhexidine, silver proteins, etc. 0.5 % silver nitrate has been the standard and most popular silver salt solution used for topical burn and wound therapy (Ovington 2005; Atiyeh *et al.*, 2007). Silver sulfadiazine consist of silver complexed to propylene glycol, stearyl alcohol and isopropyl myristate. Silver sulfadiazine binds to cell components such as DNA. Most silver products on the wound care market utilize metallic silver as the reservoir for ionic silver - the only state of silver that has antimicrobial effect. When the metallic form is used as the reservoir, the transition occurs through oxidation to form the ionic species.

One area where silver is commonly used as proven antimicrobial agent is wound management. Silver is effective against microbes at concentrations of parts per billion (Brett, 2006). Dressings are currently widely available that consist of lipid colloid contact layers containing silver sulfadiazine creams. Another area where silver has proven to be an effective antimicrobial agent is nanocrystalline silver dressing (Strohal *et al.*, 2004). Silver dressings have been found to be an effective barrier to MRSA cross-contamination. Hence they provide a localised anti-MRSA action. These dressings also demonstrate sustained antibacterial action and were very effective in preventing the spread of antimicrobial resistant microorganisms. Jones *et al.*, (2004) investigated

the wound management of hydrofiber dressings containing ionic silver. Their results showed that the hydrofiber was effective against MRSA, Vancomycin resistant *enterococci*, anaerobic organisms and yeasts. Hydroxyapatites (HA) coatings and films are potential carriers of silver ions and could potentially form strong bonds with living bone (Shirkhanzadeh, 1995). HA film coatings and films containing silver ions slowly release strongly inhibitory and bactericidal ions with broad spectrum of activity at the site of the bone-implant interface. Irrespective of the source of silver, whether released from solutions, ointments, creams or nanocrystalline silver provides an antimicrobial action in aqueous fluids that is highly toxic for micro-organisms but has relatively low toxicity for human tissue cells.

1.2.4 Mode of antimicrobial activity of silver

Silver works as an antimicrobial agent through a number of pathways. The ionic species carries a strong positive charge so it has high affinity for negatively charged groups of biological molecules (Poon and Burd, 2004). These molecules include groups such as sulfhydryl, carboxyl, phosphates and other groups commonly found on macromolecular structures distributed throughout microbial cells (Hugo, 1991; Li *et al.*, 1997b; Yin *et al.*, 1999). The binding reaction alters the molecular structure of the macromolecule, rendering it worthless to the cell. This attack effectively inactivates many functions such as cell wall synthesis, membrane transport, nucleic acids such as RNA and DNA synthesis and translation, and protein folding and function (Russell and Hugo, 1994; Sondi and Salopek-Sondi 2004). Because silver affects so many different functions of microbial cells, it is non-selective, resulting in antimicrobial activity against a broad spectrum of microorganisms including bacteria, fungi, and yeasts. Silver is also favoured because it is extremely active in small quantities against microorganisms. With certain bacteria, as little as 0.1 parts per billion may have an antimicrobial effect (Kumar and Münstedt, 2004).

However, using silver for bio-burden control in wounds is not problem-free. It also has a reputation for staining tissues and equipment. These properties are stability issues that are exacerbated in the presence of moisture. Silver is effective against gram-negative bacteria, gram-positive bacteria and mycobacteria.

1.3 Bacteria

1.3.1 Gram-negative bacteria

1.3.1.1 Surface structures

Gram-negative bacteria consist of a cell membrane where oxidative phosphorylation occurs. Outside the cell membrane is the cell wall which is composed of a thin, inner layer of peptidoglycan that functions to prevent osmotic lyses. Gram-negative bacteria have an additional outer membrane of lipopolysaccharides (LPS), protein and lipoprotein (Madigan *et al.*, 2000). The space between the outer membrane and the inner membrane is called the periplasmic space (Figure 2).

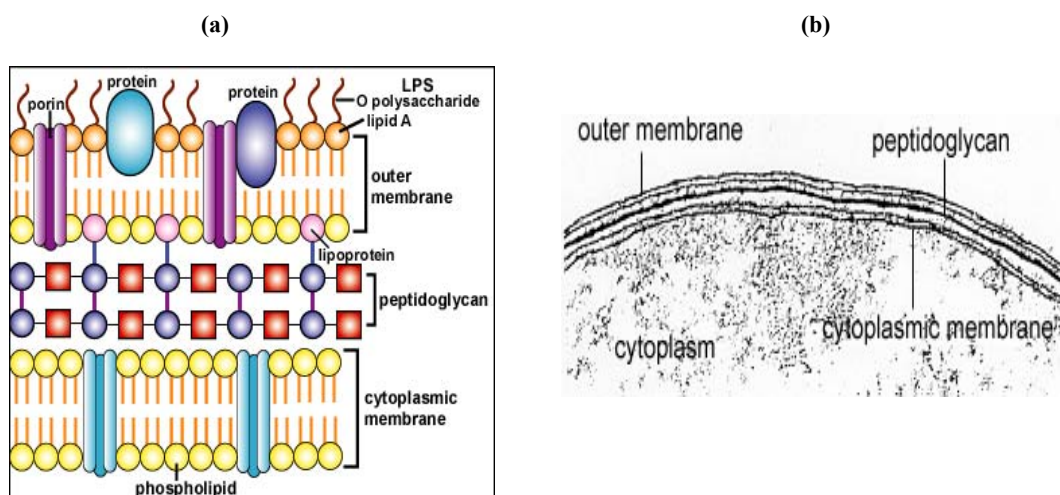


Figure 2: (a) Diagram of a gram-negative cell wall. (b) Electron Micrograph of a Gram-Negative cell wall (<http://student.cbcmd.edu/bio141>)

The outer membrane also contains a number of proteins that differ with the strain and species of the bacterium. Examples of gram-negative bacteria include *E. coli*, *P. aeruginosa*, *Salmonella* species, *Neisseria gonorrhoea* and *Neisseria meningitidis* (Madigan *et al* 2000). Phospholipids are located mainly in the inner layer of the outer membrane and lipoproteins connect the outer membrane to the peptidoglycan. The lipopolysaccharides, located in the outer layer of the outer membrane, consist of a lipid portion called lipid A, embedded in the membrane and a polysaccharide portion extending outward from the bacterial surface (Madigan *et al.*, 2000). Porins are a class of proteins that form water-filled channels across cell membranes (Madigan *et al.*, 2000) and are responsible for the selectivity and permeability of this structure.

(a) Flagella motility

Some bacterial species are mobile and possess locomotory organelles called flagella that project from the cell body (Madigan *et al.*, 2000). It is helical in shape with a sharp bend just outside the outer membrane that allows the helix to point directly away from the cell. The flagellum is driven by a rotary engine made up of proteins at the flagellum's anchor point on the inner cell membrane. The engine is powered by a proton motive force (the flow of hydrogen ions) across the bacterial cell (Rodgers *et al.*, 1990). They move the cell by rotating with a propeller-like action. Binding proteins in the periplasmic space or cell membrane bind food sources (such as sugars and amino acids) causing methylation of other cell membrane proteins which in turn affect the movement of the cell by flagella (Rodgers *et al.*, 1990).

(b) Pili

Pili are hair-like projections of the cell. Some are involved in sexual conjugation and others allow adhesion to host epithelial surfaces in infection (Madigan *et al.*, 2000).

(c) Capsules

These are structures surrounding the outside of the cell envelope. When more defined, they are referred to as a capsule when less defined as a slime layer or glycocalyx (Mittelman, 1985). They usually consist of polysaccharide; however, in certain *Bacillus* species they are composed of a polypeptide (polyglutamic acid). They are not essential to cell viability and some strains within a species will produce a capsule, whilst others do not. Capsules of pathogenic bacteria inhibit ingestion and killing by phagocytes. Capsules are often lost during *in vitro* culture.

(d) Lipoteichoic acids

Lipoteichoic acids are polymers of amphiphilic glycerophosphates with the lipophilic glycolipid and anchored in the cytoplasmic membrane. They are antigenic, cytotoxic and adhesions (Rodgers *et al.*, 1990; Madigan *et al.*, 2000).

(e) Lipopolysaccharides

One of the major components of the outer membrane of gram-negative bacteria is lipopolysaccharide (also called endotoxin). It is a complex molecule consisting of a lipid and a polysaccharide core (carbohydrates) joined by covalent bonds (Kaiser, 2001).

1.3.1.2 *Plasma membrane*

It is the membrane that surrounds the bacterial cell. It is composed primarily of proteins and phospholipids. It is permeable to specific molecules allowing nutrients and other essential elements to enter the cell and waste materials to leave the cell. Small molecules, such as oxygen, carbon dioxide, and water, are able to pass freely across the membrane, but the passage of larger molecules, such as amino acids and sugars, is carefully regulated (Madigan *et al.*, 2000).

1.3.2 Gram-positive bacteria

Gram-positive bacterium cell (Figure 3) consists of cell wall which is composed of a dense layer of peptidoglycan and teichoic acids (Rodgers *et al.*, 1990).

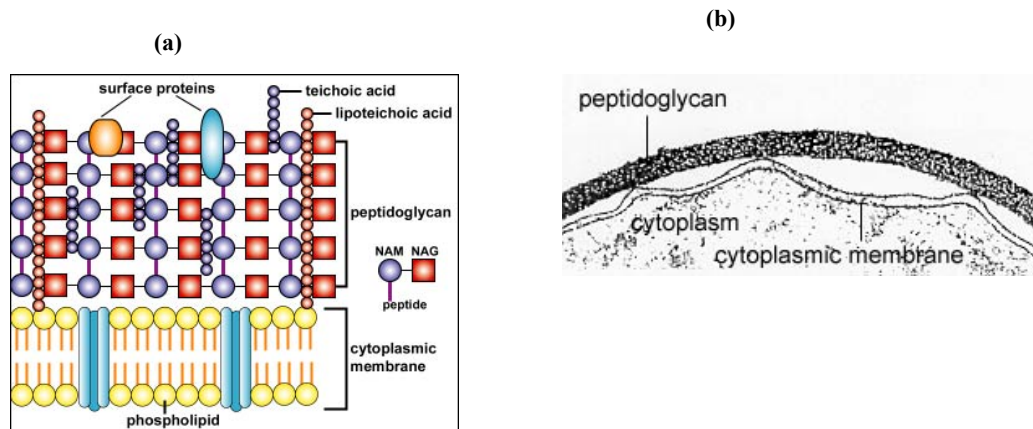


Figure 3: (a); Structure of a gram-positive bacterium and (b); Electron micrograph of a gram-positive cell wall (<http://student.cbcemd.edu/bio141>)

The cell structures consist of a numerous interconnecting layers of peptidoglycan (Figure 3). Chemically, 60 to 90% of the gram-positive cell wall is peptidoglycan. Interwoven in the cell wall of gram-positive are teichoic acids (Madigan *et al.*, 2000). Teichoic acids extend through and beyond the rest of the cell wall and are composed as polymers of glycerol, phosphates, and the sugar alcohol ribitol. Some teichoic acids have lipids attached and are called lipoteichoic acids. The outer surface of the peptidoglycan is studded with proteins that differ with the strain and bacterium species (Madigan *et al.*, 2000). Gram-positive bacteria can produce endospores when starved (Cadow, 1989; Madigan *et al.*, 2000). The spore is resistant to adverse conditions (including high temperatures and organic solvents). The spore cytoplasm is dehydrated and contains calcium dipicolinate (dipicolinic acid) which is involved in the heat resistance of the spore.

1.3.3 Mycobacterium cell

The mycobacterial cell wall composes of a thin, inner layer of peptidoglycan and large amount of glycolipids (Madigan *et al.*, 2000) such as mycolic acid, arabinogalactan-lipid complex, and lipoarabinomannan (Figure 4).

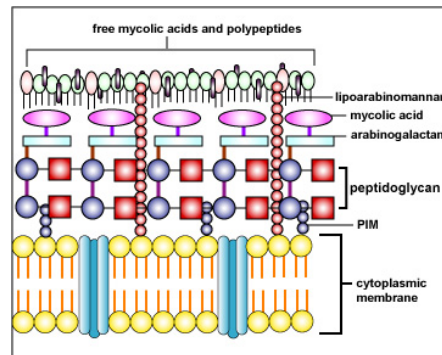


Figure 4: Structure of mycobacterial cell wall. (<http://student.ccbcmd.edu/bio141>)

The peptidoglycan layer is linked to arabinogalactan (D-arabinose and D-galactose) that is then linked to high-molecular weight mycolic acids (Madigan *et al.*, 2001). The arabinogalactan/mycolic acid layer is overlaid with a layer of polypeptides and mycolic acids consisting of free lipids, glycolipids, and phosphatidylinositol mannosides. Common acid-fast bacteria include *Mycobacterium tuberculosis*, *Mycobacterium leprae*, and *Mycobacterium avium-intracellulare* complex. The arabinogalactan/mycolic acid layer is overlaid with a layer of polypeptides and mycolic acids consisting of free lipids, glycolipids, and peptidoglycolipids (Rodgers *et al.*, 1990). Other glycolipids include lipoarabinomannan and phosphatidylinositol mannosides (PIM).

1.3.4 Bacterial growth

In most bacteria, growth involves increase in cell mass and number of ribosomes, duplication of the bacterial chromosome, synthesis of new cell wall and plasma membrane, partitioning of the two chromosomes, septum formation, and cell division (Rodgers *et al.*, 1990).

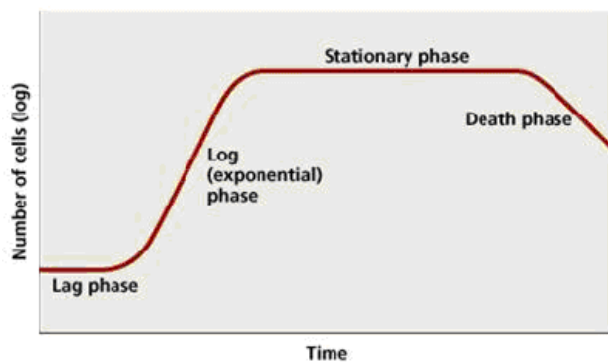


Figure 5: Hypothetical growth curve of bacteria (Madigan, 2000)

The growth of bacteria in biofilms begins with an electrostatic (physical) attraction onto a surface, resulting in a reversible adsorption (Mittelman, 1985). Cells initially adjust to the new medium (lag phase) (Figure 5) until they can start dividing regularly by the process of binary fission (exponential phase). When their growth becomes limited, the cells stop dividing (stationary phase), until eventually they show loss of viability (death phase). Growth is expressed as change in the number viable cells with respect to time (Madigan *et al.*, 2000). The length of the lag phase depends on a wide variety of factors including the size of the inoculum; time necessary to recover from physical damage or shock in the transfer; time required for synthesis of essential coenzymes or division factors; and time required for synthesis of new enzymes that are necessary to metabolize the substrates present in the medium (Rodgers *et al.*, 1990). In the

exponential phase, cells divide at a constant rate depending upon the composition of the growth medium and the conditions of incubation. Population growth is limited by: exhaustion of available nutrients, accumulation of inhibitory metabolites as well as oxygen/pH (Rodgers *et al.*, 1990; Madigan *et al.*, 2000). This results in the stationary phase where the cells do not divide and death phase where the viable cells decrease with time in an exponential order (Madigan *et al.*, 2000).

1.4 Microbial resistance

1.4.1 Microbial resistance to antimicrobial agents

Resistance has been defined as the temporary or permanent ability of an organism and its progeny to remain viable and/or multiply under conditions that destroy or inhibit other members of the strain (Levy, 1998; Cloete, 2003). Bacteria may be defined as resistant when they are not susceptible to a concentration of antibacterial agents used in practice (Gupta and Silver, 1998). For an antimicrobial agent to be effective, it must attain sufficiently high concentration at the target site in order to exert its antimicrobial activity (Cloete, 2003).

Table 3: Intrinsic resistance in bacteria to biocides (Adopted from McDonnell and Russell 1999)

Type of resistance	Example(s)	Mechanism of resistance
Impermeability Gram-negative bacteria	Quaternary ammonium compounds (QACs), triclosan, diamines	Barrier presented by outer membrane may prevent uptake of biocides; glycocalix may also be involved
Mycobacteria		Prevention of biocide entry into cell due to waxy cell wall
Bacteria spores	Chlorhexidine, QACs, formaldehyde	Prevention of biocide entry into spores by spore coat(s) and cortex
Gram-positive bacteria	Chlorhexidine, QACs, phenolics Chlorhexidine	Reduced diffusion of biocide by glycocalyx or mucoexopolysaccharide

Many microbes have both intrinsic (Table 3) and acquired resistance to antimicrobials because of their efflux pumps (Gupta *et al.*, 1999). The mechanism of antimicrobial resistance to antimicrobial may include (1): target site alteration, (2): reduction of cellular diffusion, (3): inactivation of the antimicrobial agent, and (4): active efflux of the antimicrobial agent (Table 4). Acquired resistance comes from the acquisition of plasmids (Table 4) from other microbes or through mutations whereas intrinsic resistance occurs independently of these (Russell, 1993; Russell *et al.*, 1993; Russell and Day, 1993, 1996). Acquired efflux pumps called multi-drug resistant pumps have been found in bacteria. Intrinsic resistance implies that the efflux pumps have another function in the cell and that the pumps coincidentally cause the efflux of antimicrobials (Li *et al.*, 1995; Silver, 1996; Li *et al.*, 1997b).

Table 4: Mechanisms of plasmid-encoded resistance to biocides. (Adapted from McDonnell and Russell, 1999)

Biocide	Example(s)	Mechanisms
Antiseptics or disinfectants	Chlorhexidine salts	(i) Chromosomally mediated inactivation (ii) Efflux (iii) Decreased uptake
	QACs	(i) Efflux (ii) Decreased uptake
	Formaldehyde	(i) Inactivation by Formaldehyde dehydrogenase (ii) Cell surface alterations
	Acridines Diamidines Crystal violeta	Efflux: some <i>S. aureus</i> , some <i>S. epidermidis</i> Efflux: some <i>S. aureus</i> , some <i>S. epidermidis</i> Efflux: some <i>S. aureus</i> , some <i>S. epidermidis</i>
Other biocides	Mercurials Ethidium bromide	Inactivation (reductases, lyases) Efflux: some <i>S. aureus</i> , some <i>S. epidermidis</i>

1.4.2 Microbial resistance to silver

Silver resistance has been reported for both gram- negative and gram- positive bacteria (Haefeli *et al.*, 1984; Nies, 1999). The first resistance was reported on *Pseudomonas stutzeri* isolated from a silver mine (Haefeli *et al.*, 1984; Starodub and Silver, 1990). Silver resistance in *Escherichia coli* is thought to be controlled by a chromosomally encoded efflux pump (Li *et al.*, 1997a, 1997b) that may involve the protein encoded by gene *ybdE* (Gupta *et al.*, 1999; Franke *et al.*, 2001). Silver resistance in *Salmonella* species have been reported to be mediated by genes that encode a periplasmic silver-binding protein and two parallel efflux pumps, a P-type ATPase and a cation/proton anti-porter (Silver, 1996; Silver *et al.*, 1989; Gupta *et al.*, 1999). Plasmid mediated resistance have been identified (Silver 2003). Plasmid pMG101, is 180 KB in size, it was isolated from *Salmonella enterica* and conferred resistance to silver. A cloned and sequenced region of the plasmid responsible for silver resistance contained a gene cluster of nine genes; seven named (silP, ORF105, silAB, ORF96, silC silSR, silE) the other two classified as open reading frames. silE is a gene that encodes for a silver periplasmic binding protein, which is only synthesized in the presence of silver (Gupta *et al.*, 1996; Silver 2003). This provides the first line of resistance against silver ion attack (Silver 2003). However, the formation of a protein surrounding the electron-light region of *E. coli* and *S. aureus*, may only help slow down than preventing the biocidal activity of the silver ions (Franke *et al.*, 2001). A silver efflux pump coded by SilCBA silP forms the second line of defence (Silver, 2003). It codes two parallel membrane silver ion efflux pumps that are responsible for the removal of silver from the cell cytoplasm to the outside the cell. The defence mechanism acts to block biocides by not allowing silver ions to reach their targets within the cell membrane. Recently, some molecular removal of silver resistance was done. An efflux ATPase CopB from *Enterococcus hirae* was found to transport Ag⁺ and Cu⁺ (Solioz and Odermatt, 1995). Silver resistance in *E. coli* has also been

identified (Gupta *et al.*, 1998, Gupta *et al.*, 1999). In gram-negative bacteria silver resistance may be based on RND-driven trans-envelope efflux. In gram-positive bacteria however, resistance to silver is based on the efflux by P-type ATPases and complexation by intracellular compounds (Gupta *et al.*, 1996; Silver, 2003). Biosorption of silver by living and dead fungal biomass has been investigated and have been reported to bind silver ions with high affinity (Fourest *et al.*, 1994).

1.5 Zeolites

1.5.1 Historical background

The discovery of zeolites dates back to the 18th century (Mumpton, 1978). They were first discovered in 1756 by a Swedish mineralogist, A.F. Cronstedt, who named them from two Greek words for ‘boiling stone’ (‘zein’ – boiling and ‘lithos’ – stone) (Breck, 1974; Szostak, 1989; Thompson, 1998). Following their discovery zeolites were found to be characterised by the following properties (Szostak, 1989; Van Bekkum *et al.*, 2001):

- catalytic properties;
- high hydration propensity;
- stable crystal structure when dehydrated;
- low density and high void volume when dehydrated;
- cation exchange and sorption properties.

This resulted in a number of investigations aimed at validating such properties. As cited by Van Bekkum *et al.*, (2001), Damour (1840) showed that zeolites could be reversibly dehydrated without change in their transparency or crystal morphology. As cited in Van Bekkum *et al.* (2001) Eichhorn (1858) reported for the first time the reversibility of ion exchange of zeolite minerals. Firedel and Bull (1896) cited by Szostak (1989) proposed that the structure of

dehydrated zeolites consists of open porous frameworks. As cited in Breck, (1974) the first laboratory synthesis of a zeolite is attributed to Deville, who in 1862 synthesized levynite by heating potassium silicate and sodium aluminate in a glass ampoule. The hexagonal crystals were obtained from the gel composition:



Following the successful synthesis of levynite more discovery and synthesis were made. Although the synthesis of more zeolites was reported the absence of reliable characterisation techniques made it impossible to verify that zeolites were indeed fabricated. X-ray diffraction was used in the mid-1930s for the purpose of identification of mineral species. Hence the first precise confirmation of zeolite synthesis can be traced to 1948 when Barrer (1982) reported the synthesis of an analogue of mordenite. This led to the era of adsorption and synthesis of synthetic zeolites. Within the same period Milton and Breck led the Union Carbide project and synthesised zeolite A, X and Y among others. As a result zeolite A was introduced into detergents as a replacement for phosphates and zeolite X was used as a cracking catalyst at commercial scale. Since then many new zeolite framework types have been attained thanks to the important effort of oil companies. The use of quaternary ammonium salts resulted in an increase in Si/Al ratio and the discovery of ZSM-5. Flanigen *et al.*, (1978) reported the synthesis of silicalite-1 which is the all-silica counterpart of ZSM-5.

1.5.2 Introduction to molecular sieves

As interest widened literature began to include materials which are not classical aluminosilicates but are related to them. Microporous aluminophosphates were discovered in the 1980s. The term “molecular sieves” was introduced to describe those materials that exhibit selective adsorption properties. Thus zeolites, silicalites, and aluminophosphates were classified as molecular sieves.

Nevertheless, poor thermal and hydrothermal stability of the metal-substituted analogues has hindered their commercial applications (Szostak, 1989). In recent years zeolites with extra large pore volumes have been synthesised (Nagy *et al.*, 1998). Toxicological studies on natural zeolites have shown that zeolites are inert, non-toxic and safe to use medicinally. Zeolites can be natural or synthetic with more than 150 zeolite types synthesized and 40 naturally occurring zeolites known (Szostak, 1989). Natural zeolites are formed from volcanic ash whilst synthetic zeolites are produced mainly in the laboratory.

1.5.3 Classification of zeolites

There are three classification schemes used to classify zeolite structures. Two of these are based upon specifically defined aspects of crystal structure, and the third has a more historical basis, placing zeolites with similar properties such as morphology into the same group (Barrer, 1982; Szostak, 1989). The first structural classification of zeolites is based on the framework topology, with distinct framework receiving a three-letter code (Ertl *et al.*, 1999). The second structural method for the classification of zeolites is based on a concept termed “secondary building units” (SBU). The primary building unit for zeolites is the tetrahedron and the SBUs are the geometric arrangements of tetrahedra (Breck 1974). In most cases the SBUs tend to control the morphology of the zeolites. The third broad classification scheme is similar to the SBU classification of Breck (1974), except that it includes some historical context of how the zeolites were discovered and named. This scheme uses a combination of zeolite group names which have specific SBUs and is widely used by geologists. This is the classification scheme used by Ocelli and Kessler (1997).

1.5.4 Nomenclature of zeolites

There is no systematic nomenclature developed for molecular sieve materials. Each confirmed zeolite framework type is assigned a three-letter code of three capital letters by the Structure Commission of the International Zeolite Association (IZA). Illustrative codes include FAU for the Faujasite framework (e.g. zeolite X and zeolite Y), LTA for Linde zeolite A, MOR for mordenite topology, MFI for the ZSM-5 and silicalite topologies and AlPO_4^{5-} for the AFI topology. Details of these framework types are published in the *Atlas of Zeolite Framework Types*, formerly entitled the *Atlas of Zeolite Structure Types*. All framework types, including updates between editions of the *Atlas*, are also published on the internet at <http://www.iza-structure.org/databases/>. A three-letter code preceded by a hyphen has been assigned in a few cases to zeolite-like framework types that are not fully 4-connected (i.e., interrupted frameworks such as that of the gallophosphate cloverite, whose topology has the code -CLO). In subsequent discussion, the three-letter code will be referred to as the IZA code. For this research, Linde zeolite A, Faujasite type X, High aluminium Phillipsite and Analcime have been studied and will be assigned the letters LTA, LTX, PHI and ANA.

1.5.5 Structures of zeolites

Zeolites are crystalline hydrated aluminosilicates whose framework structure consists of cavities or pores that are occupied by cations or water molecules. Both the cation and the water molecule have considerable freedom of movements and this permits ion exchange and reversible dehydration (Ocelli and Kessler, 1997). The zeolite structure is made up of a central atom commonly silicon or aluminium surrounded by four oxygen atoms (Figure 6a).

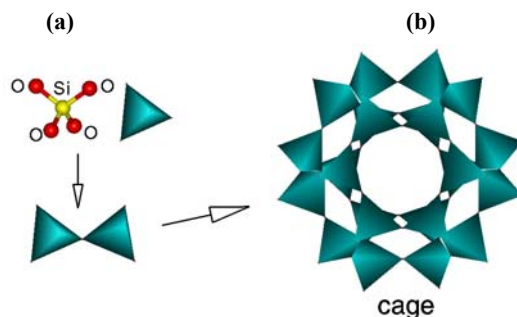


Figure 6: Tetrahedra framework structure of zeolites (l www.bza.org/zeolites.html)

The tetrahedral atoms, called T-atoms are stacked in beautiful regular three-dimensional arrays such that channels form (Figure 6b). The zeolite frameworks are typically anionic which are counterbalanced by the positive charges of cations resulting in a high cation exchange capability (Occelli and Kessler, 1997; Ertl *et al.*, 1999). Exchangeable cations include lithium, cadmium, lead, zinc, copper, ammonia, silver and protons. The zeolite channels or pores are microscopically small, and have molecular size dimensions in such a way that they are normally termed *molecular sieves* (Szostak, 1989). There are hundreds of different possible three-dimensional lattice structures. The large majority of zeolites are constructed from SBUs.

1.5.5.1 Channels and pore openings

Zeolite structures are often described according to the size of pore openings and the dimensionality of their channel system (Szostak, 1989). These pore openings are characterised by the size of the ring that defines the pore, usually designated as n-ring, where n is the number of T (= Al or Si tetrahedra) atoms in a ring. Different pore openings are assigned for different ring sizes. Hence an 8-ring is considered a small ring opening, a 10-ring opening is considered a medium ring opening and a 12-ring is considered a large ring opening (Breck, 1974; Szostak, 1989). The size and shape of the pore opening depends on (Szostak, 1989):

- the configuration of the T and O atoms relative to each other
- the Si/Al ratio
- the size of the cation
- the location of the cation
- temperature

The zeolite structure can also be examined in terms of one, two or three-dimensional tubes or channels as shown in Table 5:

Table 5: Various zeolites with their channel systems (Szostak, 1989)

Channel system	Zeolite type
One-dimensional	Analcime
Two-dimensional	Mordenite, Phillipsite
Three dimensional	Paulingite, ZSM-5, ZSM-11

Analcime consists of a system of non-intersecting one-dimensional channels running parallel to the [111] axis. An example of a two-dimensional intersecting channel system is mordenite, with 12 and 8 ring channels parallel to [100] axis. In Paulingite, there are two interpenetrating systems of three-dimensionally intersecting channels (Szostak, 1989; Ocelli and Kessler, 1997).

1.5.5.2 Secondary Building Units

The individual tetrahedra TO_4 units (where T = Al or Si) represent primary building units. Secondary building units (SBUs) consist of selected geometric groupings of those tetrahedra. Such building units (Ocelli and Kessler, 1997; Szostak, 1989) can be used to describe all the

known zeolite structures (Figure 7). There are nine such building units. These include 4, 5, 6 and 8-member single rings, 4-4, 6-6, and 8-8-member double rings, and 4-1, 5-1, and 4-4-1 branched rings. Most zeolite frameworks are derived from several different SBUs. Describing structural similarities and differences requires a building unit that takes into account the arrangement of these SBUs in space. There is more than one possibility of joining for example a 4-ring unit hence linking of each ring results in what is called extended chain building unit (Szostak, 1989). An alternative method of describing extended zeolite structures is to visualise zeolites in two-dimensional sheet units. The framework structure is generated by attaching layers to form a complex structure (Figure 7).

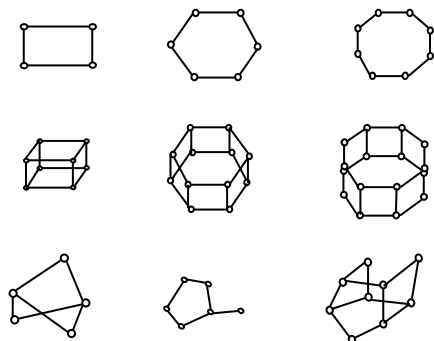


Figure 7: Secondary building units recognized in zeolite frameworks. Single 4, 6, and 8 rings (S4R, S6R and S8R), double rings (4DR, 6DR and 8DR) and complex rings (4-1, 5-1 and 4-4-1) (Adapted from

These planar projections provide information on the relative orientation of the 8, 10 and 12 ring pore openings of the different structures. They also help in understanding the area of crystal purity (Szostak, 1989; Occelli and Kessler, 1997).

1.5.6 Diffusion in zeolites

Diffusion can be defined as a phenomenon of random motion causing a system to decay towards uniform conditions (Karger and Ruthven, 1992). Diffusion is caused by the thermal motion and subsequent collision of molecules in a closed system. Two types of diffusion can be

distinguished: transport diffusion, which is initiated by a concentration gradient, and self-diffusion, which takes place in a system that is in equilibrium (Szostak, 1989, Karger and Ruthven, 1992). Diffusion of molecules through the pores of zeolites is different from diffusion in fluids or large porous solids. Since the molecules have to move through channels of molecular dimensions there is a constant interaction between the zeolite framework and the diffusion molecules (Szostak, 1989). Hence the molecular motion is highly influenced by both the size and shape of the channels instead of temperature and concentration only (Karger and Ruthven, 1992). The diffusivity in this region depends on (Szostak, 1989):

- the pore diameter
- the structure of the pore wall
- the interaction between the surface atoms and the diffusion molecules
- the shape of the diffusion molecules and
- the way they are connected.

Diffusion in zeolites can be classified in a number of different regimes depending on the pore diameter. For large pore diameters of the order of $1\mu\text{m}$ or greater, usually called macropores, collisions between the molecules occur much more frequently than the collisions with the walls (Thompson, 1998). As the size of the pores decreases, the number of collisions with walls increases until it finally becomes smaller than the mean free path (the average distance travelled by a molecule between collisions). At this point Knudsen diffusion takes over and the mobility of the molecules start to depend on the dimensions of the pore (Szostak, 1989; Thompson, 1998). At smaller pore sizes in the range of 20 \AA the interaction between the molecules and the walls is constant. Diffusion in the micropores of zeolites takes place in this region and is called configurational diffusion (Thompson, 1998).

1.5.7 Zeolite chemistry

The empirical formula of a zeolite is given by (Breck, 1974; Szostak, 1989):



Where:

x, y = stoichiometric coefficients for Al^{3+} and Si^{4+} in tetrahedral sites, respectively

M = exchangeable cations (generally a Group I or II ion)

n = valency of exchangeable cations.

Other metals, non-metals and organic cations may also balance the negative charge created by the presence of aluminium (Al^{3+}) ions in the silicate structure. Recent advances in structural zeolite chemistry have been mainly in the areas of highly siliceous zeolites, aluminophosphates and related materials (Nagy *et al.*, 1998). Zeolite chemistry is thus no longer confined to aluminosilicates. Taking into account isomorphous substitution as well as the possible presence of hydroxyl bridges and ligands, the general formula for a four-connected network of a zeolite-like molecular sieve was proposed (Nagy *et al.*, 1998). Zeolites with low Si/Al ratios have strongly polar anionic frameworks (Ocelli and Kessler, 1997). The exchangeable cations create strong local electrostatic fields and interact with highly polar molecules such as water. The cation-exchange behaviour of zeolites depends on: the nature, size and charge of the cation species, temperature, the concentration of the cationic species in the solution, the anion associated with the cation in solution, the type of solvent and the structural characteristics of the particular zeolite (Amphlett, 1964). Two theories have been proposed for the mechanism of zeolite synthesis. These are solid-solid transformation and solution crystallisation mechanism. In

a solid-solid transformation mechanism, crystallization of the zeolite occurs directly from the amorphous gel to the crystalline phase (Zhdanov, 1971). In the solution crystallization mechanism, nuclei form and grow in the liquid phase (Occelli and Kessler, 1997). The latter proposes that equilibrium exists between the solid-gel phase and the solution, and that nucleation occurs in the solution. The gel dissolves continuously, and the dissolved species are transported to the nuclei crystals in the solution. In addition to zeolite formation via either of the two transformations, there is evidence to indicate that both types of transformation can sometimes occur simultaneously. In some cases zeolites can also be crystallized from a single-solution system containing no secondary solid-gel phase (Ueda and Koizumi, 1979; Brinker and Scherer, 1990).

1.6 Structures studied in this work

1.6.1 Zeolite X

Zeolite X (Figure 8) is a synthetic counterpart of the naturally occurring mineral Faujasite (Breck, 1974; Szostak, 1989; Coker *et al.*, 1995). It has one of the largest cavities and cavity entrances of any known zeolites (Szostak, 1989). The channel structure is 3-dimensional with equidimensional channels intersecting in a perpendicular order with free aperture of 7.4 Å. (Coutinho and Balkus, 2002). There are also smaller cavities called sodalite cages which are connected to the supercages by rings of four and six tetrahedra (Szostak, 1989; Coutinho and Balkus, 2002; Novembre *et al.*, 2004).

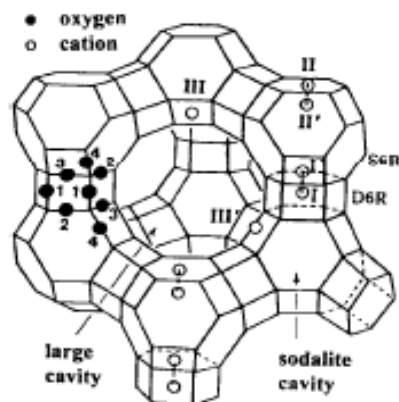


Figure 8: Framework structure of zeolite X showing location of exchangeable sites (Yeom and Kim, 1997).

Exchangeable cations, which balance the negative charge of the aluminosilicate framework, are found within the zeolite cavities. They are usually found (Yeom and Kim, 1997) at the following sites shown in Figure 8: site I at the centre of a D6R, site I' in the sodalite cavity on the opposite side of one of the D6R's 6-rings from site I, II' inside the sodalite cavity near a single 6-ring entrance to the supercage, II in the supercage adjacent to a S6R, III in the supercage opposite a 4-ring between two 12-rings, and III' off III (off the 2-fold axis) (Szostak, 1989). The chemical composition can vary according to the silicon and aluminum content from a Si/Al ratio = 1.0-1.5. Zeolite X has a wide range of industrial application primarily due to the excellent stability of the crystal structure and a large available pore volume and surface area (Kwakye-Awuah *et al.*, 2008a).

1.6.2 Zeolite A

Zeolite A exhibits the LTA (Linde Type A) structure (Figure 9). It has a 3-dimensional pore structure with pores running perpendicular to each other in the x, y, and z planes, and is made of secondary building units 4, 6, 8, and 4-4 (Szostak, 1989).

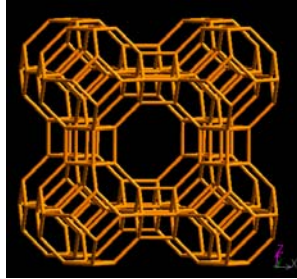


Figure 9: Framework structure of zeolite A (LTA) (http://izasc.ethz.ch/fmi/xsl/IZA-SC/ftc_fw.xsl?-db=Atlas_main&-lay=fw&-max=25&STC=LTA&-find)

The pore diameter is defined by an eight member oxygen ring and is small at 4.2\AA leading to a larger cavity of minimum free diameter 11.4\AA (Coker *et al.* 1995; Grizzetti and Artioli, 2002). The cavity is surrounded by eight sodalite cages (truncated octahedra) connected by their square faces in a cubic structure. The unit cell is cubic ($a = 24.61\text{\AA}$) with Fm-3c symmetry. Zeolite A has a void volume fraction of 0.47, with a Si/Al ratio of 1.0 (Szostak, 1989). It is stable at temperatures up to $700\text{ }^{\circ}\text{C}$ at which it thermally decomposes (Pillay and Peisach, 1990).

1.6.3 High Aluminium Phillipsite

Phillipsite is a monoclinic zeolite with pseudo-orthorhombic framework. It has two-dimensional channel system containing 8-membered ring with a free aperture of about 3.8 \AA (Franco *et al.*, 1990). The framework structure of Phillipsite is shown in Figure 10:

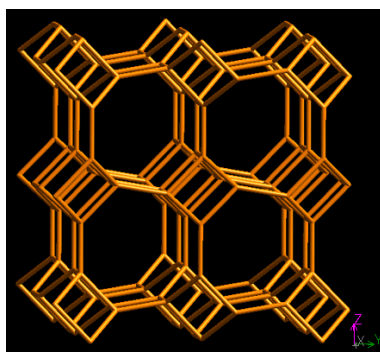


Figure 10: Framework structure of Phillipsite (PHI) (http://izasc.ethz.ch/fmi/xsl/IZA-SC/ftc_fw.xsl?-db=Atlas_main&-lay=fw&-max=25&STC=PHI&-find)

The main channel of Phillipsite is an 8-membered ring with free aperture of about 3.8 Angstrom.

1.6.4 Analcime

Generally analcime ($\text{NaAlSi}_2\text{O}_6 \cdot \text{H}_2\text{O}$) is a mineral belonging to the tectosilicate group with a zeolitic structure of a complex aluminosilicate framework (Kohoutková *et al.*, 2007; Balandis and Traidaraite, 2007). However, new examinations have shown that depending on the nature of conditions and type of impurities present natural Analcime may belong to the cubic, tetragonal, orthorhombic, monoclinic or triclinic crystallographic systems (Figure 11).

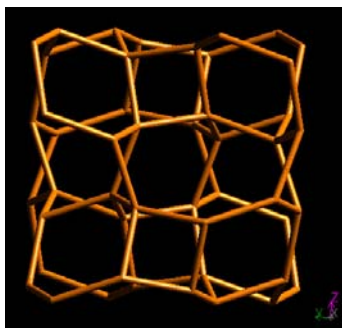


Figure 11: Framework structure of Analcime (ANA) (http://izasc.ethz.ch/fmi/xsl/IZA-SC/ftc_fw.xsl?-db=Atlas_main&-lay=fw&-max=25&STC=ANA&-find)

The framework is based on corner sharing (Al, Si)O₄ tetrahedra, arranged in four-fold, six-fold and eight-fold rings. The sixfold rings are arranged axially, forming structural channels parallel to <111> axis (Szostak, 1989). Such channel arrangements shows many possibilities for structural modification, including framework distortion, channel collapse, and ionic mobility. It is well known that Analcime is a potential precursor for the new generation of dental porcelains having high fracture resistance (Gruciani and Gualtieri, 1999; Kohoutková *et al.*, 2007). Previous work from Ueda and Koizumi (1979) showed that analcime can form from a clear aqueous solution (Gruciani and Gualtieri, 1999). In the laboratory analcime is easily synthesized under hydrothermal conditions (Giampaolo and Lombardi, 1994; Line *et al.*, 1995).

1.7 Synthesis of zeolites

1.7.1 Introduction

The synthesis of zeolites is carried out under hydrothermal conditions (Barrer, 1982; Szostak, 1989). An aluminate and silicate suspensions are mixed together in an alkaline medium to form a milky gel or in some instances, clear solution. Various cations and anions can be added to the synthesis mixture. Synthesis proceeds at elevated temperatures (60-200 °C) where crystals grow through nucleation. A systematic representation zeolite formation process (Brinker and Scherer, 1990) is shown in Figure 12:

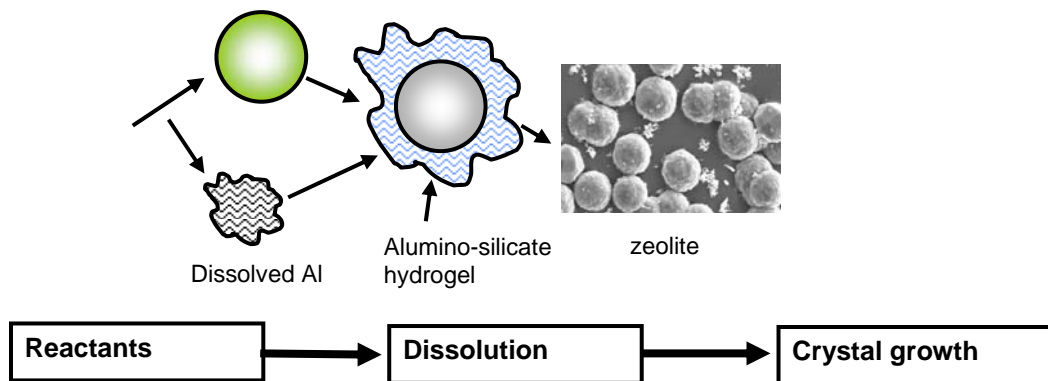


Figure 12: Schematics of zeolite synthesis

The zeolite synthesis involves two steps: nucleation and crystallization. Nucleation is a process where small aggregates of precursors give rise to nuclei (embryos), which become larger with time (Szostak, 1989). Crystallization is the formation of the zeolite crystals.

1.7.2 Factors affecting zeolite formation

The main factors influencing zeolite formation are (Szostak, 1989)

- the composition of the reaction mixture
- temperature
- time
- history-dependent factors.

1.7.2.1 Molar composition

The molar composition of all zeolite structures depends on the Si/Al ratio and/or impurities in the silicon and aluminium sources (Breck 1974; Szostak, 1989; Thompson, 1998). Thus each structure imposes a restriction on the amount of Al it can incorporate. High-silica molecular sieves such as ZSM-5 can be synthesised over wide range of Al/Si ratios from 7 to infinity (Szostak, 1989; Thompson, 1998). The molar composition also depends on the OH⁻ concentration, which act as a mineralizer (Szostak, 1989). The OH⁻ increases the solubility of silica by depolymerising amorphous silica particles resulting in the formation of oligomeric species in the solution. The OH⁻ further enables the process of condensation of aluminosilicate species which leads to the appearance of the initial crystals (Culfaz and Sand, 1973; Thompson, 1998). Other anions such as fluoride ions have been used in the area of aluminophosphates. Inorganic cations have been regarded as an important parameter influencing the structure of the zeolite formed (Szostak, 1989). They are involved in structure direction, solid yield, crystal

morphology and purity (Rollmann, 1999; 2000). Nucleation and crystal growth can be optimized by the right choice of inorganic cations (Table 6). Organic cations, such as tetramethylammonium (TMA) and tetrabutylammonium (TBA) salts act as a gel modifier resulting in the formation of structures with high Si/Al ratio. In addition, they also interact physically and chemically with the other components of the gel so as to alter the gelling process (Barth-Wirsching and Höller, 1989; Szostak, 1989; Rollmann, 1999). The concentration of water of the starting mixture also plays important role in the direction of structure in most zeolites (De’Gennaro, and Collela, 1989; Thompson, 1998).

Table 6: Sub-factors influencing zeolite crystallisation (Szostak, 1989)

Factor	Sub-factors
Reaction/gel composition	<ul style="list-style-type: none"> • SiO₂/Al₂O₃ sources • OH⁻ concentration • Cations (both organic and inorganic) • Anions other than OH⁻(for example fluoride) • Water concentration
Time	<ul style="list-style-type: none"> • Varies, depending on type of zeolite
Temperature	<ul style="list-style-type: none"> • Varies, depending on type of zeolite <ol style="list-style-type: none"> 1. Ambient (25 – 60 °C) 2 Low (90 – 120 °C) 3. Medium (120 – 200 °C) 4. High (250 °C and higher)
History-dependent factors.	<ul style="list-style-type: none"> • Ageing, stirring, nature of mixture, order of mixing

Water has been proposed to interact with the cations in the solution (Breck, 1974; Occelli and Kessler, 1997) thus itself becoming a template for structure direction. A higher H₂O/Na₂O in the initial mixture has been found to yield lower concentration of aluminium and silicon in the liquid phase and vice versa (Szostak, 1989).

1.7.2.2 Temperature

Temperature can alter the zeolite structure as well as the induction period and crystal growth kinetics (Szostak, 1989). As discussed, the rate of crystallization is directly proportional to temperature while the rate of nucleation is inversely proportional to temperature. Since both the processes undergo simultaneously for large periods of time, the operating temperature needs to be optimized for maximum zeolite yield (Thoma and Nenoff, 2000). The reaction mixture, being in a disordered state, is at higher entropy than the crystalline, ordered state (Iler, 1979; Franco *et al.*, 1990). Usually, zeolites are synthesized below 350 °C, with some exceptions (Szostak, 1989). Higher temperatures generally yield more condensed phase species. Temperature influences several factors in zeolite synthesis; it can alter the zeolite phase obtained as well as change the induction period before the start of crystallization. This induction period decreases with increasing temperature. The reaction temperature seems to influence both the d-spacing and the crystallinity of the zeolite MCM-41, in opposite ways (Terres, 1996).

1.7.2.3 Time

The optimization of time is very important in the industrial manufacturing of the zeolites. It is very important to control the time due to the fact that the same reactants may yield different products at different times at same process conditions. In the sol-gel processing of zeolites, the reaction mixture forms gel very quickly (Szostak, 1989). After some time the gel phase separates

into two phases, solid and liquid, with increase in the mixture density (Brinker and Scherer, 1990). The solid precipitates from the gel. This solid is the crystalline material-zeolite. Thus the reaction mixture forms a metastable state, which splits into two stable states, one of which is the crystalline solid phase.

1.7.2.4 History-dependent factors influencing zeolite formation

Ageing has been defined as the period between the mixing of reagents and the onset heating to the crystallization temperature (Szostak, 1989). Increased aging decreases the crystallization time (Li *et al.*, 2001). Alfaro *et al.*, (2007) recently found that aging is a critical factor for the control of particle size. Stirring rate significantly affects crystal size. Smaller crystals are obtained from stirred rather than from static batches for both zeolite Beta (Cambor *et al.*, 1991) and TS-1 (Van der Pol and van Hoof, 1992; Gontier and Tuel, 1996). The effect corresponds to the formation of large zeolite crystals in viscous systems, where convective motion is hindered and mass transfer is diffusion-controlled. Zeolite A, X and Gismondine (zeolite P) crystals up to 150 μm have been obtained by counter-diffusion of silicate and aluminate solutions in Carbopol gel (Ciric, 1992) or by synthesis in triethanolamine solution (Di Renzo, 1998). It can be observed that stirring often modifies the selectivity of zeolite crystallization. For instance, zeolite A is preferred to zeolite X in stirred systems, and MFI is formed instead of TON from several unstirred synthesis systems (Pellegrino *et al.* 1997). The nature of the mixture plays a very important role in the structure direction of zeolites. The sol-gel synthesis is carried out with inorganic as well as organic precursors. The product zeolites are influenced by the precursor (Diaz and Lazo, 2000). Depending on the type of precursor used (organic or inorganic) the final compound can have approximately the same chemical composition, but different crystalline structures. The inorganic precursors yielded more hydroxylated surfaces whereas the organic precursors easily

incorporated the metals into the network (Szostak, 1989). Seeding involves the introduction of a known zeolite into the synthesis system, just before the hydrothermal treatment in order to direct crystallization towards a given zeolite and control the size of the final crystals (Di Renzo, 1998). The seed surface provides nucleation sites resulting in rapid crystallization and growth (Ueda and Koizumi, 1979; Szostak, 1989). The effect of mixing of reagents can also affect the structure direction of the zeolite. Poorly mixed hydrogel can give rise to impurity phases (Coker *et al.*, 1995) with the amount of impurity decreasing with improved pre-mixing.

1.8 Properties of zeolites

The following are the properties of zeolites (Szostak, 1989):

- open, cage-like structures
- high cation exchange capacities
- high internal and external surface areas
- variable aggregate sizes
- high permeability

1.9 Applications of zeolites

The main applications of zeolites are adsorption, catalysis and ion exchange (Szostak, 1989; Nagy *et al.*, 1998; Thompson, 1998). These properties are described in brief-detail below:

1.9.1 Adsorption of zeolites

Zeolites are used to adsorb a variety of materials. This includes applications in drying, purification and separation. They can remove water to very low partial pressures and are very effective desiccants, with a capacity of up to more than 25% of their weight in water. They can

remove volatile organic chemicals from air streams, separate isomers and mixtures of gases. A widely used property of zeolites is that of gas separation. The porous structure of zeolites can be used to "sieve" molecules having certain dimensions and allow them to enter the pores. Other applications that can take place within the pore include polymerization of semi conducting materials and conducting polymers to produce materials having unusual physical and electrical attributes (Barthomeuf, 1996; Nagy *et al.*, 1998).

1.9.2 Zeolite catalysis

Zeolites are extremely useful as catalysts for several important reactions involving organic molecules (Szostak, 1989). The most important are cracking, isomerization and hydrocarbon synthesis. Zeolites are able to promote a diverse range of catalytic reactions including acid-base and metal induced reactions; serve as acid catalysts and can be used to support active metals or reagents (Barthomeuf, 1996). Zeolites can be shape-selective catalysts either by transition state selectivity or by exclusion of competing reactants on the basis of molecular diameter (Sobolev *et al.*, 1993). They have also been used as oxidation catalysts. The reactions can take place within the pores of the zeolite, which allows a greater degree of product control (Szostak, 1989). The main industrial application areas are: petroleum refining, synfuels production, and petrochemical production. Synthetic zeolites are the most important catalysts in petrochemical refineries

1.9.3 Ion exchange

The loosely-bound nature of extra-framework cations allows them to be readily exchanged for other types of cations including metal ions when they are in aqueous solution (Townsend, 1984; De'Gennaro and Collela, 1989; Collela, 1996). The cation-exchange behaviour of zeolites depends on: the nature, size and charge of the cation species, temperature and the concentration

of the cationic species in the solution, the anion associated with the cation in solution, the type of solvent and the structural characteristics of the particular zeolite (Szostak, 1989). Other applications where zeolites are used is in toothpaste, in water softening, oxygen production, solar energy use, latent hydraulic additive wastewater, gas treatment, and reduction of water in air to very low concentrations, allowing very effective evaporative cooling to occur (Thompson, 1998).

1.9.4 Aquaculture

Contamination in aquatic environment can be very high due to the production of ammonia by the fish themselves. This results in the pollution of the water and a consequent increase in the concentrations of toxic substances (Bergero *et al.*, 1994). Due to their high cation exchange capacity, zeolites are used to adsorb ammonia in the aquaria.

1.9.5 Swimming pool filters

Chemicals such as chlorine, algaecides and flocculants can change the pH of pool water. In addition, environmental factors as well as the quality of the fill water can create changes in the pH of a swimming pool (Dyer and White, 1999). Zeolites are able to filter particles as small as 3 μm . The zeolite also reduces backwashing requirement by up to 50% and so saves time and pool water and can be regenerated using regular salt (Anderson, 2003). The use of zeolites results in lower chlorine consumption and a better swimming environment in pools. Zeolites also adsorb ammonia and its compounds, thus reducing and preventing their formation (Bergero *et al.*, 1994; Dyer and White, 1999).

1.9.6 Removal of solids and organic matter

As zeolites are a granular material, solid and suspended particles are trapped between the grains. The porous structure also causes colloid particles from both organic and mineral origin to be removed from the water (Szostak, 1989; Thompson, 1998). The capacity for the removal of solid particles is up to 45% greater than the capacity of sand with an equivalent particle size distribution. At the moment, further investigations are still being performed in this field of interest (Papaioannou *et al.*, 2005).

1.10 Silver zeolites technology

Research is on going about silver zeolite technology. The antimicrobial activity of zeolitic matrix containing both mixture of silver and zinc have been tested on a stainless steel surface (Cowan *et al.*, 2003). It was found to exhibit strong antimicrobial activity by inactivating vegetative cells of three *Bacillus* species though no inactivation of spores was observed. The coatings were also effective against *P. aeruginosa*, which has high degree of natural resistance to many known antimicrobial agents (Cowan *et al.*, 2003). Silver ions coupled with zinc ions have been found to be more effective than silver alone. Bright *et al.*, (2002) demonstrated that a coating of 2.5 % silver and 14 % zinc had significant anti *S. aureus* properties after one hour of exposure. Unfortunately, many tests and investigations were carried out within the laboratory environment using controlled parameters. Rivera-Garza *et al.*, (2000) demonstrated the antimicrobial activity of silver zeolite. Clinoptilite (a natural zeolite found in Mexico) with a particle size of 2 mm when put into contact with concentrations of silver nitrate. The zeolite was then dried at 80 °C for five hours. The resulting silver zeolitic mineral eliminated the pathogenic microorganisms *E. coli* and *Streptococcus faecalis* from water after two hours of contact. However, the silver was at the highest possible adsorbed level on the zeolitic mineral. The silver ions bound to the zeolite

are what give it its bactericidal action as the zeolitic minerals themselves gave no antibacterial properties. The American Food and Drug Administration gave the approval for the use of silver ion technology in all types of food contact polymers. These polymers have a thin layer of silver zeolite laminated onto the food contact surface. The silver ions are released from the laminate so there is continual flow antimicrobial agent to the surface of the foodstuff during direct contact. This will minimize the chances of microbial contamination during food storage, transportation and handling. The negative side of the silver zeolite incorporated polymers is the need to be assessed for each different food item as the types of microorganism and growth rates will vary for each type of food stuff (Quintavalla and Vicini, 2002). If the introduction of silver zeolite into work places such as kitchens and hospitals is to take place further in situ tests need to be performed so that the effects of environmental factors can be taken into consideration. Results may be affected by such things such as the presence of organic matter, varying pH and ionic strengths, changes in humidity and temperature (Galeano *et al.*, 2003). However, the addition of silver/zinc ion zeolite coatings to stainless steel surfaces could prove to be very useful in settings where microbial contamination is undesirable; such as in food preparation areas and on surfaces within hospital environments such as door handles, water taps and ventilation ducts (Bright *et al.*, 2002). The main aim should be eradication or at least extreme reduction in hospital acquired infections such as MRSA.

Silver and zinc ions have also been incorporated into temporary dental filling materials. The silver and zinc zeolite at varying concentrations along with silicon oxide filler were incorporated into urethane acrylate monomer paste. The materials exhibited antimicrobial activity in vitro against *Streptococcus mutans* and *Streptococcus mitis*. Detectable amounts of silver and zinc zeolites were released even after four weeks of experimentation (Hotta *et al.*, 1998). These results suggest that small amounts of silver and zinc zeolites will confer antibacterial activity that

is sufficient for dental applications for at least four weeks. Zeolites containing silver alone have also demonstrated antimicrobial activities.

1.11 Hypothesis

Conventional silver-based antibacterial agents tend to leach their silver ions out quite quickly, producing materials with short active lifetimes. This ‘quick leaching’ of silver ions coupled with the emergence of resistance and the toxicity of some antimicrobial materials have prompted renewed interest in the use of silver as an effective antimicrobial agent (Russell & Hugo, 1994; Silver, 2003; Feng *et al.*, 2000; Dunn & Edward-Jones, 2004). Silver and silver ions are relatively less toxic to humans (Russell & Hugo, 1994) but exhibit a broad spectrum of antimicrobial activity at low concentrations (Feng *et al.*, 2000; Kawahara *et al.*, 2000; Inoue *et al.*, 2002). Silver is well known to inactivate membrane-bound proteins resulting in the failure of DNA to replicate (Feng *et al.*, 2000; Silver, 2003; Sondi & Salopek-Sondi, 2004). The silver ion also aids in the generation of reactive oxygen species, which are produced through the inhibition of respiratory enzymes by silver ions (Matsumura *et al.*, 2003). Naturally occurring zeolites (alumino-silicate minerals) are widely distributed in oceanic sediments and volcanic regions and have long been of geochemical interest. It was discovered that although they had limited activity as catalysts they can act as reservoir for antibacterial agents. Furthermore, due to the electrostatic charges and cage structure of zeolites the silver can be held within the framework for long periods of time, producing active materials with lifetimes of years rather than months. So far these zeolite antibacterial agents have only been impregnated into kitchen wipes and cooker hoods. Although conventional zeolites have been used successfully as polymer fillers in Japan for over 5 years the longevity of silver and the extent to which it persists in its antimicrobial activity has not been established. Silver-loaded zeolite X, A and High Aluminium Phillipsite

were therefore produced in the laboratory and the release activity and persistency of activity on strains of *E. coli*, *S. aureus* and *P. aeruginosa* suspended in TSB were investigated in this study.

1.12 Aims and objectives of this study

The key aims of this research are listed below:

- To produce silver-loaded zeolites using conventional ion exchange technologies
- To produce silver-doped zeolites with silver held within the zeolite framework using novel isomorphous substitution techniques
- To characterize the silver zeolites using X-ray diffraction, scanning electron microscopy, energy dispersive X-ray analysis, Fourier transformed infrared spectroscopy
- To examine the antimicrobial efficiency of the silver zeolites compared with other antimicrobial agents
- To identify the interaction of silver ions with molecular targets in the microbial cell. For example fatty acid biosynthesis

To achieve these aims the following silver zeolites were produced by ion exchange in the laboratory: zeolite A, zeolite X and high aluminium Phillipsite. Silver-doped analcime was produced by direct isomorphous substitution of silver into their framework structures.

The work is divided into seven chapters. Chapter one contains an introduction and reviews of the literature on antimicrobial agents, silver and its compounds, bacterial cells as well as silver zeolite technology. In chapter two the experimental design and methodology used in this work is presented. This includes general methods used in the synthesis of zeolites along with their characterization, the antimicrobial activity of silver-loaded zeolites on microorganisms used in this work and the effect of silver on the components of these microorganisms. Results of the synthesis, ion exchange and characterization of silver-loaded zeolites are presented in chapter

three. Chapter four focuses on the results and discussion on the influence of concentration of silver-loaded zeolites on the microorganisms used in this work. In chapter five, the results obtained from the persistency of the antimicrobial activity of silver-loaded zeolites are presented. Chapter six focuses on the effect of silver on some of the components of the microorganisms used in this work. The overall discussion and conclusion and suggestion for future work is given chapter seven.

Chapter 2

Experimental design and methodology

This chapter is divided into two parts: the general methods involved in the synthesis and characterization techniques of zeolites will be elaborated in Part A. Experimental protocols for the investigation of the antimicrobial activity of silver zeolites produced in this work will be discussed in Part B.

PART A:

Production and characterizations of silver zeolites

2.1 Synthesis of zeolites

As discussed in Section 1.7 the synthesis of zeolite is carried out under hydrothermal conditions. An aluminate solution and a silicate solution are mixed to give an alkaline medium which forms a milky gel, or in some instances, clear solutions. Various cations or anions can be added in the synthesis mixture. Synthesis proceeds at elevated temperatures (60 – 200 °C) in a sealed reaction vessel at constant pressure. The zeolite crystallizes at the required temperature.

2.1.1 Synthesis of zeolite X

Zeolite X (crystal composition: $\text{Na}_{80}[\text{Si}_{112}\text{Al}_{80}\text{O}_{384}]\cdot 260\text{H}_2\text{O}$) was synthesised following the method described by Lechert and Kacirek (1991, 1992). The batch composition for the synthesis is given by:

$\text{NaAlO}_2:4\text{SiO}_2:16\text{NaOH}:325\text{H}_2\text{O}$

3.0

97.5 g of sodium aluminate powder was added to 100 g of sodium hydroxide (Aldrich Chemicals, UK) dissolved in 195 ml of de-ionized water while stirring until a homogeneous solution was obtained. In a separate vessel, 219.7 g of sodium silicate and 100 g of sodium hydroxide were added to 612 g of distilled water in a polypropylene bottle to obtain a suspension

of silicate. The sodium aluminate suspension was added to the sodium silicate to form a gel, and stirring was continued until a homogeneous gel was obtained. The gel was poured into PTFE-vessels, with each vessel containing about 10 g of the gel. The bottles were put into an electric oven at a temperature of 90 °C for 8 hours. The reaction in the PTFE bottles was quenched by running cold water on the bottles after they were removed from the oven until they were cooled to room temperature. The synthesized samples were filtered using a Buchner vacuum funnel and Whatman No 1 filter paper. The powder samples obtained were washed copiously with 500 ml of distilled water. Following overnight drying of the powdered zeolite at 40 °C in an electrical oven, the zeolite was crushed into uniform powder with pestle and mortar, sieved and stored in a cupboard.

2.1.2 Synthesis of zeolite A

Zeolite A was synthesized following the method described by Thompson and Huber (1982). The batch composition for the synthesis is given by:



0.723g of sodium hydroxide (Aldrich Chemicals, UK) was dissolved in 80 ml of distilled water. The solution was divided into two equal halves and each transferred into plastic beakers. 0.258g of sodium aluminate (Fischer Scientific Chemicals, UK) was added to the first halve with continuous stirring until a homogeneous solution was obtained. 15.48g of sodium metasilicate (Fischer Scientific Chemicals, UK) was added to other half while mixing until the gel was homogenized. The two samples were mixed quickly and the mixture was again stirred continuously until a homogeneous solution was obtained. The gel was poured into PTFE-vessels, with each vessel containing about 10 g of the gel. The bottles were put into an electric oven at a temperature of 99 °C for 4 hours. The reaction in the PTFE bottles was quenched by running cold

water on the bottles after they were removed from the oven until they were cooled to room temperature. The synthesized samples were filtered using a Buchner vacuum funnel and Whatman No 1 filter paper. The powder samples obtained were washed copiously with 500 ml of distilled water. Following overnight drying of the powdered zeolite at 40 °C in an electrical oven, the zeolite was crushed into uniform powder with pestle and mortar, sieved and stored.

2.1.3 Synthesis of high alumina Phillipsite

High alumina Phillipsite was synthesized from the following molar gel composition:

1.53Na₂O: 0.44K₂O:Al₂O₃:5SiO₂:82.7H₂O (Cichocki, 1991) **5.0**

At room temperature 1.53 g of sodium hydroxide and 3.78 g of potassium hydroxide pellets were dissolved in 36.0 g of distilled water in a polypropylene bottle. The homogenized suspension was added to 6.0 g of silica suspension (Aldrich Chemicals, UK) in a separate polypropylene bottle. The reaction gel was produced by adding 25.22 g of sodium aluminate solution (26.6 % Al₂O₃, 19.6 % Na₂O) to the silical suspension mixture with continuous stirring until a homogenized gel was obtained. The gel was poured into PTFE-vessels, with each vessel containing about 10 g of the gel. The bottles were put into an electric oven at a temperature of 40 °C for 7 days. The reaction in the PTFE bottles was quenched by running cold water on the bottles after they were removed from the oven until they were cooled to room temperature. The synthesized samples were filtered using a Buchner vacuum funnel and Whatman No 1 filter paper. The powder samples obtained were washed copiously with 500 ml of distilled water. Following overnight drying of the powdered zeolite at 40 °C in an electrical oven, the zeolite was crushed into uniform powder with pestle and mortar, sieved, transferred into air-tight bottles and stored in a cupboard.

2.1.4 Synthesis of silver-doped analcime

The starting sols were made according to the reaction gel composition (Lechert and Kacirek, 1991, 1992):

6.5Na₂O:Al₂O₃:4.5SiO₂:380H₂O:6.1: triethanolamine (TEA) 6.0

with some modifications. 9.8 g of kaolinite was added to 55 g of distilled water and stirred until a homogeneous suspension was obtained. Simultaneously, 14.9 g of sodium silicate was added to 36.5 g distilled water, stirred continuously after which 12.2 g of triethanolamine was added and stirred until the slurry was homogenized. The kaolinite suspension and the silica suspension were mixed together under constant stirring for 15 minutes. Thoroughly homogenized synthesis mixtures were treated hydrothermally in a Teflon-lined stainless steel autoclave at 200 °C for 24 hours. Silver doped-analcime was prepared as follows: 1 M silver nitrate solution (1.96 g in 10 ml distilled water) was pre-added to 9.8 g of kaolinite suspension to obtain about 5 % silver doping. The molar composition of the sodium silicate and TEA were unaltered. The sodium silicate-TEA and the silver kaolinite suspensions were mixed with constant stirring until a homogeneous suspension was obtained. The content was hydrothermally treated and crystallized in the same conventional manner as before. Silver-doped analcime with aluminate reduction of 10 % and 20 % were prepared by pre-adding 2 M silver nitrate solution (3.92 g in 10 ml distilled water) and 4 M silver nitrate solutions (7.84 g in 10 ml distilled water) and repeating the synthesis procedure. After the hydrothermal treatment, the content of the autoclave was washed with 1-liter distilled water, vacuum filtered and dried in an electric oven at 40 °C. After drying the samples they were crushed into uniform powder with pestle and mortar, sieved and stored in a cupboard.

2.2 Characterization of zeolites

Spectroscopic, microscopic and particle size analysis were used to characterize the zeolites. Spectroscopy techniques used include X-ray Diffraction (XRD), Energy Dispersive X-ray analysis (EDX) and Fourier Transformed Infrared spectroscopy (FTIR). Microscopy method used was Scanning Electron microscopy (SEM).

2.2.1 X-ray Diffraction (XRD)

(a) Introduction

XRD provides the most comprehensive description of members of zeolite groups. The theory is based on the elastic scattering of X-rays from structures that have long range order. XRD is used to monitor the phase purity and crystallization and the purity of the zeolite particles. XRD also gives information of the particle strain and lattice size

(b) Principle of XRD

When a crystal is bombarded with X-rays of a fixed wavelength (similar to spacing of the atomic-scale crystal lattice planes) and at certain incident angles, intense reflected X-rays are produced when the wavelengths of the scattered X-rays interfere constructively (Figure 13).

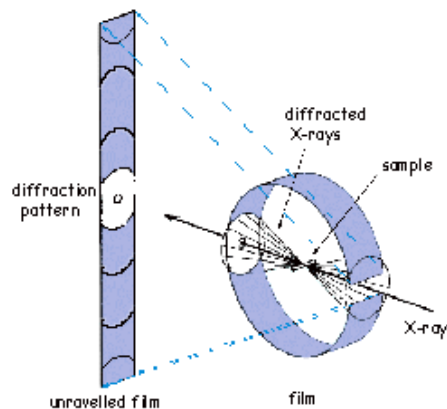


Figure 13: Schematics of the X-Ray diffraction spectrometer (British Museum 2005)

In order for the waves to interfere constructively, the differences in the travel path must be equal to integer multiples of the wavelength. When this constructive interference occurs, a diffracted beam of X-rays will leave the crystal at an angle equal to that of the incident beam. The general relationship between the wavelengths of incidence X-rays, angle of incidence and spacing between the crystal lattice planes of atoms is known as Bragg's law:

$$n\lambda = 2d \sin \theta \quad 7.0$$

Where:

n (an integer) is the "order" of reflection

λ is the wavelength of the incident X-rays

d is the inter-planar spacing of the crystal and

θ is the angle of incidence.

(c) Method

The powder X-ray diffraction patterns of the zeolite samples were recorded on a Philips PW1710 X-ray powder diffractometer over 2θ range of 5° to 55° at a scanning speed of 2° per minute and a step size of 0.05° . The instrument uses sealed Xenon detector. The diffractometer was equipped with graphite monochromated Cu radiation source (8978 eV or $\lambda = 1.5418 \text{ \AA}$). The X-ray source was operated at 40 mA and 40 kV. Data processing was carried out using Philips APD software with a search/match facility and an ICDD database on a DEC Microvax minicomputer interfaced to the diffractometer. The pattern on the computer depends on what is in the sample and by reference to standard data. X-ray powder diffraction patterns of zeolite X, A, high aluminium Phillipsite and Analcime were collected on a conventional source using a flat auto plate. Portions of the samples of the three zeolites were placed on the flat auto plate and pressed

down to fill the entire perimeter of the plate using a glass plate. After obtaining a smooth and level surface of the powder, the plates were stacked on an automatic sample chamber.

2.2.2 Energy Dispersive X-ray spectroscopy (EDX)

(a) Introduction

Energy Dispersive X-ray Analysis (EDX) is employed in Scanning Electron Microscopy (SEM) and Transmission Electron Microscopy (TEM) for local elemental identification. The incident electron beam induces X-ray fluorescence in the sample which is energy-analyzed using a cooled semiconductor detector. The element-specific spectral lines are then identified to give the local elemental composition. EDX is used in many different application areas such as in the chemical, electronic and food industries as well as refineries. It can be used with solid, powder and frozen liquid samples.

(b) Principle of EDX

Most EDX equipments are fitted in conjunction to a scanning electron microscope (SEM). The EDX measures the energy of X-rays that are generated by the atoms of the sample during interactions with the electron beam. The X-ray spectra formed are characteristic of the atoms that formed them, allowing the chemical composition of the sample to be determined.

2.2.3 Scanning electron microscopy

(a) Introduction

Scanning Electron Microscopy is a versatile and well-established complementary technique to light optical microscopy. By using a beam of electrons instead of photons, samples can be imaged at far higher magnifications.

(b) Principle of SEM

SEM can use different signals to generate contrast mechanisms. The back-scattered electron and secondary electron signals can be used to form images that can give information about the structure, topography and compositional features of a sample.

(c) Experimental method

Aluminium stubs were prepared prior to the analysis with an adhesive coating. The samples were sprinkled on the stubs. Where necessary, the samples were gold-coated using an Emscope SC500 Sputter coater to reduce static charging. Electron micrographs were obtained at various magnifications.

2.2.4 Particle size analysis

(a) Introduction

The particle size distributions per unit volume zeolites without silver ions and silver zeolites were analyzed with Mastersizer X long bed analyzer (Malvern Instruments, UK).

(b) Principle of Mastersizer X long bed analyzer

The general principle of the Mastersizer is based on the laser ensemble of light scattering. The system inherently measures the integral scattering from all particles present in the beam. The number of particles needed in the beam to obtain adequate measurement of the scattering is in the range of 100 – 10000 depending on their size. Three different types of lenses ranging from 0.1 – 80 μm , 100 – 600 μm and >600 – 2000 μm are used for measuring the size distribution.

(c) Experimental method

Samples of silver-exchanged zeolite X, A and high aluminium Phillipsite with or without silver loading and silver-doped analcime were taken for particle size analysis. Before measurements were made, the laser lenses were aligned in a straight line. Settings were set to obscuration value of 0.2. After steady conditions, 0.1 mg of each sample was loaded into an MSX 15 sample handling unit that uses mechanical action of stirring to ensure that the zeolite particles did not flocculate. Sodium Amalgam was then added to disperse adhering particles. Measurements were then recorded on a computer connected to the instrument.

2.2.5 Fourier transformed infrared spectroscopy (FTIR)

(a) Introduction

FTIR spectroscopy is used to investigate the structural features of samples. Samples of zeolites produced in this study (with or without silver loading) were analyzed with a Mattson FTIR spectrometer (Mattson Instruments, UK) equipped with a ZnSe crystal plate attached to the spectrometer with a mercury cadmium telluride A (MCTA) detector and KBr as beam splitter.

(b) Principle of FTIR

The principle of FTIR used in this study is based on the principle of diffuse reflectance. Incident light from a source radiation is scattered in all directions. These spectra can exhibit both absorbance and reflectance features due to contributions from transmission, internal and specular reflectance components, and the scattering phenomena in the collected radiation. A monochromator (usually a salt prism or a grating) separates a source radiation into different wavelengths that are collected by a slit system (Figure 14). A beam splitter separates the radiation into two: half goes through the sample and half to a reference.

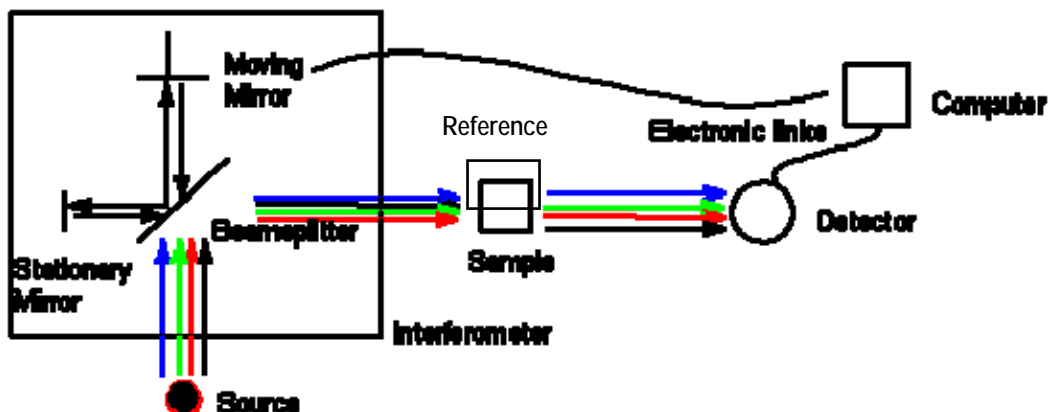


Figure 14: Schematics of the FTIR spectrometer (British Museum, 2005)

A detector collects the radiation that passes through the sample, compares its energy to that going through the reference and sends it to a recorder (computer connected to the instrument). The recorder is calibrated in such a way that it converts the radiation into energy signals which is presented as a function of frequency.

(c) Experimental method

Measurements were done using 100 scans at 4 cm^{-1} resolution, units of $\log(1/R)$ (absorbance), over the mid-IR region of $1200\text{-}400 \text{ cm}^{-1}$. An air background spectrum was collected at the start of the sample collection. A small sample of each zeolite (with or without silver) was centered on the ZnSe plate to ensure that it covered the entire crystal surface, and a pressure clamp was used to apply pressure on the filter. The zeolite samples were analyzed three times for three different samples. A background spectrum was measured before every sample to compensate for atmospheric conditions around the FT-IR instrument.

2.3 Ion exchange of zeolites

2.3.1 Cation exchange capacity of zeolites

For an exchange between two monovalent ions M_A and M_B the ion exchange equation is given by:



Where:

M_A and M_B are the two cations or anions involved

Z_A and Z_B are the valencies of the ions. The characters with a bar indicate the particular cation or anion in the exchanger phase.

The cation exchange capacity (CEC) defined as the magnitude of cation exchange is given by (Ertl *et al.*, 1999):

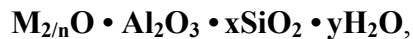
$$CEC = \frac{N_c}{A_M} \quad 9.0$$

Where

N_c = the number of cations available for exchange

A_M = the sum of the atomic weights of constituent atoms.

Thus for a zeolite of chemical formula:



Where M is a cation, A_M is given by the sum of the atomic weights of M, O, Al, Si and H taking into account the stoichiometric coefficients.

2.3.2 Ion exchange in zeolite X

Silver nitrate solution (20 ml) at a concentration of 0.5 M was added to 20.0 g of zeolite X. Subsequently the mixing was performed in plastic bottles placed in a rotation drum for five hours to obtain significant ion exchange. The slurry was filtered, washed five times with 500 ml of de-

ionized water, dried at 40 °C in an electrical oven and crushed into powder. Silver-loaded zeolite X produced was transferred into air-tight containers and kept in the dark.

2.3.3 Ion exchange in zeolite A

The protocol in Section 2.3.1 was repeated for silver-exchanged zeolite A.

2.3.4 Ion exchange in high aluminium Phillipsite

The production of silver-exchanged high alumina Phillipsite followed the protocol described in Section 2.3.1.

PART B:

Microbiology

2.4 Media preparation

2.4.1 Preparation of tryptone soya agar (TSA)

TSA is a nutrient-rich medium used for culturing many kinds of microorganisms. It is mainly used as an initial growth medium for the purposes of: observing colony morphology, developing a pure culture, achieving sufficient growth for further biochemical testing, and culture storage. In preparing the TSA (Lab M, UK) for this study, 14.8 g TSA was added to 400 ml of distilled water in 500 ml medical flasks in order to obtain 37 g l⁻¹ of TSA. The flasks were loosely capped and autoclaved at about 121 °C for about 15 minutes after which it was cooled to 50 °C. The agar was then poured on sterile Petri dishes and allowed to solidify at room temperature.

2.4.2 Preparation of tryptone soya broth (TSB)

TSB (Lab M, UK) was prepared according to the manufacturer's protocol. 6 g of the TSB were dissolved in 200 ml of de-ionized water in conical flasks. The flasks were capped with foams and further covered with aluminium foils. The flasks and their contents were autoclaved at 121 °C for 15 minutes and cooled to room temperature.

2.4.3 Preparation of ringer solution

One-quarter strength Ringer (Lab M, UK) solutions were prepared by dissolving 1 tablet in 500 ml of de-ionized water in a 1-litre flask. 4.5 ml ringers were pipetted into test tubes and capped. The test tubes and their contents were autoclaved at 121 °C for 15 minutes and cooled to room temperature.

2.5 Antimicrobial activity of silver-exchanged zeolite X

2.5.1 Introduction

The antimicrobial activity of silver-exchanged zeolite X was investigated by exposing bacterial strains of *E. coli* K12W-T, *S. aureus* NCIMB6571 and *P. aeruginosa* NCIMB8295 to silver-exchanged zeolite X in TSB. All three microorganisms were obtained from the University of Wolverhampton culture collection. The stock cultures were freeze-dried and kept at $-20\text{ }^{\circ}\text{C}$. Before use, cultures were resuscitated and grown on TSA overnight at $37\text{ }^{\circ}\text{C}$. The first stage of the investigation was the exposure of all three strains to silver-exchanged zeolite X in TSB for a duration of 24 hours. The second stage involves the exposure of all three strains to silver-exchange zeolite X in TSB over a shorter period (2 hours).

2.5.2 Influence of concentration with time

The inhibitory effect of the silver zeolite X as function of concentration and time was investigated by the method described by Bellantone *et al.*, (2002) as shown in Table 7: A single bacterial colony for each microorganism was used to inoculate a 100 ml starter culture, which was grown aerobically overnight at $37\text{ }^{\circ}\text{C}$ in a rotary shaker (150 rpm). After overnight incubation (18h) at $37\text{ }^{\circ}\text{C}$ 0.1 ml of each culture ($1 \times 10^9\text{ CFU ml}^{-1}$) was inoculated into 200 ml sterile TSB in 500 ml conical flasks to give a final concentration of $5.73 \times 10^5 \pm 4.22 \times 10^4\text{ cells ml}^{-1}$ for *E. coli*, $5.60 \times 10^5 \pm 3.57 \times 10^4$ for *S. aureus* and $5.70 \times 10^5 \pm 4.15 \times 10^4$ for *P. aeruginosa*. Flasks containing each culture, zeolite X or silver-loaded zeolite were prepared according to the protocol shown in Table 7. Flasks 1 to 3 containing *E. coli*, *S. aureus* and *P. aeruginosa* in TSB were used as controls. A second set of controls was prepared as follows: 1 g l^{-1} (0.2 g per 200 ml) of zeolite X without silver was added to flasks 4, 5 and 6 containing *E.*

coli, *S. aureus* and *P. aeruginosa*. The concentration of silver-zeolite X used was 0.15 g l⁻¹ (0.03 g per 200 ml).

Table 7: Summary of experimental procedure used in the antimicrobial testing of silver-loaded zeolite X

Flask No	TSB; ml	<i>E. coli</i> ; ml	<i>S. aureus</i> ; ml	<i>P. aeruginosa</i> ; ml	Z-X ^a ; g	AgZ-X ^b ; g
1	200	0.1	-	-	-	-
2	200	-	0.1	-	-	-
3	200	-	-	0.1	-	-
4	200	0.1	-	-	0.2	-
5	200	-	0.1	-	0.2	-
6	200	-	-	0.1	0.2	-
7	200	0.1	-	-	-	0.03
8	200	-	0.1	-	-	0.03
9	200	-	-	0.1	-	0.03
10	200	0.1	-	-	-	0.05
11	200	-	0.1	-	-	0.05
12	200	-	-	0.1	-	0.05
13	200	0.1	-	-	-	0.10
14	200	-	0.1	-	-	0.10
15	200	-	-	0.1	-	0.10
16	200	0.1	-	-	-	0.20
17	200	-	0.1	-	-	0.20
18	200	-	-	0.1	-	0.20

^a Zeolite X, ^b silver-exchanged zeolite X

In the first stage of the investigation, a sample of 5 ml of each culture was withdrawn at 2 hour intervals for 12 hours and then once more at 24 hours. 0.5 ml of each samples were serially

diluted in ringers in 10-fold steps to 10^{-7} . 100 μ l of dilutions were spread on TSA plates and incubated overnight at 37 °C. The colony counts of three plates were counted and averaged for each dilution. All these experiments were performed four times and results were expressed as CFU ml⁻¹. The remaining 4.5 ml was kept in a refrigerator at 4 °C until they were analysed by ICP-AES. For each time interval, triplicate pH measurements of the culture were taken and the average pH was calculated. The protocol was repeated with 0.25, 0.5 and 1.0 g of the silver-loaded zeolite X in 200 ml TSB.

The same protocol (Table 7) was used in investigating the influence of concentration with time for silver-exchanged zeolite A, silver-exchanged high-alumina Phillipsite and silver-doped analcime.

2.5.3 Concentration dependence over shorter time

To determine the antibacterial activity of the silver-loaded zeolites X on the microorganisms over a shorter period of time, each protocol described in the previous section was repeated with samples taken every 15 minutes for 2 hours. Silver-exchanged zeolite A, silver-exchanged high-alumina Phillipsite and silver-doped analcime were investigated in a similar manner.

2.5.4 Continuous retrieval and reuse of silver-exchanged zeolite X

The extent to which the silver-loaded zeolites persisted in their antimicrobial activity was investigated according to the method described by Kwakye-Awuah *et al.*, (2008a). 0.3 g of silver-exchanged zeolite X, silver-exchanged zeolite A, silver-exchanged high-alumina Phillipsite or silver-doped analcime was added to 200 ml of TSB containing either *E. coli* K12 W-T, *S. aureus* NCIMB 6571, *P. aeruginosa* NCIMB 8295 following the protocol described in Table 8. Samples were taken every 15 minutes for 2 hours. At the end of the two hours the

remaining culture was allowed to settle at room temperature after which the zeolite was retrieved by centrifugation ($6900 \times g$, 5 min, 15 °C). The retrieved zeolite was washed five times with 1 litre of de-ionised water and air-dried in a fume cupboard. After drying at 40 °C for five hours, the retrieved zeolite was weighed and the concentration of silver ions remaining in the zeolite determined by EDX. The retrieved, washed zeolite was added to fresh cultures in fresh TSB at the same concentration (0.3 g per 200 ml) and antimicrobial activity investigated as described as before.

Table 8: Summary of experimental procedure used in the repeated retrieval and re-use of silver-loaded zeolite X

Flask No	TSB (ml)	<i>E. coli</i> (ml)	<i>S. aureus</i> (ml)	<i>P. aeruginosa</i> (ml)	Ag Z-X (g)
1	200	0.1	-	-	-
2	200	-	0.1	-	-
3	200	-	-	0.1	-
4	200	0.1	-	-	0.3
5	200	-	0.1	-	0.3
6	200	-	-	0.1	0.3

The same protocol (Table 8) was used in investigating the persistency of antimicrobial activity of silver-exchanged zeolite A, silver-exchanged high-alumina Phillipsite and silver-doped analcime.

2.6 EDX analysis of each retrieved silver-loaded zeolites

To determine the concentration of silver ions occluded on the zeolites surface after each exposure and retrieval, EDX analysis was carried on portion each silver zeolite. Area scans were performed over four different regions and averaged.

2.7 Analysis of silver released silver-loaded zeolites by inductively coupled plasma-atomic emission spectrometer ICP-AES spectroscopy

(a) Introduction

The concentration of silver ions released from the zeolite framework into TSB for each time interval was determined by ICP-AES (SPECTRO 2005, Siemens, UK).

(b) Principle of operation

Figure 15 is a schematic presentation of the inductively coupled plasma-atomic emission spectrometer. Samples in the form of fluids are in argon plasma causing atoms and ions in the plasma vapour to be excited into a state of radiated photon emission. The emitted radiation then passed to the spectrometer optic where it was dispersed into its spectral components. The most suitable line of application was measured from the specific wavelength emitted by each atomic element by a charge couple device (CCD). The intensity of radiation is proportional to the concentration of the element within the sample. This was recalculated internally from a stored calibration curves and shown directly as a percentage or measured concentration.

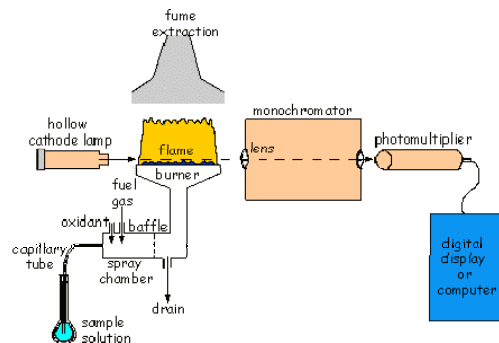


Figure 15: Schematics of ICP-AES (British museum, 2005)

(c) Experimental procedure

The 4.5 ml samples for each sampling time that were stored in a refrigerator (Section 2.5.1) were thawed to room temperature. Turbid cultures were diluted with distilled water and analysed by ICP-AES. Triplicates measurements (in ppm) were made and averaged.

2.8 Analysis of effect of silver on bacterial components

2.8.1 Introduction

The effects of silver ions uptake by *E. coli* K12W-T, *S. aureus* NCIMB6571 and *P. aeruginosa* NCIMB8395 were investigated. Flow Cytometry (FC) analysis was carried out to ascertain the uptake of silver ions by the strains. This was followed by observing changes in DNA contents and fatty acid composition before and after uptake of silver ions by *E. coli* K12W-T and *S. aureus* NCIMB6571. Silver-exchanged zeolite X was used as the source of silver ions.

2.8.2 Flow Cytometry analysis

2.8.2.1 Introduction

Flow Cytometry (FC) provides a rapid analysis of multiple characteristics of single cells (Figure 16).

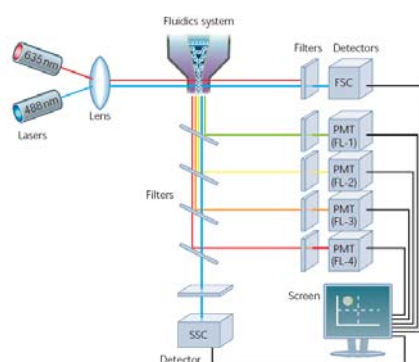


Figure 16: Schematics of the Flow Cytometer (www.ab-direct.com)

2.8.2.2 Principle of the FC

Flow cytometry (FC) is a technology that simultaneously measures and then analyzes multiple physical characteristics of single particles, usually cells, as they flow in a fluid stream through a beam of light (Melamed, 1995; Givan, 2001). The properties that can be measured by FC include a particle's relative size, relative granularity or internal complexity, and relative fluorescence intensity (Givan, 2001). These characteristics are determined using an optical-to-electronic coupling system that records how the cell or particle scatters incident laser light and emits fluorescence (Melamed, 1995; Shapiro, 1995; Givan, 2001). Inside a Flow Cytometer (Figure 16) cells in suspension are drawn into a stream created by a surrounding sheath of isotonic fluid that creates a laminar flow, allowing cells to pass through individually at an interrogation point. At the interrogation point a beam of monochromatic laser light intersects the cells. This results in the emission of light in all directions. This emitted light is collected via optics that direct the emitted light to series of filters and dichroic mirrors that isolate particular wavelength bands. The light signals are detected by photomultiplier tubes and digitized for computer analysis (converted into voltage pulse). This is proportional to the size of the cell. The size distribution of the cell is represented by a histogram. Light scattered at larger angles (side scatter) is caused by granularity and cell complexity inside the cell. The signal collected by side scatter can be presented by histogram as in forward scatter. In order to analyze the DNA content fluorescent dyes are used.

2.8.2.3 Material and media preparation

Gram-negative *E. coli* K12W-T and gram-positive *S. aureus* NCIMB6571 were obtained from the University of Wolverhampton culture collection. Tryptone soya broth (TSB) was obtained from Lab M, UK. De-ionized water used in this investigation was supplied by University of

Wolverhampton. Silver-exchanged zeolite X was produced at the University of Wolverhampton. Propidium iodide (PI) and SYTO 22 were purchased from Molecular Probes, UK. Tris-base ultra pure which was used as the Tris-base was purchased from MELFORD, UK whilst ethylenediaminetetraacetic acid (EDTA) was purchased from BDH, UK. Hydrochloric acid (HCl) was purchased from Sigma Aldrich, UK. Tryptone soya broths (TSB) were prepared following the manufacture's protocol (3 g in 100ml de-ionized water) and were sterilized by autoclaving at 121 °C for 15 minutes. Tris-HCl was prepared by adding 7.8 ml of 1 mM Tris-base (MELFORD, UK) to 66.6 ml of equimolar HCl to obtain a pH of 7.8. Stock solutions of PI and SYTO 22 (Molecular Probes, UK) were prepared as per manufacturer's protocol.

2.8.2.4 Instrumental settings

Flow Cytometry analysis was carried out with FACS Calibur instrument (Becton Dickinson, UK) equipped with Argon ion laser providing 15mW at 488 nm. The instrument was equipped with forward scatter (<15 °), side scatter (>15 °) and three fluorescent detectors, FL1 (530 ± 15 nm), FL2 (585 ± 31 nm) and FL3 (605 nm). Fluorescence emission was detected at FL3 for PI and SYTO 22 is yet to be detected. The sample flow rate was set to low and at least 10,000 cells were acquired for analysis. Triplicate counts were obtained for each procedure

2.8.2.5 Experimental procedure

A single bacterial colony *E. coli* strain was used to inoculate a 100 ml starter culture, which was grown overnight at 37 °C in a rotary shaker. After overnight incubation at 37 °C, 0.1 g of silver-exchanged zeolite X was added to the culture at this stage. After 4 hours of incubation at 37 °C aliquots were withdrawn every 30 minutes. About 10³ cells were collected after washing twice with 4 ml Tris-HCl buffer (pH = 7.8). The cells were re-suspended in 2 ml Tris-HCl buffer. The

cells were stained with 10 μ l of 5 mM SYTO 22 and 10 μ l 10 mg/ml PI. For DNA content 5 μ l of DNase free, RNase A (1:50 dilution) was added prior to staining. After 10 minutes of incubation at room temperature, the samples were analyzed by FC.

2.9 Analysis of fatty acid composition by gas chromatography (GC)

2.9.1 Introduction

In order to identify the interaction of silver ions with molecular targets in the microbial cell changes in fatty acid composition of all three strains as a result of their exposure to silver-loaded zeolites were analyzed. Fatty acids of all three strains were extracted and analyzed by gas chromatography.

2.9.2 Media preparation

Tryptone soya agar was prepared as described in Section 2.4.1. Four reagents were required to saponify cells, esterify, extract and base wash the fatty cells. Saponification reagent was prepared by first diluting 150 ml of methanol (HPLC grade; Aldrich Chemicals, UK) with 150 ml of de-ionized water and adding 45 g of sodium hydroxide. The resulting solution was stirred until the sodium hydroxide was completely dissolved. To prepare the methylation reagent, 325 ml of 6.0 N HCl was added to ethanol with constant stirring until a uniform solution was obtained. Extraction solvent was prepared by adding 200 ml of methyl tert-butyl ether (MTBE) to 200 ml hexane (HPLC grade) with uniform stirring. Finally the base wash reagent was prepared by dissolving 10.8 g of sodium hydroxide in 900 ml de-ionized water.

2.9.3 Preparation of cell cultures

A single bacterial colony of gram-negative *Escherichia coli* K12W-T or *Pseudomonas aeruginosa* NCIMB8295 or gram-positive *Staphylococcus aureus* NCIMB6571 was used to inoculate a 100 ml starter culture, which was grown aerobically overnight at 37 °C in a rotary shaker (150 rpm) (Bellantone *et al.*, 2002). Silver-exchanged zeolite X was added at a concentration of 1.0 g l⁻¹. Cultures without silver-exchanged zeolite X were used as controls. The silver-exchanged zeolite X dosed cultures and the control cultures were re-incubated at 37 °C in a rotary shaker (150 rpm) for 2 hours.

2.9.4 Fatty acid extraction

Fatty acid composition of gram-negative *Escherichia coli* K12W-T, *Pseudomonas aeruginosa* NCIMB8295 or gram-positive *Staphylococcus aureus* NCIMB6571 was determined two hours after incubation by the method described by Sasser (1990) with some modifications. Cells of *Escherichia coli* K12W-T, *S. aureus* NCIMB6571 or *P. aeruginosa* NCIMB8295 were harvested by centrifugation (6900 × g) at 15 °C for 10 minutes and transferred into culture tubes. Starting with *E. coli* K12W-T, the extraction was carried out as follows: 1.0 ml of the saponification reagent was added to the cells in the culture tubes (two replicates) to cleave the fatty acids from the lipids and convert them to their sodium salts. The tubes were then tightly sealed with a clean Teflon-lined screw cap and vortexed for 10 seconds and placed in boiling water for 5 minutes at 100 °C. After five minutes the tubes were removed from the boiling water and cooled to about 60 °C after which they were again vortexed for 10 seconds. Once no leakage was observed the tubes were heated for a further 25 minutes after which they were cooled to room temperature with cold tap water. The methylation procedure was performed by adding 2.0 ml of the methylation reagent to the content of each tube to convert the sodium form of the fatty acids into fatty acid

methyl esters. The tubes were tightly capped and vortexed for about 10 minutes. Following heating of the tubes in boiling water at 80 °C, the tubes were cooled to room temperature with cold tap water. In order to extract the fatty acid methyl esters from the acidic phase and transfer them into organic phase, 1.25 ml of the extraction reagent was added to each tube and mixed end-to-end in a laboratory rotator for 10 minutes. The aqueous (lower) phase was removed and discarded whilst the top phase was kept in the tube. 3.0 ml of the base wash reagent was added to the tube, vortexed for 10 minutes and allowed to settle. Portion of the top phase in the tube was transferred into GC vials for gas chromatography analysis. The remaining content of the culture tubes were kept in the fridge. The whole procedure was repeated for *S. aureus* NCIMB6571 and *Pseudomonas aeruginosa* NCIMB8295.

2.9.5 Determination of fatty acid composition

The strains were first identified on the basis of the cellular fatty acid profile by a Hewlett-Packard Microbial Identification System (MIS) in the University of Silesia, Poland. Fatty acid methyl ester (FAMES) were detected by a Flame Ionization Detector (FID) using the aerobic method and TSBA library version 3.9 (MIDI, USA).

2.10 Analysis of DNA content of *E. coli* K12 W-T by FTIR

2.10.1 DNA Extraction

The solvent-based extraction protocol is based on Gabor *et al.*, (2003) with some modifications. A single bacterial colony *E. coli* K12W-T strain was used to inoculate a 100 ml starter culture, which was grown overnight at 37 °C in a rotary shaker. After overnight incubation at 37 °C 0.1 ml of each culture was inoculated into 100 ml sterile TSB in 500 ml conical flasks. After 24 hours of incubation at 37 °C 1.0 g l⁻¹ of silver-doped zeolite X was added to the culture and re-

incubated for 30 minutes. 1.5 M sodium chloride and 1 % hexadecylmethylammonium bromide (CTAB; pH 8) were added and cells were homogenized by gentle vortex. 20 % SDS was then added followed by another 2 hours of incubation at 37 °C in a rotary shaker. After incubation, the samples were centrifuged at $14000 \times g$ for 10 minutes and the supernatant was placed in a clean 5 ml microtube. The remaining pellets were re-extracted twice with 500 ml of lyses buffer, homogenized, incubated at 65 °C for 10 min, and centrifuged. All supernatants of the three serial extractions were combined and subjected to further purification. For the DNA recovery test, the three fractions were purified separately for comparison. DNA was purified through two phenol/chloroform/isoamyl alcohol extractions, followed by one chloroform extraction. About 0.7 ml of isopropanol was added and DNA was precipitated overnight at 4 °C. The precipitated DNA was pelleted by centrifuging at $16,000 \times g$, 4 °C, for 10 min, followed by two 70 % alcohol washes, air dried, and redissolved in 200 ml of TE buffer.

2.10.2 FTIR analysis of extracted DNA

The FTIR spectra for the extracted DNA were acquired using a Mattson FTIR spectrometer (Mattson Instruments, UK) equipped with a ZnSe crystal plate attached to the spectrometer with a mercury cadmium telluride A (MCTA) detector and KBr as beam splitter. Measurements were done using 100 scans at 4 cm^{-1} resolution, units of $\log (1/R)$ (absorbance), over the mid-IR region of $1200\text{-}400 \text{ cm}^{-1}$. An air background spectrum was collected at the start of the sample collection. A small sample of the extracted DNA was centered on the ZnSe plate to ensure that it covered the entire crystal surface, and a pressure clamp was used to apply pressure on the filter. The DNA extract was analyzed three times for three different samples. A background spectrum was measured before every sample to compensate for atmospheric conditions around the FT-IR instrument.

2.11 Statistical analysis

All data were analyzed on a computer package SPSS, version 12 for windows and with Microsoft Excel. All experiments relating to the antimicrobial activity silver zeolites on each strain were treated as separate experiments. One-way analysis of variance (ANOVA) within the individual strains, and a two-way analysis of variance across the strains for all concentration dependent and retrieval experiments were used. Before analysis all data were tested for homogeneity of variance, to determine whether they meet the correct criteria for ANOVA. All data were also analyzed for least significant differences (LSD) within the strains for each strain.

Chapter 3

Results and discussion

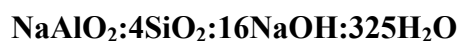
Synthesis, ion exchange and characterization of zeolites

In this chapter the results based on the synthesis and ion exchange and the characterization of silver-loaded zeolites before and after ion exchange are presented

3.1 Synthesis, ion exchange and characterization of zeolite X

3.1.1 Synthesis

As discussed in section 2.1.1 the batch composition for the synthesis is given by:



Three unsuccessful attempts using the above gel composition were made. The fourth attempt however, was successful.

3.1.2 Ion exchange

Ion exchange was carried out on as-synthesized zeolite X as described in Section 2.3.1 followed by re-characterized by, SEM, XRD EDX/X-ray microanalysis and FTIR. The value of the cation exchange capacity as calculated from equation 8.0 was found to be 2.58 meq/g

3.1.3 Characterization

The SEM micrographs in Figures 17 and 18 confirmed the phase purity of the crystal morphology.

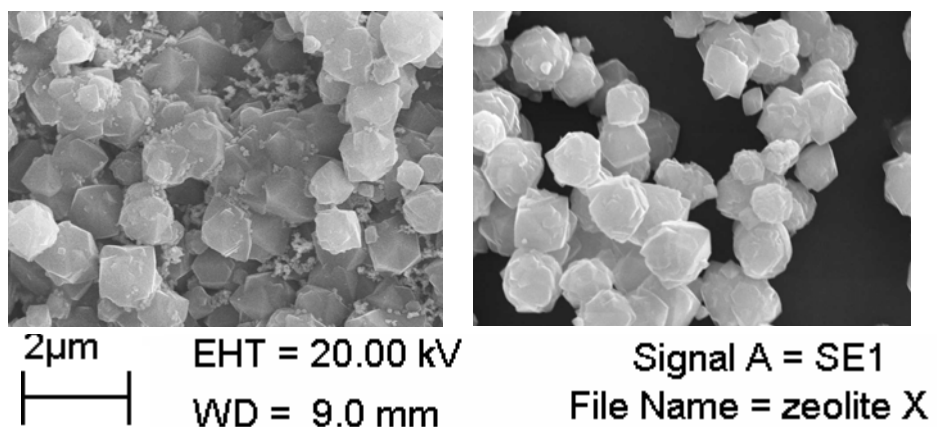


Figure 17: SEM micrographs of zeolite X with silver loadings (left) and without (right)

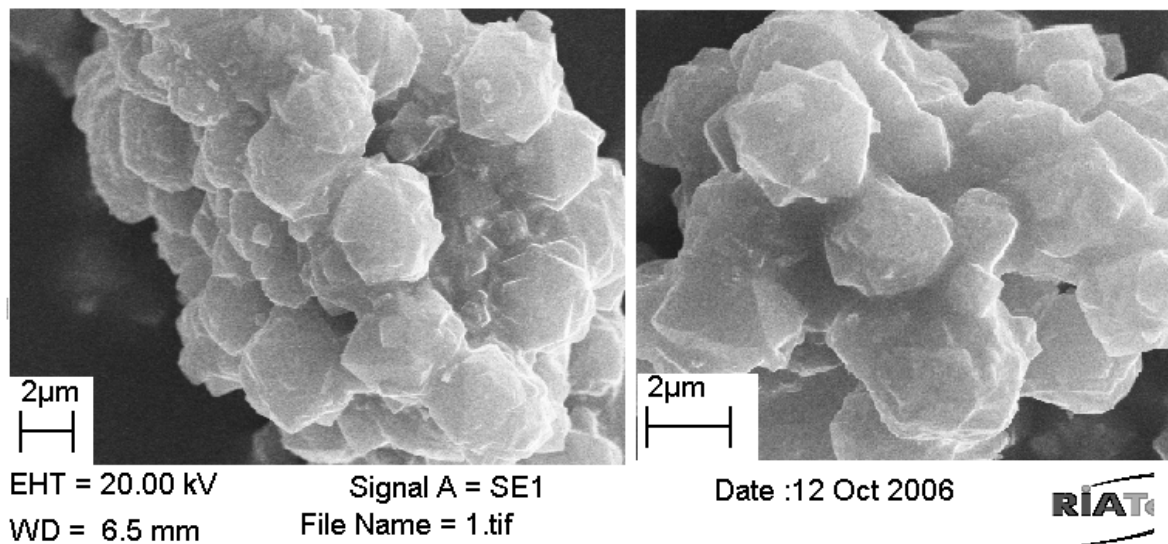


Figure 18: SEM micrographs of silver-exchanged zeolite X showing varying sizes

The SEM micrographs also showed that the particles were closely similar in size and appearance, which suggests that the loading of silver ions into the framework seems to have little or no effect on the size of the zeolite. Crystals varied between 2 – 10 µm and were octahedral with fairly uniform morphology. EDX spectrum detected silver ions in the zeolite framework after loading (Figure 19). The gold peak (arrow) detected in the spectrum is the gold coating of the samples prior to analysis.

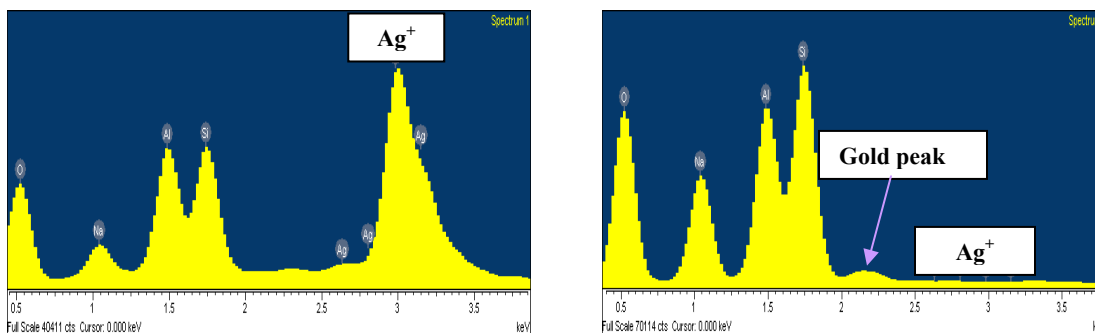


Figure 19: EDX spectra of zeolite X with (left) and without (right) silver loading

EDX also quantified the amount of Ag^+ that were trapped within the framework of zeolite X (cavities or the exchangeable sites) as well as the elemental composition of zeolite X with and without silver ions (Table 9).

Table 9: Elemental composition of zeolite X before and after ion exchange

Element	% Atomic weight	
	Before ion exchange	After ion exchange
Oxygen	56.9	52.6
Sodium	5.3	2.8
Aluminium	15.2	13.0
Silicon	22.6	21.8
Silver	0.0	7.8
Si/Al	1.45	1.56

The elemental composition obtained indicate that the atomic concentration of sodium ions decreased by 41 % after ion exchange. Aluminium ions decreased by 7.7 %. The atomic concentration of silver ions on the other hand increased from near zero to 7.8 % whilst that of silicon remained fairly constant after ion exchange. Hence the ion exchange of sodium ions by silver ions is likely to have been at the exchangeable sites within zeolite X framework.

The corresponding particle size distribution shown in Figure 20 indicates that the sizes of the zeolite particles were similar with the modal distribution being between 2 – 9 μm . The size distribution is typical of a microporous material (Ruihong *et al.*, 2006).

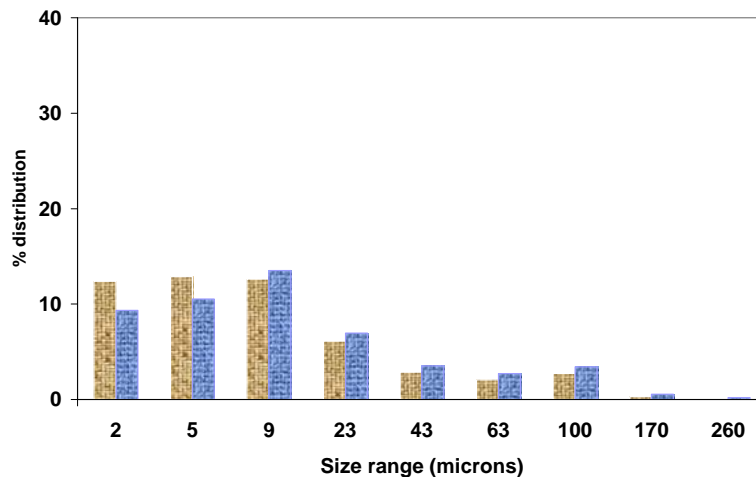


Figure 20: Particle size distribution of zeolite X with silver ions (blue bars) and without (brown bars) silver ions

XRD analysis was carried on zeolite X to monitor the phase purity and crystallization and the purity of the final product (Figure 21).

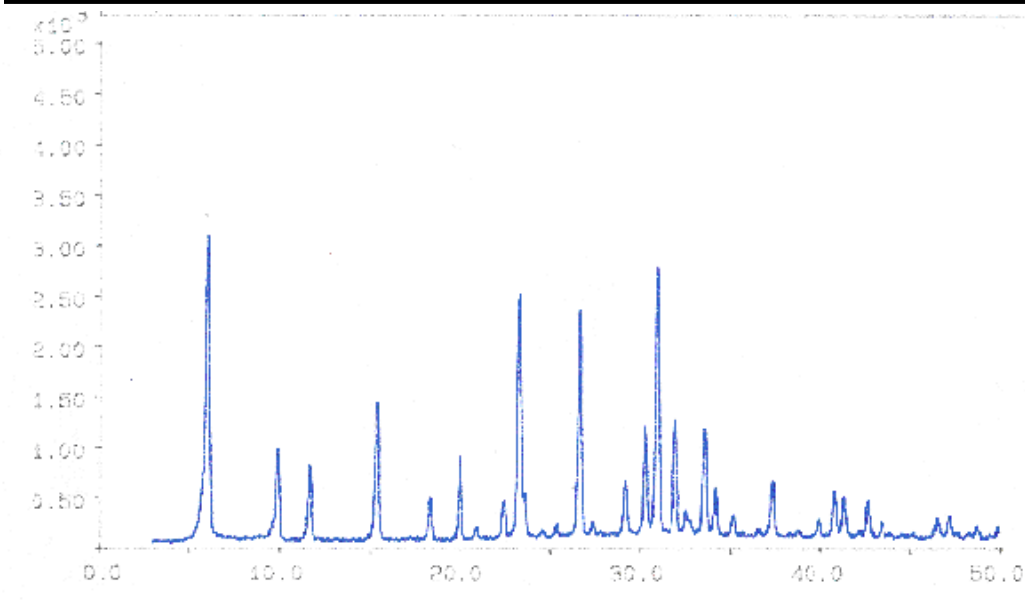


Figure: 21: XRD pattern for zeolite silver-exchanged X along with the reference pattern 38 - 237

The XRD pattern of zeolite X samples must accord with the ICCD standard reference pattern in order to be validated as an as-synthesized zeolite X (Cichocki, 1991). Highly crystalline crystals were obtained as shown by the reflection peaks (Figure 21). There were also no other phases of impurities present in the crystals. Hence, the purity of silver-exchanged zeolite X was validated.

The structural features in the zeolite X and silver-exchanged zeolite X frameworks were analyzed by FTIR which gives information on two classes of vibration:

- (1) vibrations caused by internal stretching of the framework tetrahedra
- (2) vibrations related to the external linkages between tetrahedra

The general infrared assignments in zeolites as proposed by Flanigen *et al.*, (1978) and Mozgawa, (2000) are presented in Table 10.

Table 10: General infrared assignments in zeolites (Flanigen *et al.*, 1978; Mozgawa, 2000)

Internal vibrations	
Asymmetric stretch	1250 – 950
Symmetric stretch	720 – 650
T – O bend	500 – 420
External T – O linkages	
Double ring	650 – 500
Pore opening	420 – 300
Symmetric stretch	750 – 820
Asymmetric stretch	1150 – 1050
Internal vibrations	
Asymmetric stretch	1250 – 950
Symmetric stretch	720 – 650
T – O bend	500 – 420
External T – O linkages	
Double ring	650 – 500
Pore opening	420 – 300
Symmetric stretch	750 – 820
Asymmetric stretch	1150 – 1050

Although each zeolite has a characteristic FTIR pattern some common features are observed for all zeolites.

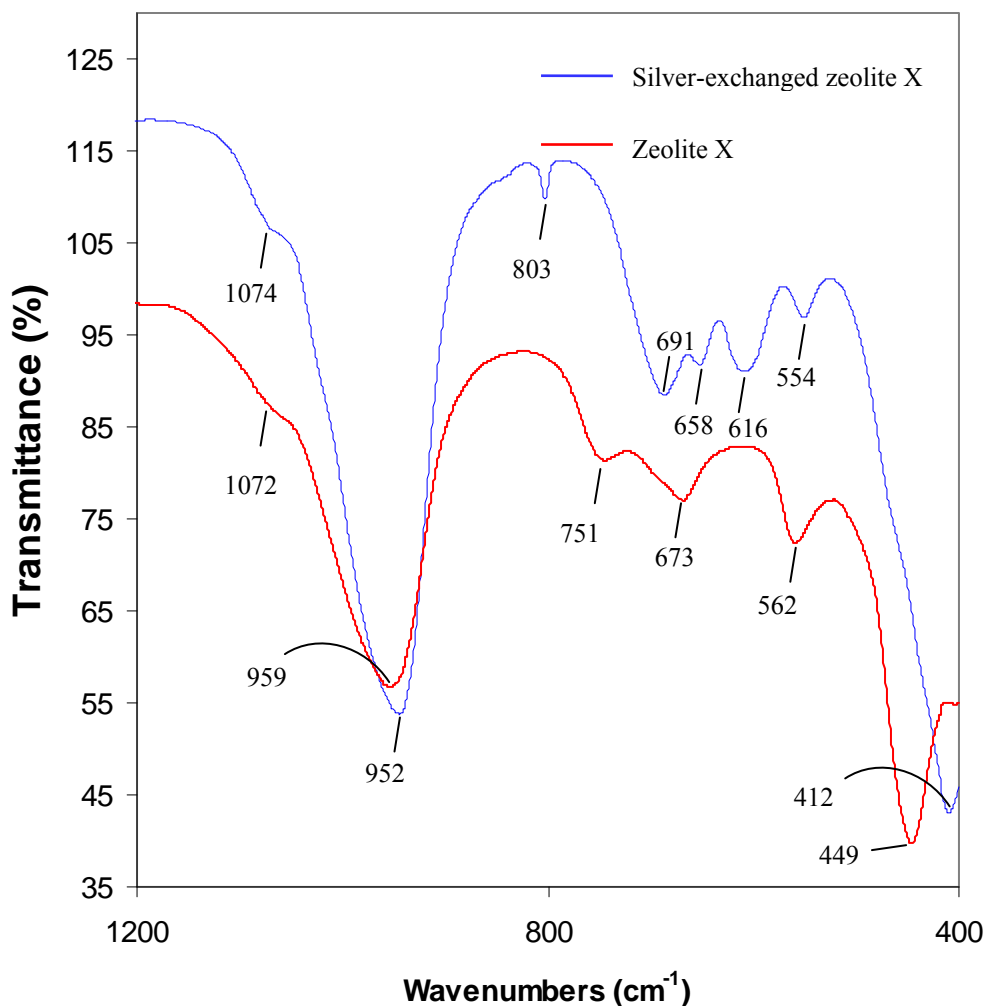


Figure 22: Results of the FTIR spectra of zeolite X with and without silver ions

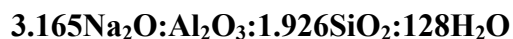
The mid-FTIR spectra of the as-synthesized zeolite X (red line) and silver-exchanged zeolite X (blue line) are given in Figure 22 in the region of lattice vibrations (1200 – 400 cm⁻¹). A large broad band was observed in the region 950 – 960 cm⁻¹ in both samples. This band can be attributed to the overlap of the asymmetric vibrations of Si – O (bridging) and Si – O⁻ (non-

bridging) bonds. The band shifted towards a slightly higher frequency of 1074 cm^{-1} . The symmetric stretching of the external T – O linkages occurred at 751 cm^{-1} whilst the symmetric stretching due to the internal vibrations of the zeolite X framework tetrahedra occurred at 673 cm^{-1} . Vibrations associated with the double six rings (D6R) that connect the sodalite cages occurred at 562 cm^{-1} . The band at 449 cm^{-1} is assigned to the internal vibrations due to the bending of the T – O tetrahedra. This band shifted toward a lower frequency of 412 cm^{-1} after ion exchange.

3.2 Synthesis, ion exchange and characterization of zeolite A

3.2.1 Synthesis of zeolite A

As discussed in section 2.1.2 the batch composition for the synthesis is given by

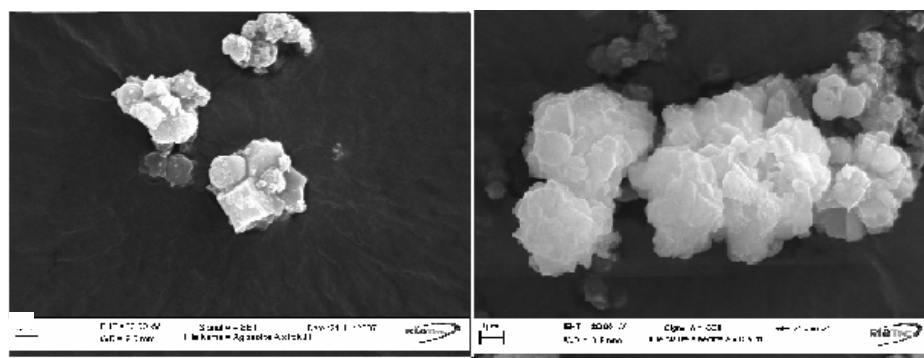


3.2.2 Ion exchange

Ion exchange was carried out on as-synthesized zeolite A as described in section 2.3.2. The exchange capacity as calculated from equation 8.0 was found to be 13.5 meq/g

3.2.3 Characterization

Similar characterization was carried out on zeolite A as described in section 3.1.3. The SEM micrograph in Figure 23 shows that zeolite A crystals were highly crystalline whereas that of silver-exchanged zeolite A appeared to be partly amorphous.



Size shown = 1 μm

Figure 23: SEM micrographs of zeolite A with silver loadings (left) and without silver loadings (right)

EDX spectrum detected silver ions in the zeolite framework after loading (Figure 24).

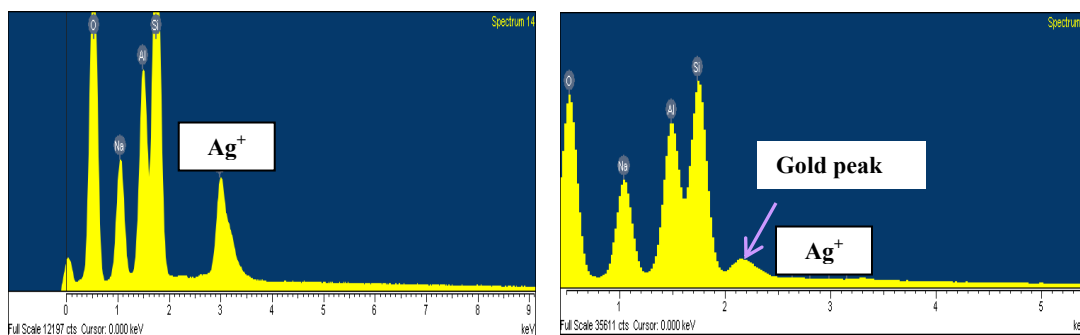


Figure 24: EDX spectra of zeolite A with silver loadings (left) and without (right) silver loading

XRD analysis was carried out on zeolite A to monitor the phase purity and crystallization and the purity of the final product. The XRD spectrum of silver-exchanged zeolite A showed highly crystalline spectrum as evident in the distinct reflected peaks Figure 25. The XRD pattern of zeolite A samples accorded with the ICDD standard reference pattern (39 - 222). Hence the sample was validated as an as-synthesized zeolite A.

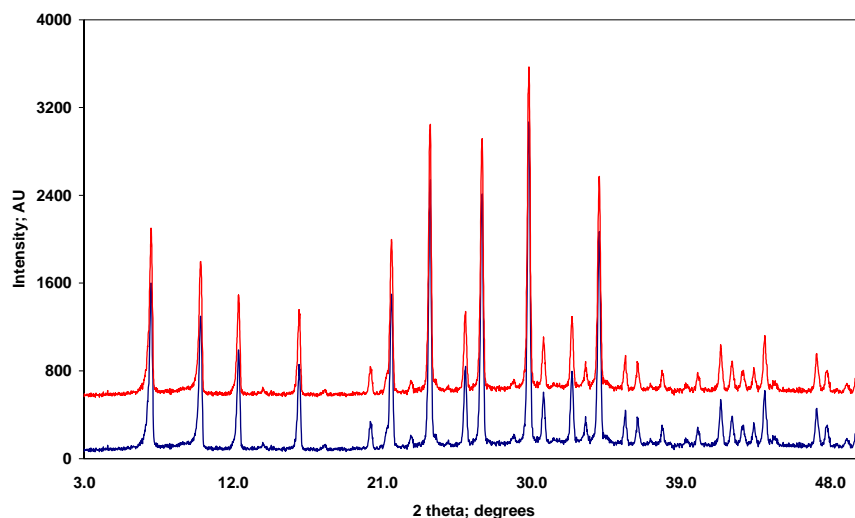


Figure: 25: XRD pattern for zeolite A with silver loadings (red line) and without silver loadings (blue line) along with the reference pattern 39 - 222

The elemental composition obtained indicates that the atomic concentration of sodium ions decreased by 42 % (w/w) after ion exchange. Aluminium ions decreased by 5 % (w/w). The atomic concentration of silver ions on the other hand increased from near zero to 6.75 % (w/w) whilst that of silicon remained fairly constant after ion exchange (Table 11).

Table 11: Elemental composition of zeolite A before and after ion exchange

Element	% Atomic weight	
	Before ion exchange	After ion exchange
Oxygen	57.4	55.1
Sodium	5.3	3.0
Aluminium	15.2	14.7
Silicon	22.1	22.0
Silver	0.0	6.8
Si/Al	1.45	1.44

Hence, the ion exchange at the exchangeable sites within zeolite A framework occurred mostly with sodium.

The particle size distribution of zeolite A with and without silver ions is shown in Figure 26. The modal distribution occurred at 2 μm for zeolite A and 9 μm for silver-exchanged zeolite A. This might be due to agglomeration of zeolite A particles.

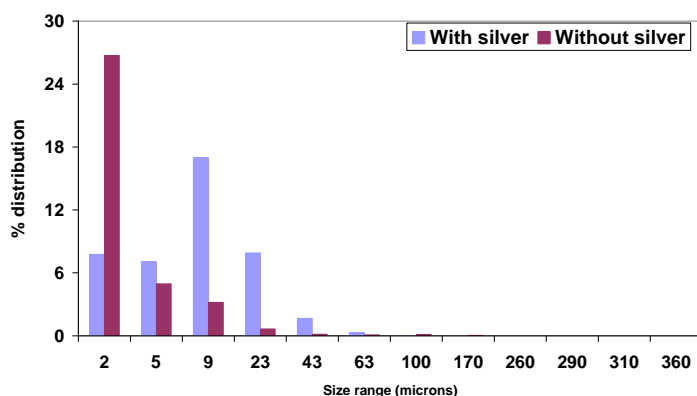


Figure 26: Particle size distribution of zeolite A with (blue bars) and without (brown bars) silver ions

The mid-FTIR spectra of the as-synthesized zeolite A (red line) and silver-exchanged zeolite A (blue line) are given in Figure 27 in the region of lattice vibrations ($1200 - 400 \text{ cm}^{-1}$). A large broad band was observed in the 977 cm^{-1} in both samples. This band can be attributed to the overlap of the asymmetric vibrations of Si – O (bridging) and Si – O⁻ (non-bridging) bonds. The band shifted towards a slightly higher frequency of 978 cm^{-1} . The symmetric stretching of the external T – O linkages occurred at 743 cm^{-1} whilst the symmetric stretching due to the internal vibrations of the zeolite A framework tetrahedra occurred at 670 cm^{-1} . These bands shifted towards slightly higher frequencies of 744 cm^{-1} and 674 cm^{-1} respectively. Vibrations associated with the double six rings (D6R) that connect the sodalite cages occurred at 533 cm^{-1} (shifted toward a slightly higher frequency of 555 cm^{-1}). The band at 449 cm^{-1} is assigned to the internal

vibrations due to the bending of the T – O tetrahedra. This band shifted toward a lower frequency of 412 cm^{-1} after ion exchange.

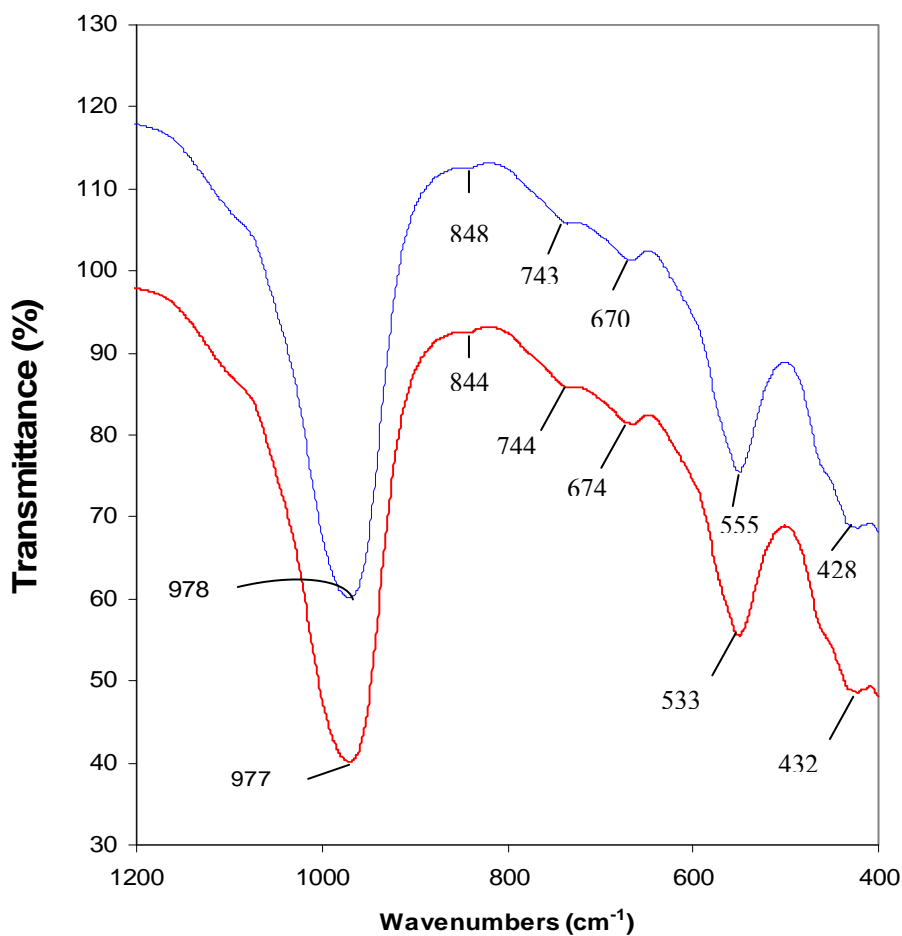


Figure 27: FTIR spectrum of zeolite A with silver-loading (blue line) and without silver loading (red line).

3.3 Synthesis, ion exchange and characterization of AgHAP

3.3.1 Synthesis

As discussed in Section 2.1.3 the synthesis of high-alumina Phillipsite was synthesized from the following molar gel composition:

1.53Na₂O: 0.44K₂O:Al₂O₃:5SiO₂:82.7H₂O (Cichocki, 1991)

3.3.2 Ion exchange

Ion exchange was carried out on as-synthesized high-alumina Phillipsite as described in section 2.3.1. The exchange capacity as calculated from equation 8.0 was found to be 3.36×10^4 meq/g. Thus high-alumina Phillipsite has the highest CEC compared with zeolite and zeolite A. Once ion exchange was established, samples were re-characterized by SEM, EDX/ X-ray microanalysis, XRD and FTIR.

3.3.3 Characterization

The SEM micrographs in Figures 28 confirmed the phase purity of the crystal morphology. The particles were similar in size and appearance which suggests that the loading of silver ions into the framework seems to have little or no effect on the size of the zeolite.

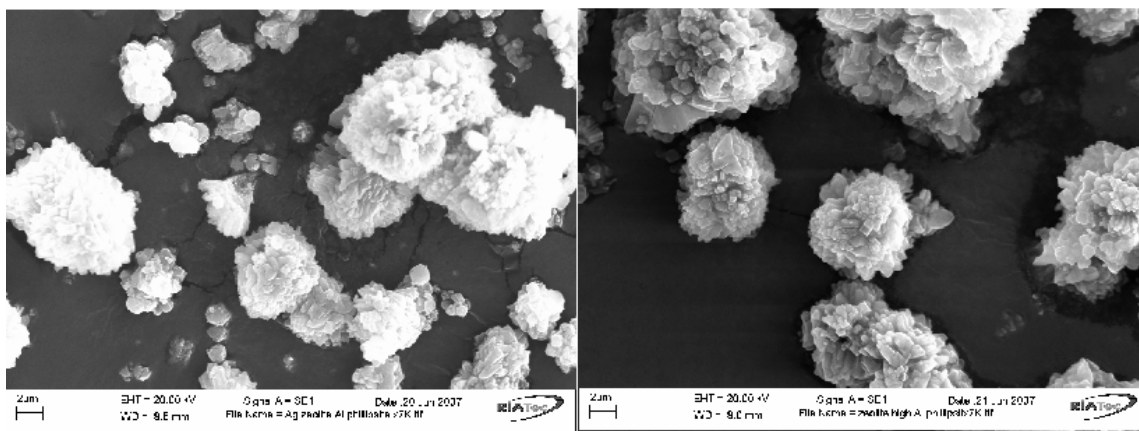


Figure 28: SEM micrograph of high aluminium Phillipsite with silver loading (left) and without silver loading (right)

EDX spectrum showed detection of silver ions in the zeolite framework after loading (Figure 29). The gold peak detected in the spectrum of silver-exchanged high alumina was due to the sample being gold-coated prior to the analysis.

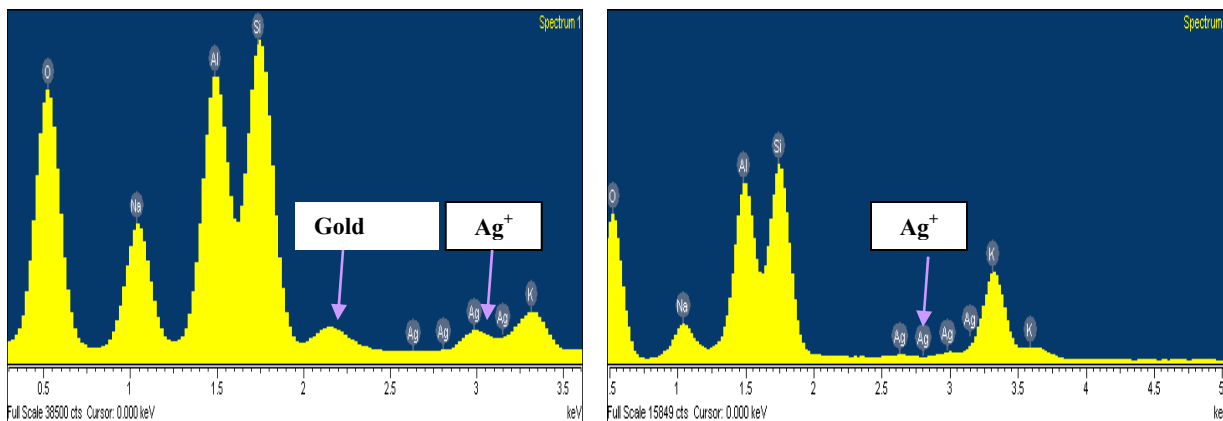


Figure 29: EDX spectra of high-alumina Phillipsite with silver loading (left) and without silver loading (right)

The elemental composition (Table 12) obtained indicates that the atomic concentration of sodium by 36.5 % after ion exchange. Aluminium ions decreased by 4.6 % and potassium by 38.7 %. The atomic concentration of silver ions on the other hand increased from near zero to 3.71 % whilst that of silicon remained fairly constant after ion exchange. From the changes in atomic concentrations, it follows that ion exchange occurred mostly with potassium than with sodium.

Table 12: EDX chemical composition analysis of high-alumina Phillipsite before and after ion exchange

Element	Atomic weight %	
	Before ion exchange	After ion exchange
O	67.6	60.5
Na	5.9	3.8
Al	13.6	13.0
Si	15.7	15.5
K	5.8	3.5
Ag	0.0	3.7
Si/Al	1.2	1.2

Highly crystalline crystals were obtained as shown by the XRD reflection peaks (Figure 30). There were also no other phases of impurities present in the crystals. Hence the purity of silver-exchanged high-alumina Phillipsite was validated.

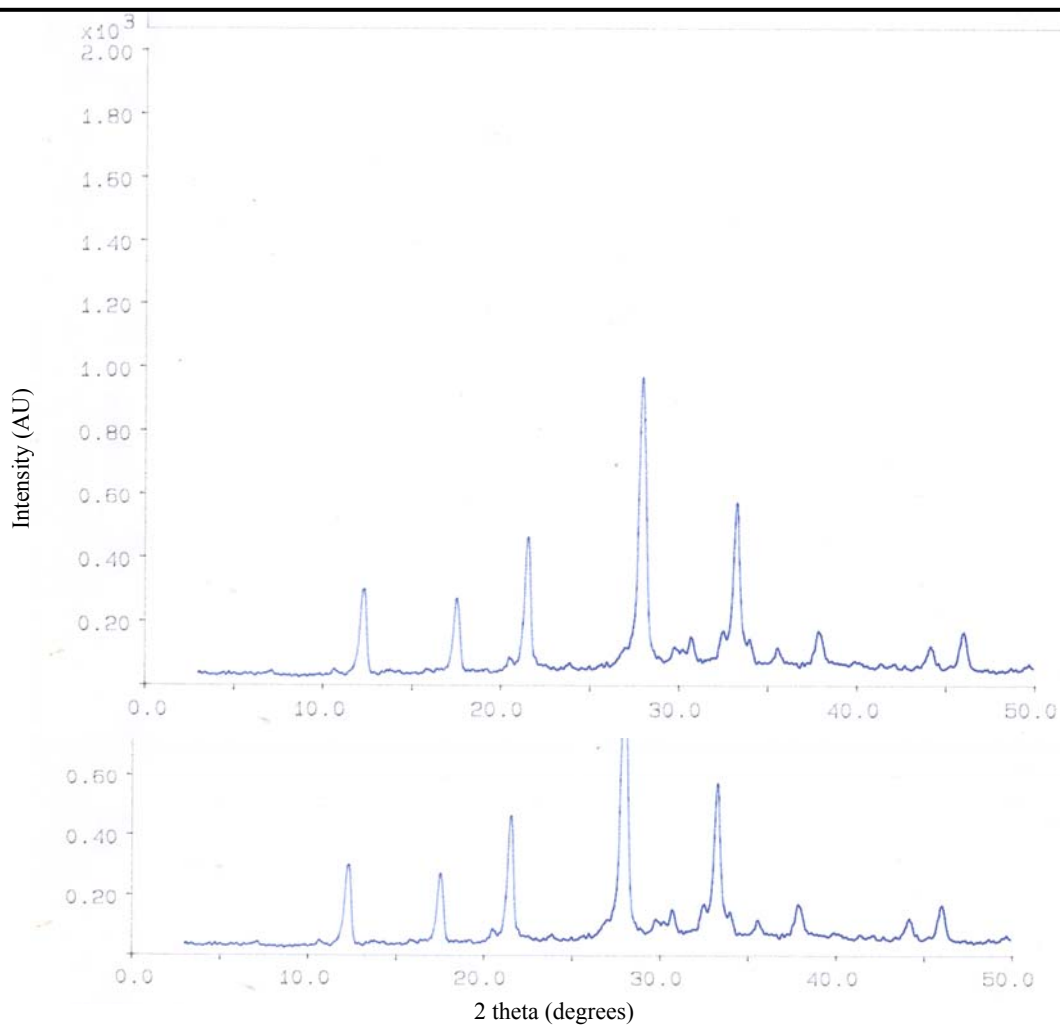


Figure 30: XRD spectra for high aluminium Phillipsite with silver loading (top) and without silver loading (bottom)

The mid-FTIR spectra of the as-synthesized high-alumina Phillipsite (red line) and silver-exchanged high-alumina Phillipsite (blue line) are given in Figure 31 in the region of lattice vibrations (1200 – 400 cm^{-1}). The larger broad band attributed to the overlap of the asymmetric vibrations of Si – O (bridging) and Si – O⁻ (non-bridging) bonds was observed 973 cm^{-1} in both samples. The band shifted towards a higher frequency of 982 cm^{-1} . The symmetric stretching of the external T – O linkages occurred at 745 cm^{-1} whilst the symmetric stretching due to the internal vibrations of the high-alumina framework tetrahedra occurred at 681 cm^{-1} . The band at 745 cm^{-1} shifted towards a slightly higher frequency of 749 cm^{-1} whereas the band at 681 cm^{-1} shifted towards a lower frequency of 749 cm^{-1} and 677 cm^{-1} respectively.

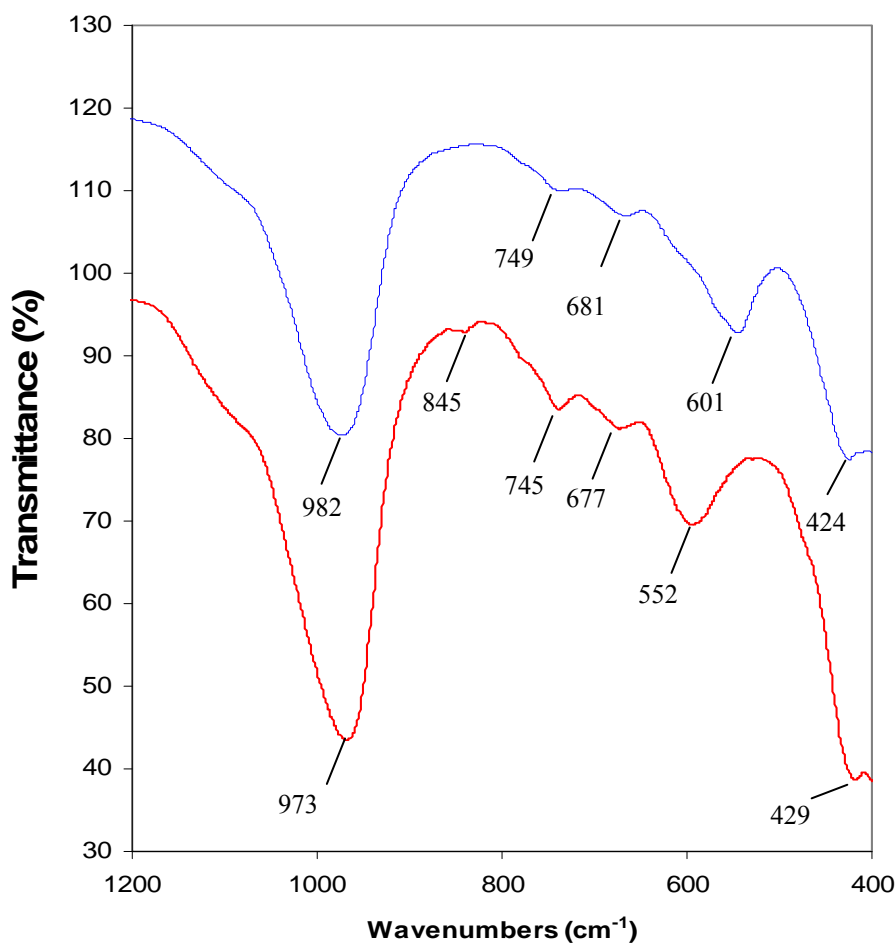


Figure 31: FTIR spectra of high aluminium Phillipsite with silver loading (blue line) and without silver loading (red line)

Vibrations associated with the double six rings (D6R) that connect the sodalite cages occurred at 601 cm^{-1} (shifted towards a lower frequency of 552 cm^{-1}). The band at 424 cm^{-1} is assigned to the internal vibrations due to the bending of the T – O tetrahedra. This band shifted toward a lower frequency of 429 cm^{-1} after ion exchange.

3.4 Analcime

3.4.1 Synthesis

The hydrothermal synthesis of analcime and silver-doped analcime is described in Section 2.1.4.

3.4.2 Characterization

XRD spectra of analcime of undoped, and of 5 %, 10 % and 20 % silver-doped samples are shown in Figure 32. Highly crystalline particles were obtained for all loadings and for the undoped analcime (Kwakye-Awuah *et al.*, 2008).

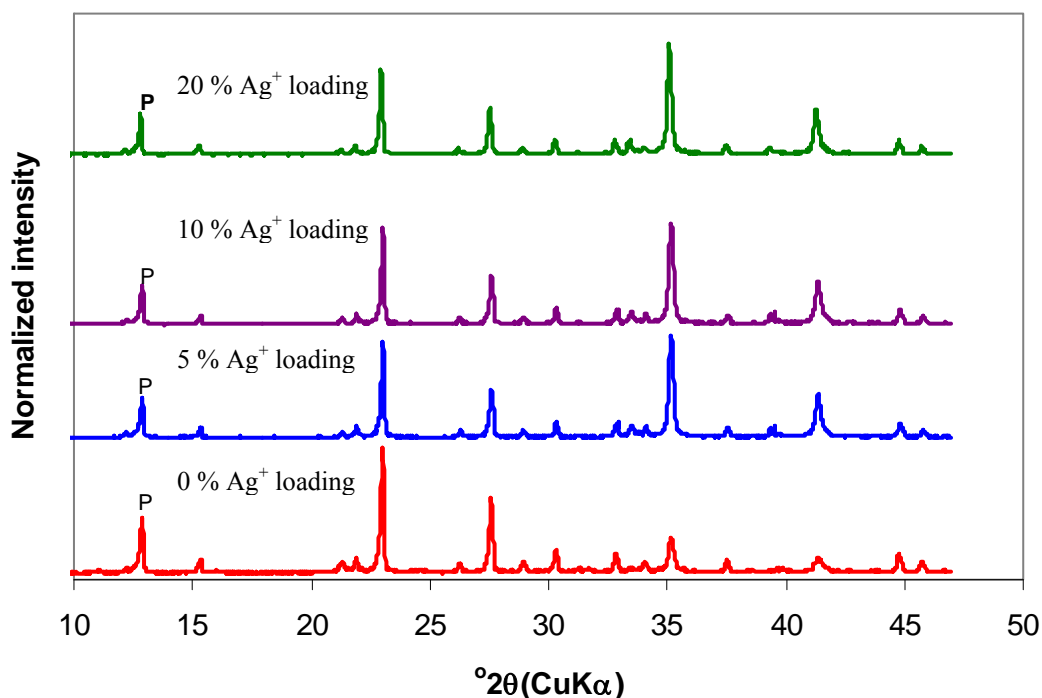
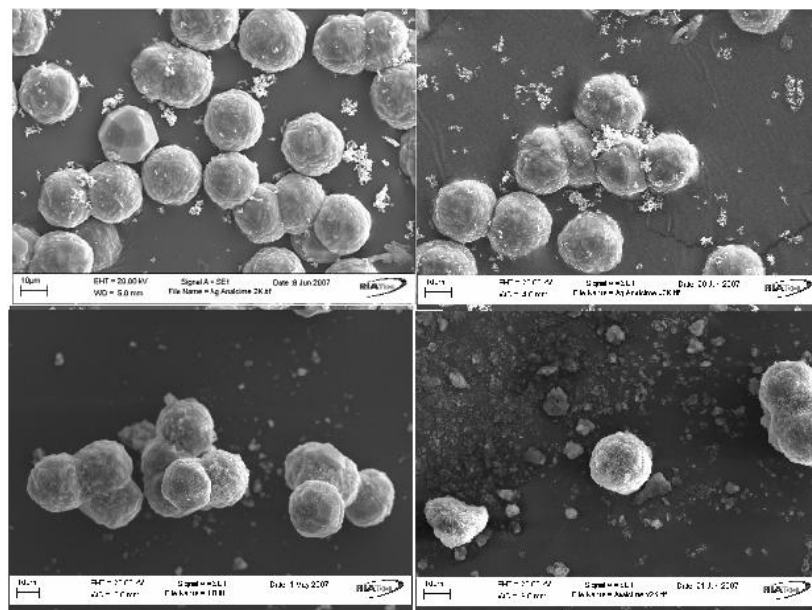


Figure 32: XRD spectra of silver-doped analcime with different loading of silver ions

The doping of analcime with Ag^+ resulted in 0.2° shift of the peaks towards the right for 20 % silver loading although the crystallinity of the crystals were retained. The peaks intensities were not reduced indicating that there were no carbonaceous materials present the analcime crystals (Balandis and Traidaraite, 2007; Kohoutková *et al.*, 2007). It is also seen from Figure 32 that traces of zeolite P is identified at 11.5° , 22° and 23° . These peaks can be considered to represent a intermediate phase which converts to analcime with time (Balandis and Traidaraite, 2007).

The SEM images of analcime with and without silver doping are shown in Figure 33.



Size shown = 10 μm

Figure 33: SEM micrograph of silver-doped analcime obtained with (top left): no loading of silver ions, (top right): 5 % loading of silver ions, (bottom left): 10 % loading of silver and (bottom right): 20 % loading of silver ions

SEM photograph confirmed that the crystallographic structure of undoped and silver-doped analcime as icositetrahedral (Dyer and White 1999). The EDX spectra detected the presence of

silver ions for all loadings (Figure 34). The loadings were higher for a 20 % (w/w) substitution of Ag^+ . The spectra also show detection of Ag^+ .

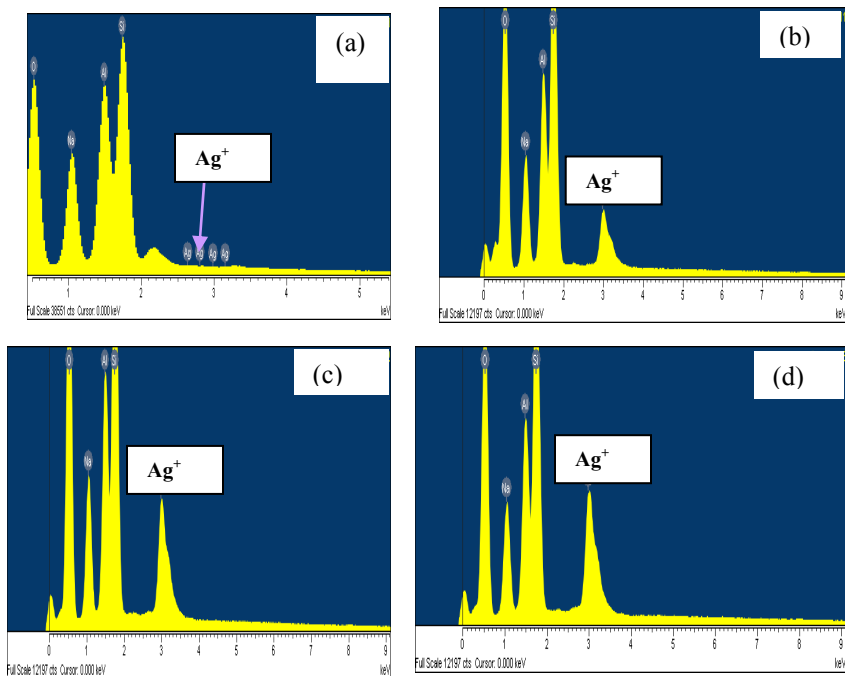


Figure 34: Energy dispersive X-ray spectra of (a): undoped analcime, (b): analcime doped with 5 % Ag^+ , (c): analcime doped with 10 % Ag^+ and (d) analcime doped with 20 % Ag^+

The elemental composition obtained from the EDX analysis is shown in Table 13. The gold peak (marked by an arrow) detected in the spectrum was due to the samples being gold coated prior to analysis.

Table 13: EDX analysis of the elemental composition with various loading of silver ions into the analcime framework ($N = 4$)

Element	Atomic weight (%) \pm stdev*			
	0 % Ag^+ loading	5 % Ag^+ loading	10 % Ag^+ loading	20 % Ag^+ loading
O	54.4	59.3 ± 0.14	71.1 ± 0.12	72.7 ± 0.12
Na	13.3	10.6 ± 0.06	8.4 ± 0.06	8.0 ± 0.06
Al	13.1	10.5 ± 0.05	6.8 ± 0.05	6.2 ± 0.05
Si	19.2	19.6 ± 0.10	12.3 ± 0.07	11.1 ± 0.06
Ag	0.0	0.4 ± 0.10	1.4 ± 0.01	2.1 ± 0.10

No Ag^+ was detected for the undoped analcime (Table 19). The EDX also quantified the amount of Ag^+ trapped within the analcime framework (cavities or the exchangeable sites). An amount of 0.3 % (w/w) of Ag^+ was either trapped within the analcime structure or at the exchangeable sites upon 5 % (w/w) substitution of Ag^+ . 1.4 % (w/w) was trapped within the cavities or at the exchangeable sites with 10 % Ag^+ with equivalent substitution of Ag^+ , and 2.1 % (w/w) was trapped within the cavities or at the exchangeable sites upon 20 % (w/w) substitution of Ag^+ . As a result there was 19 % (w/w) aluminium reduction on doping with 5 % Ag^+ , 47 % (w/w) aluminium reduction on doping with 10 % Ag^+ and 53 % aluminium reduction on doping with 20 % Ag^+ .

Figure 35 shows the particle size distribution of undoped analcime particles and analcime doped with Ag^+ .

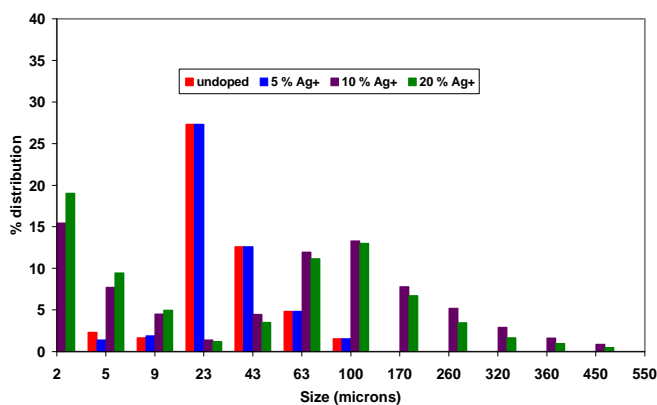


Figure 35: Particle size distribution of analcime doped with 0, 5, 10 and 20 % doping of silver ions

The sizes of the zeolite particles were not the same. The modal distribution of the particles occurred at 23 μm for undoped and for 5 % Ag^+ -doped analcime, 2.0 μm for 10 % and 20 % Ag^+ -doped analcime. Results obtained for the FTIR analysis are shown in Figure 36. The FTIR spectrum for undoped analcime is shown in the red line. The main band centered at 1026 cm^{-1} is

attributed to the asymmetric stretching of the Si – O and Al – O belonging to the SiO₄ and AlO₄ tetrahedra (Aronne *et al.*, 1997; Sitarz *et al.*, 2001).

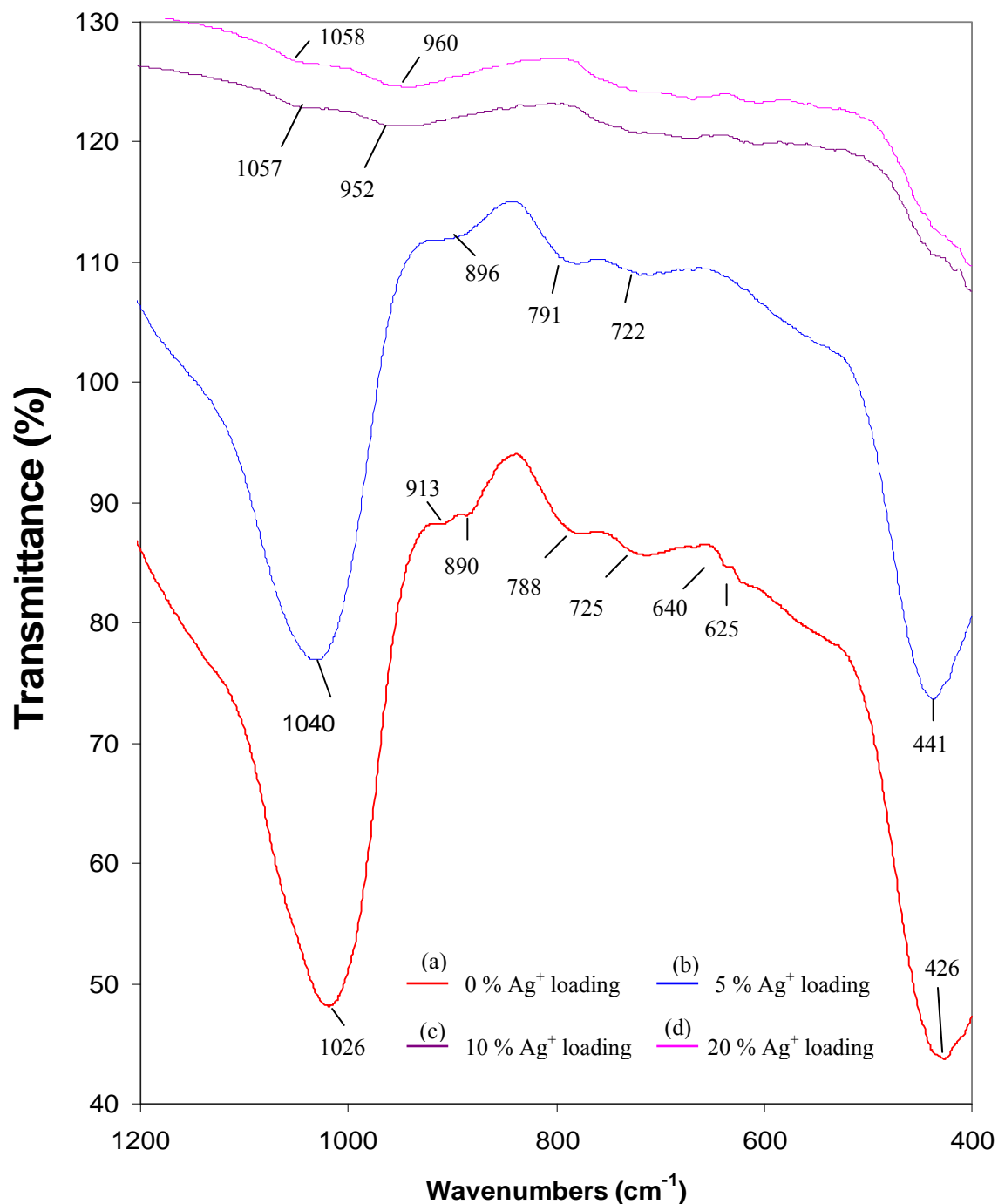


Figure 36: Fourier transformed infrared spectroscopy spectra of (a): undoped analcime, (b): analcime doped with 5 % Ag⁺, (c): analcime doped with 10 % Ag⁺ and (d) analcime doped with 20 % Ag⁺

The corresponding internal bending modes of the Si – O – Al bonds give rise to a transmission band at 426 cm^{-1} (Sitarz *et al.*, 1997; Mozgawa, 2001; Novotna *et al.*, 2003). Moreover, three bands were detected in the $500 - 800\text{ cm}^{-1}$ region. The first and second occurred at 598 cm^{-1} and 622 cm^{-1} respectively. Both bands are narrow and exhibit the lowest relative intensity. The third one occurred at 728 cm^{-1} and is broader than the first and second. According to Mozgawa (2001) these bands can be attributed to the internal vibration symmetrical stretching of the particles. In the case of analcime, these bands are attributed to the external vibrations of the 4-membered double rings (D4R) and the 6-membered single rings (S6R) units respectively (Mozgawa, 2001). The band centered at 888 cm^{-1} and 917 cm^{-1} are attributed to the asymmetric stretching mode of the Si – O – Al bonds (Mozgawa, 2001; Novotna *et al.*, 2003). On doping the analcime with 5 % Ag^+ (Figure 36) there was no change in the spectrum (with reference to the absorption bands compared with the undoped analcime) with the exception of the band centered at 888 cm^{-1} which was reduced significantly. Further doping (10 % and 20 %) of Ag^+ resulted in the loss of bands at 1026 cm^{-1} and 426 cm^{-1} in each case and the peak intensities of the remaining bands seems to have been significantly reduced. This is due to the shielding effect caused by silver ions and silver particles (Kwakye-Awuah *et al.*, 2008a) Results obtained for the ICP-AES analysis are shown in Table 14.

Table 14: Amount of Ag^+ detected in the supernatant (ICP-AES) for undoped analcime and for various loadings of Ag^+

% silver doping	[Ag^+] in supernatant (ppm)
0	0.0
5	3.8
10	7.5
20	27.9

Silver ions were not detected in the supernatant of the undoped analcime. Ag^+ ions were also detected in minute quantities in the supernatant compared with the amount trapped in the analcime framework.

3.5 Discussion

Zeolite X is aluminium-rich analogue of the naturally occurring mineral Faujasite (Yeom and Kim, 1997). Exchangeable cations that balance the negative charge of the aluminosilicate framework of zeolite X are found within the zeolite cavities at the sites shown in Figure 8. Constant trapping of heavy metal cations in zeolite structure is one of the possible ways of cation immobilization and making them harmless (Mozgawa, 2000). Chemical immobilization is based on ion exchange of alkali earth or alkaline earth metal cations with heavy metal cations. After ion exchange, the post heat treatment at a slightly higher temperature allowed the introduced Ag^+ to find and occupy the energetically stable sites in the zeolite framework. The XRD results obtained indicates that there were no changes in the structural units of zeolite X after ion exchange. Hence the total number of cations (Na^+ and Ag^+) did not change after ion exchange. Generally, the bulk zeolite X gel fully crystallizes after just 8 hours (Coutinho and Balkus Junior, 2002). XRD data also indicate that longer hydrothermal treatments of zeolite X synthesis occasionally produce the thermodynamically favoured phases such as zeolite P as in impurity in the bulk gel (Coutinho and Balkus Junior, 2002). Hence for this study zeolite X was hydrothermally synthesized for 8 hour duration.

The SEM results showed that the aggregated octahedral products were translucent crystals of Faujasite type X, with a modal diameter of 2 – 10 μm . Further EDX experiments confirmed the mean Si/Al ratio of 1.1. Araujo *et al.*, (1999) reported that the introduced silver ions are

subjected to different influences of local environment depending on the occupied site. According to Araujo *et al.*, (1999) the occupied sites include near a non-bridging oxygen (NBO) and near a bridging oxygen which surrounds an Al^{3+} ion in four fold coordination. The silver ions once exchanged are likely to be held in the ionic state in the zeolite framework. This is because silver atoms can only be reduced intrazeolitically by heating, by reaction with reducing agents or by sorption of metal atoms (Kim *et al.*, 1997). In this study the temperature at which the zeolites were dried after ion exchange was lower than the synthesis temperature. Hence reduction of silver ions to silver particles was minimal. In addition no reducing agents were used during the synthesis and ion exchange process. Hence for this study it is assumed that most of the silver within the zeolite framework were held as ions.

Replacements of Na^+ by Ag^+ causes an increase in intensity and a shift in frequency towards a lower frequency of the (Flanigen *et al.*, 1978; Mozgawa, 2000) in the range of pseudolattice vibration. For the FTIR analysis appreciable changes were observed in the region of 600 cm^{-1} – 800 cm^{-1} after ion exchange. The symmetric stretching of the external T – O linkages shifted towards a lower frequency of 691 cm^{-1} whilst the symmetric stretching due to the internal vibrations of the zeolite X framework tetrahedra shifted towards a lower frequency of 658 cm^{-1} . The vibrations associated with the double six rings (D6R) that connect the sodalite cages also shifted towards a lower frequency of 554 cm^{-1} . Two new bands were formed at 803 cm^{-1} and 616 cm^{-1} . These bands can be assigned to the symmetric stretching of the external T – O linkages and symmetric stretching of the internal vibrations within the framework of silver-exchanged zeolite X.

Silver-doped analcime was successfully synthesized from kaolinite in the laboratory (Figure 32). Ag^+ ions were detected as verified by the EDX spectra (Figure 33). The SEM photograph confirmed a crystallographic structure of icositetrahedral (Dyer and White 1999) for undoped

and for all loadings. Since the particle sizes of the particles were not the same, the surface area of the zeolite available for adsorption was also different (Figure 35). The particle size per volume of the particles showed two peaks when doped with Ag^+ as against none from the undoped analcime. It is known that the symmetric and asymmetric stretching modes of the Si – O and Al – O bonds with n bridging oxygen (where n is the number of Si – O or Al – O tetrahedra) are IR active in the $800 - 1300 \text{ cm}^{-1}$ with the Si – O bonds being stronger than the Al – O bonds (Line *et al.*, 1996; Gruciani and Gualtieri 1999; Novotna *et al.*, 2003; Kohoutková *et al.*, 2007). Consequently, the isomorphous substitution of the Al atoms with a transition Ag^+ replaced some of the Al atoms within the framework of the analcime. This is confirmed by the results obtained from the elemental composition (Table 18). It is known that the Ag – O bonds (near 995 cm^{-1}) are weaker than the Al – O bonds (Sitarz *et al.*, 2001). There is no evidence of such bonds from the FTIR spectra (Figure 36). The main absorption bands on doping the analcime with 10 % and 20 % Ag^+ are centered at lower values of 954 cm^{-1} , 956 cm^{-1} and 850 cm^{-1} , instead of absorption bands at 1200 cm^{-1} , 1100 cm^{-1} , 950 cm^{-1} , 900 cm^{-1} for undoped analcime. This can be attributed to the shielding Ag^+ provided due to the isomorphous substitution (Kwakyeh-Awuah *et al.*, 2008b). It is therefore likely that some bonds were unable to vibrate completely. The XRD patterns (Figure 32) shows the shift in diffraction peaks when doped with Ag^+ . The fact that the crystallinity of the structures was not destroyed implies that the D4R and D6R rings were unaffected by the presence of Ag^+ (Seok *et al.*, 2000). This can confirm that Ag^+ was trapped within the framework including the exchangeable sites. The position of the IR ring bands depend on the Si/Al ratio and the degree of ring deformation (Aronne *et al.*, 1997; Hovis *et al.*, 2002). The decrease in the number of ring members shifts the characteristic bands towards higher wave numbers (Aronne *et al.*, 1997). In this work however, there is no evidence of such a shift as the main absorption bands are lower. From the FTIR spectra the following findings are evident: (1)

Doping the analcime with lower amount of Ag^+ did not cause changes for internal and external stretching modes. The amount of Ag^+ trapped within the analcime framework (Table 18) is 0.3 % (w/w). This depicts that analcime can tolerate doping at this concentration (Kwakyee-Awuah *et al.*, 2008b). (2) Doping the analcime with higher amounts of Ag^+ resulted in the 1.4 % and 2.1 % (w/w) being trapped in the frame work with significant reduction of most absorption bands. This can be attributed to the shielding effect of silver ions and silver particles (Kwakyee-Awuah *et al.*, 2008b) These observations suggest that the analcime structure (particularly the D4R and S6R members) were unable to vibrate as a result of the doping with larger amounts of Ag^+ . However, it is worth noting that the results from the XRD, SEM and/or particle size analysis are not consistent with this suggestion.

Chapter 4

Results and discussion

Antimicrobial activity of silver-loaded zeolites

The antimicrobial activity includes concentration dependence of silver exchanged zeolites produced in this study are presented in this chapter

4.1 Antimicrobial activity of silver-exchanged zeolite X

4.1.1 Concentration dependence for a 24-hour duration

Antibacterial tests were performed against gram-negative *E. coli* K12W-T and *P. aeruginosa* NCIMB8295 and gram-positive *S. aureus* NCIMB6571 using TSB as the growth medium (Section 2.5.1). The results obtained (Table 15) show the presence of silver-loaded zeolite X at concentrations of 0.15, 0.25, 0.5 and 1.0 g l⁻¹ resulted in complete inhibition (minimum detection limit of the method was 33.3 CFU ml⁻¹) of *E. coli* K12W-T within two hours. Similar antimicrobial effects were obtained for *S. aureus* NCIMB6571 and *P. aeruginosa* NCIMB8295.

Table 15: Results showing the antimicrobial activity of silver exchanged zeolite X against *E. coli* K12 W-T for a duration of 24 hours with different concentrations of silver-exchanged zeolite X.

Time (h)	Average Log(cfu/ml) of <i>E. coli</i> K12 W-T with:					
	0 gl ⁻¹ AgZ-X ± stdev	Z-X ± stdev	0.15 gl ⁻¹ AgZ-X ± stdev	0.25 gl ⁻¹ AgZ-X ± stdev	0.5 gl ⁻¹ AgZ-X ±stdev	1.0 gl ⁻¹ AgZ-X ± stdev
0	5.81± 0.01	5.76±0.05	5.78±0.03	5.69±0.04	5.68±0.02	5.76±0.04
2	6.05±0.03	6.02±0.01	1.50±0.00	1.50±0.00	1.50±0.00	1.50±0.00
4	7.43±0.01	7.42±0.01	1.50±0.00	1.50±0.00	1.50±0.00	1.50±0.00
6	8.69±0.03	8.70±0.02	1.50±0.00	1.50±0.00	1.50±0.00	1.50±0.00
8	8.89±0.02	8.94±0.03	1.50±0.00	1.50±0.00	1.50±0.00	1.50±0.00
10	9.04±0.03	9.06±0.03	1.50±0.00	1.50±0.00	1.50±0.00	1.50±0.00
12	9.16±0.01	9.16±0.02	1.50±0.00	1.50±0.00	1.50±0.00	1.50±0.00
24	9.29±0.02	9.28±0.02	1.50±0.00	1.50±0.00	1.50±0.00	1.50±0.00

4.1.2 Concentration dependence over a 2-hour duration

As described in Section 2.5.3 the step-by-step inhibition of silver-exchanged zeolite X for a duration of 2 hours was investigated. The results obtained are presented in Figure 37.

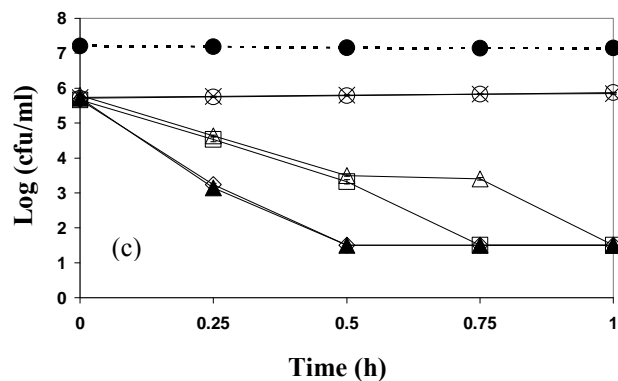
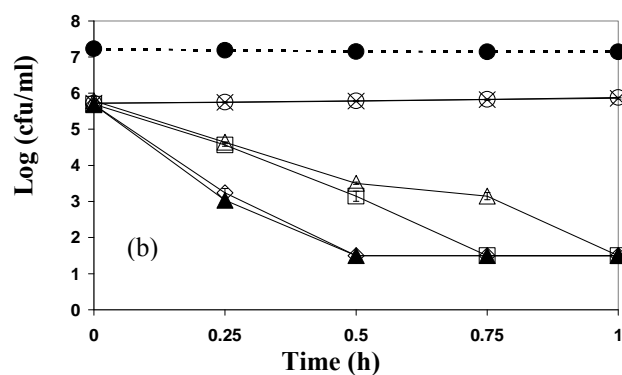
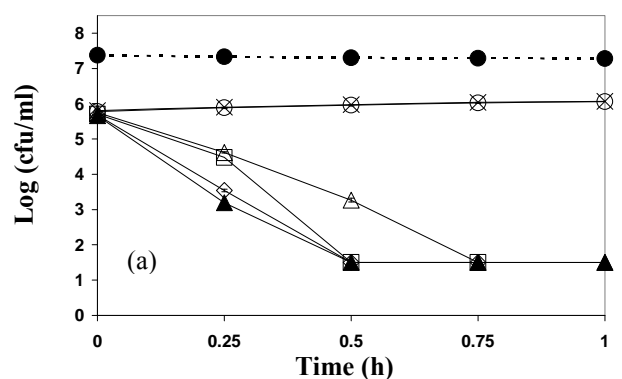


Figure 37: Bactericidal activity of silver-loaded zeolite X at 37 °C. (a): *E. coli* (b): *S. aureus* and (c): *P. aeruginosa* cells were treated with zeolite X (○) and with silver-loaded zeolite X at 0 (×), 0.15 (Δ), 0.25 (□), 0.50 (◇) and 1.00 (▲) g l⁻¹ in TSB. The pH (●) remained fairly constant within the range of 7.1 – 7.3.

After 15 minutes, the viability of *E. coli* (Figure 37a) was reduced by 1 log cycle by 0.15 and 0.25 g l⁻¹ silver zeolite while 0.5 and 1.0 g l⁻¹ reduced the viability by 2 and 2.5 log cells respectively. Similar results were achieved for *S. aureus* (Figure 37b) and *P. aeruginosa* (Figure

37c) within the same period. At lower concentrations (0.15 g l^{-1}) complete inhibition was achieved for *E. coli* in 45 minutes whilst it took 1 hour to achieve the same inhibition for *S. aureus* and *P. aeruginosa* for the same concentration.

4.1.3 ICP-AES analysis of silver ions eluted from zeolite X

The amount of silver ions eluted from zeolite X framework in TSB containing no bacteria or *E. coli*, *S. aureus* or *P. aeruginosa* are shown in Figure 38.

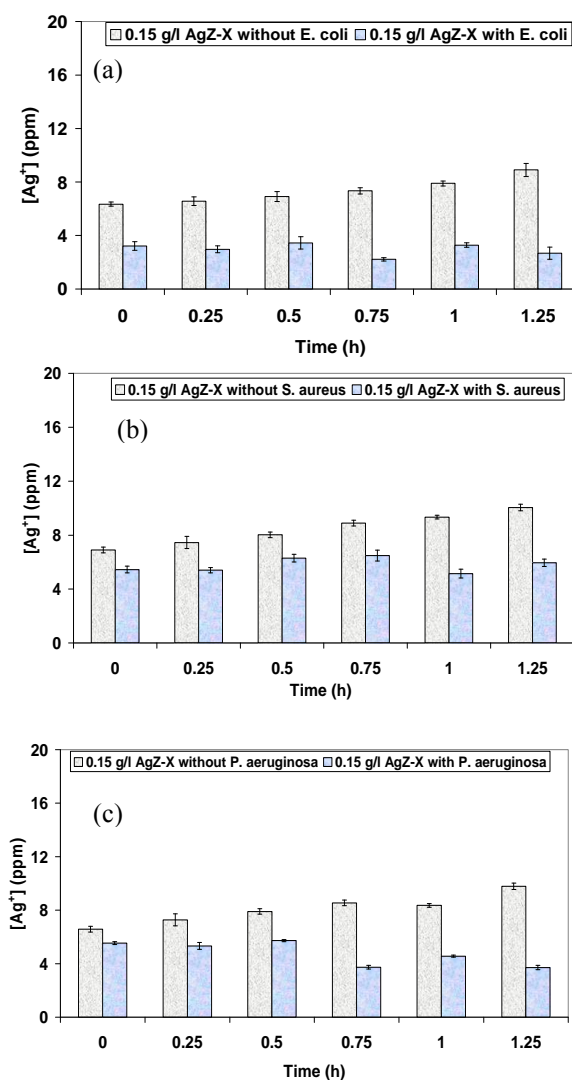


Figure 38: Silver ions released from silver-exchanged zeolite X into TSB with or without (a): *E. coli* (b): *S. aureus* and (c): *P. aeruginosa* with time at concentration of 0.15 g l^{-1} silver-exchanged zeolite X.

The release of silver ions with time was nearly uniform when no bacteria was present in TSB. In the presence of *E. coli*, *S. aureus* or *P. aeruginosa* the release rate of silver ions was anomalous for all bacterial strains. For instance, in the presence of *E. coli* (Figure 38a) there was a steady release of silver ions from 0 to 0.5 and was lower at 0.75 hours. The amount of silver ions was higher at 1 hour than at 1.25 hours. For *S. aureus* (Figure 38b), there was steady release of silver ions up to 0.75 hours but lower at 1 hour after which it increased by 0.2 ppm. The release profile for *P. aeruginosa* (Figure 38c) was fairly constant from 0 to 0.5 hours and got lower towards the end of the 2-hour duration.

Figure 39 are the results obtained on exposing *E. coli*, *S. aureus* and *P. aeruginosa* to 0.25 g l⁻¹ silver-exchanged zeolite X in TSB.

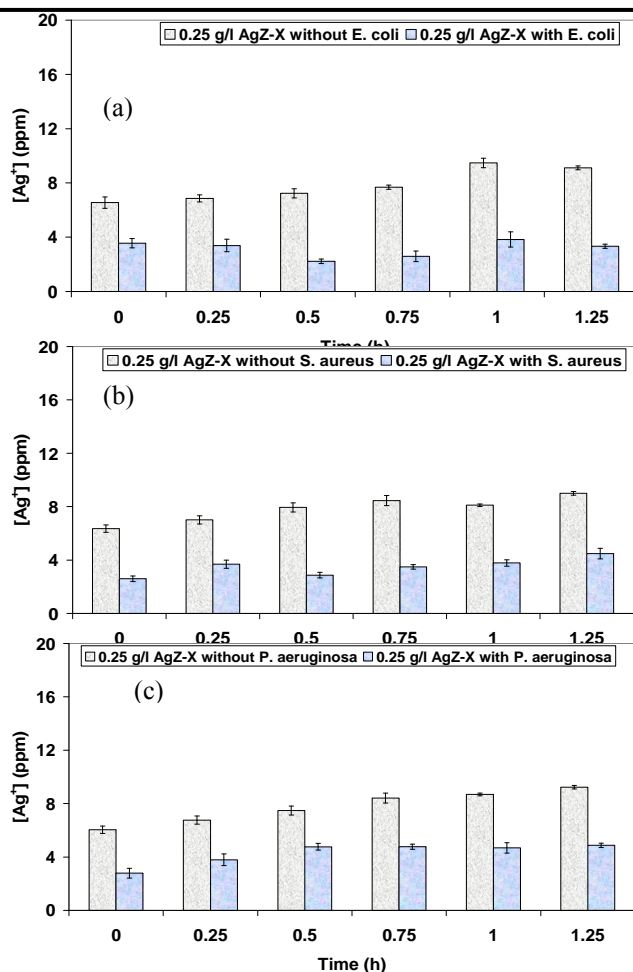


Figure 39: Silver ions released from silver-exchanged zeolite X into TSB with or without (a): *E. coli* (b): *S. aureus* and (c): *P. aeruginosa* with time at a concentration of 0.25 g l⁻¹ silver-exchanged zeolite X.

The release of silver ions from zeolite X framework in the absence of all three strains was similar to that obtained when 0.15 g l⁻¹ silver-exchanged zeolite X was added. In the presence of *E. coli* the release of silver ions was fairly constant at 0 and 0.25 hours and decreased at 0.5 hours. After 0.5 hours it increased at 0.75 hours and at 1.0 hour and decreased slightly at 1.25 hours. The release profile for *S. aureus* increased steadily after 0.5 hours after it showed a decreasing trend between 0 and 0.25 hours. In the presence of *P. aeruginosa* however, the release profile showed a progressive increasing trend at 0, 0.25 and 0.5 hours and remained fairly constant afterwards.

On exposing *E. coli*, *S. aureus* and *P. aeruginosa* to 0.50 g l⁻¹ silver-exchanged zeolite X in TSB (Figure 40), the release profiles of silver ions were different for each strain.

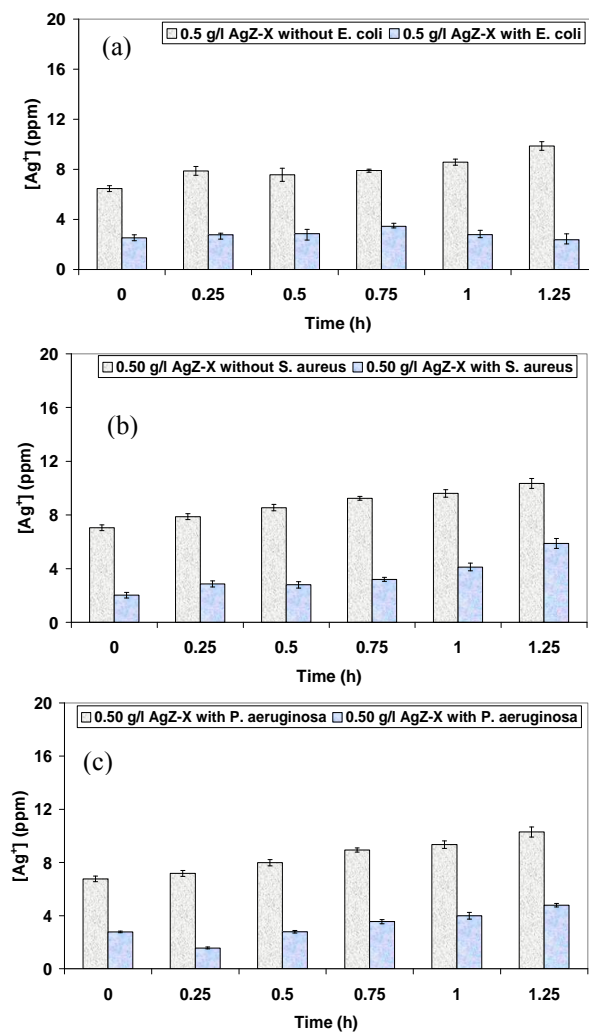


Figure 40: Silver ions released from silver-exchanged zeolite X into TSB with or without (a): *E. coli* (b): *S. aureus* and (c): *P. aeruginosa* with time at concentration of 0.50 g l⁻¹ silver-exchanged zeolite X.

In the presence of *E. coli* there was steady release of silver ions between 0 and 0.25 hours and progressive decrease in the release of silver ions towards the end of the exposure period. The release profile for *S. aureus* showed a progressive decreased in silver ions release throughout the duration of the exposure with a modal release at 1.25 hours. For *P. aeruginosa*, the release of silver ions decreased between 0 and 0.25 hours but increased progressively afterwards until the end of the exposure period.

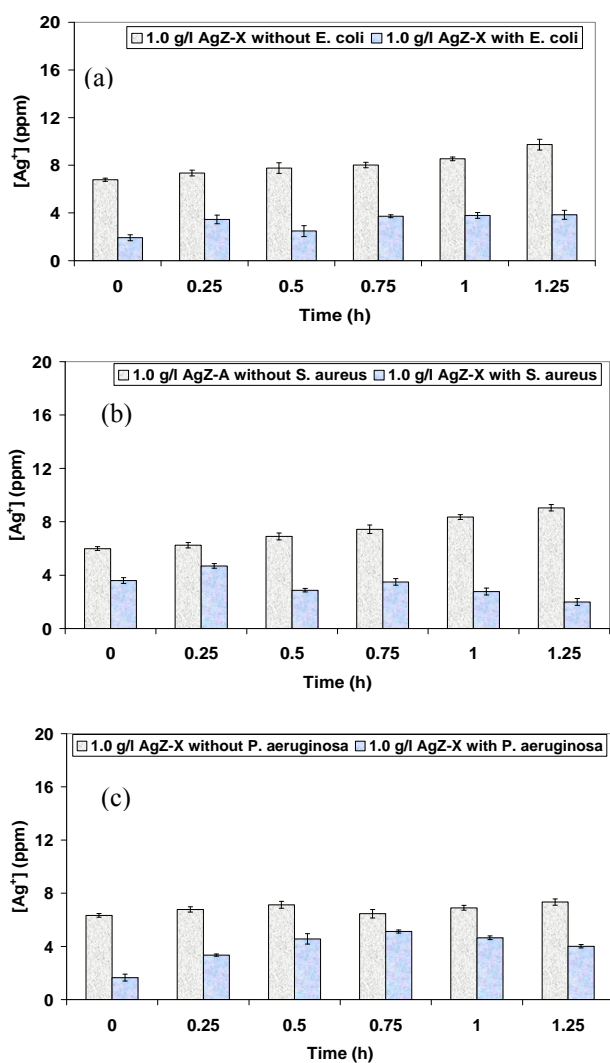


Figure 41: Silver ions released from silver-exchanged zeolite X into TSB with or without (a): *E. coli* (b): *S. aureus* and (c): *P. aeruginosa* with time at concentration of 1.0 g l⁻¹ silver-exchanged zeolite X.

In Figure 41, the release profiles of silver again varied from strain to strain on their exposure to 1.0 g l^{-1} in TSB. In the presence of *E. coli* (Figure 41a) the release profile of silver ions increased between 0 and 0.15 hours followed by a progressive decrease in the release of silver ions until the end of the exposure period. In the presence of *S. aureus* (Figure 41b), however the release profile of silver ions increased in a similar manner between 0 and 0.15 hours followed by a decrease in release between 0.75 and 1.25 hours. For *P. aeruginosa* (Figure 41c), the release in silver ions was progressive from 0 to 0.75 hours and decreased progressively until the end of the exposure period.

The results of this study have shown that the amount of silver ions needed to effect antimicrobial activity is dependent of the cell structure of the bacteria. Since the peptidoglycan of *S. aureus* is six to twenty times more than that of *E. coli*, the amount of silver ions needed to effect antimicrobial activity under similar conditions will be greater in *S. aureus* than in *E. coli*. Hence, more silver ions were released from the zeolite at each sampling time in *S. aureus* than either *E. coli* or *P. aeruginosa*.

4.2 Antimicrobial activity of silver-exchanged zeolite A

4.2.1 Concentration dependence for a 24-hour duration

Table 16 shows the results of the concentration dependence of silver-loaded zeolite A at concentrations of 0.15, 0.25, 0.5 and 1.0 g l^{-1} . At these concentrations, complete inhibition (minimum detection limit of the method was 33.3 CFU ml^{-1}) of *S. aureus* NCIMB6571 within two hours.

Table 16: Results showing the antimicrobial activity of silver exchanged zeolite A against *S. aureus* for duration of 24 hours with different concentrations of silver-exchanged zeolite A.

Time (h)	Average Log(cfu/ml) of <i>S. aureus</i> NCIMB 6571 with:					
	0 g l ⁻¹ AgZ-X ± (stdev)	Z-X ± (stdev)	0.15 g l ⁻¹ AgZ-X ± (stdev)	0.25 g l ⁻¹ AgZ-X ± (stdev)	0.5 g l ⁻¹ AgZ-X ± (stdev)	1.0 g l ⁻¹ AgZ-X ± (stdev)
0	5.77± 0.05	5.75± 0.01	5.77±0.02	5.72±0.02	5.73±0.04	5.757±0.01
2	6.05± 0.01	6.00± 0.02	1.50±0.00	1.50±0.00	1.50±0.00	1.50±0.00
4	7.43± 0.01	7.42± 0.01	1.50±0.00	1.50±0.00	1.50±0.00	1.50±0.00
6	8.73±0.07	8.69± 0.05	1.50±0.00	1.50±0.00	1.50±0.00	1.50±0.00
8	8.95±0.05	8.95± 0.01	1.50± 0.00	1.50±0.00	1.50±0.00	1.50±0.00
10	9.04±0.02	9.10± 0.02	1.50±0.00	1.50±0.00	1.50±0.00	1.50±0.00
12	9.17±0.06	9.16± 0.02	1.50 ±0.00	1.50±0.00	1.50±0.00	1.50±0.00
24	9.30±0.06	9.28± 0.02	1.50 ±0.00	1.50±0.00	1.50±0.00	1.50±0.00

4.2.2 Influence of concentration of (AgZ-A) over shorter period

To examine the step-by-step inhibition of all three microorganisms by silver-zeolite A, the protocol described in Section 2.6.3 was followed. At lower concentrations (0.15 g l⁻¹) there were between 2.0 – 2.5 log cells reduction for all strains in 30 minutes (Figure 42). At higher concentration (0.5 g l⁻¹ and 1.0 g l⁻¹) there were 4 log cells reduction for all strains. After 1 hour there were 4 log cells reduction for all concentrations of silver-exchanged zeolite A.

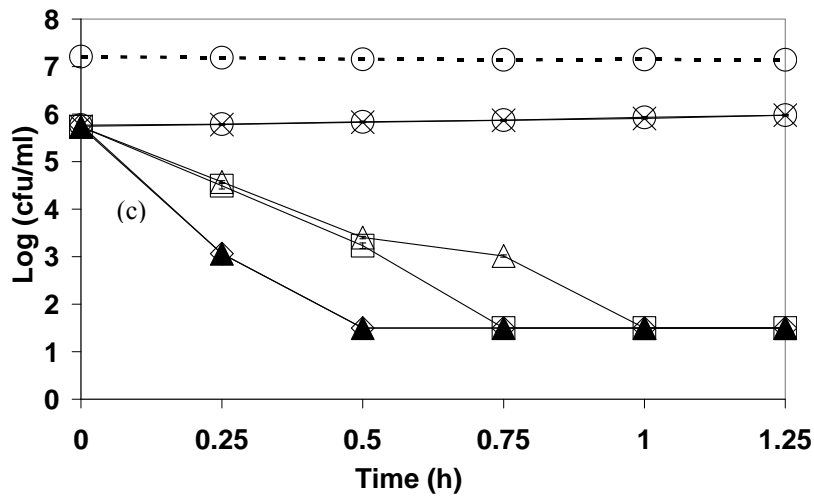
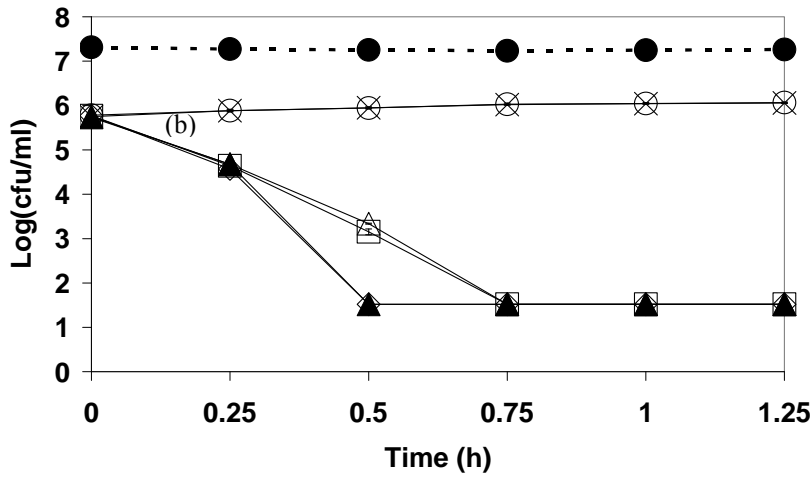
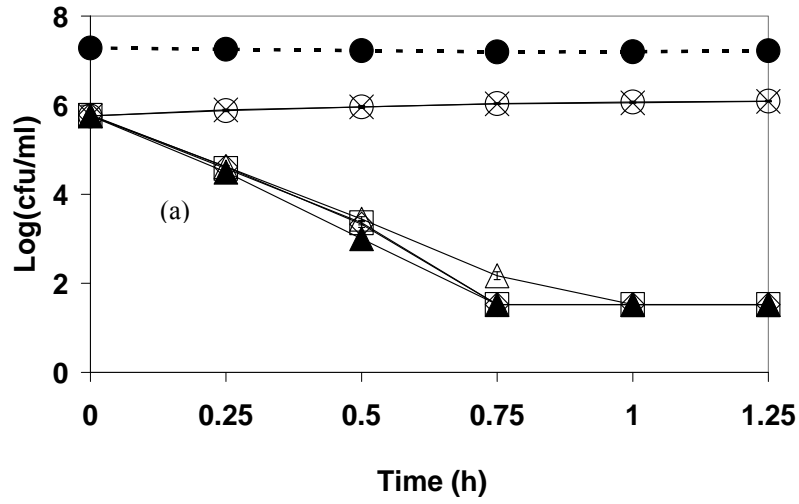


Figure 42: Bactericidal activity of silver-loaded zeolite A at 37 °C. (a): *E. coli* (b): *S. aureus* and (c): *P. aeruginosa* cells were treated with zeolite A (○) and with silver-loaded zeolite A at 0 (×), 0.15 (Δ), 0.25 (□), 0.50 (◇) and 1.00 (▲) g l⁻¹ in TSB. The pH (●) remained fairly constant within the range of 7.1 – 7.3.

4.2.3 ICP-AES analysis of silver ions eluted from (AgZ-A)

The corresponding release profiles of silver ions from silver-exchanged zeolite A are shown in Figure 43.

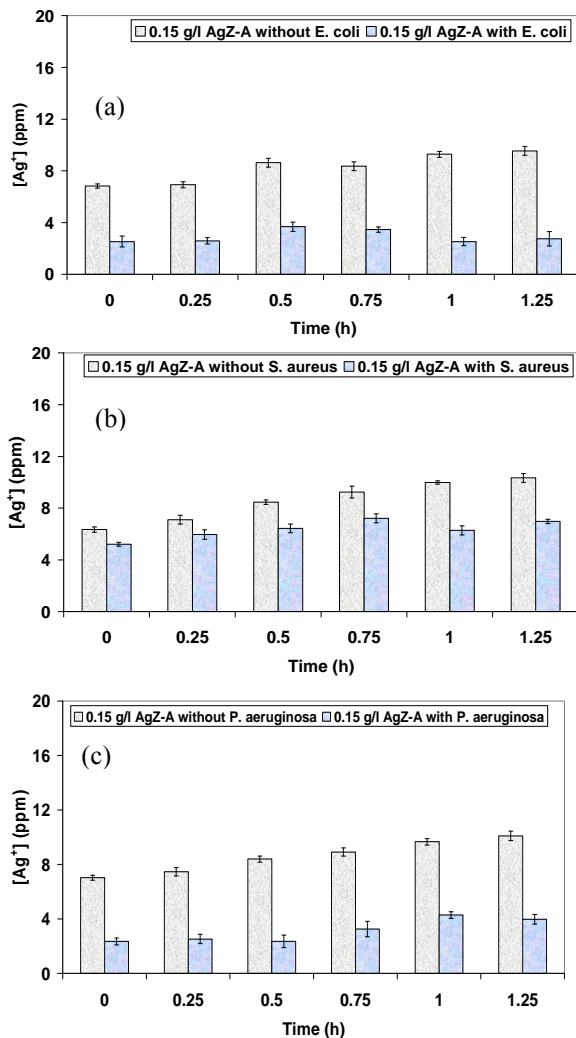


Figure 43: Silver ions released from silver-exchanged zeolite A into TSB with or without (a): *E. coli* (b): *S. aureus* and (c): *P. aeruginosa* with time at concentration of 0.15 g l⁻¹ silver-exchanged zeolite A.

At concentration of 0.15 g l⁻¹ and in the presence of *E. coli*, (Figure 43a) a fairly uniform release was observed between 0 and 0.15 hours followed by an increase in concentration at 0.5 hours (which remained fairly constant until 0.75 hours) and then a dip at 1.0 and 1.25 hours. A similar release profile was observed for *S. aureus* (Figure 43b). In the presence of *P. aeruginosa*

however, the concentration released into TSB remained fairly constant between 0 and 0.5 hours followed by a rise in concentration of silver ions released (Figure 43c).

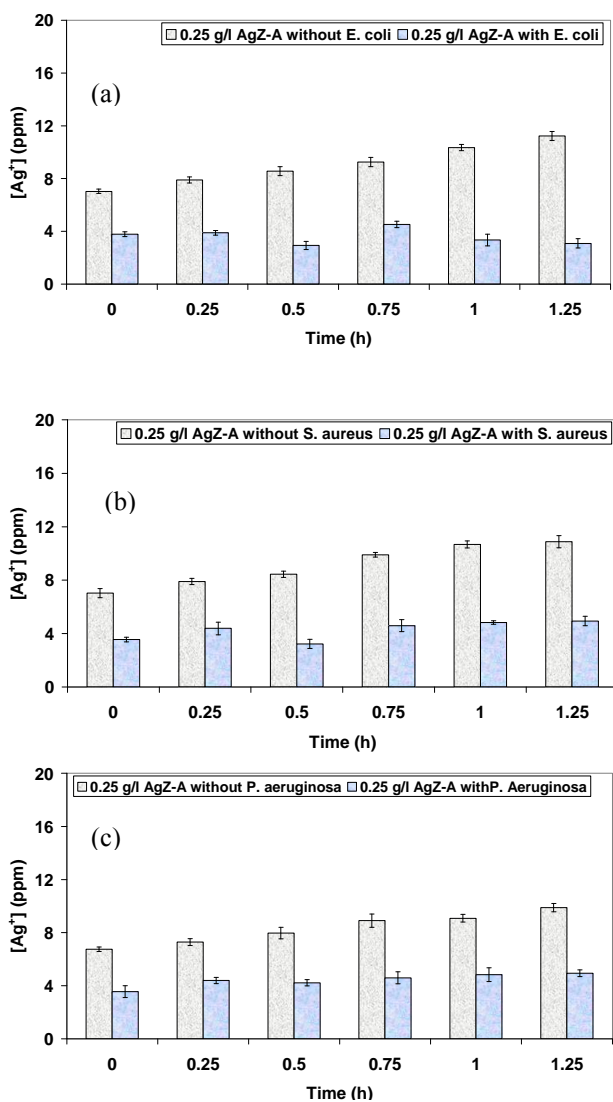


Figure 44: Silver ions released from silver-exchanged zeolite A into TSB with or without (a): *E. coli* (b): *S. aureus* and (c): *P. aeruginosa* with time at concentration of 0.25 g l⁻¹ silver-exchanged zeolite A.

When 0.25 g l⁻¹ silver exchanged zeolite A was added to the culture containing *E. coli*, *S. aureus* or *P. aeruginosa* (Figure 44), the same anomalous trend was observed. In the presence of *E. coli* (Figure 44a) the silver ions released remained fairly constant between 0 and 0.15 hours and

between 1.0 and 1.25 hours. There was a slight increase in the amount of silver ions released between 0.5 and 0.75 hours. The amount of silver ions release in the presence of *S. aureus* (Figure 44b) however, showed a steady increase from 0.5 to 1.2 hours with an increase in the amount of silver ions released between 0 and 0.25 hours. The release of silver ions seemed to be fairly uniform in the presence of *P. aeruginosa* (Figure 44c)

Figures 45 shows the amount of silver ions released from 0.50 g l⁻¹ silver-exchanged zeolite A into TSB with or without *E. coli*, *S. aureus* or *P. aeruginosa*. The profile was fairly uniform for all strains.

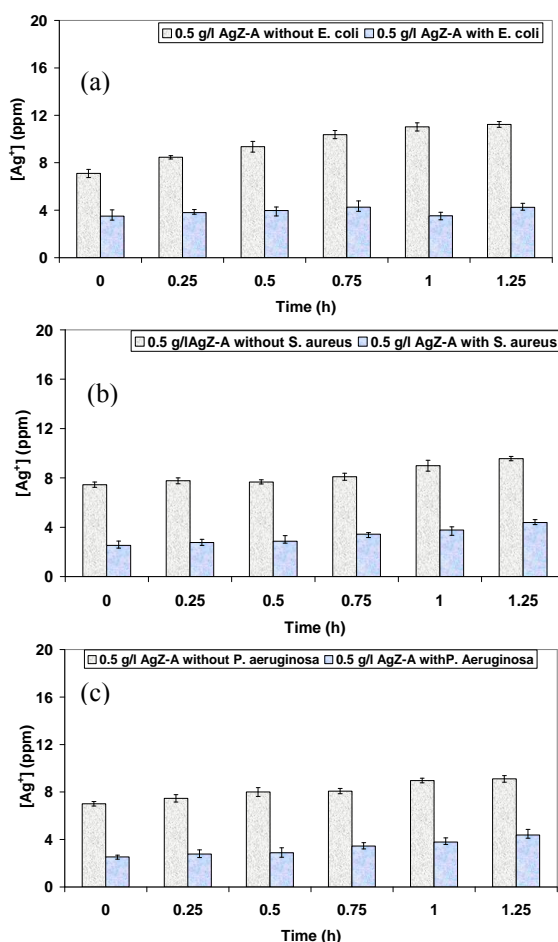


Figure 45: Silver ions released from silver-exchanged zeolite A into TSB with or without (a): *E. coli* (b): *S. aureus* and (c): *P. aeruginosa* with time at concentration of 0.50 g l⁻¹ silver-exchanged zeolite A.

When 1.0 g l^{-1} silver-exchanged zeolite A was used (Figure 46), the amount of silver eluted from zeolite A framework showed a similar trend of release in the presence of all strains.

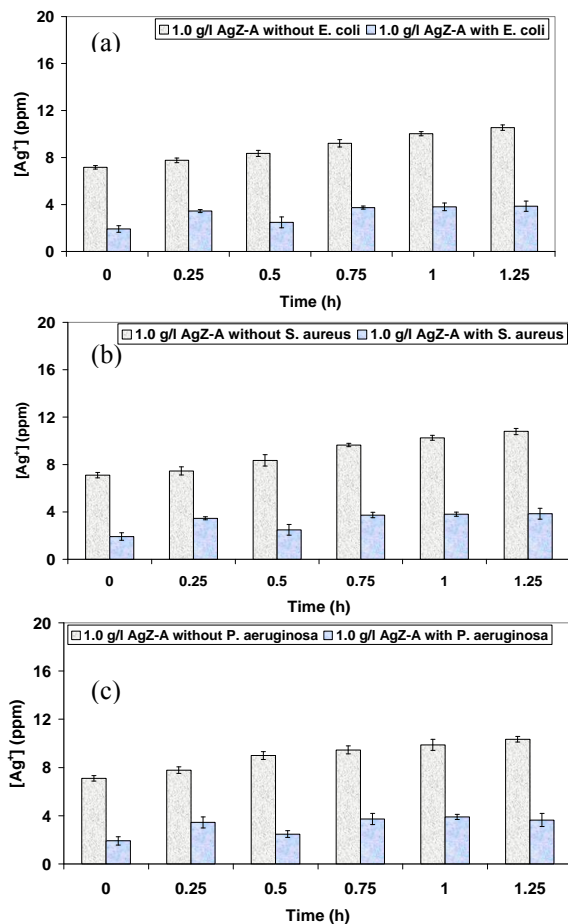


Figure 46: Silver ions released from silver-exchanged zeolite A into TSB with or without (a): *E. coli* (b): *S. aureus* and (c): *P. aeruginosa* with time at concentration of 1.0 g l^{-1} silver-exchanged zeolite A.

More silver ions were released from the zeolite framework when no strain was added to it than cultures containing *E. coli*, *S. aureus* and *P. aeruginosa* in all cases. The amount released from the zeolite were in all cases higher in *S. aureus* than in *E. coli* and *P. aeruginosa* due to the difference in structure between *S. aureus* on one hand and *E. coli* and *P. aeruginosa* on the other.

4.3 Antimicrobial activity of silver-exchanged high-alumina Phillipsite (AgHAP)

4.3.1 Concentration dependence of AgHAP over a 24-hour duration

Table 17: Results showing the antimicrobial activity of silver exchanged high-alumina Phillipsite against *P. aeruginosa* for duration of 24 hours. Different concentrations of silver-exchanged high-alumina Phillipsite used are shown in the graph

Time (h)	Average Log(cfu/ml) of <i>P. aeruginosa</i> NCIMB 8295 with:					
	0 g l ⁻¹ AgZ-X ± (stdev)	Z-X (± stdev)	0.15 g l ⁻¹ AgZ-X (± stdev)	0.25 g l ⁻¹ AgZ-X (± stdev)	0.5 g l ⁻¹ AgZ-X (±stdev)	1.0 g l ⁻¹ AgZ-X (± stdev)
0	5.89±0.01	5.75±0.06	5.78±0.05	5.73±0.04	5.73±0.05	5.74±0.04
2	6.05±0.02	6.02±0.01	1.50±0.00	1.50±0.00	1.50±0.00	1.50±0.00
4	7.43±0.01	7.42±0.01	1.50±0.00	1.50±0.00	1.50±0.00	1.50±0.00
6	8.80±0.05	8.69±0.05	1.50±0.00	1.50±0.00	1.50±0.00	1.50±0.00
8	8.98±0.05	8.95±0.04	1.50±0.00	1.50±0.00	1.50±0.00	1.50±0.00
10	9.05±0.02	9.05±0.02	1.50±0.00	1.50±0.00	1.50±0.00	1.50±0.00
12	9.16±0.01	9.16±0.02	1.50±0.00	1.50±0.00	1.50±0.00	1.50±0.00
24	9.30±0.02	9.28±0.02	1.50±0.00	1.50±0.00	1.50±0.00	1.50±0.00

The results (Table 17) showed that the presence of silver-loaded high-alumina Phillipsite at concentrations of 0.15, 0.25, 0.5 and 1.0 g l⁻¹ resulted in complete inhibition (minimum detection limit of the method was 33.3 CFU ml⁻¹) of *P. aeruginosa* NCIMB8295 1 within two hours. Similar results antimicrobial effects were obtained for *E. coli* K12W-T and *S. aureus* NCIMB657.

4.3.2 Influence of concentration of AgHAP over shorter period

The experimental protocol was repeated with samples taken at 15 minutes interval in order to ascertain the step-by-step inhibition of all three microorganisms by silver-exchanged high-alumina Phillipsite. The results obtained are presented in Figure 47.

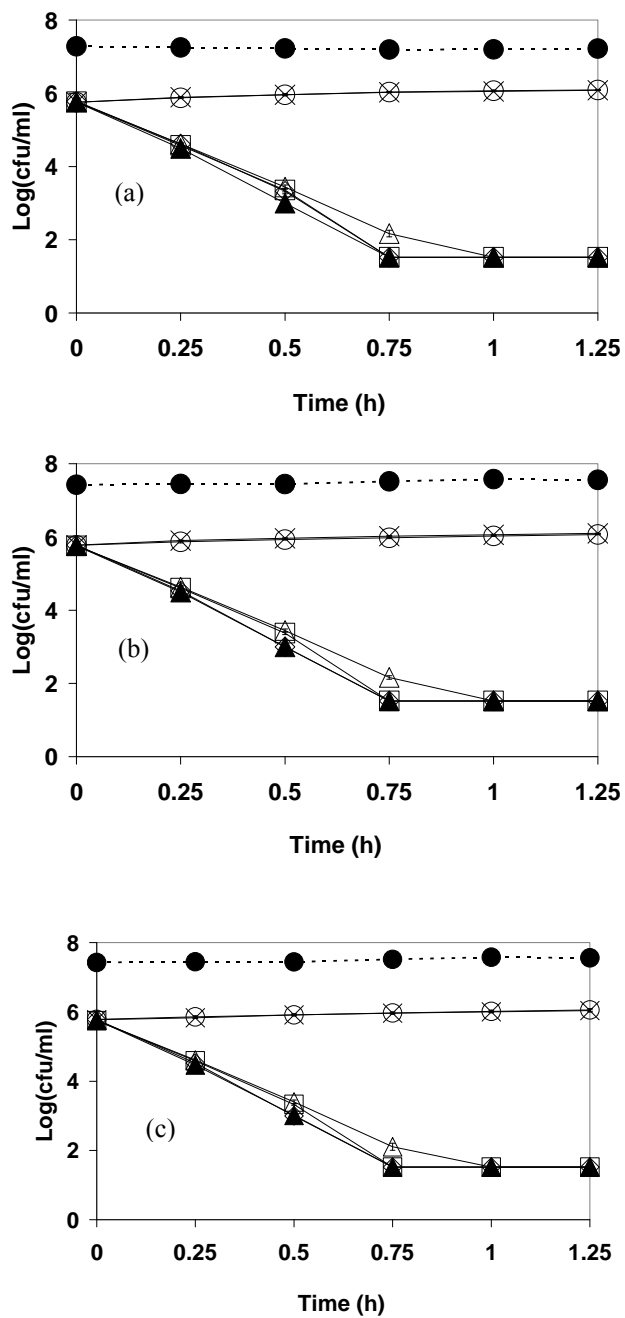


Figure 47: Bactericidal activity of silver-loaded high-alumina Phillipsite at 37 °C. (a): *E. coli* (b): *S. aureus* and (c): *P. aeruginosa* cells were treated with high-alumina Phillipsite (○) and with silver-loaded high-alumina Phillipsite at 0 (×), 0.15 (△), 0.25 (□), 0.50 (◇) and 1.00 (▲) g l⁻¹ in TSB. The pH (●) remained fairly constant within the range of 7.1 – 7.3.

After 15 minutes, the viability of *E. coli* (Figure 47a) was reduced by 1 log cells. Similar results were achieved for *S. aureus* (Figure 47b) and *P. aeruginosa* (Figure 47c) within the same period. At lower concentrations (0.15 g l^{-1}) there was 2.0 – 2.2 log cells reduction for all strains in 30 minutes. At higher concentration (0.5 g l^{-1} and 1.0 g l^{-1}) there was 3 - 4 log cells reduction for all strains. After 1 hour of exposure, 4 log cells reduction for all concentrations of silver-exchanged high-alumina Phillipsite were obtained.

4.3.3 ICP-AES analysis of silver ions eluted from AgHAP framework

The corresponding release profiles of silver ions from silver-exchanged high-alumina Phillipsite are shown in Figure 48 and Figure 49.

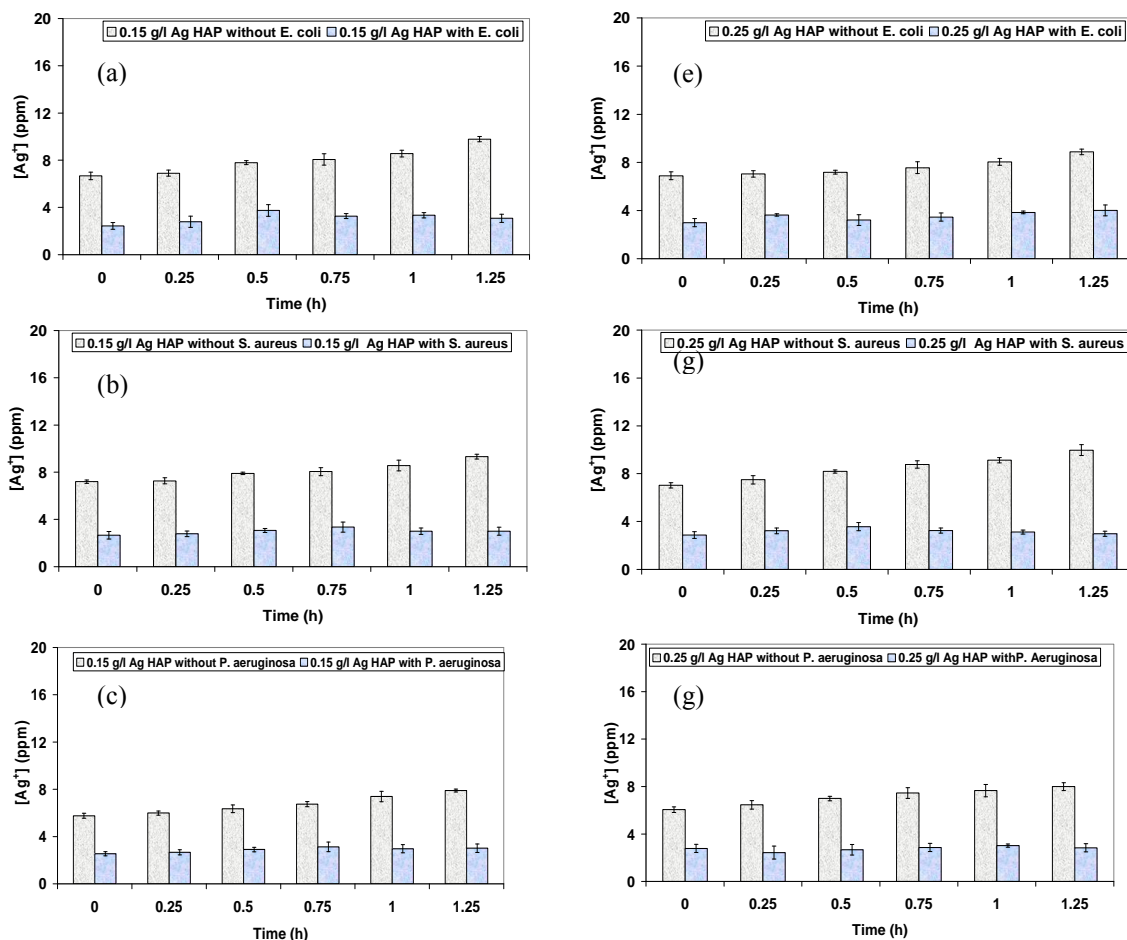


Figure 48: Left: Silver ions released from silver-exchanged high-alumina Phillipsite into TSB with or without (a): *E. coli* (b): *S. aureus* and (c): *P. aeruginosa* with time at concentration of 0.15 g l^{-1} silver-exchanged high-alumina Phillipsite. Right: Silver ions released from silver-exchanged high-alumina Phillipsite into TSB with or without (a): *E. coli* (b): *S. aureus* and (c): *P. aeruginosa* with time at concentration of 0.25 g l^{-1} silver-exchanged high-alumina Phillipsite

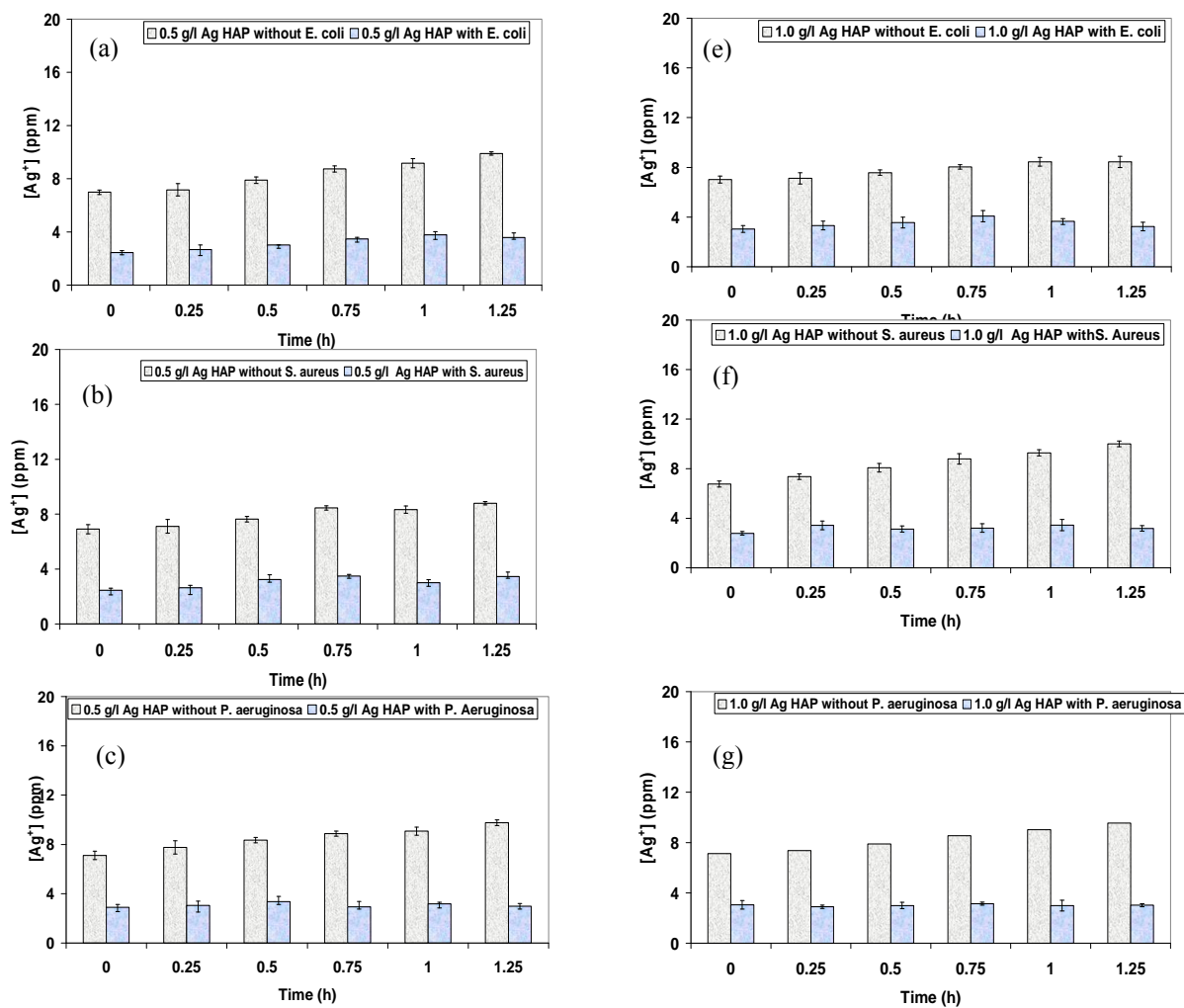


Figure 49: Left: Silver ions released from silver-exchanged high-alumina Phillipsite into TSB with or without (a): *E. coli* (b): *S. aureus* and (c): *P. aeruginosa* with time at concentration of 0.50 g l⁻¹ silver-exchanged high-alumina Phillipsite. Right: Silver ions released from silver-exchanged high-alumina Phillipsite into TSB with or without (a): *E. coli* (b): *S. aureus* and (c): *P. aeruginosa* with time at concentration of 1.0 g l⁻¹ silver-exchanged high-alumina Phillipsite

4.4 Antimicrobial activity of silver-doped analcime

4.4.1 Concentration dependence of silver-doped Analcime for a 24-hour duration

The result of the antimicrobial activity of silver-doped analcime against *P. aeruginosa* NCIMB 8295 is given in Table 18. The result showed that the presence of silver-doped analcime at concentrations of 0.15, 0.25, 0.5 and 1.0 g l⁻¹ resulted in complete inhibition (minimum detection

limit of the method was 33.3 CFU ml⁻¹) of *P. aeruginosa* NCIMB8291 within two hours. Similar results antimicrobial effects were obtained for *E. coli* K12W-T and *S. aureus* NCIMB6571.

Table 18: Results showing the antimicrobial activity of silver-doped analcime on *P. aeruginosa* for duration of 24 hours. Different concentrations of silver-exchanged zeolite X used are shown in the graph.

Time (h)	Average Log(cfu/ml) of <i>P. aeruginosa</i> NCIMB 8295 with:					
	0 gl ⁻¹ AgZ-X ± (stdev)	Z-X (± stdev)	0.15 gl ⁻¹ AgZ-X (± stdev)	0.25 gl ⁻¹ AgZ-X (± stdev)	0.5 gl ⁻¹ AgZ-X (±stdev)	1.0 gl ⁻¹ AgZ-X (± stdev)
0	5.77±0.04	5.74±0.05	5.78±0.05	5.73±0.04	5.73±0.05	5.74±0.04
2	6.04±0.01	6.04±0.02	1.50±0.00	1.50±0.00	1.50±0.00	1.50±0.00
4	7.42±0.03	7.43±0.01	1.50±0.00	1.50±0.00	1.50±0.00	1.50±0.00
6	8.80±0.05	8.69±0.05	1.50±0.00	1.50±0.00	1.50±0.00	1.50±0.00
8	8.98±0.03	8.87±0.04	1.50±0.00	1.50±0.00	1.50±0.00	1.50±0.00
10	9.04±0.01	9.06±0.02	1.50±0.00	1.50±0.00	1.50±0.00	1.50±0.00
12	9.16±0.01	9.16±0.02	1.50±0.00	1.50±0.00	1.50±0.00	1.50±0.00
24	9.28±0.02	9.28±0.01	1.50±0.00	1.50±0.00	1.50±0.00	1.50±0.00

4.4.2 Concentration dependence of silver-doped analcime over a shorter period

The experimental protocol was repeated with samples taken at 15 minutes interval in order to examine the step-by-step inhibition of all three microorganisms by silver-doped. After 15 minutes, the viability of *E. coli* (Figure 50a) remained nearly unchanged. Similar results were achieved for *S. aureus* (Figure 50b) and *P. aeruginosa* (Figure 50c) within the same period. At lower concentrations (0.15 g l⁻¹) there was a 1.0 log cells reduction of all strains achieved after 0.75 hours. At higher concentration (0.5 g l⁻¹ and 1.0 g l⁻¹) there were 2 log cells reduction for all strains after 0.75 hours. After 1.5 hours there were 4 log cells reduction of all cells and for all concentrations of silver-doped analcime

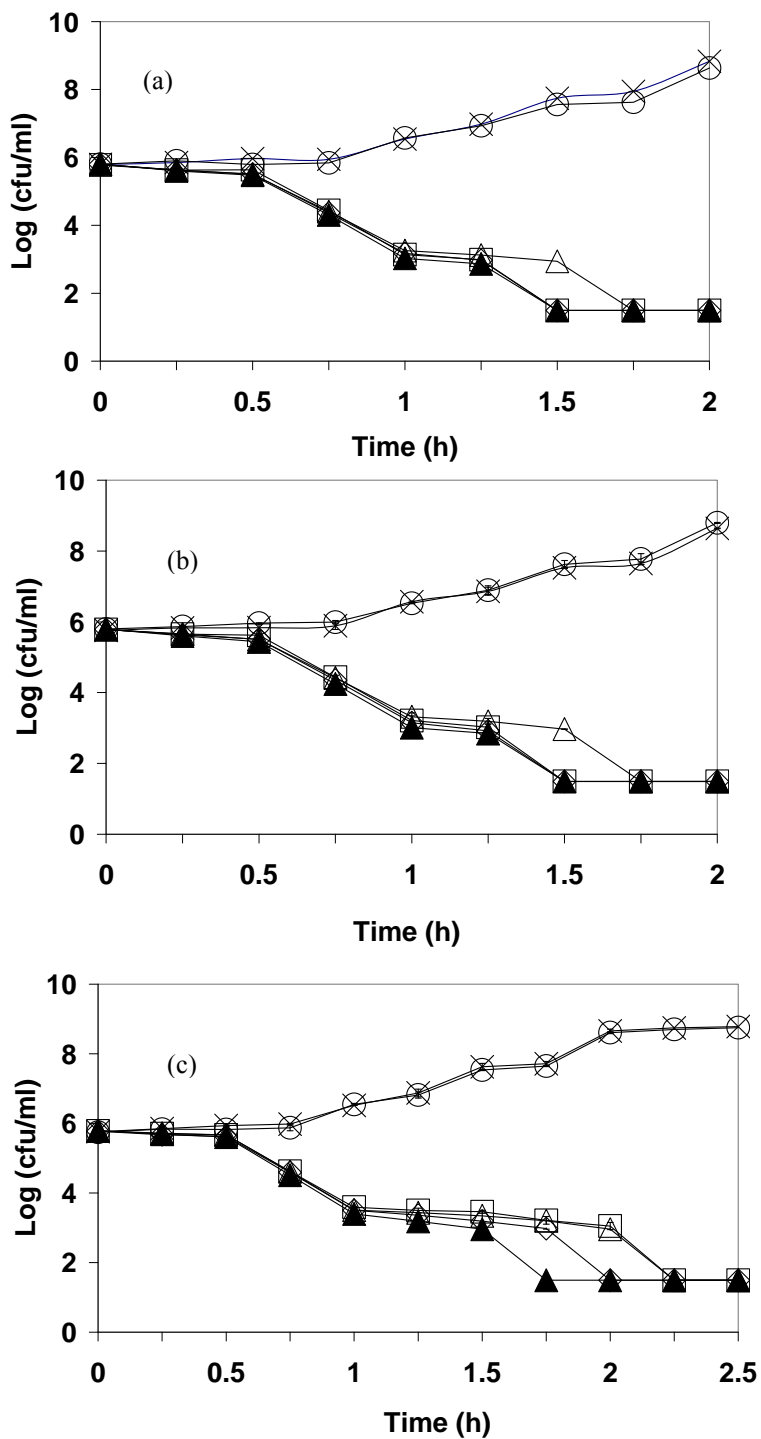


Figure 50: Bactericidal activity of silver-loaded high-doped analcime at 37 °C. (a): *E. coli* (b): *S. aureus* and (c): *P. aeruginosa* cells were treated with analcime (○) and with silver-doped analcime at 0 (×), 0.15 (Δ), 0.25 (□), 0.50 (◇) and 1.00 (▲) g l⁻¹ in TSB.

4.5 Discussion

4.5.1 Discussion of antimicrobial activity of silver-loaded zeolites used in this study

The slow and continuous release of silver ions in the bacterial environment is a critical factor needed to ensure the efficacy of silver ions as an antimicrobial agent (Brett, 2006). No antibacterial activity was observed with zeolite controls (zeolites containing no silver ions) and the zeolites did not dissolve upon solvation in TSB. Therefore the antimicrobial activity of the silver-loaded zeolites was not related to changes in the physicochemical characteristics (pH, osmotic pressure, ionic strength and composition) of the culture medium (Kumer and Musnstedt, 2004). However, silver ions released from the zeolite framework of the silver-loaded zeolites were responsible for the antimicrobial action against all three microorganisms. Comparison of antimicrobial activity of the silver-loaded zeolites with that of silver nitrate have shown that the silver ions delivered by silver-loaded zeolites showed antimicrobial power similar to that of silver nitrate (Matsumura *et al.*, 2003). The results of this study shows that the zeolites all the zeolites were responsible for the slow and sustained release of silver ions from their framework (Kwakye-Awuah *et al.*, 2008a). It is suggested that such release of silver ions can make silver-loaded zeolites a more effective antimicrobial agent clinically in both prevention and treatment of established infections than traditional antimicrobial agents that release silver rapidly (Kwakye-Awuah *et al.*, 2008a). The mechanism(s) of antimicrobial action is still not clearly understood (Nies, 1999). Earlier investigations on the bactericidal activity of silver-loaded zeolite by Matsumura *et al.*, (2003) and Abe *et al.*, (2004) suggested the following mechanism: bacterial cells first make contact with silver zeolite, take in silver ions which inhibit its essential enzymes necessary for ATP production. Antimicrobial action of silver ion has been reported to primarily affect the function of membrane-bound enzymes such as those of the respiratory chain (McDonnell and Russell 1999; Parsons *et al.*, 2003; Hardman *et al.*, 2004; Parsons *et al.*, 2005).

The inhibitory action also includes plasmolysis, the partial disruption of the cytoplasmic membrane from the cell wall (Feng *et al.*, 2000, Yamanaka *et al.*, 2005) and the disruption of the outer membrane (Yamanaka *et al.*, 2005). Furthermore, Yamanaka *et al.*, (2005) asserted that bactericidal action of silver ion is mainly due to its interaction with the cytoplasm of the cell. Since the experiments described in this paper were performed in daylight, it is possible that a fraction of the silver ions were reduced to metallic silver when silver-loaded zeolite was added to the bacterial culture. This metallic silver was likely to become a mass of tiny electrodes, making the zeolite conductive and causing it to release the silver ions (Schierholz *et al.*, 2000). The ion exchange is a slow process and this can extend the antimicrobial effect. The results of this study have shown that microbial cultures containing 10^5 CFU ml⁻¹ of *E. coli* K12 W-T, *S. aureus* NCIMB 6571 and *P. aeruginosa* NCIMB 8295 were completely inhibited by silver-loaded zeolites X in less than 2 hours. Hence future work will examine the mechanism of silver ion interaction(s) with *E. coli* K12 W-T, *S. aureus* NCIMB 6571 and *P. aeruginosa* NCIMB 8295 with time. The silver ions released from the zeolite framework were attached to the bacterial cell. The concentrations of silver ions released into the culture were sufficient for inhibition of all three microorganisms for each exposure and retrieval. The antimicrobial activity of silver has been found to be dependent of the silver cation which strongly binds to electron donor groups in biological molecules containing sulphur, oxygen or nitrogen (Feng *et al.*, 2000). It is suggested that the Ag⁺ was released from the zeolite framework and made contact with the bacterial cell (Matsumura *et al.*, 2003, Feng *et al.*, 2000; Inoue *et al.*, 2002; Sondi and Salopek-Sondi 2004). The fact that none of the microorganisms appeared to recover from the inhibition caused by Ag⁺ implies that none of the bacteria were resistant to silver, although resistance to silver has been reported elsewhere (Trevors, 1987; Silver *et al.*, 1989; Starodub and Silver, 1990; Gupta *et al.*, 1999; Silver, 2003). In summary, silver-loaded zeolites inhibited the growth of *E. coli* K12 W-T,

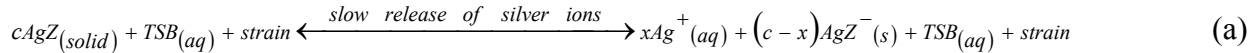
S. aureus NCIMB6571 and *P. aeruginosa* NCIMB8295 in less than one hour. There was probably, sustained release of silver ions from the zeolite framework into the bacteria culture, which exerted effective antimicrobial activity on all three microorganisms. Although the clinical applicability of the silver-loaded zeolites has not been established, it has attractive features, which make it potentially useful.

4.5.2 Discussion of silver ions eluted from zeolites frameworks

Investigations by Matsumura *et al.*, (2003) reported that silver-loaded zeolites in aqueous media would only release silver ions in the presence of the bacterial cells. However, more Ag^+ ions were released from the zeolite when silver-loaded zeolites were added to TSB solutions (without bacterial cells) and incubated in a rotary shaker for 2 hours. Similar trends were observed for the silver ions released from the frameworks of silver-loaded zeolites in the absence of bacterial cells. In the presence of *E. coli* K12 W-T, *S. aureus* NCIMB 6571 and *P. aeruginosa* NCIMB 8295 the amount of silver ions released was significantly lower ($P = 0.003$). The results are in agreement with that reported by Bellantone *et al.*, (2002). In contrast, anomalous trends were observed when the same process of silver ion release was monitored in the presence of *E. coli*, *S. aureus* or *P. aeruginosa*. It was found that as the concentration of silver-loaded zeolite and time increased, silver ions seemed to be depleted from the solution instead of increasing. The difference in the concentration profiles could be due to the binding to or the accumulation of silver ions in the cells (Efrima and Bronk, 1998; Sibbald *et al.*, 2001). The results reported in this study are consistent with silver accumulation of tested strains (Efrima and Bronk, 1998; Ghandour *et al.*, 1988; Feng *et al.*, 2000., Matsumura *et al.*, 2003). Gram-positive bacteria cell wall contains three to twenty times more peptidoglycan than their gram-negative counterpart. Since peptidoglycan are negatively charged it somewhat binds some portion of the Ag^+ .

Subsequently, more Ag^+ reach the plasma membrane of gram negative than gram positive species (Kawahara *et al.*, 2000). The peptidoglycan layer serves to shield gram positive bacteria from penetration by the Ag^+ into the cytoplasm. The mechanism of the silver ion released can be explained tentatively as follows (Kwakye-Awuah *et al.*, 2008a):

The reaction taking place in the flask can be represented by the following equation:



Where:

c is the initial concentration of silver ions in the zeolite framework;

x is the concentration of silver ions released from the zeolite framework.

The silver ions released were either attached to the bacterial cell or adsorbed back into the zeolite framework (Kwakye-Awuah *et al.*, 2008) according to the equations:



The equilibrium constant of K of the reaction is given by:

$$K = \frac{x(c-x)}{c} \quad (3)$$

Since the amount of silver ions released were far less than that left in the zeolite framework for

each exposure the term $\frac{x^2}{c} \approx 0$ and $cx \approx c$

$$K = cx$$

$$\therefore K = 1.$$

The value of the equilibrium constant indicates that the reaction in equation (b) and (c) does not lie to the left or to the right. The initial release of silver ions is likely to come from silver

particles occlude within surfaces of the silver-loaded zeolites. Such release can be instantaneous since they do not diffuse from the zeolite framework. For an oxidation and subsequent release of silver ions within the zeolite framework, diffusion of water molecules into and out of the zeolite framework also occurs. Hence, the release of silver ions into and out of the zeolite framework will be dependent of the amount of water molecules leaving or entering the zeolite framework. Since the pore dimensions were different for each zeolite, the rate of release of silver ions was different. Hence, this can explain the anomalous trend of silver ion release (Kwakyee-Awuah *et al.*, 2008a).

Chapter 5

Results and discussion

Persistency in antimicrobial activity of silver-loaded zeolites

This chapter focuses on the results of the antimicrobial action, ICP-AES analysis of the eluted silver from each zeolite framework and analysis of each silver-loaded zeolite after retrieval.

5.1 Continuous retrieval and re-use of silver-exchanged zeolite X

5.1.1 Antimicrobial activity

The extent to which silver-zeolite X persisted in its antimicrobial action was investigated by retrieving and using it in fresh broth cultures.

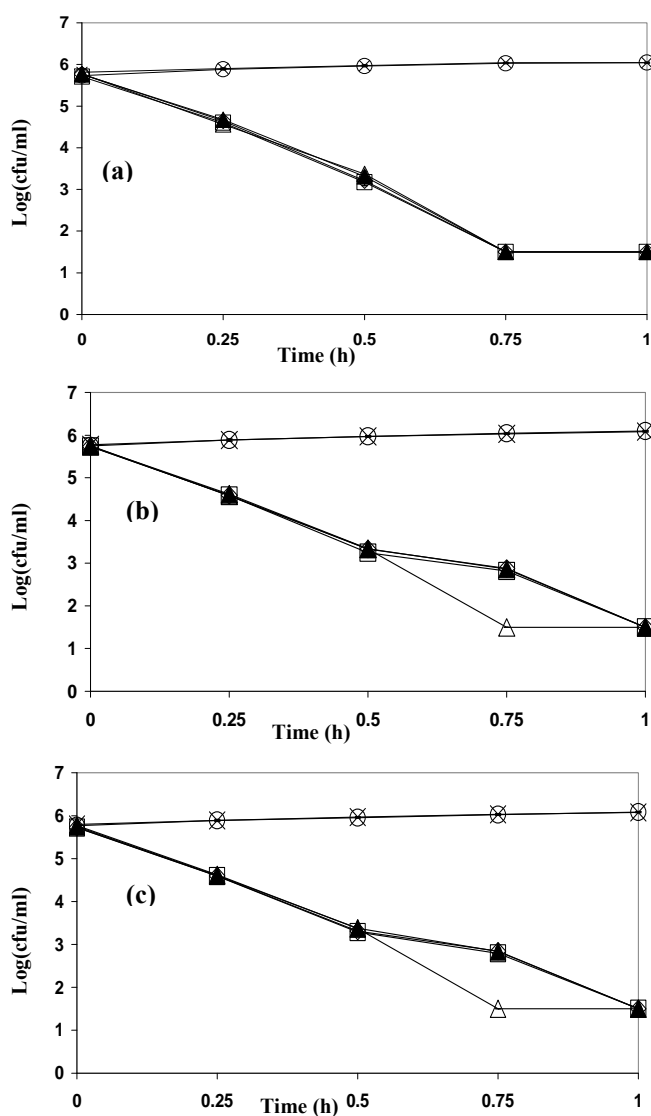


Figure 51: Results from the retrieval experiments for silver-loaded zeolite X at concentration of 1.5 g l^{-1} . Controls are represented by (O) and (X), before retrieval (▲), first retrieval (◻) second retrieval (◊) and third retrieval (△) for (a): *E. coli*, (b): *S. aureus* and (c): *P. aeruginosa*

No colonies were detected for *E. coli* in all three successive retrievals after 45 minutes (Figure 51)

5.1.2 EDX analysis of silver ions left in AgZ-X after each retrieval

The concentration of silver left in zeolite X framework for each exposure is shown in Figure 52.

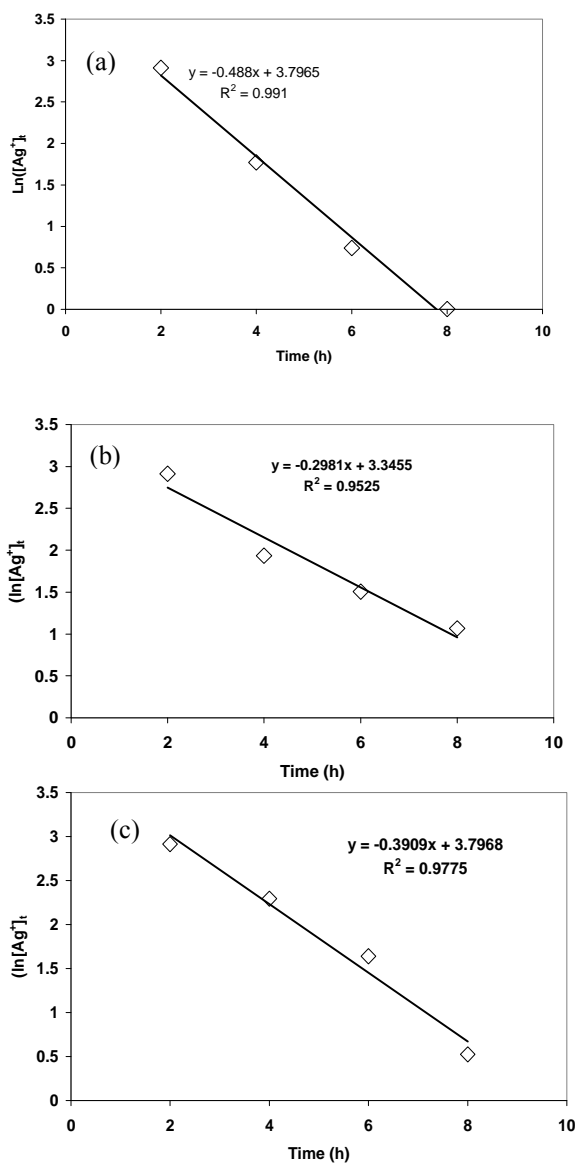


Figure 52: Concentrations of silver remaining in silver-zeolite X before and after each exposure to (a) *E. coli*, (b) *S. aureus* and (c) *P. aeruginosa* cultures. Each experiment lasted for 2 hours.

The slopes of each graph give the release constants and were used to calculate the half-life of silver release from each strain.

The high R^2 values obtained for each strain confirms the first order release of silver ions from zeolite X. If the release of silver from the zeolite is assumed to be first order then the rate equation is given by:

$$\frac{d[Ag^+]}{dt} = k[Ag^+] \quad 10.0$$

This can be re-written as:

$$\ln\left(\frac{[Ag^+]_t}{[Ag^+]_0}\right) = -k t \quad 11.0$$

where k is the rate constant (of silver ion release)

$\ln[Ag^+]_0$ and $\ln[Ag^+]_t$ are the concentrations at time $t = 0$ (before exposure to microorganisms) and $t = t$ (for each exposure and after retrieval).

Hence a plot of $\ln[Ag^+]_t$ as ordinate and t as abscissa gives a straight line where the slope is the rate constant (k).

The half-life $T_{\frac{1}{2}}$ for the decay is given by:

$$T_{\frac{1}{2}} = \frac{\ln 2}{k} \quad 12.0$$

Results obtained from the above deductions are shown in Table 19:

Table 19: Rate constants and half-lives of silver zeolite X in *E. coli* K 12W-T, *S. aureus* NCIMB6571 and *P. aeruginosa* NCIMB8295. The values of the rate constants were obtained from the slopes of the graphs in Figure 56 whilst the half-lives of zeolite X activity was determined from equation 10.0

Strain	Rate constant (h^{-1})	Half-life (h)
<i>E. coli</i> K 12W-T	0.49	1.41
<i>S. aureus</i> NCIMB6571	0.30	2.31
<i>P. aeruginosa</i> NCIMB8295	0.39	1.78

5.1.3 ICP-AES analysis of silver ions eluted from AgZ-X

The release trend of silver ions was anomalous for each treatment (first exposure, first retrieval, second retrieval and third retrieval) as shown in Figure 53.

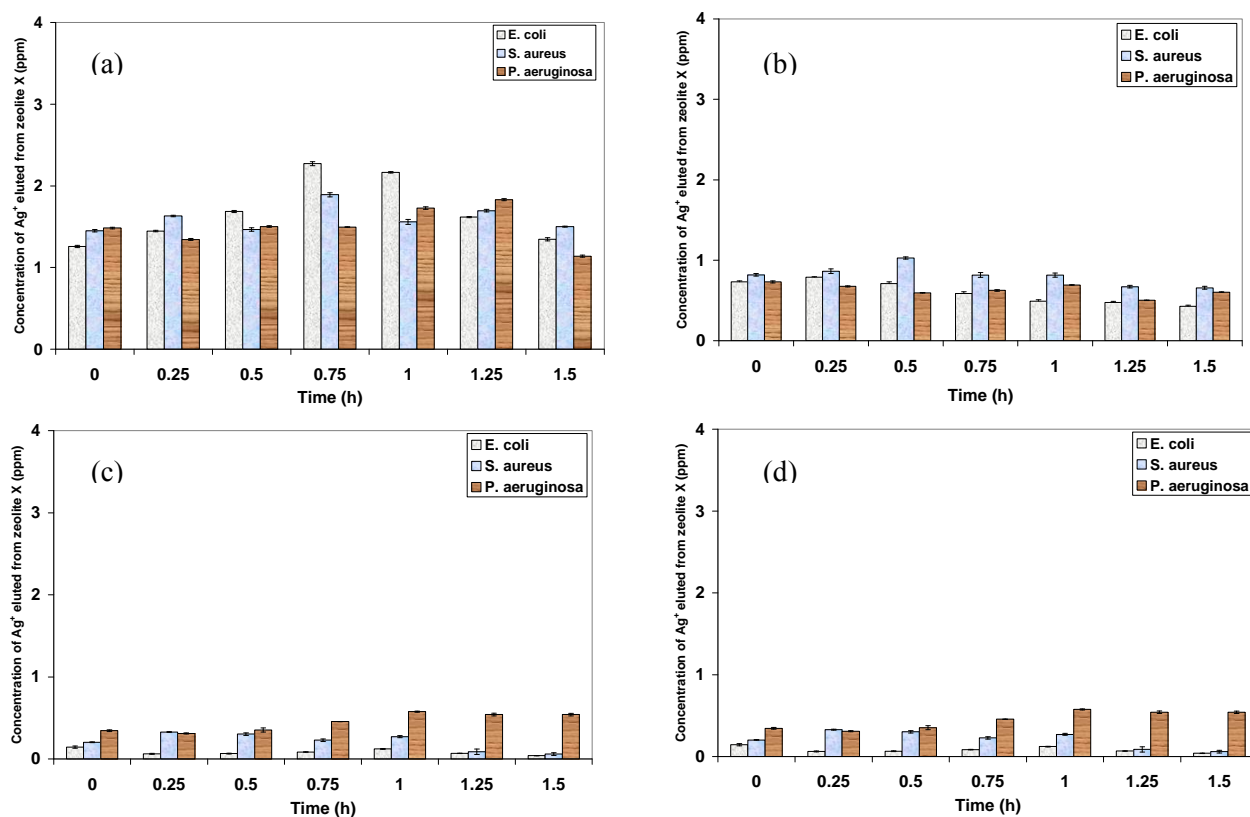


Figure 53: Concentration profile of silver ions eluted from zeolite X as a function of time for (a): first exposure, (b): first retrieval, (c): second retrieval and (c): third retrieval of silver-exchanged zeolite X.

During the first exposure of silver-exchanged zeolite X, the amount of silver ions released in the presence of *E. coli* at 0 and 0.5 hours was lower than in the presence of either *S. aureus* or *P. aeruginosa*. The highest release of silver ions was observed at 0.75 hours and 1.0 hours in the presence of *E. coli*. During the first retrieval of silver-exchanged zeolite X, the amount of silver ions released was lower compared to the first exposure. The highest release was observed at 0.5 hours in the presence of *S. aureus*. On retrieving silver-exchanged zeolite X a second time the highest release of silver ions occurred at 1 hour in the presence of *S. aureus*. However, more silver ions were released towards the end of the exposure period in the presence of *P. aeruginosa* during the third retrieval. There was no significant difference between the amount of silver ions (released from zeolite X framework) that effected antimicrobial activity for treatments of each strain at time $t = 0.5$ hours ($P = 0.0004$, $N = 4$) and $t = 1.5$ hours ($P = 0.00005$, $N = 4$) as shown in Table 20.

Table 20: Mean concentration (ppm) of silver ions released from silver-exchanged zeolite X into TSB containing either *E. coli* K12 W-T, *S. aureus* NCIMB6571 or *P. aeruginosa* NCIMB8289 at time, $t = 0.5$ hours ($N = 4$; $P \leq 0.05$)

Treatment at $t = 0.5$ hours	Concentration (ppm)		
	<i>E. coli</i> K12 W-T	<i>S. aureus</i> NCIMB6571	<i>P. aeruginosa</i> NCIMB8289
First exposure	1.686	1.470	1.502
First retrieval	0.709	1.102	0.594
Second retrieval	0.462	0.459	0.478
Third retrieval	0.065	0.272	0.352
LSD ($P \leq 0.05$) = 0.200			

However, significant difference at $t = 0.5$ hours ($P = 0.7$, $N = 4$) and $t = 1.5$ hours ($P = 0.6$, $N = 4$) was obtained for the amount of silver ions that effected antimicrobial activity for each strain (Table 21). Hence the silver ions released for each treatment at the different sample times exerted effective antimicrobial activity against all three strains.

Table 21: Mean concentration of silver ions released from silver-exchanged zeolite X into TSB containing either *E. coli* K12 W-T, *S. aureus* NCIMB657 or *P. aeruginosa* NCIMB8289 at time, $t = 1.5$ hours ($N = 4$; $P \leq 0.05$)

Treatment at $t = 1.5$ hours	Concentration (ppm)		
	<i>E. coli</i> K12 W-T	<i>S. aureus</i> NCIMB6571	<i>P. aeruginosa</i> NCIMB 8289
First exposure	1.427	2.105	1.427
First retrieval	0.848	0.737	0.787
Second retrieval	0.547	0.373	0.547
Third retrieval	0.526	0.311	0.498
LSD ($P \leq 0.05$) = 0.164			

5.2 Continuous retrieval and re-use of silver-exchanged zeolite A

5.2.1 Antimicrobial activity

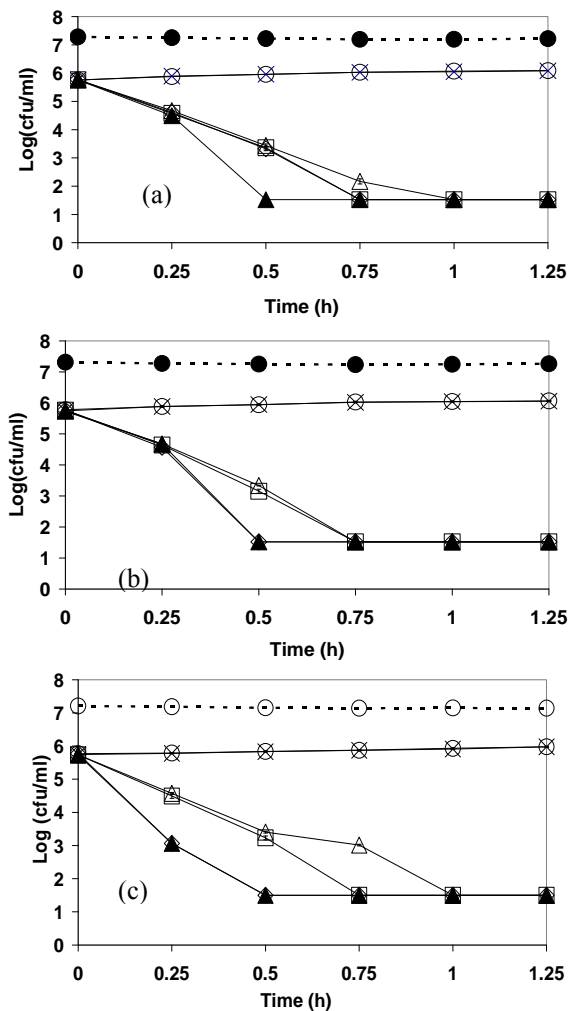


Figure 54: Results from the retrieval experiments for silver-loaded zeolite A at concentration of 1.5 g l^{-1} . Controls are represented by (○) and (×), before retrieval (△), first retrieval (◻) second retrieval (◊) and third retrieval (▲) for (a): *E. coli*, (b): *S. aureus* and (c): *P. aeruginosa*

Figure 54 shows the result obtained from the retrieval of silver-exchanged zeolite A from TSB in the presence of *E. coli*, *S. aureus* and *P. aeruginosa*.

5.2.2 Analysis of silver ions left in silver-exchanged zeolite A after each retrieval

Similar trend was observed as described in Section 55. The rate constants were used to calculate the half lives of silver-exchanged zeolite A

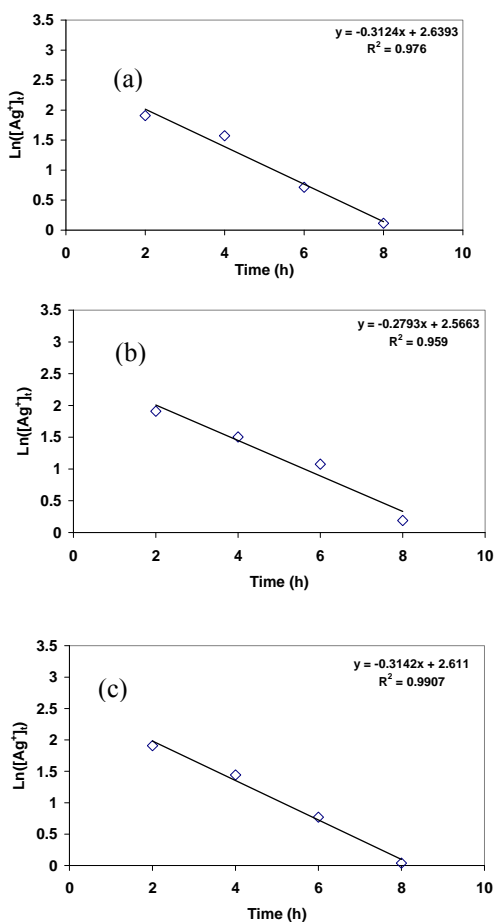


Figure 55: Concentrations of silver remaining in silver-zeolite A before and after each exposure to (a): *E. coli*, (b): *S. aureus* and (c) *P. aeruginosa* cultures

Table 22: Rate constants and half-lives of silver zeolite A in *E. coli* K 12W-T, *S. aureus* NCIMB6571 or *P. aeruginosa* NCIMB8295

Strain	Rate constant (h^{-1})	Half-life (h)
<i>E. coli</i> K 12W-T	0.23	3.01
<i>S. aureus</i> NCIMB6571	0.28	2.47
<i>P. aeruginosa</i> NCIMB8295	0.31	2.23

5.2.3 Analysis of silver ions eluted from silver-exchanged zeolite A with time

The release trend of silver ions was anomalous for each treatment (first exposure, first retrieval, second retrieval and third retrieval) as shown in Figure 56.

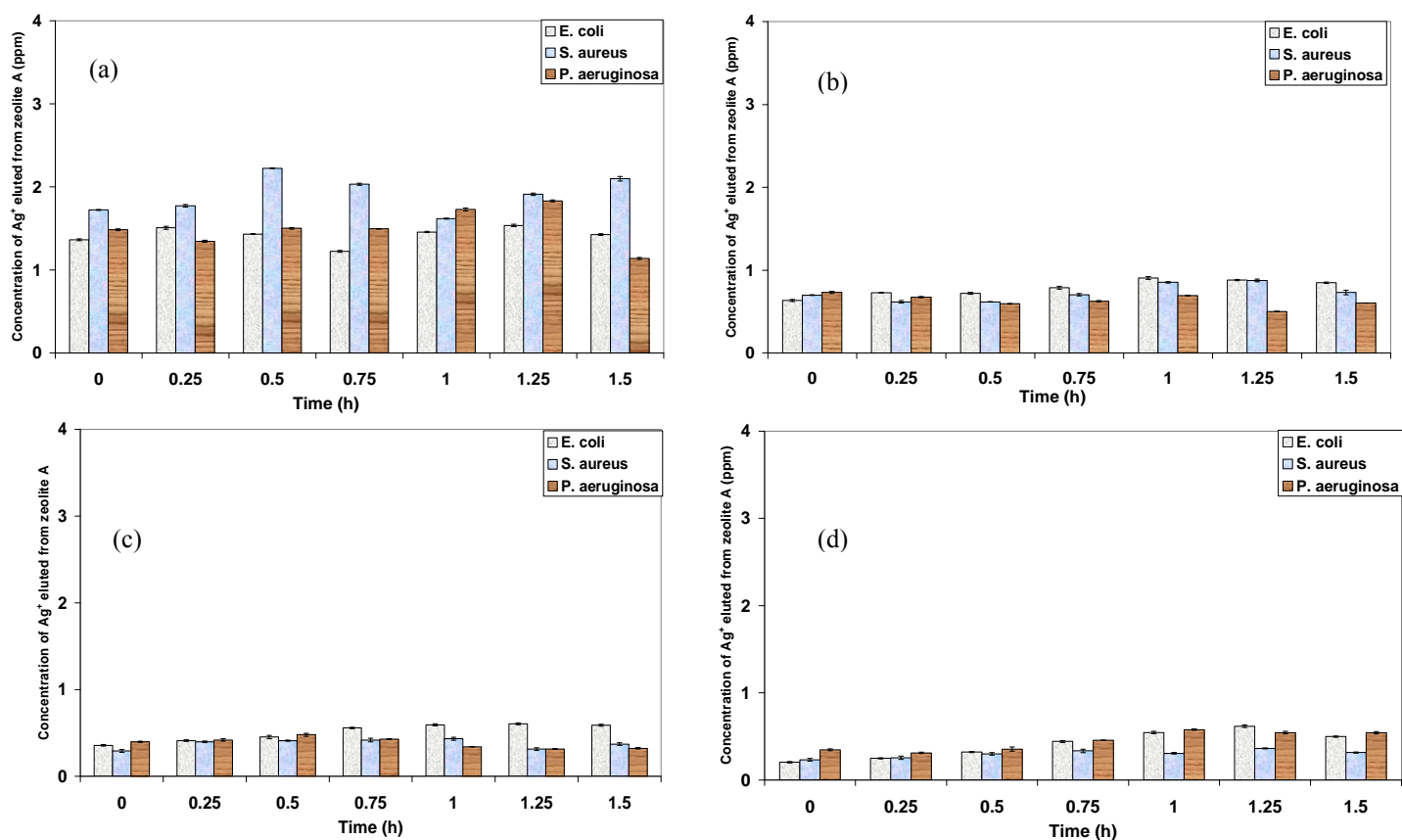


Figure 56: Concentration profile of silver ions eluted from zeolite A into TSB containing *E. coli*, *S. aureus* and *P. aeruginosa* as a function of time for (a): first exposure, (b): first retrieval, (c): second retrieval and (d): third retrieval of silver-exchanged zeolite A

During the first exposure of silver-exchanged zeolite A, the amount of silver ions released in the presence of *E. coli* than in the presence of either *S. aureus* or *P. aeruginosa*. The release of silver ions was higher towards the end of the exposure period in the presence of *E. coli*. During the first retrieval of silver-exchanged zeolite A, the amount of silver ions released was fairly uniform throughout the exposure period. For the profile obtained on second retrieval of silver-exchanged zeolite A the highest release of silver ions occurred at 1 hour in the presence of *S. aureus*. However, silver ions were released progressively throughout the exposure period in the presence of *P. aeruginosa* during the third retrieval.

There was no significant difference between the amount of silver ions (released from zeolite A framework) that effected antimicrobial activity for treatments of each strain at time $t = 0.5$ hours ($P = 0.002$, $N = 4$) and $t = 1.5$ hours ($P = 0.003$, $N = 4$) as shown in Table 23:

Table 23: Mean concentration of silver ions released from silver-exchanged zeolite A into TSB containing either *E. coli* K12 W-T, *S. aureus* NCIMB657 or *P. aeruginosa* NCIMB8289 at time, $t = 0.5$ hours ($N = 4$; $P \leq 0.05$)

	Concentration (ppm)		
Treatment at $t = 0.5$ hours	<i>E. coli</i> K12 W-T	<i>S. aureus</i> NCIMB6571	<i>P. aeruginosa</i> NCIMB 8289
First exposure	1.433	2.23	1.432
First retrieval	0.721	0.623	0.721
Second retrieval	0.527	0.411	0.527
Third retrieval	0.275	0.301	0.32
LSD ($P \leq 0.05$) = 0.220			

However, significant difference at $t = 0.5$ hours ($P = 0.6$, $N = 4$) and $t = 1.5$ hours ($P = 0.9$, $N = 4$) was obtained for the amount of silver ions that effected antimicrobial activity for each strain (Table 24).

Table 26: Mean concentration of silver ions released from silver-exchanged zeolite A into TSB containing either *E. coli* K12 W-T, *S. aureus* NCIMB657 or *P. aeruginosa* NCIMB8289 at time, $t = 1.5$ hours ($N = 4$; $P \leq 0.05$)⁴

Treatment at $t = 0.5$ hours	Concentration (ppm)		
	<i>E. coli</i> K12 W-T	<i>S. aureus</i> NCIMB6571	<i>P. aeruginosa</i> NCIMB 8289
First exposure	1.433	2.23	1.432
First retrieval	0.721	0.623	0.721
Second retrieval	0.527	0.411	0.527
Third retrieval	0.275	0.301	0.32
LSD ($P \leq 0.05$) = 0.220			

5.3 Continuous retrieval and re-use of silver-exchanged high-alumina Phillipsite

5.3.1 Antimicrobial activity

Figure 57 shows the persistency of antimicrobial activity of silver-exchanged high-alumina Phillipsite.

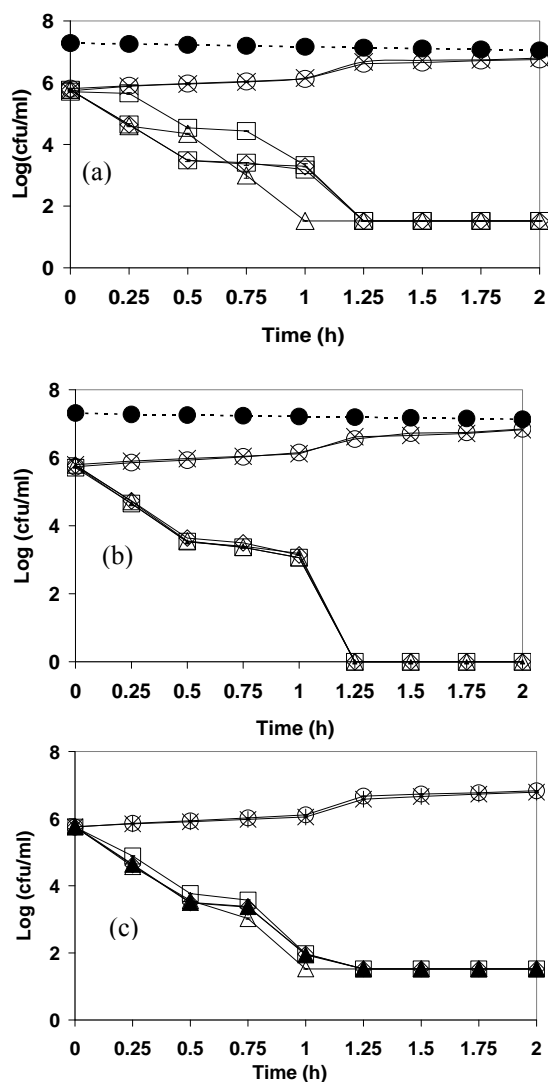


Figure 57: Results from the retrieval experiments for silver-loaded high-alumina Phillipsite at concentration of 1.5 g l⁻¹. Controls are represented by (O) and (x), before retrieval (Δ), first retrieval (□) second retrieval (◇) and third retrieval (▲) for (a): *E. coli*, (b): *S. aureus* and (c): *P. aeruginosa*

For *E. coli* 1.5 log cells reduction was achieved (Figure 57a) for all treatments after 0.75 hours. The detection limit was reached after 1.25 hours. 2 log cells reduction was achieved in 0.5 hours in the presence of *S. aureus* for all exposure treatment (Figure 57b). When the detection limit was reached after 1.25 hours the *S. aureus* colonies were reduced by 4 log cells. The activity

against *P. aeruginosa* is shown in Figure 57c. After 1 hour of exposure in the presence of *P. aeruginosa*, there was 4 log cells reduction at the detection limit.

5.3.2 EDX analysis of silver ions left in AgHAP after each retrieval

The trend was observed for silver ions remaining in high-alumina Phillipsite for each exposure treatment is shown in Table 25. The release of silver ions from high-alumina Phillipsite framework followed a first order kinetics. The rate constants were used to calculate the half-lives of silver-exchanged high-alumina Phillipsite. The results showed that the release of silver ions followed a similar trend.

Table 25: Rate constants and half-lives of AgHAP in *E. coli* K 12W-T, *S. aureus* NCIMB6571 and *P. aeruginosa* NCIMB8295

Strain	Rate constant (h ⁻¹)	Half-life (h)
<i>E. coli</i> K 12W-T	0.20	3.46
<i>S. aureus</i> NCIMB6571	0.18	3.74
<i>P. aeruginosa</i> NCIMB8295	0.22	3.11

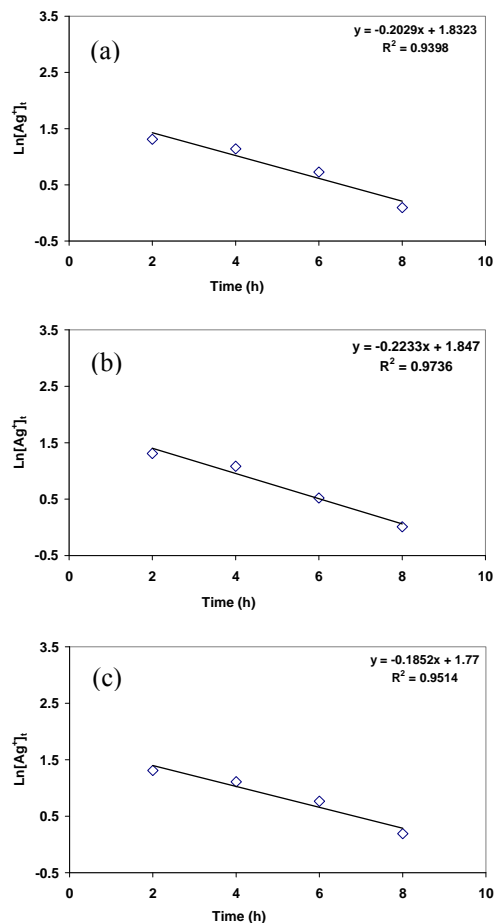


Figure 58: Concentrations of silver remaining in silver-exchanged high-alumina Phillipsite before and after each exposure to (a): *E. coli*, (b): *S. aureus* and (c) *P. aeruginosa* cultures.

Amount of silver loaded into high-alumina Phillipsite is half that of zeolite X or zeolite A (Table 26). This is because of narrow pore size of high-alumina Phillipsite structure. Compared with that of zeolite X or zeolite A which has large pore sizes

Table 26: Summary of rate constants and silver-loading for zeolites X, A and high-alumina Phillipsite

Strain	Rate constant (h^{-1})		
	Z-X	Z-A	HAP
<i>E. coli</i>	0.49	0.23	0.20
<i>S. aureus</i>	0.30	0.28	0.18
<i>P. aeruginosa</i>	0.39	0.31	0.22
Ag^+ (w/w) loaded	(7.8)	(6.8)	(3.7)

Consequently, the rate constant obtained for high-alumina Phillipsite is lower than either zeolite X or A.

5.3.3 ICP-AES analysis of silver ions eluted from AgHAP

The release trend of silver ions was anomalous after for each treatment (first exposure, first retrieval, second retrieval and third retrieval) as shown in Figure 63. During the first exposure of silver-exchanged high-alumina Phillipsite, the amount of silver ions released in the presence of *E. coli* than in the presence of either *S. aureus* or *P. aeruginosa*. The release of silver ions was higher towards the end of the exposure period in the presence of *E. coli*. During the first retrieval of silver-exchanged high-alumina Phillipsite, the amount of silver ions released was fairly uniform throughout the exposure period.

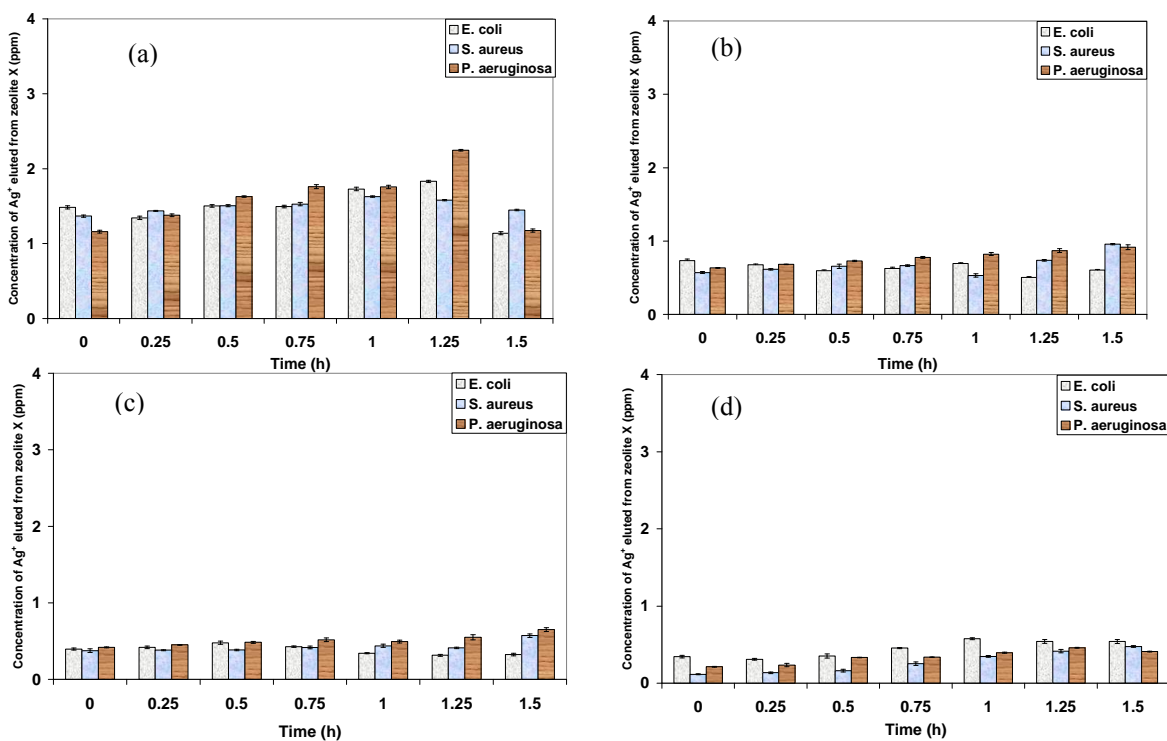


Figure 59: Concentration profile of silver ions eluted from high-alumina Phillipsite into TSB containing *E. coli*, *S. aureus* and *P. aeruginosa* as a function of time for (a): first exposure, (b): first retrieval, (c): second retrieval and (d): third retrieval of silver-exchanged high-alumina Phillipsite

For the profile obtained on second retrieval of silver-exchanged high-alumina Phillipsite the highest release of silver ions occurred at 1 hour in the presence of *S. aureus*. However, silver ions were released progressively throughout the exposure period in the presence of *P. aeruginosa* during the third retrieval.

There was no significant difference between the amount of silver ions (released from high-alumina Phillipsite framework) that effected antimicrobial activity for treatments of each strain at time $t = 0.5$ hours ($P = 0.002$, $N = 4$) and $t = 1.5$ hours ($P = 0.003$, $N = 4$) as shown in Table 27:

Table 27: Mean concentration of silver ions released from silver-exchanged high-alumina into TSB containing either *E. coli*, *S. aureus* or *P. aeruginosa* at time, $t = 0.5$ hours ($N = 4$; $P \leq 0.05$)

Treatment at $t = 1.5$ hours	Concentration (ppm)		
	<i>E. coli</i> K12 W-T	<i>S. aureus</i> NCIMB6571	<i>P. aeruginosa</i> NCIMB8289
First exposure	1.118	1.592	1.241
First retrieval	0.637	0.919	0.891
Second retrieval	0.392	0.547	0.652
Third retrieval	0.273	0.34	0.78
LSD($P \leq 0.05$) = 0.3999			

However, significant difference at $t = 0.5$ hours ($P = 0.6$, $N = 4$) and $t = 1.5$ hours ($P = 0.9$, $N = 4$) was obtained for the amount of silver ions that effected antimicrobial activity for each strain (Table 28).

Table 28: Mean concentration of silver ions released from silver-exchanged high-alumina into TSB containing either *E. coli*, *S. aureus* or *P. aeruginosa* at time, $t = 1.5$ hours ($N = 4$; $P \leq 0.05$)

Treatment at $t = 0.5$ hours	Concentration (ppm)		
	<i>E. coli</i> K12 W-T	<i>S. aureus</i> NCIMB6571	<i>P. aeruginosa</i> NCIMB8289
First exposure	1.124	1.59	1.593
First retrieval	0.516	0.721	0.693
Second retrieval	0.33	0.425	0.472
Third retrieval	0.251	0.182	0.233
LSD ($P \leq 0.05$) = 0.2745			

5.4 Continuous retrieval and re-use of silver-doped Analcime

Figure 60 represent the results from the first exposure and first retrieval of silver-doped analcime.

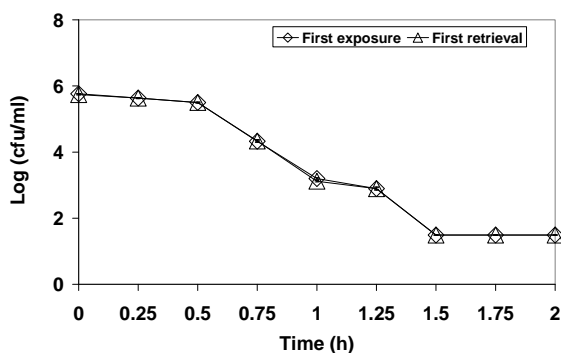


Figure 60: Retrieval and re-use of silver-doped analcime against *E. coli* K12 W-Tin TSB over time

The results indicate that there was virtually no difference in antimicrobial activity of silver-doped analcime on retrieving and adding it to a fresh broth medium. After first retrieval, the antimicrobial activity of the silver-doped analcime was retained similar to that of the silver-exchanged zeolites. Due to time constraint, the persistency in antimicrobial activity for a second and a third successive retrievals and re-use of the silver-doped analcime was not determined.

Chapter 6

Mode of antimicrobial action of silver-exchanged zeolite X

This chapter focuses on the effect of silver-exchanged zeolite X on DNA content of *E. coli* K12 W-T and fatty acid composition of *E. coli* K12 W-T, *S. aureus* NCIMB 6571 and *P. aeruginosa* NCIMB 8295. The experimental methods used in the analysis are elaborated.

6.1 Flow Cytometry analysis of *E. coli*

Figure 61 shows the fluorescence obtained when cells of *E. coli* K12 W-T and *S. aureus* NCIMB6571 were treated with silver-exchanged zeolite X with Propidium iodide (PI) and SYTO 22 dual staining.

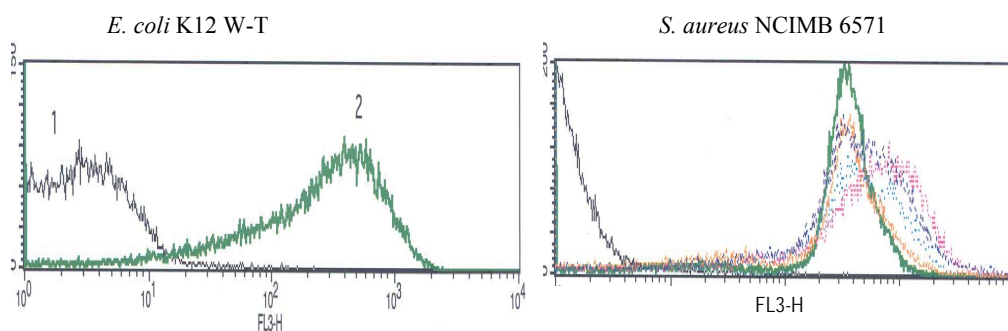


Figure 61: Typical fluorescence for SYTO 22 stained (black line) live cells and PI-stained (green line) dead cells of left: *E. coli* K12W-T and right: *S. aureus* NCIMB6571 assessed by Flow Cytometry. Lines in other colours represent fluorescence obtained for PI stained *S. aureus* NCIMB 6571 cells.

The results show an increase in uptake of PI by both cells of *E. coli* K12W-T and *S. aureus* NCIMB6571 when treated with silver-exchanged zeolite X. This suggests an effect of silver ions on the membrane permeability of both strains. For *S. aureus*, the uptake was performed with dual staining of PI and SYTOX 22. The effect of silver on DNA of *E. coli* K12 W-T is shown in Figure 61.

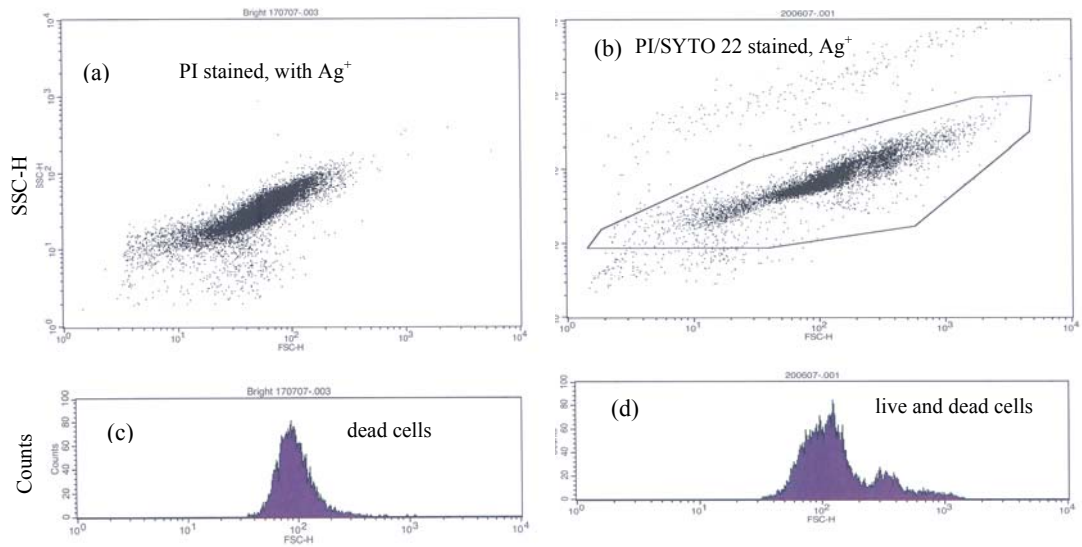


Figure 62: Above (a): Dot plot of cells of *E. coli* K12W-T without silver-exchanged zeolite X (b): with silver-exchanged zeolite X. Below: Fluorescence of *E. coli* K12W-T obtained with cells stained with (c): PI and (d): PI and SYTO 22.

There are two distinct populations of cells following treatment (Figure 62d). The denser of the two has a higher fluorescence intensity and represents the dead or dying cells. The dead cell population has a much broader light scattering distribution indicating a perturbation of the cell membrane.

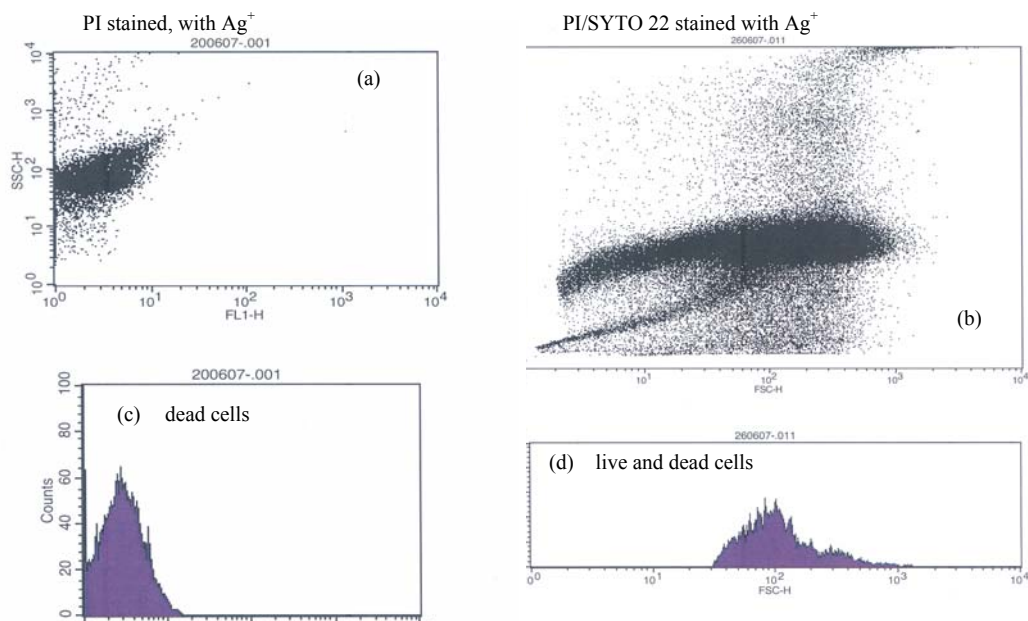


Figure 63: Above (a): Dot plot of cells of *S. aureus* NCIMB6571 without silver-exchanged zeolite X (b): with silver-exchanged zeolite X. Below: Fluorescence of *S. aureus* NCIMB6571 obtained with cells stained with (c): PI 22 and (d): PI and SYTO 22.

This is likely to have caused a loss in membrane potential and a change in cell morphology (Weichart and Kell, 2001; Amor *et al.*, 2002). The shorter population represent live cells which may have been injured during the course of the exposure with silver-exchanged zeolite X. Similar results were obtained for *S. aureus* NCIMB6571 (Figure 67). It can be hypothesized that the fluorescence of cells of *E. coli* K12W-T and *S. aureus* NCIMB without silver-exchanged zeolite X resulted in a single peak. In the presence of silver-exchanged zeolite X the peak seems to have been broadened. This suggests that the silver ions released from zeolite X framework allowed the cells to complete their cycle of DNA replication that have already begun, but caused initiation of new rounds of replication to fail (Lebaron and Joux, 1994; Hiraoka *et al.*, 2002; Baars *et al.*, 2006).

6.2 Effect on fatty acid composition

Fatty acids analysis was performed by the method of White and Ringelberg (1997).

Table 29: Profile of fatty acids obtained from *E. coli* grown without silver-exchanged zeolite X and in the presence of silver-exchanged zeolite X

Fatty acids	Without silver-exchanged zeolite			Silver-exchanged zeolite X			Changes (%)
	Exp 1	Exp 2	Average	Exp 1	Exp 2	Average	
<i>Saturated</i>							
12:0	3.96	4.12	4.04	3.44	4.55	4.00	0
14:0	7.91	8.06	7.99	8.04	8.70	8.37	0
unknown	0.91	1.91	1.41	0.73	0.00	-	0
14:0 3OH	8.18	8.30	8.24	7.29	7.81	7.55	0
16:0	36.70	36.30	36.50	39.53	38.66	39.10	-6
17:0 cy	15.43	16.15	15.79	23.35	21.56	22.46	+ 42
19:0 cy ω8c	2.98	2.84	2.91	6.56	5.51	6.04	+ 107
<i>Unsaturated</i>							
% of total fatty acids							
18:1ω7c/9t/12t	12.77	12.69	12.73	7.34	8.92	8.13	- 36
16:1 ω7c	10.29	10.41	10.35	3.06	4.26	3.66	- 65
<i>Sat/unsat</i>	76.9:23.1 = 3.3			87.5:12.5 = 7			

The nomenclature is as follows: the number of carbon atoms, followed by a colon, the number of double bonds and then by a position of the first double bond from the methyl end (ω) end of the molecule. The prefix *c* or *t* indicate *cis* or *trans* configuration of the double bond, *cy* – cyclopropane fatty acids, *Me* – the position of the position of the methyl group from the acid end, and -OH indicates the position of the hydroxyl group from the acid end of the molecule. Branched fatty acids were designed as *iso* or *anteiso*, if the methyl branch is one or two carbons from the ω end of the acyl chain (Sasser, 1990). All fatty acids detected by gas chromatography (GC) for *E. coli* K12W-T (Table 29), *S. aureus* NCIMB 6571 (Table 30) or *P. aeruginosa* NCIMB8295 (Table 31). For the interpretation of the obtained results, all isolated fatty acids were divided into two groups: saturated and unsaturated fatty acids (Mrozik *et al.*, 2004a). The first group included four subgroups: straight chain, hydroxyl, cyclopropane and branched fatty acids (*iso* or *anteiso*). The analysis of fatty acids extracted from control samples (strains with zeolite X) differed in fatty acid profiles.

Table 30: Profile of fatty acids obtained from *Staphylococcus aureus* grown in the presence of zeolite X and silver exchanged zeolite X

Fatty acid	Without silver-exchanged zeolite			Silver-exchanged zeolite X			Changes (%)
	Exp 1	Exp 2	Average	Exp 1	Exp 2	Average	
<i>Saturated</i> % of total fatty acids							
15:0 <i>iso</i>	10.85	9.83	10.34	8.39	8.05	8.22	+ 20
15:0 <i>anteiso</i>	46.64	43.12	44.88	42.73	44.05	43.39	+3
16:0	2.69	2.71	2.70	3.21	3.95	3.58	+ 32
17:0 <i>iso</i>	5.32	4.75	5.04	4.53	4.15	4.34	- 14
17:0 <i>anteiso</i>	11.55	11.66	11.61	12.74	12.71	12.73	-9
18:0	9.67	10.74	10.21	10.12	9.60	9.86	
19:0 <i>iso</i>	2.26	2.42	2.34	3.07	3.04	3.06	+ 30
19:0 <i>anteiso</i>	3.02	3.57	3.30	4.98	4.64	4.81	+ 46
20:0	8.00	9.40	8.70	10.56	9.47	10.02	+ 15
	100:0						100:0

Changes in some fatty acids could not be determined. These includes 12:0, 14:0,16:0, 14:0 3OH and an unknown fatty acid for *E. coli*; 15:0 *anteiso*, 17:0 *anteiso* and 18:0 for *S. aureus* and 10:0 3OH, 12:0, 12:0 2OH, 12:0 3OH, 14:0, 17:0 *cy*, 18:0 and 19:0 *cy ω8c* for *P. aeruginosa*. The total level of saturated fatty acids in *E. coli* was 76.9 % whereas it was 100 % for *S. aureus* and 44.6 % for *P. aeruginosa* (some values of *P. aeruginosa* could not be determined). As a result the saturated to unsaturated ratio was different for each microorganism.

Table 31: Profile of fatty acids obtained from *P. aeruginosa* grown in the presence of zeolite X and silver-exchanged zeolite X

Fatty acid	Without silver-exchanged zeolite			Silver exchanged zeolite X			Changes (%)
	Exp 1	Exp 2	Average	Exp 1	Exp 2	Average	
<i>Saturated</i> % of total fatty acids							
10:0 3OH	2.79	3.24	3.02	0.00	0.00		0
12:0	4.72	5.15	4.94	4.43	4.44	4.44	0
12:0 2OH	2.71	3.27	2.99	2.93	2.95	2.94	0
12:0 3OH	4.26	3.88	4.07	4.44	4.11	4.27	0
14:0	0.91	n.d		1.05	0.92	0.98	0
16:0	28.26	28.82	28.54	32.16	31.37	31.77	+ 11
17:0 <i>cy</i>	0.92	n.d		1.08	0.97	1.03	0
18:0	0.90	1.18	1.04	0.88	1.10	0.99	0
19:0 <i>cy ω8c</i>	1.49	n.d		1.53	1.49	1.51	0
<i>Unsaturated</i> % of total fatty acids							
16:1 <i>ω7c</i>	14.71	15.35	15.03	12.70	12.82	12.76	- 15
18:1 <i>ω9c</i> (new)	0.00	0.00	0.00	0.93	0.75	0.84	0
<i>Sat/unsat</i>	1.96						4.52

The results show that silver-exchanged zeolite X influenced the cellular fatty acid composition of all three microorganisms. The profiles of *E. coli* revealed an increase in saturated fatty acid

composition after treatment with silver-exchanged zeolite X and a reduction in the unsaturated fatty acids. Similar result was obtained for *P. aeruginosa* although the composition for the new fatty acid formed (18:1 ω 9c) could be not determined. All the fatty acids detected in *S. aureus* were saturated fatty acids. With the exception of 17:0 *iso* there was an increase in all changes to fatty acid composition in *S. aureus*.

6.3 Effect of silver-exchange zeolite X on DNA of *E. coli*,

The interaction of λ -DNA (standard) and DNA of *E. coli* K12 W-T (isolated) with silver-exchanged zeolite X (Ag-X) was investigated by FTIR. As compared to the spectrum of λ -DNA alone, changes in the FTIR spectrum of isolated DNA/Ag-X complex occurred. DNA remained in a B-form conformation in the DNA-silica complex (Naumann *et al.*, 1991). Table 32 was used tentatively for bands assignment. For λ -DNA and isolated DNA, the spectra are dominated by two broad bands at 3315 cm⁻¹ and 1646 cm⁻¹. These broad bands were also observed for Ag-X/DNA spectra (Wong *et al.*, 1991). Two additional weak bands occurred at 1122 cm⁻¹ and 1438 cm⁻¹ for isolated DNA of *E. coli* K12 W-T which shifted towards lower intensities upon Ag/DNA intercalation (Wong *et al.*, 1991; Menashi *et al.*, 1998). The most prominent changes in the DNA spectrum occurred in the 800 cm⁻¹ to 1600 cm⁻¹ region. The PO₂⁻ asymmetric stretch at 1438 cm⁻¹ increased in intensity and slightly shifted towards a lower frequency of 1254 cm⁻¹; the PO₂⁻ symmetric stretch at 1122 cm⁻¹ markedly increased in intensity and shifted towards a lower frequency of 1090 cm⁻¹. Two new bands were formed at 1419 cm⁻¹ and 1563 cm⁻¹ for Ag/ λ DNA. These bands can be assigned to the C = O symmetric stretching of the -COO⁻ functional groups and the formation of amide II structures (Naumann *et al.*, 1991; Chiriboga *et al.*, 2000). The spectrum obtained for Ag- λ DNA has a new band at 964 cm⁻¹. This band can be assigned to either the phosphodiester or the C = O stretch of DNA backbone, is significantly reduced in

intensity (Wong *et al.*, 1991; Menashi *et al.*, 1998; Chiriboga *et al.*, 2000). The region between 2000 cm^{-1} and 2222 cm^{-1} did not show a clear band for all DNA species used in the study.

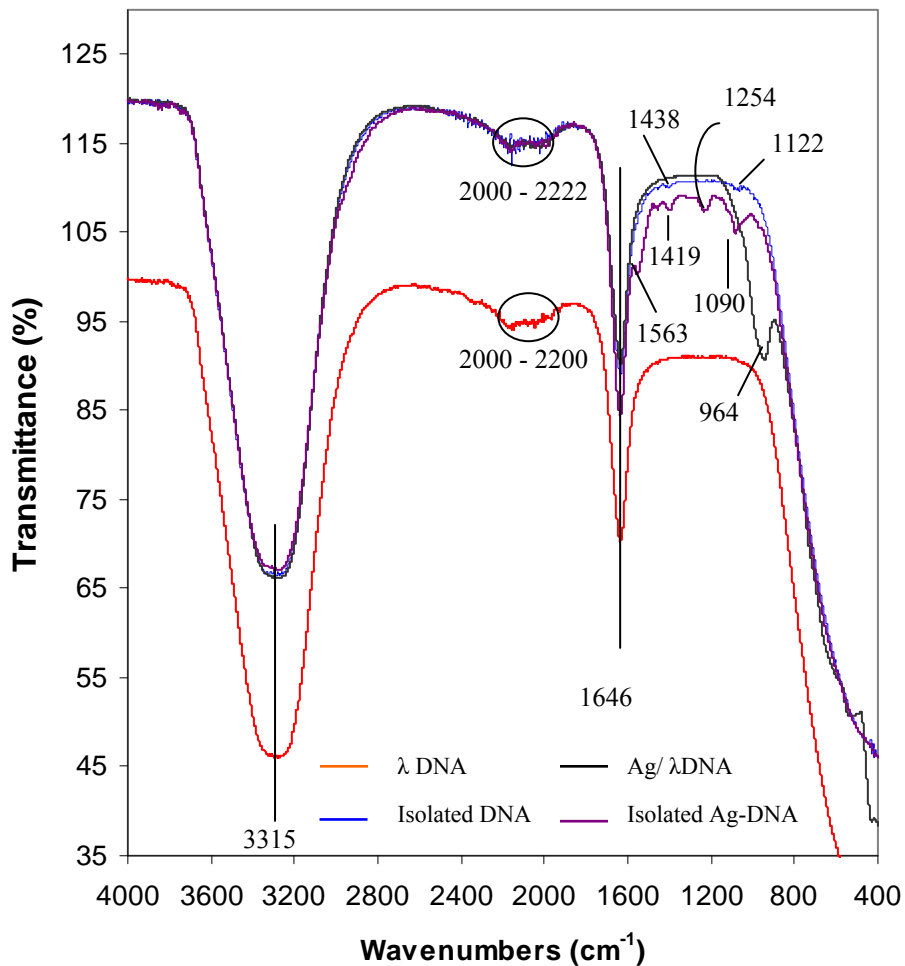


Figure 64: FTIR spectra of λ DNA, Ag/ λ DNA, isolated DNA of *E. coli* K12 W-T and isolated Ag/ λ DNA of *E. coli* K12 W-T.

The results of this study showed that silver-exchanged zeolite X intercalates to the phosphate-sugar backbone of DNA. Intercalation may contribute to DNA strand breakage produced by Ag^+ . The ability of Ag^+ to form stable complexes with DNA may play an important role in the mechanisms of Ag^+ -induced toxicity in microorganisms (Wong *et al.*, 1991; Menashi *et al.*, 1998).

Table 32: General band assignment of bacterial components (Naumann *et al.*, 1991; Menashi *et al.*, 1998; Chiriboga *et al.*, 2000)

Wave number (cm^{-1})	Definition of spectral assignment
3307	N – H and O – H stretching vibrations: Polysaccharides, proteins
2959	CH ₃ asymmetric stretch: mainly lipids
2927	CH ₂ asymmetric stretch: mainly lipids with little contribution from proteins, carbohydrates and nucleic acids
2876	CH ₃ symmetric stretch: mainly lipids with little contribution from proteins, carbohydrates and nucleic acids
2857	CH ₂ symmetric stretch: mainly lipids with little contribution from proteins, carbohydrates and nucleic acids
1739 – 1744	Ester C = O stretch: lipids, triglycerides
1657	Amide I (proteins C = O stretching): α helices
1541	Amide II (protein N – H bend, C – N stretch): α helices
1452	CH ₂ bending: lipids
1391	COO ⁻ symmetric stretch: amino acid side chains, fatty acids
1236	PO ₂ ⁻ asymmetric stretching mainly nucleic acids with little contribution from phospholipids
1152	CO-O-C asymmetric stretching: glycogen and nucleic acids
1080	PO ₂ ⁻ symmetric stretching: nucleic acids and phospholipids
969	C-N ⁺ -C stretch: nucleic acids

6.4 Discussion

The effects on *E. coli* K12 W-T and *S. aureus* NCIMB6571 components caused by their interaction with silver were investigated as follows. In the first study, the effect on membrane permeability of both strains was assessed by Flow Cytometry. The fluorescence from dead cells of both strains increased upon PI staining. This indicates that the cytoplasmic membrane became permeable. Hence it is likely that silver ions were able to reach the interior of both *E. coli* K12 W-T and *S. aureus* NCIMB 6571. Feng *et al.*, (2000) reported that the cytoplasm membrane shrank and detached from the cell wall on exposure to silver ions. In addition, observations by Yamanaka *et al.*, (2005) indicated that bactericidal actions of the silver ions are caused primarily by its interaction with the cytoplasmic membrane in the interior of the cell. The silver ion appeared to penetrate through ion channels without causing damage to the cell membranes. It can therefore be speculated silver ions were likely to have denatured the ribosome and suppressed the expression of enzymes and proteins essential to ATP production (Yin *et al.*, 1999; Sondi and Salopek-Sondi, 2004). The results obtained from this study indicate that the cell wall as well as the cytoplasmic membranes of *E. coli* K12 W-T and *S. aureus* NCIMB 6571 were likely to have been affected by the action of silver-exchanged zeolite X. However, the interaction of silver with bacterial components has been reported to primarily affect the function of membrane-bound enzymes, such as those in the respiratory chain (Bragg and Rainnie, 1974, McDonnell and Russell, 1999). The sensitivities of bacterial species may not be determined by changes in a single cellular parameter (McDonnell and Russell, 1999). However, flow cytometry provided a qualitative means of monitoring the dynamic cellular events that occurred in *E. coli* K12 W-T and *S. aureus* NCIMB 6571.

The second study involved the investigation of the changes in the fatty acid composition in *E. coli* K-12 W-T, *S. aureus* NCIMB6571 and *P. aeruginosa* NCIMB8295. All the analyses demonstrated that there was significant effect relating to the bacteriostatic effect of silver-exchanged zeolite X on *E. coli* K-12W-T and where applicable *S. aureus* and *P. aeruginosa*. For the fatty acid composition analysis, the saturated/unsaturated ratio in *E. coli* increased on exposure to silver-exchanged zeolite X. Similar results were obtained for *P. aeruginosa* although not all the fatty acid compositions in *P. aeruginosa* were determined. Mrozik *et al.*, (2004a) obtained similar results of fatty acid profiles for *P. aeruginosa* when they studied the influence of naphthalene on fatty acid composition of *Pseudomonas* sp. JS 150. Cells of *E. coli* contained significant proportion of 17:0 *cy* and 19:0 *cy* ω 8c. Similar results were obtained by Mrozik *et al.*, (2005) when they detected an increase in cyclopropane fatty acid composition in response to naphthalene. Low content of fatty acid composition in *P. putida* and *P. stutzeri* upon their exposure to catechol, phenol, and toluene was also reported by Ramos *et al.*, (1997) and Mrozik *et al.*, (2004a).

Exposure to silver-exchanged zeolite X also changed the composition of branched and hydroxyl fatty acids (Table 30 – 32). *S. aureus* NCIMB 6571, nearly all the fatty acids detected were saturated with an increase in the composition of branched fatty acids. Tsitko *et al.*, (1999) obtained similar results when he studied the impact of different aromatic compounds on whole cell fatty acid composition of *Rhodococcus opacus* strains GM-14, GM-24 and 1CP. According to Sikkema *et al.*, (1995) and Sajbidor, (1997), changes in the ratio of straight to branched chain fatty acids is a possible mechanism for the production for the protection of bacteria from the aromatic substrate toxicity. Thus it is possible that a similar protection mechanism could be adapted by bacteria towards other antimicrobial agents such as antibiotics.

Another type of change in the fatty acids composition was the appearance of new fatty acid in *S. aureus* NCIMB 6571 (Table 31). The mechanism of formation of new fatty acids have not been documented (Allen *et al.*, 1997; Gutierrez *et al.*, 1999; Mrozik *et al.*, 2004a, 2004b). However, they may be involved in the protection of strains tested against disruptions of the membrane-cell wall structure (Heipieper *et al.*, 1992; Heipieper *et al.*, 1994; Heipieper *et al.*, 2003; Mrozik *et al.*, 2005).

In the third study, vibrations associated with spectral changes in intensity and shift in wavelengths in DNA of *E. coli* K12 W-T was investigated by FTIR spectroscopy. DNA contains two kinds of potential nucleophilic sites which can function as hydrogen receptors: the exocyclic nitrogens or carbonyl oxygens of the purine and pyrimidine bases, and the phosphate oxygen atoms (Rodgers *et al.*, 1990; Madigan *et al.*, 2000). Each of these groups is capable of forming a hydrogen bond with a hydrogen donor molecule under specific chemical conditions (Ruddon, 1990). The molecular vibrations arising from these different moieties of DNA can be analyzed and observed in specific regions of the IR spectrum. This study demonstrates that DNA binds strongly to silver ions. Specific binding of silver ions to DNA *in vitro* (Chiriboga *et al.*, 2000) had been reported. It is possible that the binding was likely to have been enhanced by the positive charge on the silver ions and the negative charge on the phosphate moieties. The most meaningful changes observed in the FTIR spectra of DNA in a silica-DNA complexes appeared in the region between 1600 and 800 cm^{-1} (Mao *et al.*, 1994). The shift in frequency and increase in intensity of the PO_2^- asymmetric stretch at 1438 cm^{-1} suggests that the phosphate group is an important site with which silver interacts on DNA, and is the direct target for silver binding. Interaction of silver ions with DNA at phosphate/base pair sites can results in proton displacement and a possible disruption of base pairing within the DNA-duplex.

Chapter 7

Overall Discussion and Conclusion

7.1 Overall discussion

7.1.1 Silver release and uptake by microorganisms

Currently, information available on the release of silver ions from silver compounds is very little since results reported in literature are conflicting (Brett, 2006). While results showed that the amount of silver ions released to effect antimicrobial activity has been found to be directly proportional to the rate of kill *in vitro* (Schierholz *et al.*, 1998; Ovington, 1999; Thibon *et al.*, 2000; Ovington, 2001; Ovington, 2005) other literatures (Ovington, 2004; Parsons *et al.*, 2005) showed the contrary. The results obtained from this study showed that silver ions were released from the zeolite in an anomalous trend and inhibition of growth rate. The discrepancies between results have been attributed to the lack of detail on how some tests are performed and the established chemical principles of solubility (Brett, 2006). As an example it has been shown that a hydrofiber dressing containing the silver and carboxymethylcellulose (Ag/CMC) released 0.8 ppm of silver in water and in saline (Parsons *et al.*, 2005) but released 85 ppm of silver in thiosulfate (Wright *et al.*, 1998). Nanocrystalline silver released 50 ppm (Parsons *et al.*, 2003) or 70 ppm in water (depending on experimental conditions), 0.8 ppm in saline for the same analysis and 640,000 ppm in thiosulfate (Wright *et al.*, 1998). Hence, extent of silver elution depends on the nature of the type of media and the experimental conditions. The anomalous release trend observed in this study can be explained by Le Chatelier's principles of chemical equilibrium and solubility products (Zumdahl, 1986).

Recalling equation (c) from Section 4.1.2:



As samples were withdrawn from the flask silver ions in the culture were reduced. This implies that more silver needed to be released from the zeolite framework to replace what was removed.

According to Le Chatelier's principle the position of the equilibrium will shift to the right hence

more silver ions were likely to be released from the zeolite framework. However, the release of silver ions is controlled by the zeolite framework. Hence the amount of silver ions released at any time depends on the location of ions in the framework. Silver ions at exchangeable sites are normally more difficult to displace than those at the surface or in the pores (Yeom and Kim 1997). It is likely that this observation might account for the anomalous trend of the silver release from the zeolite framework into the TSB.

The uptake of silver ions in bacteria depends on the type of strain being inhibited or killed (Haefeli *et al.*, 1984). Some strains can be inhibited or killed with very low levels of silver. Other strains require significantly higher levels of silver to exert effective antimicrobial activity. In some literature the strain is not mentioned making the determination of the relevance of some data unrealistic. An example is given by Yin *et al.*, (1999) and Spacciapoli *et al.*, (2001). They performed experiments on five different strains of *Pseudomonas*. Their results showed that higher levels of silver result in rapid, bactericidal activity on all or most (five with nanocrystalline silver, four with silver sulfadiazine) strains tested; whereas lower levels of silver had an effect on only one of the strains tested.

More silver ions were released from the zeolites frameworks (in TSB) in the absence of *E. coli* K12 W-T, *S. aureus*, NCIMB6571 or *P. aeruginosa* NCIMB 8295 than when the strains was present. Such observation might imply that there was a possible binding and uptake of silver ions by each strain. For instance, in a study by Ghandour *et al.*, (1988), incubation of non-growing cells in HEPES buffer (pH 7.4) at increasing levels of Ag^+ resulted in the progressive saturation of two types of binding sites. The first site was found to be intracellular because the silver ions were not released by washing the cells with 0.1 M nitric acid. The silver ions bound to the second site were released when the cells were washed with 0.1 M nitric acid but not with buffer washing and were assumed to be surface-bound. Gadd *et al.*, (1989) reported that *P. stutzeri* did

not grow in the presence of 0.5 mM AgNO₃ in contrast to silver-free controls with silver accumulation in the cells occurring within one minute of contact time. In another study by Starodub and Trevors (1990), silver ions accumulation were detected in both Ag⁺-sensitive *E. coli* S1 strain and Ag⁺-resistant *E. coli* R1 strain. The accumulation in *E. coli* S1 was found to be 5-fold higher than that in *E. coli* R1. Silver accumulation has also been reported in yeast (Pümpel and Schinner, 1985). Silver-tolerant microorganisms isolated from soil materials of silver mine showed the following accumulation capacity (Pümpel and Schinner, 1985): bacteria accumulated a mean 23 mg Ag⁺/g dry weight, hyphomycetes 6.7 mg/g dry wt. and yeasts 0.46 mg/g dry wt. The accumulation process of the hyphomycete with the highest accumulation capacity (20 mg/g dry wt.) was shown to be completed after about 30 minutes.

The amount of silver ions released from the frameworks of the zeolites used in this study and detected by ICP-AES at any sampling time was within the range of 5 ppm – 12 ppm. The total concentration of silver ions in (ppm) released from the zeolites frameworks were inversely proportional to the mass of silver zeolites added to the TSB. Antibacterial activity of silver at concentration of 1 ppm has been reported to show at least 1 log reduction (Spacciapoli *et al.*, 2001). Furthermore, 16 % of the published *in vitro* data showed >3 log reductions (bactericidal); whereas, for silver concentrations >36 ppm, 67.9% of the data showed log reductions greater than 3 (Hall *et al.*, 1987; Spacciapoli *et al.*, 2001). Although the amount of silver released at the detection limit in this study were less than 36 ppm it showed 2.5-3 log reductions of viable cells of the strains. The difference in concentrations in this work compared to literature might be due to the source of silver ions and the presence or absence of organic/inorganic compounds (Brett, 2006). Since silver ion is extremely reactive, it can react with a variety of anions such a chloride, sulphates, phosphates, carbonates, and acetates found in biological fluids to form relatively insoluble complexes or precipitates (Hall, *et al.*, 1987; Yin *et al.*, 1999; Feng *et al.*, 2000;

Spacciapoli *et al.*, 2001). This complexation phenomenon is likely to necessitate less delivery of an adequate concentration of silver for antimicrobial activity to be observed. In addition, silver ions binds to proteins and nucleic acids. This is can further reduce the amount of available silver. Consequently, the antimicrobial efficacy of the silver can be reduced since less silver will be available to interact with the microorganism (Yin *et al.*, 1999).

7.1.2 Mode of action of antimicrobial activity of silver

The antibacterial activity of silver-exchanged zeolite X, A, high-alumina Phillipsite and silver-doped analcime on *E. coli* K12W-T, *S. aureus* NCIMB6571 and *P. aeruginosa* NCIMB 8295 in TSB was investigated. Figure 36, Figure 41, Figure 47 and Figure 53 shows the changes in the viable cell counts of *E. coli* K12W-T, *S. aureus* NCIMB6571 and *P. aeruginosa* in the suspension. The controls: *E. coli* K12 W-T, *S. aureus* NCIMB 6571 or *P. aeruginosa* NCIMB 8295 in TSB on one hand and *E. coli* K12 W-T, *S. aureus* NCIMB 6571 or *P. aeruginosa* NCIMB 8295 plus 1.0 g l^{-1} of zeolites (zeolite X, A, high-alumina Phillipsite or Analcime) in TSB on the other hand showed no loss in colony forming ability within 24 hours of contact time. In the presence of silver-loaded zeolites (used in this study) it was clearly observed that all three strains in TSB lost their colony forming ability within two hours. This showed that the inhibition of *E. coli*, *S. aureus* or *P. aeruginosa* was the resultant effect of silver and not the zeolites.

Silver ions held in the zeolites are effective against a wide range of microorganisms and appear to have multiple target sites of microorganisms (Russell and Hugo, 1994). It also interferes with a wide range of molecular processes within the microorganisms. While the exact mechanism(s) of action are not fully understood, three possible ways have been suggested. First, silver ions interact with the cell wall, attached to the cell envelope resulting in the loss of membrane integrity as a result of disruption of the cell envelope (Liau *et al.*, 1997; Feng *et al.*, 2000). The

ionic species carries a strong positive charge so it has high affinity for negatively charged groups of biological molecules. These include groups such as sulfhydryl, carboxyl, phosphates, and other groups commonly found on macromolecular structures distributed throughout microbial cells. The binding reaction alters the molecular structure of the macromolecule, rendering it worthless to the cell. This attack on multiple sites within a cell simultaneously inactivates many functions such as cell wall synthesis, membrane transport, nucleic acids such as RNA and DNA synthesis and translation, and protein folding and function. Without these functions, the bacterium is either inhibited from growth or, more commonly, dies.

The mechanism of antimicrobial action of silver has been found to depend on both concentration of silver ions present and the sensitivity of the microbial species to silver. Very recently antibacterial assay and spectroscopic study revealed that light irradiation enabled Ag-Z to reduce dioxygen to form a reactive oxygen species, which led to bactericidal activity (Inoue *et al.*, 2008). These results indicate that the onset of bactericidal activity can be controlled by light irradiation. Although the contact time, temperature, pH and the presence of free water impact on the rate and extent of antimicrobial activity, the spectrum of activity is wide (Rees *et al.*, 1998; Matsumura *et al.*, 2003) and the development of resistance relatively low (Cooper, 2004). All the silver-loaded zeolites produced in this study inhibited the growth of *E. coli* K12W-T, *S. aureus* NCIMB6571 or *P. aeruginosa* NCIMB8295. This is a clear proof that silver-loaded zeolites exhibit bacteriostatic *in vitro* (Kawahara *et al.*, 2000; Inoue *et al.*, 2002). The results obtained from the antimicrobial activity of silver-loaded zeolites used in this study showed that gram-negative bacteria *E. coli* K12W-T was more susceptible to silver ions than gram-positive *S. aureus* NCIMB6571. Kawahara *et al.*, (2000) observed a similar result on *Porphyromonas gingivalis* and *S. aureus* and concluded that the structural difference in their structural cell wall may have played a role in their susceptibility. Gram-positive bacteria cell wall contains three to

twenty times more peptidoglycan than their gram-negative counterpart (Feng *et al.*, 2000; Kawahara *et al.*, 2000). Since peptidoglycans are negatively charged, it binds some portion of silver. Consequently more silver ions reach the plasma membrane of gram-negative than gram positive bacteria. However, *P. aeruginosa* exhibited less susceptibility than *S. aureus* in this study since it took a slightly longer time to reach the detection limit (33.3 cfu/ml). This might be due to the fact that different microorganisms have different multiple strains and different strains can require different levels of silver to effect antimicrobial action (Brett, 2006).

7.1.3 Bacterial resistance to silver

The genetic and molecular basis for silver resistance in pathogenic microorganisms has been proposed (Gupta *et al.*, 1999). Silver-resistant pathogens have been developed in the laboratory by growing microbes and introducing sub-lethal levels of silver using a multiple step exposure protocol (Li *et al.*, 1997). Resistance to silver compounds as determined by bacterial plasmids and genes has been defined by molecular genetics (Silver, 2003). Silver resistance conferred by the *Salmonella* plasmid pMGH100 involves nine genes in three transcription units (Silver, 2003). A sensor/responder (*SilRS*) two-component transcriptional regulatory system governs synthesis of a periplasmic Ag(I)-binding protein (*SilE*) and two efflux pumps (a P-type ATPase (*SilP*) plus a three-protein chemiosmotic RND Ag(I)/H⁺ exchange system (*SilCBA*)). The *sil* determinant is governed by a two-component membrane sensor and transcriptional responder comprising *SilS* and *SilR*, which are co-transcribed (Gupta *et al.*, 1999). The centrally located six genes are found and functional in the chromosome of *E. coli* K-12, and also occur on the genome of *E. coli* O157:H. In this study the resistance to the silver-loaded zeolites were not determined. However, since all the silver-loaded zeolites persisted in their antimicrobial activity upon successive retrievals, resistance from any of the strains was unlikely.

7.2 Overall Conclusion

The antimicrobial activity of both silver-exchanged zeolites X, A, and high-alumina Phillipsite and silver-doped Analcime have been confirmed. The efficacy of antimicrobial activity was independent of the type of silver-loaded zeolite applied on all three strains. The silver ions released from the zeolites' frameworks either attached to the bacteria cell envelope or were reversibly adsorbed back into the zeolites' frameworks. Consequently, this resulted in the anomalous trends in the release profiles of silver ions into TSB. There was no significant difference in the release of silver ions for all silver-loaded zeolites in all experiments. Hence this suggests that there was probably, sustained release of silver ions from the zeolite framework into the bacterial cultures, which exerted effective antimicrobial activity on all three microorganisms. The mechanism of antimicrobial activity of silver is still unclear. The results obtained in this study suggest that the action of silver on bacteria begins with an uptake of silver ions by the bacteria as shown by the flow cytometry analysis of *E. coli* K12 W-T. The uptake resulted in an increase in PI uptake suggesting an effect on the membrane permeability of *E. coli* K12 W-T. Silver ions are likely to be transported possibly by the gradient resulting from the protomotive force as nutrients essential to ATP production are affected. Furthermore DNA replication is significantly affected as evidenced by the spectral changes in DNA observed by FTIR analysis. Consequently the fatty acid composition of the bacteria is significantly altered.

Although the clinical applicability of the silver-loaded zeolites has not been established, it has attractive features, which make it potentially useful in many areas such as health and chemical and petrochemical industries.

7.3 Limitations of this study

As the antimicrobial activity of the silver-loaded zeolites were performed only one strain of *E. coli*, *S. aureus* and *P. aeruginosa* under similar conditions, the results might be different for other microorganisms under different conditions. Hence the results obtained in this study can be used as a model for other microorganisms. As some zeolites were lost during the retrieval of zeolites from TSB the accuracy of the concentrations of silver left in the zeolite frameworks might be prone to some small errors.

7.4 Suggestions for future work

The ion exchange technique can be repeated over two or three successive times in order to optimize the loading of silver ions into the zeolite framework. The characterizations of silver-loaded zeolites in this study can also be optimized in future work. In order to specify the location of silver ions in the zeolite framework, elemental analysis on the silver-loaded zeolites can be performed. A model describing loading limits of silver for zeolites needs to be developed in order to compare with theoretical loading limits. Work can also be carried to determine the exchange isotherms for Ag – Na ion exchange. In addition, work can also be carried towards the formulation of silver zeolite products after performing toxicity tests.

This study has provided the basis for investigating further the attractive features of silver-loaded zeolites as antimicrobial agents. Since the microorganisms used in this study were bacteria, antiviral and antifungal investigation of the silver-loaded zeolites can be studied. The mechanism of antimicrobial action presented in this work can be validated by performing further flow cytometry analysis on different strains of bacteria and/or microorganisms. In addition the

location of silver ions in the bacteria can be analyzed by transmission electron microscopy (TEM) to give us a better understanding of the mode of antimicrobial activity of silver.

List of Abbreviations, reagents, suppliers and instrumentations

Table 32: List of reagents, suppliers and abbreviations or chemical formula

Reagent	Purity	Supplier	Abbreviation/Chemical formula
Sodium hydroxide	97 + %	Sigma Aldrich	NaOH
Potassium hydroxide	85 + %	Sigma Aldrich	KOH
Sodium silicate	98 %	Fisher Chemicals	Na ₂ SiO ₃
Sodium aluminate	98 %	Fisher Chemicals	NaAlO ₂
Sodium metasilicate	98 %	Fisher Chemicals	NaAlO ₂
Silver nitrate	99 %	Aldrich	AgNO ₃
Dimethyl sulphide	99 %	Fischer	SDS
RNAseA	99 %	Sigma Aldrich	----
Propidium Iodide	99 %	Molecular Probes	PI
SYTO 22	99 %	Molecular Probes	-----
Tris-base	99 %	MELFORD	C ₄ H ₁₁ NO ₃ .
Methanol (HPLC grade)	99 %	Sigma Aldrich	CH ₃ OH
LUDOX AS-30 (30 % wt in water)	-----	Sigma Aldrich	-----
LUDOX AS-40 (40 % wt in water)	-----	Sigma Aldrich	-----
Ethylenediaminetetraacetic acid	----	BDH	EDTA
Hydrochloric acid	37 %	Sigma Aldrich	HCl
Triethanolamine amide	----	Sigma Aldrich	TEA
Methyl-tert-butyl ether	----	Sigma Aldrich	MTBE
Hexadecylmethylammonium bromide	----	BDH	CTAB

Table 33: List of abbreviations for silver-loaded zeolites

Zeolite type	Abbreviation
Zeolite X	Z-X
Silver-exchanged zeolite X	AgZ-X
Zeolite A	Z-A
Silver-exchanged zeolite A	AgZ-A
High-Alumina Phillipsite	HAP
Silver-exchanged high-alumina Phillipsite	AgHAP
Faujasite	FAU
Linde type A	LTA
Analcime	ANA
Phillipsite	PHI

Table 34: List of media/microorganisms, suppliers and their abbreviations

Media/microorganism	Supplier	Abbreviation
Tryptone soya broth	Lab M, UK	TSB
Ringer	Lab M, UK	----
Tryptone soya agar	Lab M, UK	TSA
<i>Escherichia coli</i> K12 W-T	Lab M, UK	<i>E. coli</i> K12 W-T
<i>Staphylococcus aureus</i> NCIMB 6571	Lab M, UK	<i>S. aureus</i> NCIMB 6571
<i>Pseudomonas aeruginosa</i> NCIMB 8295	Lab M, UK	<i>P. aeruginosa</i> NCIMB 8295

Table 35: List of instruments, their abbreviations and location

Instrument	Abbreviation	Location
X-ray diffraction	XRD	UoW
Scanning electron microscope	SEM	UoW
Energy dispersive X-ray analysis	EDX	UoW
Fourier transformed infrared spectrometer	FTIR	UoW
Mastersizer X long bed particle size analyzer	----	UoW
Inductively coupled plasma –atomic emission spectrometer	ICP-AES	UoW
Flow Cytometer	FC	UoW
Gas chromatograph	GC	UoS

UoW = University of Wolverhampton, United Kingdom

UoS = University of Silesia, Poland

References

- Abe, Y., Ueshige, M., Takeuchi, M., Ishii, M. and Akagawa, Y. (2004). Effect of saliva on an antimicrobial tissue conditioner containing silver–zeolite. *International Journal of Prosthodont* **16**(2): 141 – 144.
- Alfaro, S., Rodriguez, C., Valenzuela, M. A. and Bosch, P. (2007). Aging time effect on the synthesis of small crystal LTA zeolites in the absence of organic template. *Material Letters* **61**: 4655 – 4658.
- Allen, C. C. R., Boyd, D. R., Larkin, M. J., Reid, K. A., Sharma, N. D. and Wilson, K. (1997). Metabolism of naphthalene, 1-naphthol, indene and indole by *Rhodococcus* sp. Strain NCIMB-12038. *Applied and Environmental Microbiology* **63**: 151 – 155.
- Amor, K. B., Breeuwer, P., Verbaarschot, P., Rombouts, F. M., Akkermans, A. D. L., De Vos, W. M. and Abee, T. (2002). Multiparametric Flow Cytometry and Cell Sorting for the Assessment of Viable, Injured, and Dead Bifidobacterium Cells during Bile Salt Stress. *Journal of Applied and Environmental Microbiology* **68**: 5209 – 5216.
- Amphlett, C. B. (1964). Inorganic ion exchange materials. Elsevier, New York.
- Anderson, J. (2003). The Environmental Benefits of Water Recycling and Reuse. *Water Science and Technology*. *Water Supply* **3**(4): 1 – 10.
- Araujo, A. S., Fernandes, V. J. J., Diniz, J. C., Silva, C. C. and Santos, R. H. A. (1999). Hydrothermal synthesis and crystallographic properties of silicoaluminophosphate with different content of silicon. *Material Research Bulletin* **34**(9): 1369 – 1373.
- Aronne, A., Esposito, S. and Pernice, P. (1997). FTIR and DTA study of lanthanum aluminosilicate glasses. *Material Chemistry and Physics* **51**: 163.
- Atiyeh, B. S., Facs, S. N. and Hayek, M. D. (2007). The safety and efficacy of dressings with silver - addressing clinical concerns. *International Wound Journal* **4**(3): 283–284.
- Baars, L., Ytterberg, A. J., Drew, D., Wagner, S., Thilo, C., van Wijk, K. J. and de Gier, J.-W. (2006). Defining the Role of the *Escherichia coli* Chaperone SecB Using Comparative Proteomics. *Journal of Biological Chemistry* **281**: 10024 – 10034.
- Balandis, A. and Traidaraite, A. (2007). The influence of Al containing component of synthesis of analcime of various crystallographic systems. *Material Science-Poland* **25**(3): 637 – 647.
- Barrer, R. M. (1982). Hydrothermal chemistry of zeolites. Academic Press, New York.

Barthomeuf, D. (1996). Basic Zeolites: Characterization and Uses in Adsorption and Catalysis. *Catalysis Reviews* **38**(4): 521 – 612.

Barth-Wirsching, U. and Höller, H. (1989). Experimental studies on zeolite formation conditions. *European Journal of Mineralogy* **1**: 489-506.

Bellantone, M., Williams, H. D. and Hench, L. L. (2002). Broad-spectrum bactericidal activity of Ag₂O-doped bioactive glass. *Antimicrobial Agents and Chemotherapy* **46**(6): 1940 – 1945.

Bergero, D., Boccignone, M., Di Natale, F., Forneris, G., Palmegiano, G. B. Roagna, L. and Sicuro, B. (1994). Ammonia removal capacity of European natural zeolite tuffs: Application to aquaculture waste water. *Aquaculture Research [AQUACULT. FISH. MANAGE.]* **25**(8): 813 – 821.

Blondelle, S. E. and Houghten, R. A. (1996). Novel antimicrobial compounds identified using synthetic combinatorial library technology. *Trends in Biotechnology* **14**(2): 60 – 65.

Bloomfield, S. F. (1974). The effect of the phenolic antibacterial agent Fenticlor on energy coupling in *Staphylococcus aureus*. *Journal of Applied Bacteriology* **37**:117 – 131.

Bragg, P. D. and Rainnie, D. J. (1974). The effect of silver ions on the respiratory chains of *Escherichia coli*. *Canadian Journal of Microbiology* **20**: 883.

Breck, D. W. (1974). In: *Zeolite Molecular Sieves, Structure Chemistry and Use*, Wiley, New York, NY.

Brett, D. W. (2006) A discussion of silver as an antimicrobial agent: Alleviating the confusion. *Ostomy/Wound Management* **52**(1): 34 – 41.

Bright, K. R., Gerba, C. P., and Rusin, P. A. (2002). Rapid reduction of *Staphylococcus aureus* populations on stainless steel surfaces by zeolite ceramic coatings containing silver and zinc ions. *Journal of Hospital Infection* **52**(4): 307 – 309.

Brinker, C. J., Scherer, G.W. (1990). *Sol-Gel Science: The Physics and Chemistry of Sol-Gel Processing*. Academic Press, Boston.

British museum (2005) Atomic absorption spectrometer [online]. The British Museum, [cited 9th March, 2006].

Bruch, M. K. (1996). Chloroxyleneol: an old-new antimicrobial. In: *Handbook of disinfectants and antiseptics*. Ascenzi J. M. (Ed) New York, N.Y: Marcel Dekker, Inc. 265–294.

Caddow, P. (1989). Microorganisms and their properties In: *Applied Microbiology* 1st ed. London, England: Scutari Press: 17– 42.

Cambor, M. A., Mifsud, A. and Perez-Pariente J. (1991). Influence of the synthesis conditions on the crystallization of zeolite beta. *Zeolites* **11**: 792.

Castillo, J. A., Clapes, P. Infante, M. R. Comas, J. and Manresa, A. (2006). Comparative study of the antimicrobial activity of bis(N-caproyl-L-arginine)-1,3-propanediamine dihydrochloride and chlorhexidine dihydrochloride against *Staphylococcus aureus* and *Escherichia coli*. *Journal of Antimicrobial Chemotherapy* **57**: 691 – 698.

Chambon, M., Bailly, J.-L., and Peigue-Lafeuille, H. (1992). Activity of glutaraldehyde at low concentration against capsid proteins of polio virus type 1 and echovirus type 25. *Applied and Environmental Microbiology* **58**: 3517 – 3521.

Chiriboga, L., Yee, H., and Diem, M. (2000). Infrared Spectroscopy of Human cells and tissues. Part VII: FT-IR Microspectroscopy of Dnase- and RNAase- Treated normal, cirrhotic, and neoplastic liver tissue. *Applied Spectroscopy* **54**: 480 – 485.

Cichocki, A. (1991). Synthesis of High Aluminium Phillipsite. In: *Verified Synthesis of Zeolitic Materials*. Robson, H. (Ed). Elsevier Publications, Amsterdam. 246 – 248.

Ciric, J. (1992). Synthetic Zeolites: Growth of Larger Single Crystals. *Science* 689.

Cloete, T. E. (2003). Resistance mechanisms of bacteria to antimicrobial compounds. *International Biodeterioration and Biodegradation* **51**: 277 – 282.

Coker, E. N., Dixon, A. G., Thompson, R. W. and Sacco, A. Jr. (1995). Zeolite synthesis in unstirred batch reactors II. Effect of non-uniform pre-mixing on the crystallization of zeolites A and X. *Microporous Materials* **3**: 637 – 646.

Collela, C. (1996). Ion exchange equilibria in zeolite materials. *Mineralium Deposita* **31**: 554 – 562.

Coutinho, D. and Balkus, K. Jr. (2002). Preparation and characterization of zeolite X membranes via pulsed-laser. *Microporous and Mesoporous Materials* **52**(2): 79 – 91.

Cowan, M. M., Abshire, K. Z., Houk, S. L. and Evans, S. N. (2003). Antibacterial efficacy of a silver zeolite-matrix coating on stainless steel. *Journal of Industrial Microbiology and Biotechnology* **30**(2): 102 – 106.

Culfaz, A. and Sand, L. B. (1973). Mechanism of nucleation and crystallization of zeolites from gels. *Advance Chemistry Series* **121**: 141 – 151.

De'Gennaro, M and Collela, C. (1989). Use of thermal analysis for the evaluation of zeolite content in mixtures of hydrated phases. *Thermochim Acta* **154**: 345 – 353.

Denyer, S. P. (1995). Mechanisms of action of antibacterial biocides. *International Biodeterioration and Biodegradation*. **36**: 227–245.

Denyer, S. P., Gorman, S. P. and Sussman, M. (1993). Microbial biofilms: formation and control. *Society for Applied Bacteriology Technical Series* **30**: 51-94.

Di Renzo, F. (1998). Zeolites as tailor-made catalysts: Control of the crystal size. *Catalysis Today* **41**(1 – 3): 37 – 40.

Diaz, R. and Lazo, M. A. F. (2000). Spectroscopic Study of CuO/CoO Catalysts Supported by Si-Al-Y Zeolite Matrices Prepared by Two Sol-Gel Methods. *Journal of Sol-gel Science and Technology* **17**: 137-144.

Dunn, K. and Edward-Jones, V. (2004). The role of Acticoat with nanocrystalline silver in the management of burns. *Burns* **30**(1): S1 – S9.

Dyer, A. and White, K. J. (1999). Cation diffusion in the natural zeolite clinoptilolite. *Chemochimica Acta* **340 – 341**: 341 – 348.

Efrima, S. and Bronk, B. V. (1998). Silver colloids impregnating or coating bacteria. *Journal of Physical Chemistry B* **102**: 5947 – 5950.

El-Falaha, B. M. A., Rogers, D. T. Furr, J. R. and Russell, A. D (1985a). Effect of some antibacterial agents on the hydrophobicity of wild type and envelope mutants. *Escherichia coli. Current Microbiology* **12**: 187 – 190.

El-Falaha, B. M. A., Furr, J. R. and Russell, A. D. (1985b). Effects of chlorhexidene diacetate and benzalkonium chloride on the viability of wild type and envelope mutant of *Escherichia coli* and *Pseudomonas aeruginosa* *Letters in Applied Microbiology* **1**: 21 – 24.

Ertl, G., Knözinger, H. and Weitkamp. J. (1999). Preparation of solid catalysts. Wiley-VCH Verlag GmbH, Weinheim.

Feng, Q. L., Wu, J., Chen, G. Q., Cui, F. Z., Kim, T. N. and Kim, J. O. (2000). A mechanistic study of the antibacterial effect of silver ions on *Escherichia coli* and *Staphylococcus aureus*. *Journal of Biomedical Material Research* **52**(4): 662 – 668.

Flanigen, E. M., Parton, R. L. and Katonah, W. P. (1978). Silica polymorph and process for preparing same. C01B 33/12. 4073865.

- Fourest, E., Canal, C. and Roux, J. C. (1994). Improvement of heavy metal biosorption by mycelial dead biomasses (*Rhizopus arrhizus*, *Mucor miehei* and *Penicillium chrysogenum*): pH control and cationic activation. *FEMS Microbiological Reviews* **14**(4):325 – 332.
- Franco, M. J., Perez-Pariente, J. and Fornes, V. (1990). Synthesis of zeolite Phillipsite. *Zeolites* **11**: 349 – 355.
- Franke, S., Grass, G. and Nies, D. H. (2001). The product of the ybdE gene of the *Escherichia coli* chromosome is involved in detoxification of silver ions. *Microbiology* **147**(4): 965 – 972.
- Fraud, S., Maillard, J.-Y., and Russell, A. D. (2001). Comparism of the mycobactericidal activity of ortho-phthalaldehyde, gluteraldehyde and other dialdehydes by a quantitative suspension test. *Journal of Hospital Infection* **48**: 214 – 221.
- Gabor, E. M., De Vries, E. J. and Janssen, D. B. (2003). Efficient recovery of environmental DNA for expression cloning by indirect extraction methods. *FEMS Microbiology Ecology* **44** (2): 153–163
- Gadd, G. M., Laurence, O. S., Briscoe, D. A. and Trevors, J. T. (1989). Silver accumulation in *Pseudomonas stutzeri* AG 259. *Biology of Metals* **2**: 168 – 173.
- Galeano, B., Korff, E. and Nicholson, W. L. (2003). Inactivation of Vegetative Cells, but Not Spores, of *Bacillus anthracis*, *B. cereus*, and *B. subtilis* on Stainless Steel Surfaces Coated with an Antimicrobial Silver- and Zinc-Containing Zeolite Formulation. *Applied Environmental Microbiology* **69**(7): 4329 – 4331.
- Ghandour, W., Hubbard, J. A., Deistrung, J., Hughes, M. N. and Poole, R. K. (1988). The uptake of silver ions in *Escherichia coli* K12: toxic effects and interaction with copper ions. *Applied Microbiology and Biotechnology* **28**: 314 – 319.
- Giampaolo, C. and Lombardi, G. (1994). Thermal behaviour of analcimes from two different genetic environments. *European Journal of Mineralogy* **6**(2): 285 – 289.
- Gilbert, P., Pemberton, D. and Wilkinson, D. E. (1990). Barrier properties of the Gram-negative cell envelope towards high molecular weight polyhexamethylene biguanides. *Journal of Applied Bacteriology* **69**:585 – 592.
- Givan, A. L. (2001). *Flow Cytometry: First Principles* New York, NY: Wiley-Less.
- Gontier, S., and Tuel, A. (1996). Incorporation and stability of trivalent cations in mesoporous silicas prepared using primary amines as surfactants. *Applied Catalysis A: General* **143**: 125 – 135.

Gorman, S. P. and Scott, E. M. (1977). Uptake and media reactivity of glutaraldehyde solutions related to structure and biocidal activity. *Microbios Letters* **5**:163–169.

Gorman, S. P., Scott, E. M., Russell, A. D. (1980). Antimicrobial activity, uses and mechanism of action of glutaraldehyde. *Journal of Applied Bacteriology* **48**:161–190.

Gottardi, W. 1985. The influence of the chemical behavior of iodine on the germicidal action of disinfectant solutions containing iodine. *Journal of Hospital Infection* **6**(A):1 – 11.

Grier, N. (2000). Silver and its compounds: disinfection, sterilization and preservation. Philadelphia Lea and Febiger Philadelphia, PA 375 – 389.

Grizzetti, R. and Artioli, G. (2002). Kinetics of nucleation and growth of zeolite LTA from clear solution by in situ and ex situ XRPD. *Microporous and Mesoporous Materials* **54**(1-2): 105 – 112.

Gruciani, G. and Gualtieri, A. (1999). Dehydration dynamics of analcime by in situ synchrotron powder diffraction. *American Mineralogist* **84**: 112.

Gupta, A. and Silver, S. (1998). Silver as a biocide: will resistance become a problem? *Nature Biotechnology* **16**: 888.

Gupta, A., Maynes, M. and Silver, S. (1998). Effects of halides on plasmid-mediated silver resistance in *Escherichia coli*. *Applied Environmental Microbiology* **12**: 5042–5045.

Gupta, A., Matsui, K., Lo, F. and Silver, S. (1999). Molecular basis for resistance of silver cations in *Salmonella*. *Nature Medicine* **5**(2): 183 – 188.

Gutierrez, J. A., Nichols, P. and Couperwhite, I. (1999). Changes in whole cell-derived fatty acids induced by benzene and occurrence of the unusual 16:1 ω 6c in *Rhodococcus* sp. 33. *FEMS Microbiology Letters* **176**: 213 – 218.

Habgood, H. W. (1964). Adsorptive and gas chromatographic properties of various cationic forms of zeolite X. *Canadian Journal of Chemistry* **42**(10): 2340 – 2350.

Haefeli, C., Franklin, C. and Hardy, K. (1984). Plasmid-mediated resistance in *Pseudomonas stutzeri* isolated from a silver mine *Journal of Bacteriology* **158**(1): 389 – 392.

Hall, R. E., Bender, G. and Marquis, R. E. (1987). Inhibitory and cidal antimicrobial actions of electrically generated silver ions. *Journal of Oral Maxillofacial Surgery* **45**:779–784

Hardman, S., Cope, A., Swann, A., Bell, P. R., Naylor, A. R. and Hayes, P. D. (2004). An *in vitro* to compare the antimicrobial activity silver coated versus rifampicin-soaked vascular grafts. *Annals of Vascular Surgery* **18**(3): 308 – 313.

Heipieper, H. J., Diefenbach, R. and Keweloh, H. (1992). Conversion of *cis* unsaturated fatty acids to *trans*, a possible mechanism for the protection of phenol-degrading *Pseudomonas Putida* P8 from substrate toxicity. *Applied and Environmental Microbiology* **58**: 1847 – 1852.

Heipieper, H. J. and de Bont, J. A. M. (1994). Adaptation of *Pseudomonas Putida* S12 to ethanol and toluene at the level of fatty acid composition membranes. *Applied and Environmental Microbiology* **60**: 4440 – 4444.

Heipieper, H. J., Meinhardt, F. and Segura, A. (2003). The *cis-trans* isomerase of unsaturated fatty acids in *Pseudomonas* and *Vibrio*: biochemistry, molecular biology and physiological function of a unique stress adaptive mechanism. *FEMS Microbiology Letters* **229**(1): 1 – 7.

Hiom, S. J., Furr, J. R., Russell, A. D. and Hann, A. C. (1996). The possible role of yeast cell walls in modifying cellular response to chlorhexidine diacetate. *Cytobios* **86**: 123–135.

Hiraoka, H., Yamada, T., Tone, K., Futaesaku, Y. and Kimbara, K. (2002). Flow Cytometry Analysis of Changes in the DNA Content of the Polychlorinated Biphenyl Degradator *Comamonas testosteroni* TK102: Effect of Metabolites on Cell-Cell Separation. *Journal of Applied and Environmental Microbiology* **68**(10): 5104 – 5112.

Hotta, M, H. Nakajima, K. Yamamoto and Aono, M. (1998): Antibacterial temporary filling materials: the effect of adding various ratios of Ag-Zn Zeolites. *Journal of Oral Rehabilitation* **25**: 485 – 489.

Hovis, G. L., Roux, J. and Rodrigues, E. (2002). Thermodynamic mixing properties of nepheline-kalsilite crystalline solutions. *American Mineralogist* **87** : 1108 – 1127.

Hughes, R. C. and Thurman, P. F. (1970). Cross-linking of bacterial cell walls with glutaraldehyde. *Biochemical Journal* **119**: 925–926.

Hugo W B. (1991). The degradation of preservatives by micro-organisms. *International Biodeterioration and Biodegradation*. **27**: 185–194

Iler, R.K. (1979). The Chemistry of Silica: Solubility, Polymerization, Colloid and Surface Properties, and Biochemistry. John Wiley & Sons, New York.

Inoue, Y., Hoshino, M., Takahashi, H., Noguchi, T., Murata, T., Kanzaki, Y., Hamashima, H. and Sasatsu M. (2002). Bactericidal activity of Ag-zeolite mediated by reactive oxygen species under aerated conditions. *Journal of Inorganic Biochemistry* **92**: 37 – 42

Inoue, Y., Kogure, M., Matsumoto, K., Hamashima, H., Tsukada, M., Kazutoyo Endo, K. and Tanaka, T. (2008). Light Irradiation Is a Factor in the Bactericidal Activity of Silver-Loaded Zeolite. *Chemical and Pharmaceutical Bulletin* **56**(5): 592

International Zeolite Commission (2000). *Database of zeolite structures [online]* (IZA atlas) [cited 16th March 2008].

Jones, S. A., Bowler, P. G., Walker, M. and Parsons D. (2004). Controlling wound bioburden with a novel silver-containing Hydrofiber dressing. *Wound Repair and Regeneration* **12**(3): 288 – 294.

Joswick, H. L., Corner, T. R., Silvernale, J. N. and Gerhardt, P. (1971). Antimicrobial actions of hexachlorophane: release of cytoplasmic materials. *Journal of Bacteriology* **108**: 492–500.

Karger, J. and Ruthven, D. M. (1992). *Diffusion in zeolites and other microporous solids*, John Wiley and Sons. New York

Kawahara, K., Tsuruda, K., Morishita, M. and Uchida M. (2000). Antibacterial effect of silver-zeolite on oral bacteria under anaerobic conditions. *Dental Material* **16**: 452 – 455.

Kim, Y., Han, Y. W. and Seff, K. (1993). Structure of the Tetrahedral Na₅⁴⁺ Cluster in Zeolite X. *Journal of Physical Chemistry* **97**: 12663-12664

Kloužková, A. Mrázová, M. and Kohoutková, M. (2007). Synthesis of partially stabilised leucite. *Journal of Physics and Chemistry of Solids*. **68**(5-6): 1207 – 1210.

Kohoutková, M. Kloužková, A. Maixner, J. and Mrázová, M. (2007). Preparation and Characterization of Analcime Powders by X-ray and SEM Analyses. *Ceramics-Silikáty* **51**(1): 9 – 14.

Kumar, R. and Münstedt, H. (2004). Silver ion release from antimicrobial polyamide/silver composites. *Biomaterials* **26**(14): 2081 – 2088.

Kwakye-Awuah, B., Williams, C., Kenward, M. A. and Radecka, I. (2008a). Antimicrobial action and efficiency of silver-loaded zeolite X. *Journal of Applied Microbiology* **104**(5): 1516 – 1524.

Kwakye-Awuah, B., Radecka, I., Kenward, M. A. and Williams, C. (2008b). Production of silver-doped analcime by isomorphous substitution technique. *Journal of Chemical Technology and Biotechnology* **83**(9): 1255 – 1260.

Lebaron, P. and Joux, F. (1994). Flow cytometric analysis of the cellular DNA content of *Salmonella typhimurium* and *Alteromonas haloplanktis* during starvation and recovery in seawater. *Journal of Applied and Environmental Microbiology* **60**(12): 4345–4350

- Lechert, H. and Kacirek, H. (1991) Synthesis of zeolitic materials. *Zeolites* **11**: 720.
- Lechert, H. and Kacirek, H. (1992) Synthesis of zeolitic materials. *Zeolites* **13**: 192.
- Levy, S. B. (1998). The challenge of antibiotic resistance *Scientific American* **3**: 32–39
- Li, X-Z., Nikaido, H. and Poole, K. (1995). Role of MexA-MexB-OprM in antibiotic efflux in *Pseudomonas aeruginosa*. *Antimicrobial Agents and Chemotherapy* **39**: 1948–1953.
- Li, X-Z, Nikaido H, Williams, K. E. (1997a). Silver-resistant mutants of *Escherichia coli* display active efflux of Ag⁺ and are deficient in porins. *Journal of Bacteriology*. **179**(19): 6127–6132
- Li, X-C., Cai, L. and Wu, C. D. (1997b). Antimicrobial compounds from *Ceanothus americanus* against oral pathogens. *Phytochemistry* **46**(1): 97 – 102.
- Li, Q., Mihailova, B., Creaser, D. and Sterte, J. (2001). Aging effects on the nucleation and characterization kinetics of colloidal TPA-siliclite-1. *Microporous and Mesoporous Materials* **43**: 51 – 59.
- Liau, S. Y., Read, D. C., Pugh, W. J., Furr, J. R. and Russell, A. D. (1997). Interaction of silver nitrate with readily identifiable groups: relationship to the antibacterial action of silver ions. *Letters to Applied Microbiology* **25**(4): 279-83.
- Line, C. M. B., Putnis, A. Putnis, C. and Giampaolo, C. (1995). The dehydration kinetics and microtexture of analcime from two parageneses. *American Mineralogist* **80**: 268 – 279.
- Madigan M. T., Martinko, J. M. and Parker, J. (2000). Brock Biology of microorganism. 9th ed. Upper Saddle River: New Jersey.
- Maillard, J-Y. (2002). Bacterial target sites for microbial action. *Journal of Applied Microbiology* **92**(1): 16S -27S.
- Mao, Y., Daniel, L. N., Whittaker, N. and Saffiotti, U. (1994). DNA Binding to Crystalline Silica Characterized by Fourier-Transform Infrared Spectroscopy. *Environmental Health Perspectives* **102**(10): 165 – 171.
- Matsumura, Y., Yoshikata, K., Kunisaki, S., Tsuchido, T (2003). Mode of bacterial action of silver zeolites and its comparison with that of silver nitrate. *Applied Environmental Microbiology* **69**(7): 4278 – 4281.
- McDonnell, G. and Russell A. D. (1999). Antiseptics and Disinfectants: Activity, Action, and Resistance. *Clinical Microbiological Reviews* **12**(1): 147 – 179.

- McMurry, L.M., Oethinger, M. and Levy, S. B. (1998). Triclosan targets lipid synthesis. *Nature* **394**: 531–532.
- Melamed, M. R. (1990). *Flow Cytometry and Sorting* New York, NY: Wiley-Liss;
- Menashi, S., Dehem, M., Souliac, I., Legrand, Y., Fridman, R. (1998). Density-dependent regulation of cell-surface association of 76 matrix metalloproteinase-2 (MMP-2) in breast-carcinoma cells. *International Journal of Cancer* **75**(2): 259 – 65.
- Mittelman, M. W. (1985). Biological Fouling of Purified-Water Systems: Part 2, Detection and Enumeration. *Microcontamination* **3**(11): 42 – 58.
- Mozgawa, (2000). The influence of some heavy metals cations on the FTIR spectra of zeolites. *Journal of Molecular Structures* **555**: 299–304.
- Mozgawa, W. (2001). The relation between structure and vibrational spectra of natural zeolites. *Journal of Molecular Structure* **596**: 129 – 137.
- Mrozik, A., Łabużek, S. and Piotrowska-Seget, Z. (2004a). Changes in cellular fatty acid composition induced by phenol, catechol in *Pseudomonas vesicularis* and *Pseudomonas stutzeri*. *Biotechnologia* **1**: 89 – 97.
- Mrozik, A., Piotrowska-Seget, Z. and Łabużek, S. (2004b). Changes in whole cell-derived fatty acids induced by naphthalene in bacteria from genus *Pseudomonas* *Microbiological Research* **159**(1): 87 – 95.
- Mrozik, A., Łabużek, S., and Piotrowska-Seget, Z. (2005). Changes in fatty acid composition in *Pseudomonas putida* and *Pseudomonas stutzeri* during naphthalene degradation. *Microbiological Research* **160**(2): 149 – 157.
- Nagy, J. B., Bodart, P., Hannus, I. and Kiricsi, I. (1998). *Synthesis, Characterization and use of zeolitic microporous materials*. Konya, Z. and Tubak, V. (Eds) DecaGen Publishers Ltd, Szeged, Hungary.
- Naumann, D., Helm, D., and Labischinski, H. (1991). Microbiological characterizations by FT-IR Spectroscopy. *Nature* **351**: 81 – 82.
- Nies, D. H. (1999). Microbial heavy-metal resistance. *Applied Microbiology and Biotechnology* **51**(6): 730 – 50.
- Niku-Paavola, M.–L., Laitila, A., Mattila-Sandholm, T. and Haikara, A. (1999). New types of antimicrobial compounds produced by *Lactobacillus plantarum*. *Journal of Applied Microbiology* **86**(1): 29 – 35.

- Novembre, D., Sabatino, B. D., Gimeno, D., Garcia-Valles, M. and Martinez-Manent, S. (2004). Synthesis of Na-X zeolites from tripolaceous deposits (Crotone, Italy) and volcanic zeolitized rocks (Vico volcano, Italy). *Microporous and Mesoporous Materials* **75**: 1 – 11.
- Novotna, M. Satava, V. Lezal, D. Klouzkova, A. and Kostka, P. (2003). Preparation and characterization of analcime powders. *Journal of Optoelectronics and Advanced Materials* **5**(5): S1405-S1409.
- Occelli, M. I. and Kessler, H. (Eds). 1997. Synthesis of Porous Materials: Zeolites, Clays and Nanostructures. New York, CRC Press.
- Ovington, L. G. (1999). The value of silver in wound management. *Podiatry Today* **12**: 59–62.
- Ovington, L. G. (2001). The role of silver technology in wound healing part 2: why silver is superior. *WOUNDS* **13**(B2): 5 – 10.
- Ovington, L. G. (2004). The truth about silver. *Ostomy Wound Management* **50**(9A): 1S–10S.
- Ovington, L. G. (2005). The role of silver technology in wound healing, part 2: why is nanocrystalline silver superior?’’ *WOUNDS* **13**(1B2): 5–10.
- Papaioannou, D., Katsoulos, P. D. N. Panousis, N. and Karatzias, H. (2005). The role of natural and synthetic zeolites as feed additives on the prevention and/or the treatment of certain farm animal diseases: A review. *Microporous and Mesoporous Materials* **84**(1-3): 161 – 170.
- Parsons, D. Bowler, P. G. and Walker, M. (2003). Letter to the editor: polishing the information on silver. *Ostomy Wound Management* **49**(8): 10–18.
- Parsons, D., Bowler, P. G., Myles, V. and Jones, S. (2005). Silver antimicrobial dressings in wound management: a comparison of antibacterial, physical and chemical characteristics, *WOUNDS* **17**(8): 222–232.
- Passagot, J., Crance, J. M., Biziagos, E., Laveran, H., Agbalika, F. and Deloince, R. (1987). Effect of glutaraldehyde on the antigenicity and infectivity of hepatitis A virus. *Journal of Virological Methods*. **16**: 21–28.
- Pellegrino, C., Aiello, R., Testa, F., Crea, F., Tuel A. and Nagy, J. B. (1997). Multinuclear high resolution solid state NMR characterization of zeolites Nu-10 and ZSM-5 synthesized in the presence of tetraethylenepentamine and diaminopropane. *Microporous and Mesoporous Materials* **47**(1): 85 – 96.

Phan, T-N., and Marquis, R. E. (2006). Triclosan inhibition of membrane enzymes and glycolysis of *Streptococcus mutans* in suspensions and biofilms. *Canadian Journal of Microbiology* **52**(10): 977–983.

Pillay, A. and Peisach, M. (1990). Zeolite analysis PIXE, XRF or neutron activation. *Journal of Radioanalytical and Nuclear Chemistry* **153**(2): 75 – 84.

Poon, K. M. and Burd, A. (2004). In vitro toxicity of silver: implication for clinical wound care. *Burns* **30**: 140–147.

Power, E. G. M. (1995). Aldehydes as biocides. *Progress in Medical Chemistry* **34**:149–201.

Power, E. G. and Russell, A. D. (1989). Glutaraldehyde: its uptake by sporing and non-sporing bacteria, rubber, plastic and an endoscope. *Journal of Applied Bacteriology* **67**(3):329 – 342.

Power, E. G. M. (1995). Aldehydes as biocides. *Progress in Medical Chemistry* **34**: 149 – 201.

Pümpel, T. and Schinner, F. (1985). Silver tolerance and silver accumulation of microorganisms from soil materials of a silver mine. *Journal of Applied Microbiology and Biotechnology* **24**(3): 244 – 247.

Quintavalla, S. and Vicini, L. (2002). Antimicrobial food packaging in meat industry, *Meat Science*. **62**(3): 373-380.

Ramos, J. L., Duque, E., Rodriguez-Herva, J. J., Godoy, P., Haidour, A., Reyes, F. and Fernandez-Barrero, A. (1997). Mechanism of solvent tolerance in bacteria. *Journal of Biological Chemistry* **272**: 3887 – 3890.

Rees, E. N., Tebbs, S. E. and Elliott, T. S. J. (1998). Role of Antimicrobial-impregnated polymer and Teflon in the prevention of biliary stent blockage. *Journal of Hospital Infection* **39**: 323 – 329.

Rivera-Garza, M., Olguin, M. T., Garcia-Sosa, J., Alcantara, D. and Rodriguez-Fuentes, G. (2000). Silver supported on natural Mexican zeolite as an antibacterial material. *Microporous and Mesoporous Materials* **39**: 431 – 444.

Robson, H. (2001). *Verified Synthesis of Zeolitic Materials*, Elsevier Science, Amsterdam.

Rodgers, F. G., Blakemore, R. P., Blakemore, N. A. , Frankel, R. B., Bazylnski, D. A. Maratea, D and Rodgers, C. (1990). Intercellular structure in a many-celled magnetotactic prokaryote. *Archives of Microbiology* **154**: 18 – 22.

Rollmann, D., Schlenker, J. L., Lawton, S. L. and Kennedy, C. L. (1999). On the Role of Small Amines in Zeolite Synthesis, *Journal of Physical Chemistry B* **103**: 7175-7183.

Rollmann, L. D., Schlenker, J. L., Lawton, S. L. and Kennedy, C. L. (2000). On the Role of Small Amines in Zeolite Synthesis 2. *Journal of Physical Chemistry B* **104**: 721-726.

Ruddon, R. W. (1990). Chemical mutagenesis. In: *Principles of Drug Action: The Basis of Pharmacology* Pratt, W. B. and Taylor P. (Eds). New York: Churchill Livingstone: 691-733.

Russell, A. D. (1990a). Bacterial spores and chemical sporicidal agents. *Clinical Microbiology Reviews* **3**: 99–119.

Russell, A. D. (1990b). Mechanisms of bacterial resistance to non-antibiotics: food additives and food and pharmaceutical preservatives. *Journal of Applied Bacteriology* **71**: 191–201.

Russell A D. (1994). Gluteraldehyde: current status and uses. *Infection Control in Hospital Epidemiology* **15**: 724–733

Russell, A. D. (1996). Activity of biocides against mycobacteria. *Journal of Applied Bacteriology, Symposium on Supplement* **81**: 87S–101S.

Russell, A. D. (2003). Similarities and differences in the responses of microorganisms to biocides. *Journal of Antimicrobial Chemotherapy* **52**: 750-763.

Russell, A. D. and Day M. J. (1993). Antibacterial activity of chlorhexidine. *Journal of Hospital Infection* **25**: 229–238.

Russell, A. D. and Hugo, W. B. (1994). Antibacterial activity and action of silver. *Progress in Medicinal Chemistry*. **31**: 351 – 370.

Russell A D and Day M J. (1996). Antibiotic and biocide resistance in bacteria. *Microbios* **85**: 45–65.

Russell, A. D., Dancer, B. N., Power, E. G. M. (1991). Effects of chemical agents on bacterial sporulation, germination and outgrowth. *Society for Applied Bacteriology. Technical Series* **27**: 23–44.

Russell, A. D. and Chopra, I. (1996). Understanding antibacterial action and resistance, p. 226-237. , 266-269. Ellis Horwood, Chichester, United Kingdom.

Russell, A. D., Furr, R. J. and Maillard, J. Y. (1997). Microbial susceptibility and resistance to biocide. *ASM News* **63**: 481 – 487.

Sajbidor, J. (1997). Effect of some environmental factors on the content and composition of microbial membrane lipids. *Critical Reviews in Biotechnology* **17**: 87 – 103.

- Sasser, M. (1990). Identification of Bacteria by Gas Chromatography of Cellular Fatty Acids. MIDI Technical Note 101, Microbial ID, Inc., Newark, DE, USA (1990).
- Schierholz, J. M., Fleck, C., Beuth, J. and Pulverer, G. (2000). The antimicrobial efficacy of a new central venous catheter with long-term broad-spectrum activity. *Journal of Antimicrobial Chemotherapy* **46**: 45 - 50
- Schierholz, J. M., Wachol-Drewe, Z., Lucas, L. J. and Pulvere G. (1998). Activity of silver in different media. *Zentralblatt fur Bacteriologie* **287**: 411– 420.
- Schweizer, H. P. (2001). Triclosan: a widely used biocide and its link to antibiotics. *FEMS Microbiology Letters* **202**: 1 – 7.
- Shapiro, H. (1995). Practical Flow Cytometry. 3rd ed. Alan R. Liss (Eds) New York, NY.
- Shirkhazadeh, M. (1995). Prosthetic implant with self-generated current for early fixation in skeletal bone. 005383935A. 5383935.
- Sibbald, R.G., Brown, A. C., Coutts, P. and Queen, D. (2001). Screening evaluation of an ionized nanocrystalline silver dressing in chronic wound care. *Ostomy Wound Management* **47**(10): 38 – 43.
- Sikka, R., Sabherwal, U. and Arora, D. R. (1987). Susceptibility of Klebsiella pneumoniae to heavy metal ions in vitro. *Indian Journal of Medicine* **86**: 437–440.
- Sikkema, J., de Bont, J. A. and Poolman, B. (1995). Mechanisms of membrane toxicity of hydrocarbons. *Microbiology and Molecular Biology Reviews* **59**(2): 201-222
- Silver, S. (1996). Bacterial heavy metal resistance: New surprises. *Annual Revision Microbiology* **50**: 753 – 789.
- Silver, S. (2003). Bacterial silver resistance: molecular biology and uses and misuses of silver compounds misuse. *FEM Microbiology Reviews* **27**: 341 – 353.
- Silver, S., Nucifora, G., Chu, L. and Misra, T. K. (1989). Bacterial resistance ATPases: primary pumps for exporting cations and anions. *TIBS* **14**: 76 – 80.
- Silvernale, J. N., Joswick, H. L., Corner, T. R. and Gerhardt, P. (1971). Antimicrobial actions of hexachlorophane: cytological manifestations. *Journal of Bacteriology* **108**: 482–491.
- Sitarz, M. Handke, M. and Mozgawa, W. (2001) FTIR studies of the Cyclosilicate-like structures. *Journal of Molecular Structure* **596**: 185-189.

Sliva, A., Samolejova, A., Brazda, R., Zegzulka, J. and Polak, J. (2004). Optical parameter adjustment for silica nano and micro-particle size distribution measurement using Mastersizer 2000. *Microwave and Optical Technology* **5445**: 160 – 163.

Sobolev, V. I., Panov, G. I. Kharitonov, A. S. Romanikov, V. N. Volodin, A. M. and Ione, K. G. (1993). Catalytic properties of ZSM-5 zeolites in N₂O decomposition: the role of iron. *Journal of Catalysis* **139**(2): 435 – 443.

Soloz, M. and Odermatt, A. (1995). Copper and Silver transport by CopB-ATPase in membrane vesicles of *Enterococcus hirae* by copper (I) and copper (II). *Journal of Biology and Chemistry* **270**: 19217 – 19222.

Sondi, I and Salopek-Sondi, B. (2004). Silver nanoparticles as antimicrobial agent: a case study on *E. coli* as a model for gram-negative bacteria. *Journal of Colloid and Interface Science* **275**(1): 177 – 182.

Spacciapoli, P., Buxton, D., Rothstein, D. and Friden, P. (2001). Antimicrobial activity of silver nitrate against periodontal pathogens. *Journal of Periodontal Research* **36**:108–113.

SPECTRO (2005) *Working principle of the SPECTRO CIROS CCD [online]*. Spectro, 2005 [cited 5th March, 2008]

Starodub, M. E. and Silver, J. T. (1990). Silver accumulation and resistance in *Escherichia coli* R1. *Journal of Inorganic Biochemistry* **39**: 317–325

Strohal, R., Schelling, M., Takacs, M., Jurecka, W., Gruber, U. and Offner, F. (2004). Second World Union of Wound Healing Societies Meeting. Paris, France. Presented Nanocrystalline silver dressings as an efficient anti-MRSA barrier: a new solution to an increasing problem. Oral presentation.

Szostak, R. (1989). *Molecular Sieves, Science and Technology*. Weitkamp, J. J. (Ed). Springer, Berlin

Tennen, R., Setlow, B.,K.L. Davis, K. L., Loshon, C. A. and Setlow, P. (2000). Mechanisms of killing of spores of *Bacillus subtilis* by iodine, glutaraldehyde and nitrous acid. *Journal of Applied Microbiology* **89**(2): 330–338.

Terres, E. (1996). Influence of the Synthesis Parameters on Textural and Structural Properties of MCM-41. *Microporous and Mesoporous Materials* **431**: 111-116.

Thibon, P., Le Coutour, X., Leroyer, R. and Fabry, J. (2000). Randomized multi-centre trial of the effects of a catheter coated with hydrogel and silver salts on the incidence of hospital-acquired urinary tract infections. *Journal of Hospital Infection* **45**(2):117–124.

- Thoma, S. G. and Nenoff, T. M. (2000). Vapour phase transport synthesis of zeolites from sol-gel precursors. *Microporous and Mesoporous Materials* **41**: 295.
- Thompson, R. W. (1998). Molecular Sieves, Science and Technology, Weitkamp, I. J. (Ed). Springer, Berlin.
- Thompson, R. W. and Huber, M. J. (1982). Novel synthesis to prepare zeolite crystal coating on carbon nanotubes. *Journal of Crystal Growth* **56**: 771.
- Townsend, R. P. (1984). Ion exchange in zeolites-basic principles. *The American Mineralogist* **17**: 128 – 134.
- Trevors, J. T. (1987). Silver resistance and accumulation in bacteria. *Enzyme Microbiology Technology* **9**: 331 – 333.
- Tsitko, I. V., Zaitsev, G. M., Lobanok, A. G. and Salkinoja-Salonen, M. S. (1999). Effect of aromatic compounds on cellular fatty acid composition of *Rhodococcus opacus*. *Applied and Environmental Microbiology* **65**: 853 – 855.
- Ueda, S. and Koizumi, M. (1979). Crystallisation of analcime solid solutions from aqueous solutions. *American Mineralogist*. **68**: 172
- Van Bekkum, H., Flanigen, E. M., Jacobs, P. A. and Jansen, J. C. (2001). Introduction to zeolite science and practice. In *Studies in Surface Science and Catalysis*, Elsevier Science Publishers, Amsterdam **137**: 469 – 472 .
- Van der Pol, A and van Hoof, J. H. C. (1992). Parameters affecting the synthesis of titanium silicalite 1. *Applied Catalysis A: General* **92**(22): 93 – 111.
- Vanscheidt, W., Lazareth, I. and Routkovsky-Norval C. (2003). Safety evaluation of a new ionic silver dressing in the management of chronic ulcers. *WOUNDS* **15**(11): 371–378.
- Walsh, S. E., Maillard, J.-Y., and Russell, A. D and Hann, A. C. (2001). Possible mechanisms for the relative efficacies of ortho-phthalaldehyde, gluteraldehyde against gluteraldehyde-resistant *Mycobacterium chelonae*. *Journal of Applied Microbiology* **91**: 80 – 92.
- Walsh, S. E., Maillard, J.-Y., and Russell, A. D. (1999). Ortho-phthalaldehyde: a possible alternative to gluteraldehyde for high level disinfection. *Journal of Applied Microbiology* **87**: 702 – 710.
- Weichart, D. H. and Kell, D. B. (2001). Characterization of an autostimulatory substance produced by *Escherichia coli*. *Microbiology* **147**: 1875 – 1885.

Wong, P. T. T., Wong, R. K., Caputo, T. A., Godwin, T. A. and Rigas, B. (1991). Infrared spectroscopy of exfoliated human cervical cells: Evidence of extensive structural changes during carcinogenesis. *Biochemistry* **88**: 10988-10992.

Wright, J. B., Hansen, L. and Burrell, R. E. (1998). The comparative efficacy of two antimicrobial barrier dressings: in-vitro examination of two controlled-release silver dressings. *WOUNDS* **10**(6): 179–188.

Yamanaka, M., Hara, K. and Kudo, J. (2005) Bactericidal actions of silver ion solution on *Escherichia coli*, studied by Energy-Filtering Transmission Electron Microscopy and Proteomic Analysis. *Applied and Environmental Microbiology* **71**(11), 7589 – 7593.

Yeom, Y. H. and Kim, Y. (1997). Crystal structure of zeolite X exchanged with Pb(II) at pH 6.0 and dehydrated: $(\text{Pb}^{4+})_{14}(\text{Pb}^{2+})_{18}(\text{Pb}_4\text{O}_4)_8\text{Si}_{100}\text{Al}_{92}\text{O}_{384}$. *Journal of Physical Chemistry B*, **101** (27): 5314 -5318

Yin, H. Q., Langford, R., Burrell, R. E. (1999). Comparative evaluation of the antimicrobial activity of Acticoat antimicrobial barrier dressing. *Journal of Burn Care Rehabilitation* **20**: 195–200.

Zhdanov, S. P. (1971). Some problems of zeolite crystallisation. *Advances in Chemical. Series* **101**: 20 – 43.

Zumdahl, S. S. (1986). Chemistry, 1st ed. Lexington, Mass: DC Heath and Company 547–548.

Appendices

1. Synthesis of silver-loaded zeolites

1.1 SEM micrographs of zeolite X with and without silver loading

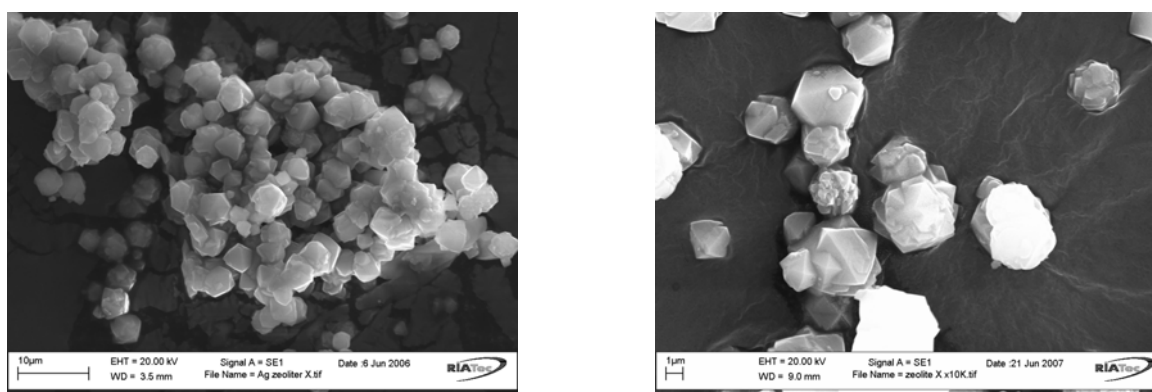


Figure 1.1: SEM micrographs of zeolite X with silver loading (left) and without silver loading (right) with different magnifications.

1.2 SEM micrographs of zeolite A with and without silver loading

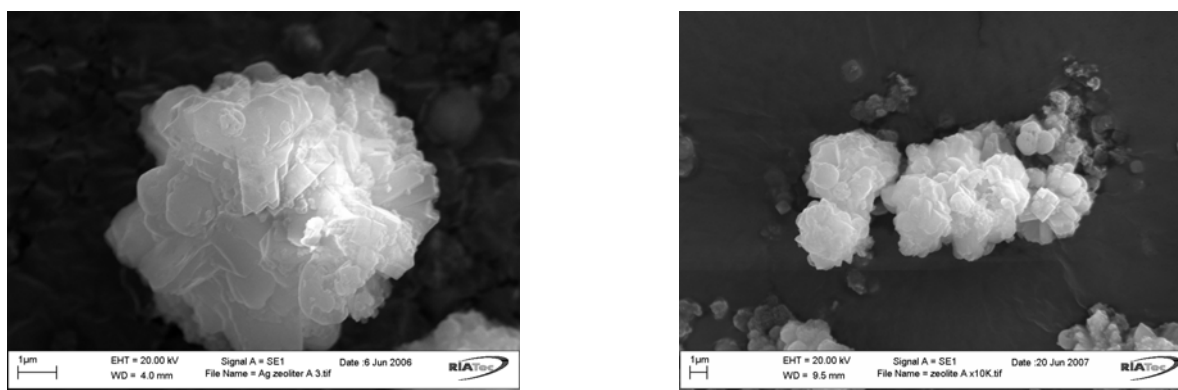


Figure 1.2: SEM micrographs of zeolite A with silver loading (left) and without silver loading (right) with different magnifications.

1.3 SEM micrographs of zeolite exchanged high-alumina Phillipsite with and without silver loading

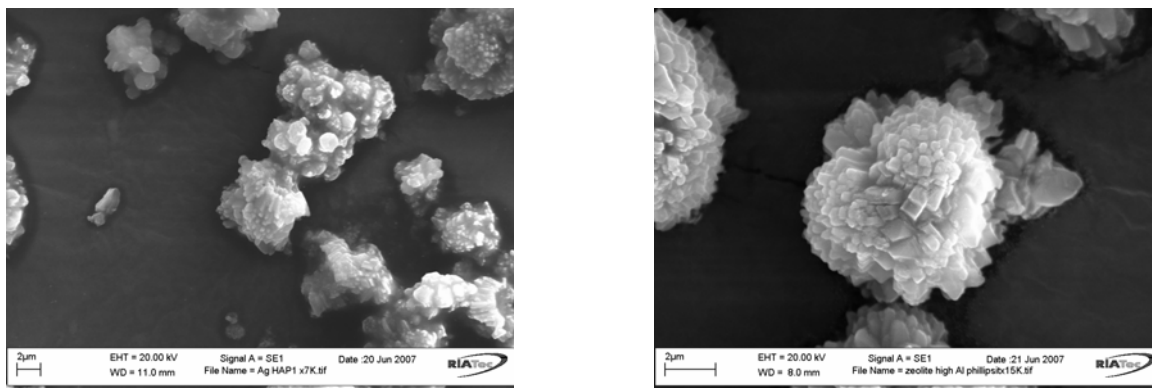


Figure 1.3: SEM micrographs of high-alumina Phillipsite with silver loading (left) and without silver loading (right) with different magnifications.

1.4 SEM micrographs of Analcime and silver-doped Analcime

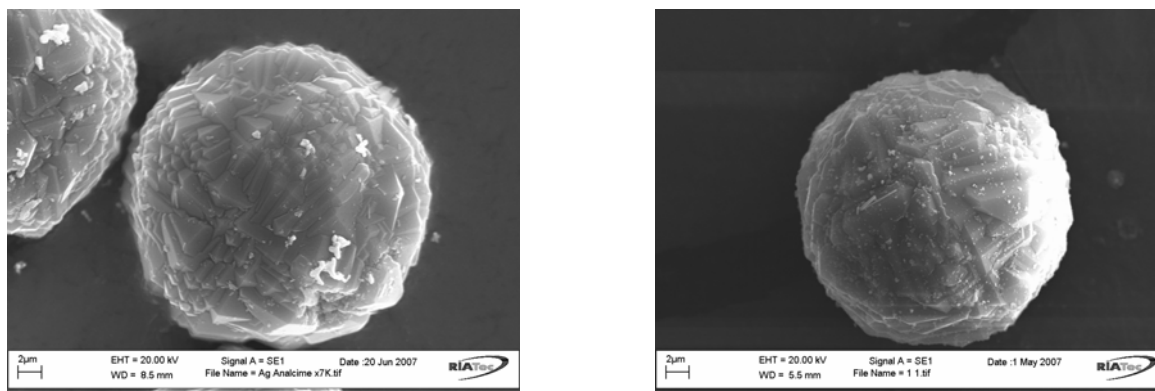


Figure 1.4: SEM micrographs of Analcime with silver loading (left) and without silver loading (right) with same magnifications.

2. Descriptive statistics of antibacterial testing of silver-exchanged zeolite X

2.1 Descriptive statistics of silver loaded zeolite X on *E. coli* K12W-T, *S. aureus* NCIMB6571 and *P. aeruginosa* NCIMB8295

Treatment	Time (h)	Zeolite X Mean Log(cfu/ml) (ppm) ± (SE)		
		<i>E. coli</i>	<i>S. aureus</i>	<i>P. aeruginosa</i>
Strain + TSB	0.00	5.734 (0.014)	5.736(0.013)	5.752(0.014)
	0.25	5.884 (0.014)	5.885(0.014)	5.899(0.013)
	0.50	5.957 (0.12)	5.957(0.013)	5.947(0.012)
	0.75	6.025 (0.010)	6.026(0.009)	6.044(0.010)
	1.00	6.114(0.021)	6.109(0.034)	6.120(0.042)
Strain +Z-X+TSB	0.00	5.808(0.097)	5.808(0.012)	5.775(0.012)
	0.25	5.899(0.012)	5.899(0.011)	5.877(0.012)
	0.50	5.974(0.011)	5.992(0.006)	5.955(0.007)
	0.75	6.041(0.07)	6.041(0.026)	6.039(0.027)
	1.00	6.117(0.030)	6.114(0.014)	6.121(0.011)
First exposure	0.00	5.766(0.011)	5.744(0.025)	5.782(0.015)
	0.25	4.558(0.024)	4.615(0.012)	4.626(0.009)
	0.50	3.370(0.038)	3.341(0.022)	3.373(0.012)
	0.75	0.000(0.000)	.000(0.000)	0.000(0.000)
	1.00	0.000(0.000)	0.000(0.000)	3.102(0.000)
First retrieval	0.00	5.707(0.010)	5.726(0.021)	5.729(0.014)
	0.25	4.601(0.016)	4.589(0.025)	4.586(0.023)
	0.50	3.171(0.046)	3.162(0.044)	3.292(0.019)
	0.75	0.000(0.000)	3.011(0.036)	2.027(0.013)
	1.00	0.000(0.000)	0.000(0.000)	2.027(0.000)
Second retrieval	0.00	5.767(0.017)	5.701(0.014)	5.701(0.012)
	0.25	4.642(0.017)	4.558(0.028)	4.596(0.032)
	0.50	3.210(0.070)	3.232(0.050)	3.293(0.077)
	0.75	0.000(0.000)	2.206(0.026)	3.102(0.011)
	1.00	0.000(0.000)	0.000(0.000)	3.102(0.000)
Third retrieval	0.00	5.763(0.013)	5.735(0.031)	5.752(0.017)
	0.25	4.675(0.080)	4.580(0.056)	4.630(0.039)
	0.50	3.311(0.041)	3.269(0.084)	3.401(0.030)
	0.75	0.000(0.000)	2.013(0.013)	3.136(0.044)
	1.00	0.000(0.000)	0.000(0.000)	0.000(0.000)

2.2 One-way ANOVA analysis

		Sum of Squares	df	Mean Square	F	Sig.
<i>E. coli</i> +TSB	Between Groups	0.140	3	0.047	96.976	0.000
	Within Groups	0.004	8	0.000		
	Total	0.143	11			
First exposure	Between Groups	55.494	3	18.498	11205.666	0.000
	Within Groups	0.013	8	0.002		
	Total	55.507	11			
First retrieval	Between Groups	55.129	3	18.376	9649.098	0.000
	Within Groups	0.015	8	0.002		
	Total	55.144	11			
Second retrieval	Between Groups	56.239	3	18.746	4458.913	0.000
	Within Groups	0.034	8	0.004		
	Total	56.273	11			
Third retrieval	Between Groups	56.316	3	18.772	13117.379	0.000
	Within Groups	0.011	8	0.001		
	Total	56.327	11			

2.3: Statistical descriptives of viable cell counts obtained by one-way ANOVA analysis for the retrieval and reuse of silver-exchanged zeolite X on *S. aureus* NCIMB6571

		Sum of Squares	df	Mean Square	F	Sig.
<i>S. aureus</i> in TSB	Between Groups	0.224	4	5.603E-02	87.883	0.000
	Within Groups	6.375E-03	10	6.375E-04		
	Total	0.230	14			
First exposure	Between Groups	83.762	4	20.941	26625.665	0.000
	Within Groups	7.865E-03	10	7.865E-04		
	Total	83.770	14			
First retrieval	Between Groups	55.622	4	13.906	5264.357	0.000
	Within Groups	2.641E-02	10	2.641E-03		
	Total	55.649	14			
Second retrieval	Between Groups	59.027	4	14.757	5876.344	0.000
	Within Groups	2.511E-02	10	2.511E-03		
	Total	59.052	14			
Third retrieval	Between Groups	59.859	4	14.965	2157.676	0.000
	Within Groups	6.936E-02	10	6.936E-03		
	Total	59.928	14			

2.4 Statistical descriptives of viable cell counts obtained by one-way ANOVA analysis for the retrieval and reuse of silver-exchanged zeolite X on *P. aeruginosa* NCIM8295

		Sum of Squares	df	Mean Square	F	Sig.
<i>P. aeruginosa</i> +TSB	Between Groups	0.238	4	5.954E-02	118.095	0.000
	Within Groups	7.562E-03	15	5.042E-04		
	Total	0.246	19			
First exposure	Between Groups	112.617	4	28.154	462055.657	0.000
	Within Groups	9.140E-04	15	6.093E-05		
	Total	112.618	19			
First retrieval	Between Groups	74.655	4	18.664	353.981	0.000
	Within Groups	0.791	15	5.273E-02		
	Total	75.446	19			
Second retrieval	Between Groups	75.152	4	18.788	383.396	0.000
	Within Groups	0.735	15	4.900E-02		
	Total	75.887	19			
Third retrieval	Between Groups	75.104	4	18.776	345.137	0.000
	Within Groups	0.816	15	5.440E-02		
	Total	75.920	19			

3. Descriptive statistics of silver ions eluted from silver-exchanged zeolite X

3.1 Statistical descriptives of silver ions eluted from silver-exchanged zeolite X obtained by one-way ANOVA analysis during exposure of *E. coli* K12W-T.

		Sum of Squares	df	Mean Square	F	Significance
First exposure	Between Groups	3.746	6	0.624	8.856	0.000
	Within Groups	1.480	21	0.070		
	Total	5.226	27			
First retrieval	Between Groups	0.493	6	0.082	3.442	0.016
	Within Groups	0.502	21	0.024		
	Total	0.995	27			
Second retrieval	Between Groups	0.252	6	0.042	2.005	0.110
	Within Groups	0.439	21	0.021		
	Total	0.691	27			
Third retrieval	Between Groups	0.032	6	0.005	1.085	0.403
	Within Groups	0.105	21	0.005		
	Total	0.137	27			

3.2 Statistical descriptives of silver ions eluted from silver-exchanged zeolite X obtained by one-way ANOVA analysis during exposure of *S. aureus* NCIMB6571

		Sum of Squares	df	Mean Square	F	Significance
1st exposure	Between Groups	0.582	6	0.097	0.562	0.756
	Within Groups	3.627	21	0.173		
	Total	4.209	27			
1st retrieval	Between Groups	0.357	6	0.059	0.708	0.647
	Within Groups	1.762	21	0.084		
	Total	2.119	27			
2nd retrieval	Between Groups	0.176	6	0.029	0.799	0.582
	Within Groups	0.773	21	0.037		
	Total	0.950	27			
3rd retrieval	Between Groups	0.258	6	0.043	1.658	0.181
	Within Groups	0.544	21	0.026		
	Total	0.802	27			

3.3 Statistical descriptives of silver ions eluted from silver-exchanged zeolite X obtained by one-way ANOVA analysis during exposure of *P. aeruginosa* NCIMB8295

		Sum of Squares	df	Mean Square	F	Significance
exposure1	Between Groups	1.266	6	0.211	3.222	0.021
	Within Groups	1.375	21	0.065		
	Total	2.641	27			
retrieval1	Between Groups	0.138	6	0.023	2.132	0.092
	Within Groups	0.226	21	0.011		
	Total	0.364	27			
retrieval2	Between Groups	0.091	6	0.015	1.007	0.447
	Within Groups	0.315	21	0.015		
	Total	0.406	27			
retrieval3	Between Groups	0.291	6	0.048	2.457	0.059
	Within Groups	0.414	21	0.020		
	Total	0.705	27			

4. Descriptive statistics of antibacterial testing of silver-exchanged zeolite A

4.1 Statistical descriptives of silver ions eluted from silver-exchanged zeolite A obtained by one-way ANOVA analysis during exposure of *E. coli* K12W-T.

		Sum of Squares	df	Mean Square	F	Sig.
<i>E. coli</i> + TSB	Between Groups	0.305	4	7.618E-02	743.162	0.000
	Within Groups	1.538E-03	15	1.025E-04		
	Total	0.306	19			
First exposure	Between Groups	130.437	4	32.609	111274.371	0.000
	Within Groups	4.396E-03	15	2.931E-04		
	Total	130.442	19			
First retrieval	Between Groups	129.581	4	32.395	57712.308	0.000
	Within Groups	8.420E-03	15	5.613E-04		
	Total	129.589	19			
Second retrieval	Between Groups	114.224	4	28.556	517.095	0.000
	Within Groups	0.828	15	5.522E-02		
	Total	115.052	19			
Third retrieval	Between Groups	112.533	4	28.133	27881.271	0.000
	Within Groups	1.514E-02	15	1.009E-03		
	Total	112.548	19			

4.2 Statistical descriptives of silver ions eluted from silver-exchanged zeolite A obtained by one-way ANOVA analysis during exposure of *S. aureus* NCIMB6571

		Sum of Squares	df	Mean Square	F	Sig.
<i>S. aureus</i> + TSB	Between Groups	0.308	4	7.689E-02	235.416	0.000
	Within Groups	4.899E-03	15	3.266E-04		
	Total	0.312	19			
First exposure	Between Groups	127.996	4	31.999	15139.616	0.000
	Within Groups	3.170E-02	15	2.114E-03		
	Total	128.028	19			
First retrieval	Between Groups	129.252	4	32.313	154377.778	0.000
	Within Groups	3.140E-03	15	2.093E-04		
	Total	129.255	19			
Second retrieval	Between Groups	111.382	4	27.845	20276.328	0.000
	Within Groups	2.060E-02	15	1.373E-03		
	Total	111.402	19			
Third retrieval	Between Groups	112.310	4	28.077	35545.154	0.000
	Within Groups	1.185E-02	15	7.899E-04		
	Total	112.322	19			

4.3 Statistical descriptives of silver ions eluted from silver-exchanged zeolite A obtained by one-way ANOVA analysis during exposure of *P. aeruginosa* NCIMB8295

		Sum of Squares	df	Mean Square	F	Sig.
<i>P. aeruginosa</i> + TSB	Between Groups	0.253	4	6.334E-02	112.487	0.000
	Within Groups	8.447E-03	15	5.631E-04		
	Total	0.262	19			
First exposure	Between Groups	129.981	4	32.495	13125.498	0.000
	Within Groups	3.714E-02	15	2.476E-03		
	Total	130.018	19			
First retrieval	Between Groups	129.601	4	32.400	14904.239	0.000
	Within Groups	3.261E-02	15	2.174E-03		
	Total	129.633	19			
Second retrieval	Between Groups	131.126	4	32.782	41581.796	0.000
	Within Groups	1.183E-02	15	7.884E-04		
	Total	131.138	19			
Third retrieval	Between Groups	110.927	4	27.732	81389.978	0.000
	Within Groups	5.111E-03	15	3.407E-04		
	Total	110.932	19			

4.4 Viable cell counts obtained for *E. coli* K12W-T, *S. aureus* NCIMB6571 and *P. aeruginosa* NCIMB8295 for the retrieval and reuse of silver-exchanged zeolite A

Treatment	Time (h)	Zeolite A		
		Mean Ag ⁺ concentration released (ppm) ± (SE)		
		<i>E. coli</i>	<i>S. aureus</i>	<i>P. aeruginosa</i>
First exposure	0.00	1.364 (0.107)	1.720 (0.212)	1.364 (0.107)
	0.25	1.507 (0.170)	1.774(0.238)	1.508(0.170)
	0.50	1.433 (0.177)	2.230(0.304)	1.432(0.177)
	0.75	1.224 (0.268)	2.204(0.310)	1.224(0.268)
	1.00	1.457 (0.219)	1.612 (0.257)	1.457(0.220)
	1.25	1.536 (0.248)	1.922 (0.348)	1.535 (0.247)
	1.50	1.427 (0.095)	2.105 (0.398)	1.427 (0.095)
First retrieval	0.00	0.635 (0.029)	0.704 (0.160)	0.635 (0.293)
	0.25	0.729 (0.027)	0.615(0.127)	0.729(0.275)
	0.50	0.721 (0.045)	0.623(0.099)	0.721(0.457)
	0.75	0.789 (0.075)	0.705(0.088)	0.789(0.755)
	1.00	0.906 (0.089)	0.862(0.140)	0.906(0.895)
	1.25	0.881 (0.114)	0.881(0.065)	0.881(0.114)
	1.50	0.848 (0.122)	0.737(0.109)	0.787(0.122)
Second retrieval	0.00	0.435 (0.048)	0.290 (0.086)	0.435(0.048)
	0.25	0.484 (0.060)	0.391(0.094)	0.484(0.060)
	0.50	0.527 (0.079)	0.411(0.118)	0.527(0.080)
	0.75	0.615 (0.089)	0.418(0.167)	0.615(0.090)
	1.00	0.607 (0.028)	0.434 (0.154)	0.607(0.028)
	1.25	0.532 (0.045)	0.315(0.133)	0.532(0.045)
	1.50	0.547 (0.045)	0.373(0.238)	0.547(0.046)
Third retrieval	0.00	0.177 (0.031)	0.233 (0.055)	0.205(0.034)
	0.25	0.211 (0.017)	0.257(0.052)	0.248(0.039)
	0.50	0.275 (0.027)	0.301 (0.064)	0.320(0.056)
	0.75	0.397 (0.041)	0.331(0.065)	0.442(0.066)
	1.00	0.498 (0.040)	0.331(0.071)	0.543(0.092)
	1.25	0.615 (0.091)	0.362(0.114)	0.617(0.067)
	1.50	0.526 (0.080)	0.311(0.072)	0.498(0.033)

4.5 Statistical descriptives of silver ions eluted from silver-exchanged zeolite A obtained by one-way ANOVA analysis during exposure of *E. coli* K12W-T

		Sum of Squares	df	Mean Square	F	Significance
First exposure	Between Groups	0.256	6	0.043	0.284	0.938
	Within Groups	3.149	21	0.150		
	Total	3.405	27			
First retrieval	Between Groups	0.231	6	0.038	1.477	0.234
	Within Groups	0.547	21	0.026		
	Total	0.778	27			
Second retrieval	Between Groups	0.098	6	0.016	1.125	0.382
	Within Groups	0.305	21	0.015		
	Total	0.402	27			
Third retrieval	Between Groups	0.686	6	0.114	10.047	0.000
	Within Groups	0.239	21	0.011		
	Total	0.925	27			

4.6 Statistical descriptives of silver ions eluted from silver-exchanged zeolite A obtained by one-way ANOVA analysis during exposure of *S. aureus* NCIMB6571

		Sum of Squares	df	Mean Square	F	Significance
First exposure	Between Groups	1.197	6	0.200	0.548	0.766
	Within Groups	7.651	21	0.364		
	Total	8.849	27			
First retrieval	Between Groups	0.265	6	0.044	0.811	0.573
	Within Groups	1.145	21	0.055		
	Total	1.410	27			
Second retrieval	Between Groups	0.070	6	0.012	0.131	0.991
	Within Groups	1.886	21	0.090		
	Total	1.956	27			
Third retrieval	Between Groups	0.045	6	0.007	0.347	0.904
	Within Groups	0.452	21	0.022		
	Total	0.497	27			

4.7 Statistical descriptives of silver ions eluted from silver-exchanged zeolite A obtained by one-way ANOVA analysis during exposure of *P. aeruginosa* NCIMB8295

		Sum of Squares	df	Mean Square	F	Significance
First exposure	Between Groups	0.256	6	0.043	0.284	0.938
	Within Groups	3.149	21	0.150		
	Total	3.405	27			
First retrieval	Between Groups	0.231	6	0.038	1.477	0.234
	Within Groups	0.547	21	0.026		
	Total	0.778	27			
Second retrieval	Between Groups	0.098	6	0.016	1.125	0.382
	Within Groups	0.305	21	0.015		
	Total	0.402	27			
Third retrieval	Between Groups	0.582	6	0.097	6.996	0.000
	Within Groups	0.291	21	0.014		
	Total	0.874	27			

4.8 Statistical descriptives of silver ions eluted from silver-exchanged high-alumina Phillipsite obtained by one-way ANOVA analysis during exposure of *E. coli* K12W-T

		Sum of Squares	df	Mean Square	F	Significance
First exposure	Between Groups	0.771	6	0.129	0.807	0.576
	Within Groups	3.346	21	0.159		
	Total	4.118	27			
First retrieval	Between Groups	0.107	6	0.018	0.967	0.471
	Within Groups	0.387	21	0.018		
	Total	0.494	27			
Second retrieval	Between Groups	0.047	6	0.008	3.132	0.024
	Within Groups	0.052	21	0.002		
	Total	0.099	27			
Third retrieval	Between Groups	0.012	6	0.002	0.478	0.817
	Within Groups	0.091	21	0.004		
	Total	0.103	27			

4.9 Statistical descriptives of silver ions eluted from silver-exchanged high-alumina Phillipsite obtained by one-way ANOVA analysis during exposure of *S. aureus* NCIMB6571

		Sum of Squares	df	Mean Square	F	Significance
First exposure	Between Groups	0.199	6	0.033	1.471	0.236
	Within Groups	0.474	21	0.023		
	Total	0.673	27			
First retrieval	Between Groups	0.227	6	0.038	1.554	0.210
	Within Groups	0.511	21	0.024		
	Total	0.739	27			
Second retrieval	Between Groups	0.087	6	0.015	2.489	0.056
	Within Groups	0.123	21	0.006		
	Total	0.210	27			
Third retrieval	Between Groups	0.145	6	0.024	6.281	0.001
	Within Groups	0.081	21	0.004		
	Total	0.226	27			

4.10 Statistical descriptives of silver ions eluted from silver-exchanged high-alumina Phillipsite obtained by one-way ANOVA analysis during exposure of *P. aeruginosa* NCIMB8295

		Sum of Squares	df	Mean Square	F	Significance
First exposure	Between Groups	0.780	6	0.130	1.627	0.189
	Within Groups	1.678	21	0.080		
	Total	2.457	27			
First retrieval	Between Groups	0.208	6	0.035	4.588	0.004
	Within Groups	0.158	21	0.008		
	Total	0.366	27			
second retrieval	Between Groups	0.171	6	0.028	1.959	0.118
	Within Groups	0.305	21	0.015		
	Total	0.476	27			
Third retrieval	Between Groups	0.176	6	0.029	4.382	0.005
	Within Groups	0.141	21	0.007		
	Total	0.317	27			

5. List of publications, posters and conferences attended

Publications from PhD thesis

Bright Kwakye-Awuah, C. Williams, M. A. Kenward and I Radecka. (2007). Antimicrobial action and efficiency of silver-loaded zeolite X. *Journal of Applied Microbiology* **104(5)**: 1516 – 1524(9).

B. Kwakye-Awuah, I. Radecka, M. A. Kenward, C. D. Williams (2008). Production of silver-doped analcime by isomorphous substitution technique. *Journal of Chemical Technology & Biotechnology* DOI: 10.1002/jctb.1938.

Bright Kwakye-Awuah, Piotrowska-Seget Z., Mrozik, A., Williams, C. D., Kenward M. A. and Radecka, I. (2008). Effects of silver-loaded zeolite X on DNA content and fatty acid composition of bacterial cells. *Journal of Applied Microbiology* (Under review).

Posters from PhD thesis presented at national/international conferences

B. Kwakye-Awuah, I. Radecka, C. D. Williams, M. A. Kenward (2007). Antimicrobial action and efficacy of silver-loaded zeolite X.

B. Kwakye-Awuah, I. Radecka, C. D. Williams, M. A. Kenward (2007). Antimicrobial action and efficacy of silver-loaded zeolite X.

B. Kwakye-Awuah, I. Radecka, C. D. Williams, M. A. Kenward (2006). Antimicrobial action of silver-loaded zeolite X.

B. Kwakye-Awuah, I. Radecka, C. D. Williams, M. A. Kenward (2005). Towards the antimicrobial action of silver-loaded zeolite X.

6. Theoretical calculations of Ag in zeolites

6.1 Number of moles of Ag in zeolite X

$$\text{Number of moles of Na}^+ \text{ per 100 g before ion exchange (Table 9)} = \frac{5.3 \times 2}{62} = 0.171$$

$$\text{Number of moles of Na}^+ \text{ per 100 g after ion exchange} = \frac{2.8 \times 2}{62} = 0.090$$

Hence Loss of Na^+ ions = $0.171 - 0.090 = 0.081$ moles.

Thus 0.08 moles of Ag^+ were exchanged with Na during the ion exchange

6.2 Number of moles of Ag in zeolite A

$$\text{Number of moles of Na}^+ \text{ per 100 g before ion exchange (Table 11)} = \frac{5.3 \times 2}{62} = 0.171 \text{ moles}$$

$$\text{Number of moles of Na}^+ \text{ per 100 g after ion exchange} = \frac{3 \times 2}{62} = 0.097 \text{ moles}$$

Hence Loss of Na^+ ions = $0.171 - 0.097 = 0.073$ moles.

Thus 0.07 moles of Ag^+ were exchanged with Na during the ion exchange

6.3 Number of moles of Ag in high-alumina Phillipsite

$$\text{Number of moles of Na}^+ \text{ per 100 g before ion exchange (Table 12)} = \frac{5.9 \times 2}{62} = 0.190 \text{ moles}$$

$$\text{Number of moles of Na}^+ \text{ per 100 g after ion exchange} = \frac{3.8 \times 2}{62} = 0.122 \text{ moles}$$

$$\text{Number of moles of K}^+ \text{ per 100 g before ion exchange} = \frac{5.8 \times 2}{94} = 0.123 \text{ moles}$$

$$\text{Number of moles of K}^+ \text{ per 100 g after ion exchange} = \frac{3.8 \times 2}{94} = 0.081 \text{ moles}$$

Hence Loss of K^+ ions = $0.123 - 0.081 = 0.042$ moles.

Total loss of Na^+ and K^+ = $0.122 + 0.042 = 0.164$ moles

Thus 0.164 moles of Ag^+ were exchanged with Na^+ and K^+ during the ion exchange

6.4 Number of moles of Ag in analcime

Number of moles of Na^+ per 100 g with no Ag^+ doping (Table 13) = $\frac{13.3 \times 2}{62} = 0.429$ moles

Number of moles of Na^+ per 100 g on doping with 5 % Ag^+ = $\frac{10.5 \times 2}{62} = 0.338$ moles

Hence Loss of Na^+ ions = $0.429 - 0.338 = 0.09$ moles.

Number of moles of Na^+ per 100 g on doping with 10 % Ag^+ = $\frac{8.4 \times 2}{62} = 0.271$ moles

Hence Loss of Na^+ ions = $0.429 - 0.271 = 0.158$ moles.

Number of moles of Na^+ per 100 g on doping with 20 % Ag^+ = $\frac{7.9 \times 2}{62} = 0.254$ moles

Hence Loss of Na^+ ions = $0.429 - 0.254 = 0.174$ moles.

7. Conferences attended during time of study

- 2008: The microbiology of water in work, rest and play. Society for Applied Microbiology summer conference, Wellington Park Hotel, Belfast, Northern Ireland, United Kingdom.
- 2007: The microbiology of fresh produce. Society for Applied Microbiology summer conference, Park Plaza Hotel, Cardiff, Wales.
- 2007: 30th Annual BZA conference, University of York, United Kingdom
- 2006: 29th Annual BZA conference, St Martin's College, Ambleside, Lake District, United Kingdom.
- 2005: 28th Annual BZA conference, University of Bath, United Kingdom.